CURRENT ADVANCES IN AGRICULTURAL AND ENVIRONMENTAL SCIENCES II

Editors
Prof. Dr. Vecihi AKSAKAL
Assoc. Prof. Dr. Ümit YILDIRIM
Lecturer Onur GÜVEN

İKSAD
Publishing House

CURRENT ADVANCES IN AGRICULTURAL AND ENVIRONMENTAL SCIENCES II

Editors
Prof. Dr. Vecihi AKSAKAL
Assoc. Prof. Dr. Ümit YILDIRIM
Lecturer Onur GÜVEN

Authors
Prof. Dr. Ayhan CEYHAN
Prof. Dr. Cüneyt GÜLER
Prof. Dr. Mehmet Ali KURT
Prof. Dr. Ümmügülsüm ERDOĞAN
Assoc. Prof. Dr. Betül GIDIK
Assoc. Prof. Dr. Bünyamin ALIM
Assoc. Prof. Dr. Erdem ŞAKAR
Assoc. Prof. Dr. Ümit YILDIRIM
Assoc. Prof. Dr. Yaşar ERDOĞAN
Assist. Prof. Dr. Cihan PALOLUOĞLU
Lecturer Onur GÜVEN
MSc. Beyza YILMAZ
MSc. Nazire ORTAK

İKSAD
Publishing House

(The Licence Number of Publicator: 2014/31220)
TÜRKİYE TR: +90 342 606 06 75
USA: +1 631 685 0 853
E mail: iksadyayinevi@gmail.com
www.iksadyayinevi.com

ISBN: 978-625-378-421-8
Cover Design: İbrahim KAYA
December / 2025
Ankara / Türkiye
Size: 16x24cm

CONTENTS

PREFACE

“Current Advances in Agricultural and Environmental Sciences II" presents modern perspectives on the fast-changing fields of agriculture and environmental sciences. In a world where environmental pressures, climate variability, population growth, and the declining capacity of natural resources increasingly influence global priorities, the relationship between productive agriculture and responsible environmental management has never been more crucial. This volume aims to offer an integrated and future-oriented framework by presenting recent research rooted in scientific rigor and interdisciplinary collaboration.

This book presents a wide range of research, from melatonin applications to the effects of air pollution on plant quality, from the assessment of water and soil resources to robotic pollination and the impact of climate change on biological systems. Furthermore, the study of heavy metal pollution using X-ray techniques makes a significant contribution to environmental monitoring approaches.

The studies in this book align closely with the United Nations Sustainable Development Goals (SDGs), particularly in advancing agricultural productivity, protecting water and soil resources, addressing environmental challenges, and supporting the sustainable use of ecosystems. In doing so, the book strengthens scientific knowledge while contributing to global sustainable development efforts.

We believe this volume will be a valuable resource for researchers, students, practitioners, and policymakers working toward building a more resilient and sustainable future. We sincerely thank all contributing authors and scholars, whose work keeps inspiring new paths of inquiry and innovation.

Editors

Prof. Dr. Vecihi AKSAKAL
Assoc. Prof. Dr. Ümit YILDIRIM
Lecturer Onur GÜVEN

CHAPTER 1

PHYSIOLOGICAL AND PRODUCTION EFFECTS OF MELATONIN APPLICATIONS IN SMALL RUMINANTS

Prof. Dr. Ayhan CEYHAN[1]

MSc. Beyza YILMAZ[2]

DOI: https://dx.doi.org/10.5281/zenodo.17847549

[1] Niğde Ömer Halisdemir University, Faculty of Agricultural Sciences and Technologies, Department of Animal Production and Technologies, Niğde, Türkiye. aceyhan@ohu.edu.tr, ORCID ID: 0000-0003-2862-7369

[2] Niğde Ömer Halisdemir University, Institute of Science, Department of Animal Production and Technologies, Niğde, Türkiye. byzylmz.95@gmail.com, ORCID ID: 0000-0001-6696-5006

INTRODUCTION

Melatonin is a hormone secreted by the pineal gland, with its production increasing especially during dark periods. Also known as the "hormone of darkness," this compound plays a role in many physiological functions in small ruminants, such as regulating the reproductive cycle, supporting the immune system, and reducing oxidative stress (Ndhlala et al., 2024; Kal, 2023). While it plays a fundamental role in regulating circadian rhythm, it is also a crucial tool for managing breeding seasons in seasonal breeders due to its sensitivity to environmental photoperiod (Garip, 2021). Increased melatonin levels due to shorter day length stimulate the production of gonadotropin-releasing hormone (GnRH) via the hypothalamus, which in turn triggers the release of follicle-stimulating hormone (FSH) and luteinizing hormone (LH) from the pituitary gland, initiating ovarian activity (Kal, 2023; Aladağ, 2024). This mechanism is critically important for the initiation and management of reproduction, especially in seasonally polyestrous sheep and goats. Melatonin, scientifically known as N-acetyl-5-methoxytryptamine, was first isolated from the bovine pineal gland by Aaron Lerner in 1958 (Jumnake et al., 2024). Its secretion mechanism involves the transmission of light signals from retinal photoreceptors to pinealocytes in the pineal gland via the suprachiasmatic nucleus (SCN) in the hypothalamus and the sympathetic nervous system. Secretion increases in the dark, while light exposure suppresses this process (Kárpáti et al., 2023). In small ruminants, melatonin serves multi-faceted roles beyond the seasonal regulation of reproductive physiology, including maintaining metabolic homeostasis, strengthening the immune system, and supporting antioxidant defense mechanisms (Canto & Abecia, 2024; Jumnake et al., 2024). By influencing the hypothalamic-pituitary-gonadal (HPG) axis through photoperiod, it regulates gonadotropin secretion, and the increase in LH and FSH levels regulates reproductive functions in both female and male animals (Garza-Brenner et al., 2024). Additionally, melatonin is a potent antioxidant that can directly scavenge reactive oxygen species (ROS) (Akbulut et al., 2025). It stabilizes cell membranes, protects mitochondrial function, and reduces oxidative stress. These properties allow it to mitigate the negative effects of metabolic stress that can occur during pregnancy, lactation, growth periods (Viola et al., 2023). It is also critically important in regulating energy metabolism, supporting bone mineralization, and modulating immunity. Its

interaction with IGF-1 and thyroid hormones can positively influence growth performance and feed efficiency (Tezcanlı et al., 2025).

With all these properties, melatonin is considered a biotechnological tool—naturally produced or externally administered—for increasing both physiological and production-related efficiency in small ruminant farming.

1. ENDOGENOUS PRODUCTION AND MECHANISM OF ACTION OF MELATONIN IN SMALL RUMINANTS

Melatonin is primarily synthesized in the pineal gland in mammals, and its secretion is regulated by ambient light conditions (Figure 1). Photoperiod, or the duration of daylight, is the key determinant of melatonin synthesis. Secretion increases during the shorter days of the autumn-winter period, which directly influences the onset of the breeding season in seasonally polyestrous sheep and goats (Garip, 2021; Sarıbay, 2023). The melatonin secretion process occurs via the retina–hypothalamus–sympathetic nervous system axis. Light signals reaching the retina are transmitted to the suprachiasmatic nucleus (SCN) via the optic nerve. The SCN activates the neuronal pathways that carry photoperiod information to the pineal gland, initiating melatonin synthesis. In the dark period, an increase in norepinephrine release stimulates the synthesis of melatonin from serotonin in pinealocytes; during daylight hours, light suppresses norepinephrine signals, halting production (Jumnake et al., 2024; Kárpáti et al., 2023; Garip, 2021).

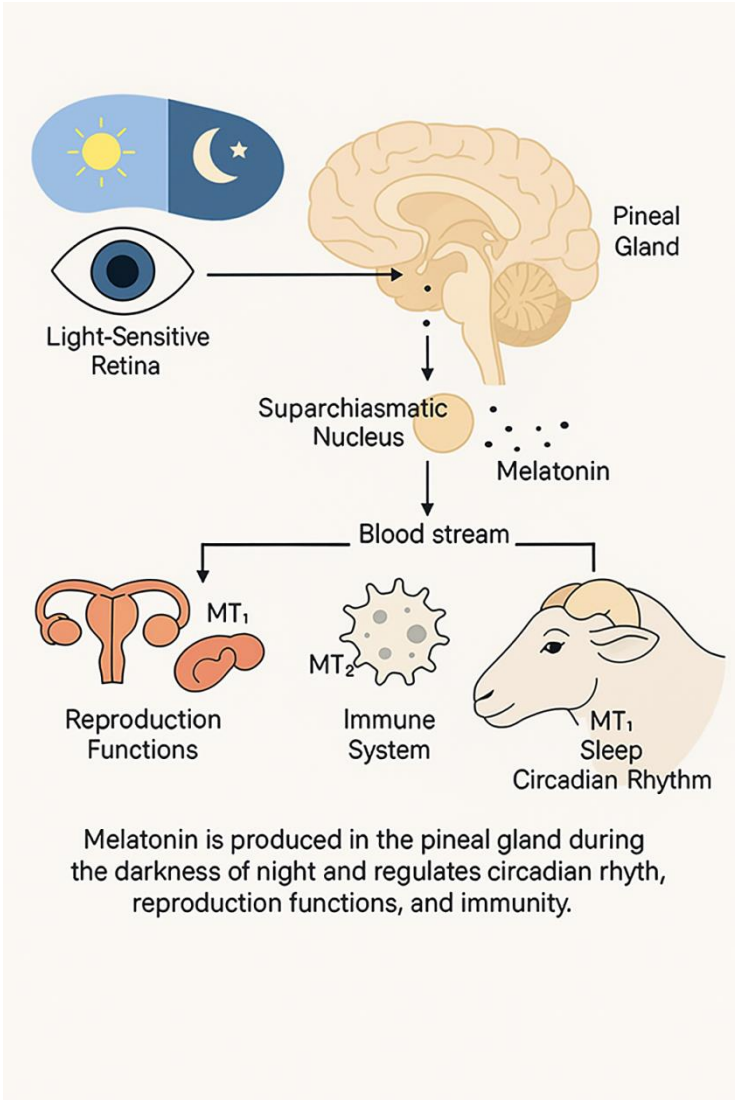

Figure 1: Melatonin Production in Small Ruminants

1.1. Synthesis and Secretion Process

Melatonin is synthesized from the amino acid tryptophan, via serotonin. Secretion peaks during the nighttime hours, and this cycle plays a critical role in maintaining circadian rhythm (Ndhlala et al., 2024).

1.2. Photoperiod and Seasonal Reproduction

In seasonally polyestrous species sensitive to short-day photoperiods, such as sheep and goats, increased melatonin production due to shorter days stimulates the hypothalamic-pituitary-gonadal (HPG) axis. This process increases gonadotropin-releasing hormone (GnRH) secretion, which in turn causes the pituitary gland to secrete luteinizing hormone (LH) and follicle-stimulating hormone (FSH) (Figure 2). LH triggers ovulation in females and supports testosterone production in males, while FSH promotes follicular development and spermatogenesis (Garza-Brenner et al., 2024; Kal, 2023; Aladağ, 2024; Kárpáti et al., 2023). Additionally, melatonin suppresses prolactin production, thereby reducing the inhibitory effects of long-day photoperiods on reproduction (Türkoğlu and Bozkurt, 2024).

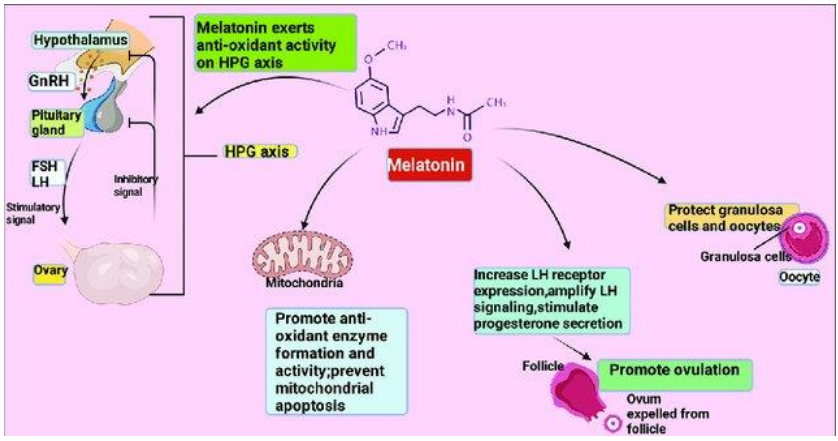

Figure 2: Mechanism of Action of Melatonin (Haque et al., 2025)

1.3. Receptors and Target Organs

The effects of melatonin are mediated through MT1 and MT2 type G-protein coupled receptors. MT1 receptors regulate reproduction and metabolism, while MT2 receptors regulate circadian rhythm and immune functions (Kárpáti et al., 2023). These receptors are found in high concentrations in the ovary, testis, pituitary gland, and hypothalamus. MTNR1A gene polymorphisms can affect seasonal reproductive adaptation among individuals (Turgut and Koca, 2024).

1.4. Extra-Reproductive Functions

Melatonin is effective not only on the reproductive system but also on immune and antioxidant defense. At the cellular level, it neutralizes reactive oxygen species (ROS), prevents lipid peroxidation, and protects mitochondrial function. These mechanisms protect animal health by reducing metabolic stress, especially during pregnancy, lactation, and growth periods (Akbulut et al., 2025; Viola et al., 2023).

1.5. Role of Environmental Light Regime

In addition to the natural light regime, melatonin secretion can be manipulated with artificial photoperiod applications. In indoor livestock farming, the artificial regulation of the photoperiod can control melatonin levels to activate the reproductive cycle (Yiğit, 2022). A study by Şirin et al. (2022) reported that a 13-hour darkness application in Akkaraman sheep significantly increased plasma melatonin levels and contributed to hormonal synchronization.

2. EFFECTS OF MELATONIN HORMONE ON THE REPRODUCTIVE SYSTEM

Melatonin is a potent bioregulator that affects the reproductive system in small ruminants through both direct and indirect pathways. In seasonally polyestrous sheep and goats, its increased secretion during short-day photoperiods plays a central role in initiating the breeding season and enhancing fertility (Aladağ, 2024; Kal, 2023; Bakış, 2021). These effects stem from its regulatory functions on the hypothalamic–pituitary–gonadal (HPG) axis via photoperiod and its antioxidant capacity, which provides protection against environmental stressors (Kárpáti et al., 2023; Garza-Brenner et al., 2024). Melatonin has multifaceted functions, including regulating the breeding season, inducing ovulation, maintaining pregnancy, and increasing offspring survival.

2.1. Effects on Female Small Ruminants

Administering melatonin implants during the anestrous period can stimulate ovulation, advance the mating season, and allow for births to be

scheduled for different times of the year (Kárpáti et al., 2023). It supports follicular development by increasing gonadotropin secretion, raises progesterone levels, and prepares a suitable uterine environment for embryo implantation (Akbulut et al., 2025). Melatonin applications in the final stage of pregnancy can increase the protein and lactose content of colostrum, enhancing the immune capacity of lambs (Canto and Abecia, 2024). It also supports the formation of brown adipose tissue (BAT), reducing the risk of hypothermia and increasing neonatal survival rates. Applications during the birthing period can even increase the weaning weight, especially in male lambs (Canto and Abecia, 2024).

2.2. Effects on Male Small Ruminants

In rams, melatonin promotes spermatogenesis, increases sperm count and motility, and supports testicular function (Figure 3). It has been reported to increase sexual behavior and libido even outside the breeding season (Garza-Brenner et al., 2024). These effects are linked to both photoperiod-induced hormonal stimulation and the reduction of heat and oxidative stress.

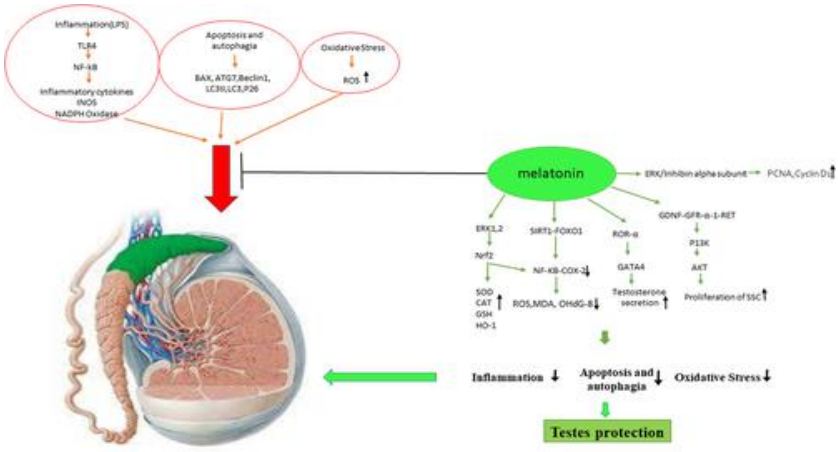

Figure 3: Schematic Representation of the Proposed Ways in which Melatonin Protects Testicular Tissue (Heidarizadi et al., 2022)

2.3. Combination with Assisted Reproductive Technologies

When combined with hormones like progesterone, GnRH, or eCG, melatonin can significantly increase estrus synchronization and pregnancy rates (Skliarov et al., 2021). Its ability to support oocyte maturation, accelerate

embryo development, and preserve the viability of frozen embryos makes melatonin a valuable tool in assisted reproductive techniques (ART) (Kárpáti et al., 2023).

2.4. Antioxidant Protection and Reproductive Success

Melatonin's ROS-scavenging effect reduces cellular damage in the ovaries and testes, improving the quality of oocytes and sperm. This can contribute to higher pregnancy rates in both natural mating and artificial insemination (Akbulut et al., 2025).

2.5. Effects on the GnRH–FSH–LH Axis

Melatonin stimulates GnRH secretion in the hypothalamus, which increases FSH and LH secretion from the pituitary gland (Figure 4). This, in turn, triggers follicular development, ovulation, and progesterone production (Kırkpınar, 2020; Kal, 2023). When administered during the anestrous period, it reactivates the ovaries (Sarıbay, 2023). Öztürk and Tölü (2025) reported that an 18-mg melatonin implant in Tahirova sheep increased estrogen and progesterone levels, triggering estrus behavior.

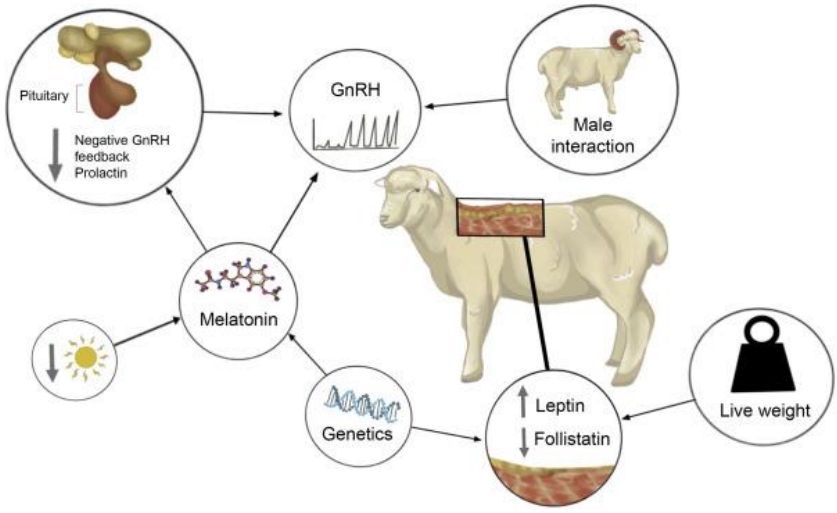

Figure 4: Endocrine, Genetic, Social, and Metabolic Factors and Their Potential Interactions Affecting the Onset of Puberty in Lambs (Pool et al., 2020)

2.6. Regulation of the Breeding Season and Estrus Synchronization

Melatonin implants, such as Regulin, are applied subcutaneously approximately 30–35 days before the introduction of rams. Their slow release synchronously activates the reproductive system (Duymaz and Koyuncu, 2021). This method allows for out-of-season lamb production (Birdane and Avdatek, 2020). Çınar and Ceyhan (2024) reported that a melatonin implant in Akkaraman sheep increased fertility, lambing rate, and twinning rate, and that a similar effect was observed with an FGA sponge combination.

2.7. Sexual Behavior and Mating Success

Melatonin positively influences not only hormonal levels but also sexual behavior (Figure 5). Öztürk and Tölü (2025) noted that the rates of sexual interaction (ESIR) were statistically significantly higher in groups that received melatonin compared to the control group. With its regulatory effects on mating rate, time to conception, and birthing time, melatonin applications provide significant advantages for farm management. Türkoğlu and Bozkurt (2024) reported that among different doses of melatonin (10 mg, 20 mg, 40 mg) given to sheep, the best results were obtained with the 10-mg application, while the 40-mg dose did not show the expected effect. These results indicate that the effect of melatonin is dose-dependent and that high doses can negatively impact hormonal balance.

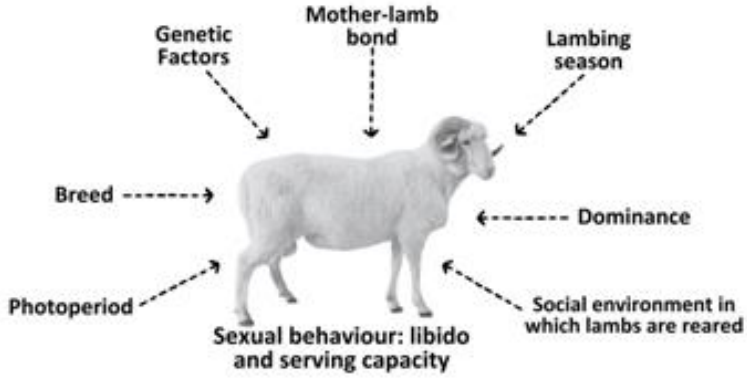

Figure 5: Factors Influencing Sexual Behavior in Rams (Orihuela Trujillo, 2014)

2.8. Heat Stress, Embryo Loss, and a Protective Role

High temperatures can lead to embryo loss and a decline in fertility. Melatonin's antioxidant capacity provides protection against these negative effects (Akbulut et al., 2023; Birdane and Avdatek, 2020). It facilitates embryo implantation by maintaining progesterone levels during early pregnancy, supports corpus luteum functions, and exhibits a luteotropic effect (Akbulut et al., 2025). Therefore, melatonin supplementation during hot summer months or under an artificial light regime helps maintain reproductive efficiency. It has multifaceted functions in small ruminants, such as regulating the breeding season, stimulating ovulation, maintaining pregnancy, and increasing offspring survival. These effects are largely due to its regulatory role on the hypothalamic-pituitary-gonadal (HPG) axis via photoperiod and its strong antioxidant properties (Kárpáti et al., 2023; Garza-Brenner et al., 2024).

3. IMPORTANCE OF DOSE, TIMING, AND APPLICATION METHODS IN MELATONIN ADMINISTRATION

Melatonin administration can provide significant benefits for productivity and physiological balance in small ruminants. However, to achieve these effects, the dosage, timing, and method of application are crucial. Doses that are either too low or too high can negate the desired positive effects or lead to adverse reactions. Various findings in the literature indicate that the optimal dose and duration of application can vary depending on the species, breed, season, and environmental conditions. Melatonin applications in small ruminants can have significant effects on reproductive success, pregnancy, growth performance, and offspring survival. However, achieving this effect depends on correctly determining the dose, timing, and application method (Figure 6). Doses that fall below or exceed physiological limits can not only eliminate the desired positive effects but also lead to reverse biological responses. Literature data show that the optimal dose and application duration vary according to species, breed, season, and environmental conditions.

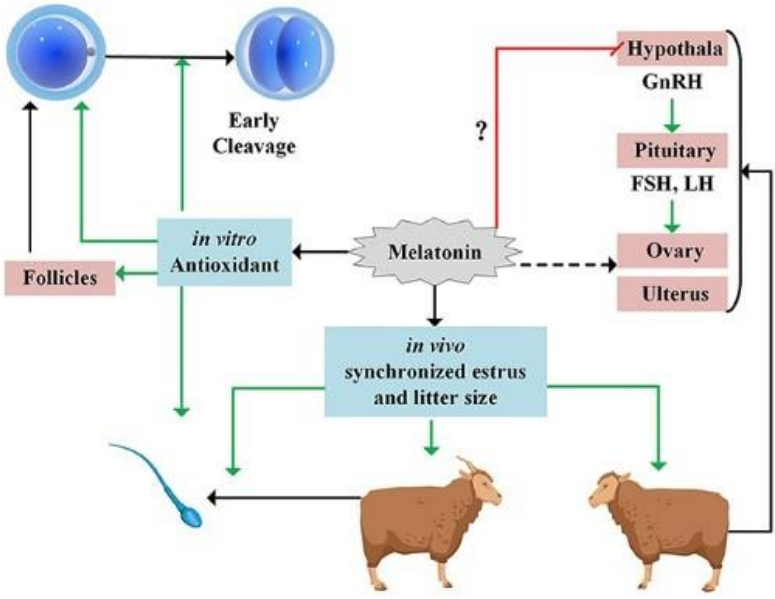

Figure 6: The Proposed Mechanism of Action of Melatonin in Relation to Oocyte Development in Sheep (Chen et al., 2022)

3.1. Dosing Strategies and Effects

The most common form of administration in small ruminants is subcutaneous implants. Most commercial implants contain 18 mg of melatonin and are effective for 60–90 days through slow release (Kárpáti et al., 2023). While the duration of efficacy can be extended with two implants in some protocols, high-dose applications can lead to receptor desensitization and a reduction in physiological responses (Kárpáti et al., 2023). Türkoğlu and Bozkurt (2024) reported that 10 mg (MEL10) and 20 mg (MEL20) doses of melatonin increased estrus, mating, and pregnancy rates. In contrast, a 40 mg (MEL40) application was ineffective and caused negative changes. In the MEL10 group, the estrus rate was 75.71%, mating rate was 61.42%, and pregnancy rate was 60%. In the MEL40 group, no significant hormonal increase was observed. This suggests that high doses might suppress endogenous melatonin production through negative feedback mechanisms.

3.2. Timing: Preparation Before Ram Introduction

When administered during the long-day period (spring-summer) when endogenous secretion is at its lowest, melatonin mimics a short-day effect, advancing the breeding season (Garza-Brenner et al., 2024). In most protocols, implants are applied 30–45 days before the introduction of rams (Duymaz and Koyuncu, 2021). Duymaz and Koyuncu (2021) reported that an 18-mg implant given 35 days before ram introduction increased fertility, birth timing, and multiple birth rates. Öztürk and Tölü (2025) showed that combining melatonin administration with a 15-day flushing protocol enhanced hormonal activity and led to an earlier onset of sexual behavior. Melatonin administered 30 days before birth during the gestation period can increase the protein and immunoglobulin content of colostrum, enhancing lamb survival (Canto and Abecia, 2024).

3.3. Application Methods

Subcutaneous Implant: Implants placed behind the ear provide a long-lasting and controlled release.

- Subcutaneous Injection: Melatonin given in an oily solution has a short-term effect and is usually administered in combination with GnRH or progesterone protocols (Akbulut et al., 2025).
- Oral Forms: Can be used in monogastrics, but their bioavailability is low in small ruminants due to ruminal metabolism.
- Dark Environment Application: Photoperiod manipulation increases endogenous melatonin secretion. Şirin et al. (2022) reported that a 13-hour darkness application in Akkaraman sheep improved plasma melatonin levels and estrus behavior.

3.4. Combination Protocols

When melatonin is combined with intravaginal sponges containing progesterone, $PGF_2\alpha$ injections, GnRH, or eCG, pregnancy rates and embryo quality can increase (Birdane and Avdatek, 2020; Akbulut et al., 2023). Melatonin + progesterone protocols, in particular, stabilize progesterone levels at the start of pregnancy, increasing the likelihood of embryo implantation (Akbulut et al., 2025).

3.5. Management Considerations

When administering melatonin, the animal's season, age, breed, reproductive status, and body condition score should be considered. The correct dose and timing maximize the stimulatory effect on the HPG axis, whereas excessive or improper applications can disrupt endogenous secretion.

4. MELATONIN'S ANTIOXIDANT PROPERTIES AND PROTECTIVE ROLE DURING PREGNANCY

Melatonin not only regulates circadian rhythm and reproductive hormones but also plays significant biological roles through its powerful antioxidant properties. Pregnancy in small ruminants is a period of heightened oxidative stress due to increased metabolic load and hormonal changes. In this context, melatonin's ability to scavenge free radicals and increase antioxidant enzyme activity provides critical benefits for both maternal health and offspring development (Ndhlala et al., 2024; Tekin, 2022). Melatonin provides dual protection; it directly neutralizes reactive oxygen species (ROS) and indirectly stimulates the activity of antioxidant enzymes like superoxide dismutase (SOD), glutathione peroxidase (GSH-Px), and catalase (Jumnake et al., 2024; Kárpáti et al., 2023). These properties help limit oxidative damage throughout pregnancy, supporting the function of placental, fetal, and maternal tissues (Figure 7).

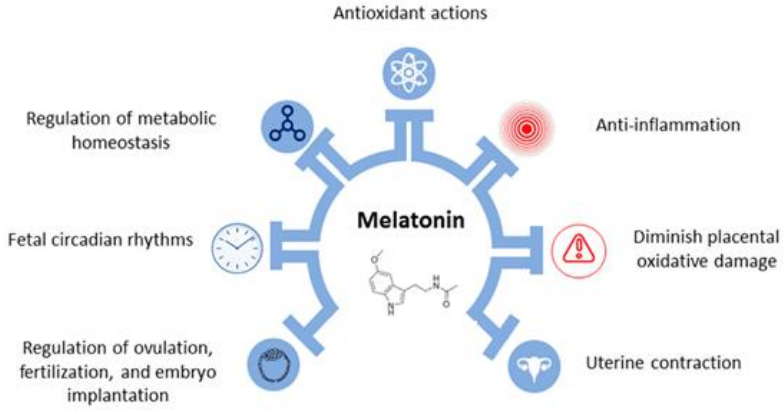

Figure 7: Schematic Representation of the Relationship Between Oxidative Stress and Fetal Programming in Early Life (Tain and Hsu, 2024).

4.1. Oxidative Stress and Cellular Protective Effects

Increased ROS production during pregnancy can cause damage to cell membranes, DNA structure, and organelle integrity. Melatonin prevents lipid peroxidation, stabilizing cell membranes, protecting mitochondrial DNA, and reducing the oxidative load that can negatively affect oocyte quality (Akbulut et al., 2025). Tekin (2022) showed that melatonin administration in late-pregnant Awassi sheep significantly increased total antioxidant capacity (TAS) while reducing total oxidant status (TOS) and the oxidative stress index (OSI).

4.2. Placental and Fetal Protection, Colostrum Quality

Melatonin can cross the placenta and reach the fetus directly (Canto and Abecia, 2024). This helps prevent developmental disorders caused by oxidative stress in the fetus and supports brown adipose tissue (BAT) development, reducing the risk of postpartum hypothermia (Figure 8). Furthermore, melatonin implants have been reported to increase the immunoglobulin G (IgG) content of colostrum, thereby enhancing passive immunity transfer (Canto and Abecia, 2024; Tekin, 2022). In his study, Tekin (2022) emphasized that this effect was more pronounced in sheep that had twin births or male lambs.

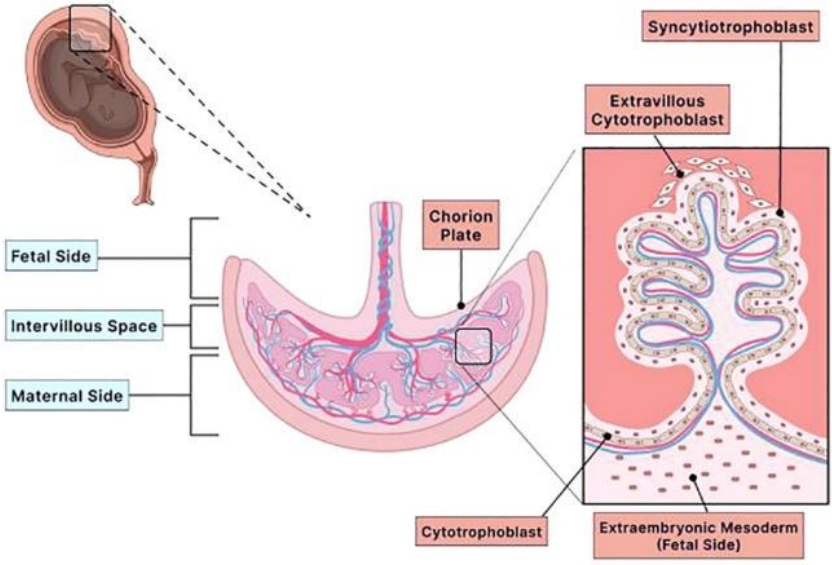

Figure 8: The Structure of the Placenta (Joseph et al., 2024)

4.3. Progesterone Support and Embryo Viability

Through its luteotropic effect, melatonin supports corpus luteum function, increasing progesterone production (Akbulut et al., 2025). Progesterone is critical for preparing the endometrium for implantation, maintaining pregnancy, and preserving embryo viability. Akbulut et al. (2025) reported that melatonin + progestagen protocols significantly increased progesterone levels on day 17 of pregnancy and supported embryo development.

4.4. Fetal Development, Protection Against Hypoxia, and Post-Natal Viability

Melatonin also has positive effects on fetal oxygenation during pregnancy. Melatonin secreted by the pineal gland can cross the placental barrier, directly reaching the fetus and contributing to the developing organism's protection against oxidative stress (İder and Ertürk, 2023). Melatonin is said to increase uterine blood flow, which helps reduce neonatal risks such as hypoxic-ischemic encephalopathy. İder and Ertürk (2023) suggested that melatonin could be used as a protective agent to prevent post-natal losses and may have a neuroprotective effect against brain damage. It's noted that prenatal melatonin administration can positively influence the nervous system, respiratory capacity, and overall viability of newborn lambs. In contrast, Yeşilkaya (2023) examined the effects of melatonin on embryo yield before superovulation, but this application led to negative results in terms of embryo number and quality. This finding indicates that the timing and protocol compatibility of melatonin administration are critical, especially in MOET (multiple ovulation and embryo transfer) systems, and should be carefully evaluated.

5. POTENTIAL EFFECTS AND RISKS OF UNDER- OR OVER-USE OF MELATONIN

While melatonin administration offers many benefits in small ruminant farming such as managing the reproductive cycle, enabling out of season breeding, and increasing pregnancy success improper dosage, incorrect timing, or unnecessary use can lead to undesirable outcomes. The powerful effects of

melatonin on the endocrine system require careful consideration of both insufficient and excessive doses (Kárpáti et al., 2023). Dosage and timing are critical to the success of melatonin application. Inadequate doses may fail to produce the targeted hormonal response, while excessive doses can disrupt physiological rhythms, decrease receptor sensitivity, and negatively impact reproductive performance. Moreover, long-term or unnecessary use can disrupt natural cycles and weaken hormonal responses.

5.1. Potential Consequences of Insufficient Dosing

Melatonin applications below the physiological level may not adequately stimulate the GnRH–FSH–LH axis, leading to failed ovulation induction, insufficient follicular development, and a lack of estrus behavior (Birdane and Avdatek, 2020; Türkoğlu and Bozkurt, 2024; Öztürk and Tölü, 2025). With single-dose subcutaneous injections, the duration of effectiveness can be shortened if the hormone's half-life and elimination time are not taken into account.

5.2. Risks of Excessive Dosing

High doses of melatonin can lead to down-regulation and desensitization of MT1 and MT2 receptors, reducing the hormone's effectiveness (Kárpáti et al., 2023). Türkoğlu and Bozkurt (2024) reported that while doses of 10–20 mg yielded high success rates, estrus and pregnancy rates dropped in the group that received 40 mg. Excessive doses can over-suppress prolactin levels, disrupting the seasonal hormonal cycle, which may result in a halt in ovarian activity and irregular ovulation (Aladağ, 2024).

5.3. Effects of High Doses During Pregnancy

Although melatonin provides antioxidant protection during pregnancy, excessive doses can negatively affect placental hormone synthesis. The suppression of LH can weaken corpus luteum function, making embryo implantation difficult (Akbulut et al., 2023). Yeşilkaya (2023) reported a decrease in embryo count, total cell count, and corpus luteum numbers in sheep administered melatonin implants before superovulation.

5.4. Effects of Prolonged or Unnecessary Use

Applications during the normal breeding season or in individuals who already have high melatonin levels can disrupt hormonal balance and cause a departure from natural cycles. Continuous administration can lead to receptor desensitization and a weakened hormonal response (Sarıbay, 2023; Turgut and Koca, 2024). Furthermore, genetic differences, such as MTNR1A gene polymorphisms, can affect an individual's sensitivity to melatonin, which may reduce the effectiveness of flock-based applications.

5.5. Key Findings from the Literature

- Out-of-Season Use: Melatonin application during the transition and anestrous periods stimulates ovarian activity, initiates estrus behavior, and increases pregnancy rates (Çınar and Ceyhan, 2024; Öztürk and Tölü, 2025).
- Dose-Response Relationship: Doses in the 10–20 mg range yield positive results, while doses of 40 mg and above can become ineffective due to negative feedback (Türkoğlu and Bozkurt, 2024).
- Antioxidant Effect: During pregnancy, melatonin reduces oxidative stress, improves colostrum quality, and strengthens neonatal immunity (Tekin, 2022; İder and Ertürk, 2023).
- Embryo Yield: Incorrect timing and dosage errors can negatively affect embryo development (Yeşilkaya, 2023).
- Genetic Factors: MTNR1A polymorphisms can influence the success of the application (Turgut and Koca, 2024).

5.6. Practical Application Recommendations

- Timing: Implants should be applied 30–45 days before ram introduction, and light exposure should be minimized.
- Dose Selection: For subcutaneous applications, 10–20 mg should be preferred, and high doses should be avoided.
- Hormone Combination: Combinations with progesterone, eCG, and $PGF_2\alpha$ should be planned considering the reproductive cycle and body condition.

- Genetic Consideration: Individual differences should be considered in flock-based applications due to genetic variability.
- Neonatal Health: Administration during pregnancy can support colostrum quality and lamb health.

6. CONCLUSION AND RECOMMENDATIONS

Melatonin is a critical bioregulator with key functions in the physiological, hormonal, and productive processes of small ruminants. Especially in seasonally polyestrous species (sheep and goats), it offers multifaceted benefits, such as initiating the breeding season, synchronizing estrus, increasing fertility, preserving embryo viability, and reducing oxidative stress. Due to its antioxidant capacity, it provides a protective effect at both maternal and fetal levels during pregnancy, enhancing pregnancy success, improving colostrum quality, and strengthening neonatal immunity. Literature findings demonstrate that factors like dose, timing, application method, and the animal's physiological state directly influence the success of melatonin applications. Insufficient doses fail to produce the desired endocrine response, while excessive doses can lead to receptor desensitization, hormonal imbalances, and a decline in reproductive performance. Furthermore, incorrect dosing or timing during pregnancy can negatively affect embryo development and placental functions.

Practical Recommendations:

- Melatonin applications should be planned based on the animal's age, breed, body condition score, and reproductive stage.
- The most effective results are obtained with applications of 10–20 mg, given approximately 30–45 days before the introduction of rams.
- Application during the non-breeding season is more effective for increasing synchronization and pregnancy rates.
- Melatonin use during pregnancy can be considered to reduce oxidative stress and support neonatal health, but the dose and timing must be determined with precision.
- Since genetic factors (e.g., MTNR1A polymorphisms) can affect the melatonin response, individual differences should be taken into account in flock-based applications.

In conclusion, melatonin is a powerful tool for managing reproduction and increasing pregnancy success in small ruminant farming. However, it provides optimal results only when the risk–benefit balance is considered and the application is planned in light of scientific data. Future research will help optimize application protocols by more clearly defining the dose-response relationship, differences in genetic sensitivity, and the long-term effects on production performance.

REFERENCES

Akbulut, K., Kırbaş, M., Harman, H., & Yavuz, H. (2023). Effects of melatonin on reproductive performance, plasma progesterone and malondialdehyde concentrations during breeding season in ewes.

Akbulut, N. K., Kırbaş, M., Harman, H., & Yavuz, H. (2025). Effect of melatonin and melatonin plus progestagen protocols on some reproductive performance and blood parameters at the beginning of the breeding season in Hasmer ewes. Revista Cientifica de la Facultade de Veterinaria, 35(1).

Aladağ, F. (2024). Koyunlarda doğan yavru sayısının immunoglobulinler ve oksidatif stres üzerine etkisi.

Bakış, F. G. (2021). Koyunlarda östrüs senkronizasyonu başarısı üzerine etkili faktörlere güncel bakış.

Birdane, M. K., & Avdatek, F. (2020). Effect of vitamin A, D_3, E treatment on fertility in the Pırlak sheep.

Canto, F., & Abecia, J. A. (2024). Effects of melatonin implants in late gestation and at lambing on colostrum and milk quality of ewes, birth temperature and growth performance of their lambs. Small Ruminant Research, 232, 107210.

Chen, Y., Shan, X., Jiang, H., & Guo, Z. (2022). Exogenous melatonin directly and indirectly influences sheep oocytes. Frontiers in Veterinary Science, 9, 903195.

Çınar, M., & Ceyhan, A. (2024). Geçiş dönemindeki Akkaraman koyunlarda uygulanan farklı senkronizasyon protokollerinin döl verimi üzerine etkisi. Kahramanmaraş Sütçü İmam Üniversitesi Tarım ve Doğa Dergisi, 27(5), 1217–1225.

Duymaz, Y., & Koyuncu, M. (2021). Kıvırcık koyunlarında anöstrus döneminde farklı senkronizasyon yöntemlerinin döl verimi üzerine etkisi. Mediterranean Agricultural Sciences, 34(2), 255–260.

Garip, R. (2021). Türk siyah alaca sağmal ineklerde gece aydınlatmasının süt ve kan melatonin düzeylerine etkileri.

Garza-Brenner, E., Sánchez-Dávila, F., Mauleón-Tolentino, K., Zapata-Campos, C. C., Luna-Palomera, C., Hernandez-Melendez, J., ... &

Vázquez-Armijo, J. F. (2024). Systematic review of hormonal strategies to improve fertility in rams. Animal Reproduction, 21(2), e20240007.

Haque, F., Deeba, F., Banu, J., Ishrat, S., Akhter, A., Sinha, S., ... & Haque, M. (2025). Melatonin and Dehydroepiandrosterone: An Observation vis-à-vis Infertility. Advances in Human Biology, 10-4103.

Heidarizadi, S., Rashidi, Z., Jalili, C., & Gholami, M. (2022). Overview of biological effects of melatonin on testis: A review. Andrologia, 54(11), e14597.

İder, M., & Ertürk, A. (2023). Koyun ve keçilerde neonatal kayıpların önlenmesi. In Sağlıklı ve Sürdürülebilir Koyun ve Keçi Yetiştiriciliği (pp. 28–35). Türkiye Klinikleri, Ankara.

Joseph, T. T., Schuch, V., Hossack, D. J., Chakraborty, R., & Johnson, E. L. (2024). Melatonin: the placental antioxidant and anti-inflammatory. Front Immunol. 2024; 15: 1339304.

Jumnake, A. R., Patodkar, V. R., Gavali, N. E., Sardar, V. M., & Mehere, P. V. (2024). Advances in Melatonin Research–A Review. Chron. Aquat. Sci., 1, 152-174.

Kal, Y. (2023). Akkaraman ırkı koyunlarda embriyonik ölümlerin azaltılmasına yönelik aşım sonrası ketoprofen uygulamasının etkinliğinin araştırılması (Yüksek lisans tezi).

Kárpáti, E., Fürlinger, D., Pleskó, A. M., Gulyás, L., Gáspárdy, A., & Becskei, Z. (2023). Various approaches to influence melatonin level in sheep reproduction. Veterinarski glasnik, 77(1), 16-34.

Kırkpınar, S. (2020). Anöstrus döneminde Kıvırcık ırkı koyunlarda farklı uygulamalar ile ovaryum aktivitesinin uyarılması.

Ndhlala, A. R., Yüksel, A. K., & Çelebi, N. (2024). Effects of melatonin on human, animal and plant metabolisms.

Orihuela Trujillo, A. (2014). La conducta sexual del carnero: Revisión. Revista mexicana de ciencias pecuarias, 5(1), 49-89.

Öztürk, N., & Tölü, C. (2025). Effect of melatonin treatment on reproductive hormones and sexual behaviors in sheep. Tekirdağ Ziraat Fakültesi Dergisi, 22(1), 221–232.

Pool, K. R., Rickard, J. P., & de Graaf, S. P. (2020). Overcoming neuroendocrine and metabolic barriers to puberty: the role of melatonin

in advancing puberty in ewe lambs. Domestic Animal Endocrinology, 72, 106457.

Sarıbay, M. K. (2023). Koyunlarda Üreme Mevsimi Dışında Ovaryum Aktivitesinin Uyarılması. 190.

Skliarov, P., Pérez, C., Petrusha, V., Fedorenko, S., & Bilyi, D. (2021). Induction and synchronization of oestrus in sheep and goats. Journal of Central European Agriculture, 22(1), 39-53.

Şirin, E., Karakaya, S., & Şen, U. (2022). The effect of darkness treatment on plasma melatonin concentrations and reproductive performance in Akkaraman ewes.

Tain, Y. L., & Hsu, C. N. (2024). Melatonin use during pregnancy and lactation complicated by oxidative stress: focus on offspring's Cardiovascular–Kidney–Metabolic health in animal models. Antioxidants, 13(2), 226.

Tekin, T. B. (2022). İleri gebe İvesi ırkı koyunlara melatonin uygulamasının kolostrum IgG düzeyi ve oksidatif stres üzerine etkisi (Doktora tezi).

Tezcanlı, Ö., Üstüner, H., Selvi, T. N., & Gök, A. (2025). Effect of melatonin on growth performance in Saanen kids. Acta Veterinaria Brno, 93(11), 47-53.

Turgut, A. O., & Koca, D. (2024). Melatonin receptor 1A (MTNR1A) gene polymorphism in cross-bred Hamdani sheep: A preliminary study. ISPEC Journal of Agricultural Sciences, 8(1), 127–133.

Türkoğlu, O., & Bozkurt, G. (2024). The effect of subcutaneously administered melatonin crystal's oily solution on estrus and conception rates in ewes. Animal Health, Production & Hygiene, 13(1).

Viola, I., Canto, F., & Abecia, J. A. (2023). Effects of melatonin implants on locomotor activity, body temperature, and growth of lambs fed a concentrate-based diet. Journal of Veterinary Behavior, 68, 24-31.

Yeşilkaya, Ö. F. (2023). Assaf ırkı koyunlarda süperovulasyon öncesi eksojen melatonin uygulamasının embriyo verimi üzerine etkisi (Doktora tezi).

Yiğit, O. (2022). Progesteron temelli östrus senkronizasyon protokollerinde eCG kullanımının ve koç etkisinin sabit zamanlı suni tohumlama sonrasında koyunlarda fertiliteye etkisi (Master's thesis, Balikesir University (Turkey)).

CHAPTER 2

EFFECT OF AIR POLLUTANTS ON STRAWBERRY (Fragaria × ananassa Duch.) FRUIT QUALITY

Prof. Dr. Ümmügülsüm ERDOĞAN[1]

DOI: https://dx.doi.org/10.5281/zenodo.17847575

[1] Bayburt University, Engineering Faculty, Department of Food Engineering, Bayburt, Turkey. gulsum25@gmail.com, ORCID ID: 0000-0002-0490-2285

INTRODUCTION

Strawberry (*Fragaria* × *ananassa* Duch.), a perennial plant belonging to the Fragaria genus of the Rosaceae family, is one of the world's most important berry species, with a production volume of approximately 10 million tons (FAO, 2022). Its long history of cultivation, its ability to grow within wide ecological limits, its flavor and aroma, and its availability to consumers at times when many other fruits are unavailable in the market have made it the most widely cultivated berry fruit (Hancock, 2000). Strawberries are not only consumed fresh but also have a place in many sectors of the food industry, including frozen products, jams and marmalades, alcoholic beverages, soft drinks, dried products, milk and dairy products, confectionery, and cake decorating. 45% of the world's strawberries are grown in Asia, 27% in the Americas, 20.6% in Europe, 6.8% in Africa, and 0.6% in Oceania. China, the United States, and Mexico rank among the top five countries in global strawberry production, while Turkey is among the top five (FAO, 2022).

Strawberry fruit quality is significantly affected by environmental conditions. High temperatures reduce strawberry fruit size and yield, while altering sugar-acid balance and phenolic compound profiles, which can negatively impact taste and nutritional value (Balasooriya et al., 2017). Air pollution has profound and multifaceted negative effects on plant physiological and biochemical processes. Common pollutants, particularly tropospheric ozone (O_3), nitrogen oxides (NO_x), and particulate matter, penetrate plant tissues through stomatal conduction, damaging the photosynthetic system. This leads to stomatal closure or dysfunction, reducing CO_2 uptake and carbon fixation, leading to a decrease in chlorophyll content and oxidative damage to cell membranes (Winner & Atkinson, 1986).

Increasing industrialization worldwide, traffic congestion, and the use of fossil fuels for heating and energy production have led to the transport of pollutants such as ozone, NO_x, SO_2, and PM into agricultural areas. These pollutants can cause a decrease in photosynthesis in the strawberry plant, accelerate chlorophyll degradation, increase oxidative stress, slow fruit development, disrupt sugar and acid balance, and reduce flavor and color quality. Strawberries are considered a functional food due to their high antioxidant capacity, phenolic compounds, and sensory properties. However, the plant's biological structure and fruit tissue create a high sensitivity to

atmospheric pollutants. Therefore, air pollutants are a multifaceted problem with nutritional and toxicological dimensions, not just yield loss.

1. AIR POLLUTION

Air pollutants are defined as substances that alter the natural composition of the atmosphere and have adverse effects on human health and ecosystems. These pollutants, released into the atmosphere as a result of natural or anthropogenic activities, can have different physical, chemical, and biological properties (Singh et al., 2023). Air pollution alters atmospheric composition, altering temperature and precipitation patterns and causing contamination of water, air, and soil (Fuller & Amegah, 2022).

The layer of the atmosphere where pollutants are effective is the troposphere, which extends from 6.5 to 16 km above the earth's surface. While the atmosphere has the ability to neutralize harmful substances introduced into it through natural mechanisms, when the concentration of these substances increases, it cannot fulfill this function, and the air pollution problem arises (Demirbaş, 2025.). Atmospheric composition is a significant environmental factor that limits plant and animal husbandry, causing changes in the yield values of agricultural and livestock products (Singh et al., 2023).

Air pollutants are classified as primary and secondary pollutants depending on their access to the atmosphere. Primary pollutants are those emitted directly into the atmosphere from the source and do not undergo any change. These include sulfur dioxide (SO_2), hydrogen sulfide (H_2S), nitrogen monoxide (NO), nitrogen dioxide (NO_2), carbon monoxide (CO), carbon dioxide (CO_2), and particulates. Secondary pollutants are compounds that react with other substances in the atmosphere after leaving the source and are formed as a result of these reactions. These include sulfur trioxide (SO_3), sulfuric acid (H_2SO_4), ozone (O_3), aldehydes and ketones, peroxyacetyl nitrate, and heavy metals (Demirbaş, 2025; Goutam Mukherjee et al., 2022).

2. EFFECTS OF PRIMARY POLLUTANTS ON STRAWBERRY FRUIT QUALITY

2.1. Sulfur Oxides (SOx)

Sulfur dioxide (SO_2) is one of the most frequently occurring harmful compounds in the atmosphere. Sulfur, an essential element for plants, contributes to the elimination of some nutrient deficiencies at low levels and has positive effects in reducing Fe deficiency (Muneer et al., 2014). Sulfur is also an essential component of amino acids, proteins, vitamins, and chlorophyll (De Kok, 1990; Yang et al., 2006). It also plays a role in nodule formation and nitrogen fixation, as well as molecular metabolism. However, the harmful effects of SO_2 on plants depend on the duration and extent of exposure (Li & Yi, 2012). High levels of SO_2 uptake can cause growth retardation, such as leaf chlorosis and necrosis, and, in later stages, plant death (Agrawal et al., 2003). SO_2 gas is easily taken up from the leaf surface through stomata and can be converted into sulfate (SO_4^{2-}) and sulfite (SO_3^{2-}) by hydration in the leaf mesophyll tissue (Considine & Foyer, 2015). These transformations can disrupt the photosynthetic electron transport chain, reduce chlorophyll and photosynthetic pigment levels, and thus reduce carbon assimilation capacity (Çepel, 2006; Li et al., 2022). At the same time, symptoms such as chlorosis, necrosis, and tissue deterioration can be observed in leaves (Muneer et al., 2014; Schubert, 1984) showed that high-dose CO, NOx, and SO_2 stress in strawberries causes high levels of reactive oxygen species production, increased lipid peroxidation products, and decreased photosynthetic physiology.

2.2. Nitrogen Oxides (NOx)

Nitrogen oxides (NO_x) are among the most common pollutants in the atmosphere. These gases are released into the atmosphere through vehicle exhausts, energy production, and various industrial processes and can have both direct and indirect effects on plant tissue. In a global study, Lobell et al. (2022) found significant negative correlations between NO_2 exposure and agricultural yield. Honour et al. (2009) emphasized the negative impact of excessive nitrogen oxides on urban vegetation. NO_2 mostly affects leaves and seedlings, and its effect decreases with increasing age of the plant and tissue. Muneer et al. (2014) study, strawberry plants were exposed to CO, NO_x, and SO_2 gas

stress; reduced photosynthesis, decreased sugar and sucrose content, and changes in antioxidant enzyme activity were observed.

2.3. Particulates

Particulate matter suspended in the atmosphere is formed by production, traffic, industrial activities, and dirt-road-related activities. These substances are important not only for human health but also for agricultural systems. High levels of particulates in polluted air can reduce light transmission to chloroplasts and gas exchange efficiency. Particulate pollution also interferes with other physiological processes such as bud burst, pollination, and light absorption/reflection. Particulates have also been reported to increase plant susceptibility to pathogen infection and cause long-term changes in their genetic makeup (Emberson, 2003). Particulates disrupt water balance and assimilation processes in plants, causing growth disorders and reduced yield and quality. On the other hand, in crowded residential and industrial areas, various metals, such as lead, contained in airborne dust are taken up by plants and stored in roots, stems, and leaves. This negatively impacts many physiological processes, particularly photosynthesis (Singh et al., 1997). Rodríguez-Rodríguez et al. (2023) demonstrated in their study that strawberry fruit poses a potential risk in terms of particulate matter and heavy metal accumulation.

3. Effects Of Secondary Pollutants On Strawberry Fruıt Qualıty

3.1. Ozone (O_3)

Ozone can be absorbed into the plant body from the environment via the leaf or fruit surface. There is a wide variation among plant species in terms of sensitivity to ozone. High ozone concentrations cause leaf deformation and symptoms such as chlorosis, bleaching, bronzing, spotting, mottling, and unilateral and bilateral necrosis in broadleaf plants. Visible leaf damage leads to reduced growth (Emberson, 2003; Müezzinoğlu, 2003). Keutgen and Pawelzik (2008) exposed Korona and Elsanta strawberry varieties to 78 ppb ozone during the growing season under greenhouse conditions. They determined that ozone exposure reduced leaf area, leaf number, water content,

and specific leaf area. A study conducted on the Cambridge Favorite strawberry variety in 2000 and 2001 measured carbon flow to the fruit and other plant organs in plants exposed to 92 ppb ozone for 69 days. It was determined that ozone affected carbon flow to the fruit. This was predicted to indirectly affect fruit growth, ripening rate, and potential quality (sugar accumulation, indirect metabolic effects) (Drogoudi & Ashmore, 2000).

3.2. Acid Deposition

Acid deposition is the deposition of acidic components in rain, snow, fog-cloud, dew, or dry particles. Acid deposition is of two types: dry and wet. Dry deposition refers to acidic gases and particles, while wet deposition refers to rain, snow, and dew (Özdemir, 2005). Acid rain occurs when SO_2 and NO_x emissions from industrial activities and traffic are converted in the atmosphere and reach the surface as sulfuric and nitric acid precipitation. Acid rain increases the concentration of heavy metals in the soil. Increased heavy metal concentrations have a toxic effect on plants. The toxicity of heavy metals is observed in the form of nutritional deficiencies due to nutrient imbalances in the soil, and burns and accumulations on plant leaves due to acid rain (Kant & Kızıloğlu, 2011). During dry seasons, heavy metal concentrations and heavy metal toxicity increase in the soil due to water evaporation. Acid rain affects the chemical structure and biological conditions of the soil. It leaches beneficial elements such as calcium and magnesium from the soil and carries them to the groundwater. It causes soil acidification, thereby reducing agricultural yields (Prakash et al., 2023; Sedyaaw et al., 2024). Under field conditions, the Chandler strawberry variety was exposed to fog at varying acidity levels from pH 1.6 to pH 3.2. At very low pH exposures, plants died within 8 weeks. At higher pH values, no significant adverse effects on growth, yield, or soluble sugars were observed, but spotting was observed on the calyx (Musselman et al., 1988).

3.3. Peroxy Acetyl Nitrate (PAN)

The most visible symptoms in plants are chlorosis and necrosis in the leaves, which inhibit the absorption and synthesis of carbohydrates and proteins (Gheorghe & Ion, 2011). Plants damaged by PAN also experience premature leaf senescence and consequent leaf drop. Conversely, due to its role as a

photooxidant, PAN damage increases at high light intensity, causing net photosynthesis losses by promoting plant respiration (Hatipoğlu et al., 1988).

3.4. Heavy Metals

Heavy metal pollution is one of the greatest threats to the safe production of agricultural products, posing potential risks to both food safety and human health. Strawberry plants grown in cadmium contaminated soils undergo various physiological and biochemical changes that directly affect nutrient uptake, ionic balance, yield, and fruit quality (Doğan et al., 2022). The accumulation of heavy metals such as lead and cadmium in the soil is absorbed by strawberry root systems and enriched in the fruits, affecting their nutritional composition and flavor (Yang et al., 2006). In general, the damage caused by heavy metals not only affects the growth and quality of strawberries, but more importantly, eating strawberries contaminated with heavy metals causes a range of health problems that are difficult to detect initially (Rachappanavar et al., 2024).

Some heavy metals are essential micronutrients for plants at low doses. However, high doses inhibit the growth of most plant species and can cause metabolic disorders. When heavy metals accumulate excessively in plant tissues, mineral nutrition, transpiration, photosynthesis, enzyme activity, nucleic acid structure, chlorophyll synthesis, and germination are negatively affected. Additionally, damage to membranes, disruption of hormone balance, and altered water relations can also be observed (Okcu et al., 2009). Şener and Cantemur (2023) compared fruit quality parameters and Zn, Cu, Pb, and Cd levels in organic and conventional strawberry production in Turkey. An advantage was observed in organic production in terms of fruit quality criteria (fruit weight, TSS, firmness), but heavy metal accumulation remained below the limit values in both systems.

A study conducted in Slovakia evaluated the relationships between Pb and Cd levels in strawberry varieties and total phenolic content (TPC) and antioxidant activity (AA). Decreases in phenolic and antioxidant values were observed in samples with high heavy metal levels (Lidiková, 2024).

4. CONCLUSION AND RECOMMENDATIONS

Among fruit species, berries, in particular, are of great health importance due to their high content of bioactive substances and the known anticarcinogenic, antimutagenic, and antioxidant properties of these substances. Strawberry cultivation, the most important fruit species in the berries group, has shown a continuous increase in Turkey over the last 55 years. Due to its high adaptability, strawberries are one of the most widely cultivated fruit species worldwide. In Turkey, strawberry cultivation is economically feasible from sea level to 2,000 meters. In addition to its high adaptability, a rich variety of varieties plays a significant role in the widespread cultivation of strawberries. However, ecologies with warm temperate climates are more important for economical strawberry cultivation.

Air pollution is one of the environmental stress factors that directly affects agricultural production systems. Because plants are immobile and more sensitive to air pollution in terms of physiological responses than humans and animals, they better reflect local conditions. Even prolonged exposure to low concentrations of air pollution can have harmful effects on plant leaves. The strawberry plant (*Fragaria* × *ananassa*) is sensitive to atmospheric pollutants due to its relatively shallow root structure, thin leaf tissue, and high metabolic activity. Recent research has shown that various air pollutants, particularly ozone (O_3), sulfur dioxide (SO_2), nitrogen oxides (NO_x), and particulate matter ($PM_{2.5}$, PM_{10}), cause oxidative stress, reduced photosynthetic capacity, and metabolic disruptions in strawberry plants. As a result of these effects, decreases in total soluble solids, ascorbic acid, anthocyanins, and total phenolic compounds, and increases in acidity, lipid peroxidation, and reactive oxygen species levels are observed in strawberry fruits. Furthermore, dust particles accumulated on the leaf surface reduce photosynthetic activity, negatively impacting fruit size and yield.

Air pollution causes both yield losses and decreases in sensory and nutritional quality in strawberry production. This situation not only reduces the product's economic value but also weakens the functional food value of strawberries, which play a vital role in human nutrition. These findings clearly demonstrate the importance of monitoring air quality in agricultural production. Therefore, it is necessary to adopt integrated environmental-agricultural management approaches, protect clean production areas, and expand scientific

monitoring methods. Supporting interdisciplinary studies to mitigate the effects of environmental stressors to ensure sustainability in strawberry production is considered a strategic necessity for agricultural sciences.

REFERENCES

Agrawal, M., Singh, B., Rajput, M., Marshall, F., & Bell, J. (2003). Effect of air pollution on peri-urban agriculture: a case study. Environmental Pollution, 126(3), 323-329.

Balasooriya, B., Dassanayake, K., & Ajlouni, S. (2017). High temperature effects on strawberry fruit quality and antioxidant contents. IV International Conference on Postharvest and Quality Management of Horticultural Products of Interest for Tropical Regions 1278,

Considine, M. J., & Foyer, C. H. (2015). Metabolic responses to sulfur dioxide in grapevine (Vitis vinifera L.): photosynthetic tissues and berries. Frontiers in plant science, 6, 60.

Çepel, N. (2006). Ekoloji, doğal yaşam dünyaları ve insan. Palme Yayıncılık.

De Kok, L. J. J. H. p. (1990). SULFUR METABOL18M IN PLANTS EXPOSED TO ATMOSPHERIC SULFUR. 111.

Demirbaş, İ. (2025.). Hava Kirliliği. In book: Çevre Sorunları (Dünü, Bugünü, Geleceği) PEGEM AKADEMİ.

Doğan, B., Ghosh, S., Hoang, D. P., & Chu, L. K. (2022). Are economic complexity and eco-innovation mutually exclusive to control energy demand and environmental quality in E7 and G7 countries? Technology in Society, 68, 101867.

Drogoudi, P., & Ashmore, M. (2000). Does elevated ozone have differing effects in flowering and deblossomed strawberry? The New Phytologist, 147(3), 561-569.

Emberson, L. (2003). Air pollution impacts on crops and forests: an introduction.

FAO. (2022). World Food and Agriculture Statistical Yearbook. https://doi.org/https://doi.org/10.4060/cc2211en

Fuller, C. H., & Amegah, A. K. (2022). Limited air pollution research on the African continent: time to fill the gap. International Journal of Environmental Research Public Health, 19(11), 6359.

Gheorghe, I. F., & Ion, B. (2011). The effects of air pollutants on vegetation and the role of vegetation in reducing atmospheric pollution. The impact of air pollution on health, economy, environment agricultural sources, 29, 241-280.

Goutam Mukherjee, A., Ramesh Wanjari, U., Eladl, M. A., El-Sherbiny, M., Elsherbini, D. M. A., Sukumar, A.,…Vellingiri, B. (2022). Mixed contaminants: occurrence, interactions, toxicity, detection, and remediation. Molecules, 27(8), 2577.

Hancock, J. F. (2000). Strawberries. In Temperate fruit crops in warm climates (pp. 445-455). Springer.

Hatipoğlu, R., Tükel, T., & Koç, M. (1988). Çevre kirlenmesinin bitkiler üzerindeki etkileri. Çukurova Üniversitesi Ziraat Fakültesi Dergisi, 2(3), 119-133.

Honour, S. L., Bell, J. N. B., Ashenden, T. W., Cape, J. N., & Power, S. A. (2009). Responses of herbaceous plants to urban air pollution: effects on growth, phenology and leaf surface characteristics. Environmental Pollution, 157(4), 1279-1286.

Kant, C., & Kızıloğlu, T. (2011). Asit Yağmurlarının Canlılar Üzerine Etkileri/The Effects on Organsms of Acid Rains. Atatürk Üniversitesi Ziraat Fakültesi Dergisi, 34(2).

Keutgen, A. J., & Pawelzik, E. (2008). Contribution of amino acids to strawberry fruit quality and their relevance as stress indicators under NaCl salinity. Food chemistry, 111(3), 642-647.

Li, L., & Yi, H. (2012). Effect of sulfur dioxide on ROS production, gene expression and antioxidant enzyme activity in Arabidopsis plants. Plant Physiology Biochemistry, 58, 46-53.

Li, Z.-G., Li, X.-E., & Chen, H. Y. (2022). Sulfur dioxide: an emerging signaling molecule in plants. Frontiers in plant science, 13, 891626.

Lidiková, J., Natália Čeryová, Grygorieva, O., Brindza, J., Demianová, A., & Jurčaga, L. . (2024). Heavy Metal Content and Antioxidant Activity of Strawberries (Fragaria vesca L.). Agrobiodiversity for Improving Nutrition, Health and Life Quality, 8(2).

Lobell, D. B., Di Tommaso, S., & Burney, J. A. (2022). Globally ubiquitous negative effects of nitrogen dioxide on crop growth. Science Advances, 8(22), eabm9909.

Muneer, S., Kim, T. H., Choi, B. C., Lee, B. S., & Lee, J. H. (2014). Effect of CO, NOx and SO2 on ROS production, photosynthesis and ascorbate–glutathione pathway to induce Fragaria× annasa as a hyperaccumulator. Redox biology, 2, 91-98.

Musselman, R. C., Sterrett, J. L., & Voth, V. (1988). Effects of simulated acidic fog on strawberry productivity. HortScience, 23(1), 128-130.

Müezzinoğlu, A. (2003). Atmosfer Kimyası. İzmir: Dokuz Eylül Üniversitesi Mühendislik Fakültesi Yayınları(305).

Okcu, M., Tozlu, E., Metin Kumlay, A., & Pehluvan, M. (2009). Ağır metallerin bitkiler üzerine etkileri. Alinteri Journal of Agriculture Science, 17(2), 14-26.

Özdemir, O. (2005). Görünmeyen tehlİke: AsİT yağişlari the invisible threat: Acid rain.

Prakash, J., Agrawal, S. B., & Agrawal, M. (2023). Global trends of acidity in rainfall and its impact on plants and soil. Journal of Soil Science Plant Nutrition, 23(1), 398-419.

Rachappanavar, V., Gupta, S. K., Jayaprakash, G. K., & Abbas, M. (2024). Silicon mediated heavy metal stress amelioration in fruit crops. Heliyon, 10(18).

Rodríguez-Rodríguez, I., Pérez-Vázquez, L., de Pablos-Pons, F., & Fernández-Espinosa, A. J. (2023). Toxic metals from atmospheric particulate matter in food species of tomato (Solanum lycopersicum) and strawberry (Fragaria x ananassa) used in urban gardening. A closed chamber study. Chemosphere, 340, 139921.

Schubert, T. (1984). Sulfer Dioxide Injury to Plants. Florida Department of Agriculture and Consumer Services.

Sedyaaw, P., Pandey, A., Kawade, S. S., Ade, P. J., Nimbarte, P. V., Bhaladhare, D. R., & Kamble, P. A. t. (2024). A review on acid rain it's causes, effects and management measures. International Journal of Creative Research Though, 12(4), q959-q968.

Singh, A. K., Kumar, M., Bauddh, K., Singh, A., Singh, P., Madhav, S., & Shukla, S. K. (2023). Environmental impacts of air pollution and its abatement by plant species: A comprehensive review. Environmental Science Pollution Research, 30(33), 79587-79616.

Singh, R. P., Tripathi, R. D., Sinha, S., Maheshwari, R., & Srivastava, H. (1997). Response of higher plants to lead contaminated environment. Chemosphere, 34(11), 2467-2493.

Şener, S., & Cantemur, M. H. (2023). Comparison of fruit quality criteria and heavy metal contents of strawberries grown in organic and conventional agriculture. Applied Sciences, 13(13), 7919.

Winner, W. E., & Atkinson, C. (1986). Absorption of air pollution by plants, and consequences for growth. Trends in Ecology Evolution, 1(1), 15-18.

Yang, L., Stulen, I., & De Kok, L. (2006). Sulfur dioxide: relevance of toxic and nutritional effects for Chinese cabbage. Environmental experimental botany, 57(3), 236-245.

CHAPTER 3

THE PAST AND PRESENT OF THE TARSUS COASTAL PLAIN (MERSİN, TÜRKİYE) IN TERMS OF WATER AND SOIL RESOURCES

Prof. Dr. Cüneyt GÜLER[1]

Prof. Dr. Mehmet Ali KURT[2]

Assoc. Prof. Dr. Ümit YILDIRIM[3]

Lecturer Onur GÜVEN[4]

DOI: https://dx.doi.org/10.5281/zenodo.17847582

[1] Mersin University, Engineering Faculty, Department of Geological Engineering, Mersin, Türkiye. cguler@mersin.edu.tr, ORCID: ID: 0000-0001-8821-6532

[2] Mersin University, Engineering Faculty, Department of Environmental Engineering, Mersin, Türkiye. malikurt@mersin.edu.tr, ORCID ID: 0000-0001-7255-2056

[3] Bayburt University, Faculty of Applied Sciences, Emergency Aid and Disaster Management Department, Bayburt, Türkiye. umityildirim@bayburt.edu.tr, ORCID ID: 0000-0002-7631-7245

[4] Bayburt University, Central Research Laboratory and Research Centre, Bayburt, Türkiye. onurguven@bayburt.edu.tr, ORCID ID: 0000-0001-5608-7633

INTRODUCTION

Tarsus Coastal Plain (TCP) in Mersin (Türkiye) has historically been devoted to agriculture (e.g., orchards, traditional vegetable farms, and greenhouses) owing to the existence of fertile alluvial soils and a mild climate that enables crops to be cultivated multiple times a year. Today, this area provides space for agriculture, heavy industry, settlements, and transport, and offers a natural habitat for several sea turtle species (i.e., Caretta caretta and Chelonia mydas) that are under threat globally. TCP is located in the southeast of Türkiye, in the easternmost part of the Mersin Province, and covers an area of approximately 240 km2. Bordered by the Deliçay River to the west and Tarsus (a.k.a. Berdan) River to the east, the aquifer has abundant water, which is currently intensely utilized to meet agricultural and industrial needs using numerous shallow (<40 m) and deep (<300 m) wells drilled through the underlying Quaternary-Recent fluvio-deltaic coastal aquifer. The thickness of the coastal aquifer ranges from 30 m in the northwest to around 500 m in the southeast of the study area. TCP can be designated as a “rural area” in terms of population and of sociological and cultural conditions. There are 26 settlements scattered throughout the coastal plain, with a total population of 65,818. In contrast, the city of Tarsus in the northeast is a major population center, with 342,373 inhabitants. Main agricultural commodities produced in the region include citrus fruits, stone fruits, grapes, pomegranate, banana, fig, vegetables, leaves/salad herbs, cereals, oil-bearing crops, and forage crops. Currently, tourism plays no role in the economy of this agricultural-industrial area.

Since the early 1960s, the water and soil resources of the site are under the influence of widespread environmental pollution and degradation resulting from intense agricultural activities and excessive use of agrochemicals (pesticides, fertilizers, etc.), rapid industrial and urban growth, land use/land cover (LULC) changes and hydrological modifications (e.g., building dams and irrigation-drainage systems, dewatering marshland areas, overpumping of aquifers, etc.). The environmental problems caused by anthropogenic pollution from various point and diffuse sources are greatly exacerbated by the lack of basin-wide management strategies and monitoring efforts. As demonstrated by the earlier studies, especially the coastal parts of TCP is highly vulnerable to pollution from various sources and to seawater intrusion due to anthropogenic and climatic forcing. In addition, dissolution of the evaporitic series (e.g.,

gypsum, anhydrite, halite, etc.) formed (in Handere formation) during the Messinian Salinity Crisis is also important in terms of salinization, in certain parts of the aquifer system. In TCP, high water levels, water logging, flooding, sand extraction, coastal erosion, and sea-level rise are also important environmental problems affecting large areas and results in degradation of water quality and economic losses in agricultural areas. Despite their importance, surface water resources in the area have received comparatively little attention in the literature. However, research has demonstrated that these resources are subject to pollution from waste discharges originating from domestic, industrial, and agricultural sources. The contemporary situation exerts a significant pressure on the ecosystem, which has resulted in a number of detrimental consequences. These include the loss of critical habitats, a decline in biodiversity, and the degradation of water and soil quality in the area.

TCP lies within the extreme northwest part of the Cilicia-Adana Basin Complex (CABC), of which stratigraphic and structural framework have reasonably well defined by the studies conducted over the course of the last two decades. TCP has also benefited from these studies to a certain degree, nonetheless there is still a considerable amount of work to be done to adequately characterize the 3D geologic framework of the basin, which will certainly improve our understanding of the aquifer's functioning and heterogeneity.

This chapter will discuss the hydrological, hydrogeological, and geological properties of TCP, as well as other relevant factors, with a view to providing further insight into the current situation of environmental conditions and pressures acting upon its complex aquifer system and soil/water resources.

1. GENERAL CHARACTERISTICS OF TCP

1.1. Location

Specifically, TCP is bounded by the state road D-400 to the north, Mediterranean Sea to the south, Deliçay River to the west, and Tarsus River to the east and resides within the boundaries of the "Eastern Mediterranean River Basin" of Türkiye. TCP, covering an area of 239.66 km^2, is located in the easternmost region of Mersin Province, and the geographic coordinates of the site are limited by latitudes between 36.74° and 36.92° N and longitudes between 34.70° and 34.97° E (see Figure 1). TCP includes small but a highly populated part of the Tarsus city, as well as the plain part comprising rural

settlements dispersed throughout the region, with the most prominent of these being Kazanlı, Adanalıoğlu, and Bahşiş (see Figure 1).

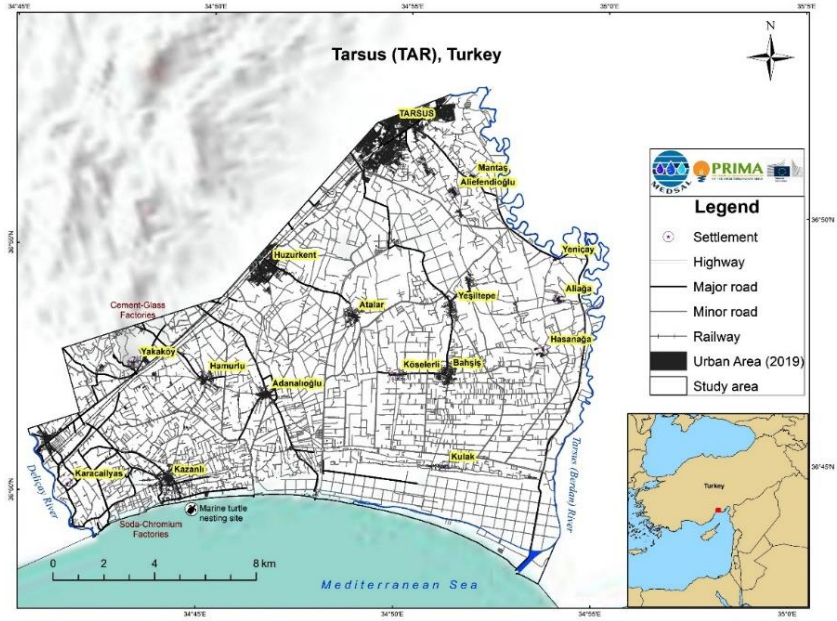

Figure 1: Location of Tarsus Coastal Plain in Mersin, SE Türkiye

1.2. Climate

The prevailing climatic conditions in the area are typified by a semi-arid Mediterranean climate (Güler et al., 2012). This climate is characterized by hot and dry summers, mild and rainy winters, accompanied by high potential evapotranspiration and low precipitation during the dry season, which extends from June to September (Güler et al., 2012). The mean annual temperature is around 18 °C in the coastal zone, where temperatures on occasion exceed 30 °C in summer and seldom fall below 5 °C in winter (Kafalı Yılmaz, 2008; Güler et al., 2012). Long-term records obtained from the climate-monitoring stations located in the coastal zone indicate that mean monthly temperatures during the dry season generally range from 25 to 28 °C (TSMS, 2019). However, alpine climate conditions prevail in the Bolkar Mountain range (a.k.a. Central Taurides) in the north, with peaks as high as 3,113 m above mean sea level (amsl).

1.3. Water and Land Use

TCP is a deltaic system fed by two perennial rivers (i.e., Deliçay and Tarsus) originating from the Bolkar Mountain range. The Seyhan River, discharging to the Mediterranean Sea only at 10 km east of the natural mouth of the Tarsus River, is estimated to account for more than 50% of the alluvial surface of the Çukurova (a.k.a. Cilicia) delta (Russell, 1954). Recently, Tarsus River was artificially connected to the sea by opening a large canal (160 m in width) located 7.2 km east of its natural discharge point (Figure 2). The Tarsus River is a "losing stream" along most of its meandering course within the Tarsus Plain.

Based on data obtained from the General Directorate of State Hydraulic Works (DSİ, 2019), the long-term average total surface runoff (Q_m) from the mountainous terrain at north is 40.1 m^3/s via Deliçay River (Q_m = 1.45 m^3/s at Puğkaraağaç in the period 1966-2015) and Tarsus River (Q_m = 38.65 m^3/s at Muhat Bridge in the period 1953-1993), the latter accounting for 96.38% of this sum. Lengths of these rivers are 51.17 km (for Deliçay River) and 124.85 km (for Tarsus River), where the latter differs from the former in its meandering character within the Tarsus Plain (Figure 2). The area of the Deliçay River basin is 439.3 km^2, which is only one-fifth the size of the Tarsus River basin (2,315.2 km^2). The flow regimes of the Deliçay and Tarsus rivers are significantly different despite their neighboring watersheds, where the peak flow (Q_p) occurs in Deliçay River (Q_p = 3.39 m^3/s in March) two months earlier than the Tarsus River (Q_p = 84.87 m^3/s in May). The differences in the flow regimes of these rivers can be attributed to areal/altitudinal differences (see Figure 2), dominant precipitation regime (rain- vs. snow-dominated) and wintertime snow coverages in their watersheds, which collectively affect spring snow melt timing, intensity, and duration. The Deliçay River flows violently during floods because of its higher channel gradient compared to the meandering Tarsus River, and could transport boulders up to 60-70 cm in diameter to within 8 km of the coast.

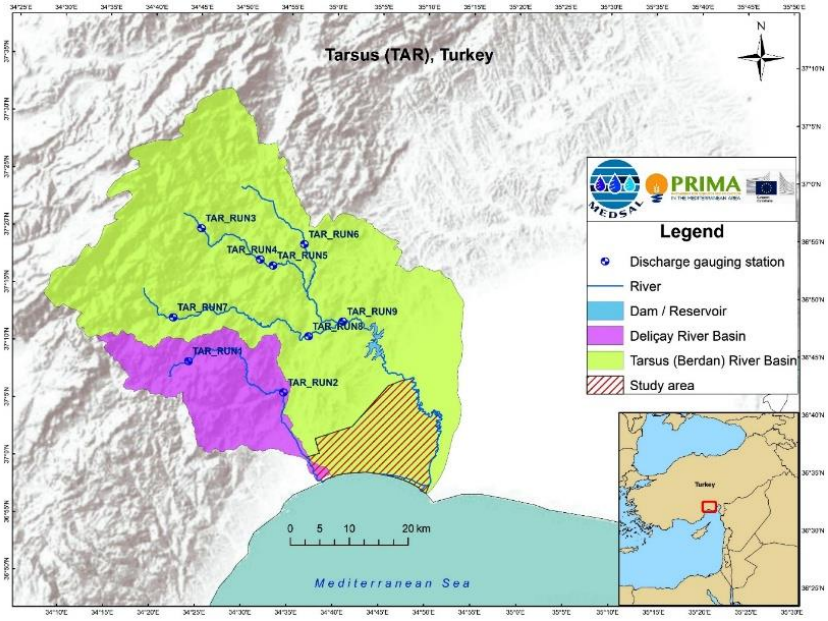

Figure 2: Discharge-Gauging Stations Established on Rivers (i.e., Deliçay and Tarsus) and the Locations of the Dam Reservoirs.

The Tarsus River was the first site in Türkiye to utilize its hydroelectric potential (in 1902), with a micro-scale hydroelectric power plant (2 kW) illuminating the main streets of the city of Tarsus (Öztürk, 2004). Later, two modern hydroelectric power plants (HEPPs) had been built on the Tarsus River, i.e., Kadıncık I HEPP (in 1971) and Kadıncık II HEPP (in 1974) with installed capacities of 70 and 56 MW, respectively. Eventually, the government has privatized these HEPPs on November 16, 2015 (Enerji Atlası, 2020). The multi-purpose Berdan Dam was built on the Tarsus River in 1984 to meet the increasing water demands of agricultural, industrial, and municipal users, to control seasonal flooding, and to produce energy (installed capacity is 10.2 MW) (Enerji Atlası, 2020). The active volume of the Berdan Dam is 71.1 hm^3, of which 75.9% is being utilized for irrigation, 11.2% for flood control, 7.2% for energy production, and 5.7% for water supply (Özgüler, 2007). The construction of another multi-purpose dam (named Pamukluk) on the Tarsus River was completed in 2023. After completion of the Berdan I and II irrigation/drainage canal projects in 1960s, the groundwater levels throughout the plain have declined, which subsequently resulted in drying up of marshland

areas (e.g., Karabucak and Aynaz marshlands) (Güler et al., 2012). According to official government documents, the State Hydraulic Works (DSİ) implemented deliberate dewatering projects in the Aynaz marshland for a period exceeding 10 years, from 1958 to April 1969, which encompassed an area of 62.55 km^2 (Resmi Gazete, 1969). The completion of the irrigation-drainage and dewatering infrastructures have resulted in marked increases in irrigation water availability and cultivable land. Because of this, by the 1970s, the cotton planting areas around the region were largely replaced by orchards (mainly citrus fruit) and vegetable farms (Sandal and Gürbüz, 2003). At present, water logging due to floods/heavy rains and rise in water table, are the major problems faced by local farmers and residents, especially in settlements situated in the eastern part of TCP near Yeşiltepe-Hasanağa-Kulak triangle (see Figure 1). A dense drainage canal network (totaling in length 186.94 km) laid across the plain, together with Aynaz and Kulak drainage pump stations (installed in 1968 and 1992, respectively), are jointly utilized to control groundwater levels in TCP. There is also a very dense network of irrigation canals (totaling in length 288.22 km) on the Tarsus Plain. According to field observations made in 2019, the water in the irrigation-drainage canal system is also subject to pollution caused by occasional industrial wastewater discharges and dumping agricultural wastes (e.g., plastics and plant residues).

The presence of substantial Quaternary unconsolidated deposits (see Gürbüz, 1999) with favorable aquifer characteristics in the region has facilitated the utilization of groundwater resources for various purposes. In this region, the majority of irrigation water for agricultural activities is supplied by a substantial number of privately owned driven-point shallow wells (<40 m in depth) that are equipped with hand/motor pumps or by drilled deep wells (<300 m in depth) that are equipped with motor pumps. The number of groundwater wells within TCP remains unknown due to challenges in locating them, primarily caused by restricted views and access due to greenhouses, residential houses, fences, and trees. Additionally, there is a lack of proper registration, which further complicates the situation. According to the most recent provincial environmental status report (PDEU, 2018), there are 1,315 registered wells in the Tarsus (Berdan) plain, with a groundwater withdrawal rate of 72,018,428 m^3/year. It is estimated that probably around 1,500-2,000 wells are actively being used for agricultural irrigation and industrial water supply in the area.

During the field studies, a significant number of abandoned wells were identified, the majority of which were old and required substantial repair. The reasons for abandonment included loss of functionality due to factors, such as well clogging, corrosion, collapse, groundwater level decline, and salinization/pollution.

According to historical records (see Sandal and Gürbüz, 2003 and references therein), during the period from 1860-1940, cotton was the most prominent agricultural product produced in the Çukurova region, where a port in Mersin and connection to the Baghdad-İstanbul-Berlin railway had been established by 1886 to export the surplus cotton abroad (Ünlü and Ünlü, 2009). Following the completion of crucial modernization projects at the Mersin port (1954-1962), the establishment of the ATAŞ petroleum refinery (1957-1962), the Mersin thermal power plant (1966-1969), and a fertilizer factory (1969) in Karaduvar near Deliçay River's outlet, has spurred an unprecedented industrial and population growth in the area (Sandal and Gürbüz, 2003; Güler, 2009; Güler et al., 2010; 2012). The industrialization trend in TCP continued in 1970s onwards without slowing down, but mainly restricted to the westernmost part, near Kazanlı, and to the northernmost part, along the D-400 state road and railroad from Mersin to Tarsus and Adana (see Figure 1). The industrial and urban development of TCP is largely attributable to its close proximity to the Mersin International Port (MIP) and the Free Trade Zone, located approximately 4 km to the west, where Mersin-Tarsus-Adana road/railroad provides an easy access to many national and international destinations. Within TCP, six primary industrial economic sectors have been identified, including the production of heavy machinery and associated components, textiles, building materials (e.g., cement, plaster, brick, glass, and ceramics), chemical products (e.g., sodium-chromium compounds and plastics), food and fruit processing, and petroleum hydrocarbon product storage facilities (above-ground storage tanks) (Güler et al., 2012).

In addition to industrial investments, agriculture currently represents the most significant economic activity in TCP (Güler et al., 2012). The region is characterized by the presence of densely cultivated orchards, traditional vegetable farms, and greenhouse cultivation. This enables planting of a wide variety of crop species, including (in the order of importance) citrus fruits (e.g., orange, lemon, tangerine, and grapefruit), stone fruits (e.g., nectarine, peach,

apricot, plum, loquat, cherry, and olive), grape, pomegranate, banana, fig, vegetables (e.g., pepper, zucchini, eggplant, tomato, cucumber, onion, leek, radish, okra, bean varieties, cabbage, cauliflower, broccoli, and melons), leaves and salad herbs (e.g., spinach, lettuce, parsley, cress, mint, arugula, and purslane), corn, wheat, soybean, cotton, vetch, potato, sunflower, sesame, rice, peanut, clover, barley, and chickpeas (MDPAF, 2018). Since the last four decades, however, TCP has been witnessing a marked decrease in agricultural areas due to industrial and urban expansions (Sandal and Gürbüz, 2003; Güler et al., 2010; 2012).

The quantification of the changes in land use and land cover (LULC) in TCP was performed using high-resolution satellite imagery (acquired in 2019) through the manual digitization and classification of pertinent LULC features. The present (2019) LULC map was then compared to the past LULC map (2004) created by Güler et al. (2012). The outcomes obtained from the manual image classification, although a tedious process, are deemed extremely satisfactory and far more superior to the freely available online LULC products, such as CORINE (resolution is 100 m). As shown by the data obtained from digitization of satellite imagery (Figure 3), land use in the area has a complex pattern, where most of the area can be associated with agricultural activities, e.g., open-field farms, greenhouses, orchards (mainly citrus) (see Table 1).

Although currently there are no permanent lakes in TCP study site, a total of 339 artificial water bodies (very small ponds) were identified and digitized using the high-resolution satellite imagery. These artificial water bodies, covering 0.38 km^2 in 2004 and 0.31 km^2 in 2019, mostly originated from the extraction of sediment/soil material throughout the site. The excavated material is used to level the uneven topography in and around the greenhouses caused by sand dunes or in places, to raise the base level of the property to protect it from flooding (Güler et al., 2012). The rainwater or groundwater quickly fills the excavated pit in places where water level is near surface (Özdemir, 2024). These features are mostly temporary in nature, where new pits are dug and old ones are filled in case the farmer needs the land for other uses (e.g., building a new greenhouse, expanding the existing one, etc.). Therefore, the number of these features show a high variability between different years and even seasons.

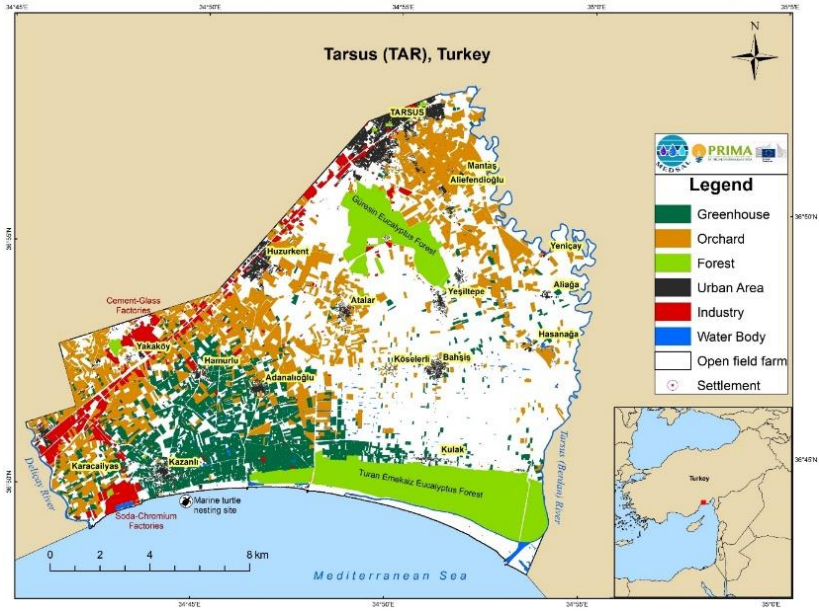

Figure 3: The Present (2019) Land Use and Land Cover Classes of Tarsus Coastal Plain

Table 1: Land Use and Land Cover Changes Between 2004 and 2019 in Tarsus Coastal Plain.

LULC class	Percentage of total area in 2004	Percentage of total area in 2019	Change (%)
Open-field farm	59.04	57.44	-1.60
Greenhouse	13.47	9.34	-4.13
Orchard (citrus)	11.56	16.55	+4.99
Forest	11.11	11.16	+0.05
Industrial area	2.84	3.39	+0.55
Residential area	1.60	1.81	+0.21
Water body	0.38	0.31	-0.07
Total	**100.0**	**100.0**	–

1.4. Environmental Conditions and Pressures

TCP is a unique coastal environment that provides space for vulnerable natural habitats as well as many industrial facilities, urban-rural settlements, agriculture/horticulture areas. It is also home to heavily trafficked roads and railways (Figure 3), which are linked to the nearby Mersin International Port (MIP) and other national and international destinations (Güler et al., 2012). Since the early 1990s, numerous studies have examined the surface water, groundwater, and sediment-soil resources of TCP. These studies mainly address the nature and extent of pollution from various sources and the impact of

anthropogenic activities on coastal ecosystems.

TCP is an ecologically significant area that supports delicate and internationally important terrestrial and marine ecosystems. For instance, the area contains one of the largest coastal dune formations in Türkiye (Uslu, 1989). Unfortunately, the coastal dune fields are seriously threatened by several natural and anthropogenic factors, including coastal erosion (Ozaner, 1994; MEDASSET, 2019), sand extraction (Yilmaz, 1998; Erol, 2003; Leloğlu et al., 2003), urban development (Sandal and Gürbüz, 2003; Burak et al., 2004; Duran et al., 2012), modifications involving landscape (leveling) and drainage patterns (Güler et al., 2012), and construction of dams on the Tarsus and Seyhan Rivers (Gürbüz, 1999; 2003). It is crucial to protect the coastal dune fields because the 4.5-km stretch of Kazanlı Beach is one of the top three most important nesting sites in the Mediterranean for marine turtles such as the loggerhead turtle (*Caretta caretta*) and green turtle (*Chelonia mydas*) (Baran and Kasparek, 1989; Kasparek et al., 2001; Canbolat, 2004). Both of these marine turtle species are protected under the CITES and Bern conventions, and currently they are listed in categories of "Vulnerable" and "Endangered", respectively (IUCN, 2020). In the area, industrial and agricultural pollution, and disordered urbanization (see Güler, 2009; Güler et al., 2012) are important threats to these marine turtle species (Wolf, 2001). These activities have co-existed for more than 50 years at the site and have profoundly affected the environment. For example, carcasses of marine turtles found on Kazanlı Beach (Kaska et al., 2004) and marine bivalve species sampled near the Deliçay River (Karayakar et al., 2007) were found to have high concentrations of potentially toxic elements, such as cadmium (Cd), chromium (Cr), copper (Cu), lead (Pb), and zinc (Zn), in their soft tissues. Another study by Çelik et al. (2006) showed elevated levels of cadmium (Cd), chromium (Cr), and lead (Pb) in plant and sediment samples collected from terrestrial and marine environments near marine turtle nesting grounds. The soda-chromium chemical industry in Kazanlı was criticized for the exceptionally high levels of potentially toxic elements in soil and water (see Koleli and Halisdemir, 2005), as well as for stockpiling approximately 1.5 million tons of toxic chromium waste on alluvial soils and releasing various toxic chemicals into the marine turtle nesting beach and sea (Wolf, 2001; MEDASSET, 2019). Soil salinity is also a major problem in the area, especially in places where water levels are close to surface

(Scheumann, 1997). Soil and sediment samples collected throughout TCP have been extensively studied to characterize their trace element and nitrate-nitrite levels, affected by different anthropogenic activities (e.g., industrial and agricultural) (Kurt et al., 2008a; 2008b; 2009a; 2010a; 2011a).

Groundwater investigations conducted by various researchers have noted the presence of elevated salinity, especially in groundwater wells located in and around the Kazanlı, Adanalıoğlu, and Kulak settlements (Demirel, 2004; Hatipoğlu, 2004; Demirel and Külege, 2005; Kumbur et al., 2008; Güler et al., 2010; 2012; Akbulut et al., 2011). As noted by Güler et al. (2012), the source of groundwater salinization is not solely caused by the seawater intrusion, but also other processes, including water-rock interaction (WRI), ion exchange, and dissolution of evaporitic series (e.g., gypsum, anhydrite, halite, etc.) formed during the Messinian Salinity Crisis are also important. A substantial number of groundwater samples from the area encompassing Kazanlı and Tarsus were found to have boron, iron, zinc, chromium, sodium, chloride, sulfate, nitrate, and nitrite levels well above drinking water standards (see Alpaslan et al., 2009; Korkut, 2009; Korkut et al., 2011; Kurt, 2010; Kurt et al., 2009b; 2011b; 2012; Hatipoglu-Bagci and Bayari, 2020). Güler et al. (2013) demonstrated that these parts of TCP are highly vulnerable to pollution from point and diffuse (non-point) sources, including seawater intrusion. Despite their importance, surface water resources in the region have received scant attention in the literature. However, they were found to be contaminated by waste discharged from domestic, industrial, and agricultural sources (see Kumbur and Vural, 1989; Özer, 2001; Ergene et al., 2007).

In TCP, high water levels, water logging, and flooding are important environmental problems affecting large areas and results in degradation of water quality and economic losses in agricultural areas (see Akgül, 2018). Due to climate change, this low-lying (<30 m) deltaic setting and the shoreline along the Eastern Mediterranean, especially the agricultural areas in the Çukurova region, are vulnerable to sea level rise (Karaca and Nicholls, 2008; Güven et al., 2024). GIS-based inundation mapping, which is based on the estimated sea level rise rate from satellite altimetry data, indicates up to 6.7 m increase in sea level by 2100 in the Çukurova region. This increase would result in the inundation of 69% of the current coastal land in the area (see Simav et al., 2013).

2. GEOLOGICAL-GEOMORPHOLOGICAL FRAMEWORK

2.1. General Geological Framework

The geological formations found in the vicinity of TCP span in age from Paleozoic to Cenozoic and display very complex tectonic and stratigraphic relationships (Ternek, 1953; 1957). The geologic units found in the area are: 1) Paleozoic-Mesozoic Basement rocks, 2) Tertiary sedimentary rocks, and 3) Quaternary deposits (Schmidt, 1961; Şenol et al., 1998; Alan et al., 2007). Table 2 gives a short description of the geological formations depicted in the Reference Geological Map (RGM) (see Figure 4) of TCP. A stratigraphic column showing the geological units found in the vicinity of TCP is presented in Figure 5. Situated at the foothills of the Bolkar Mountain range, TCP only includes Kuzgun and Handere formations, together with Quaternary deposits of diverse nature (e.g., caliche, unconsolidated fluvio-deltaic sediments, and coastal sand dune deposits).

Table 2: The Geological Formations Found in the Tarsus Coastal Plain.

LGF [1]	Age [2]	Description [3]
Kuzgun Formation	Middle-Upper Miocene	Shallow marine and lagoon sediments
Handere Formation	Upper Miocene-Pliocene	Shallow marine, lagoon, and terrestrial sediments with gypsum (evaporites)
Caliche	Middle Pleistocene	Terrestrial carbonate deposits (a.k.a. calcrete)
Unconsolidated fluvio-deltaic sediments	Upper Pleistocene	Unconsolidated alluvial fan deposits, deltaic-coastal sediments, and stream alluvium/conglomerate
Coastal sand dune deposits	Holocene-Recent	Coastal aeolian sand dune deposits

[1] LGF: Local Geological Formation (basic geological units of the Reference Geological Map, RGM).
[2] Age: The geological age of the LGF.
[3] Description: A brief description of the lithology.

In the region, basement rocks consist of Permo-Carboniferous Karahamzauşağı Formation and Upper Cretaceous Mersin ophiolite/ophiolitic mélange, which are unconformably overlain by younger formations of Tertiary and Quaternary period (Avşar, 1992).

The oldest geological unit in the region is Karahamzauşağı formation, which consists of recrystallized limestone/dolomite, marble, schist, and quartzite (Ternek, 1953; Ünlügenç, 1986; Demirkol, 1989). This weakly metamorphosed formation occurs as small outcrops directly north of TCP,

within the headwater region of the Tarsus (a.k.a. Berdan) River. Even though the formation's lower contact is not exposed (Demirkol, 1989), its thickness was estimated to be over 500 m based on field observations (Şenol et al., 1998). Lithological features and fossil assemblages identified in the formation suggest a shelf depositional environment (Demirkol, 1989). Minerals found in the Karahamzauşağı formation include calcite, quartz, muscovite, plagioclase, sericite, and iron-rich opaque minerals (Şenol et al., 1998).

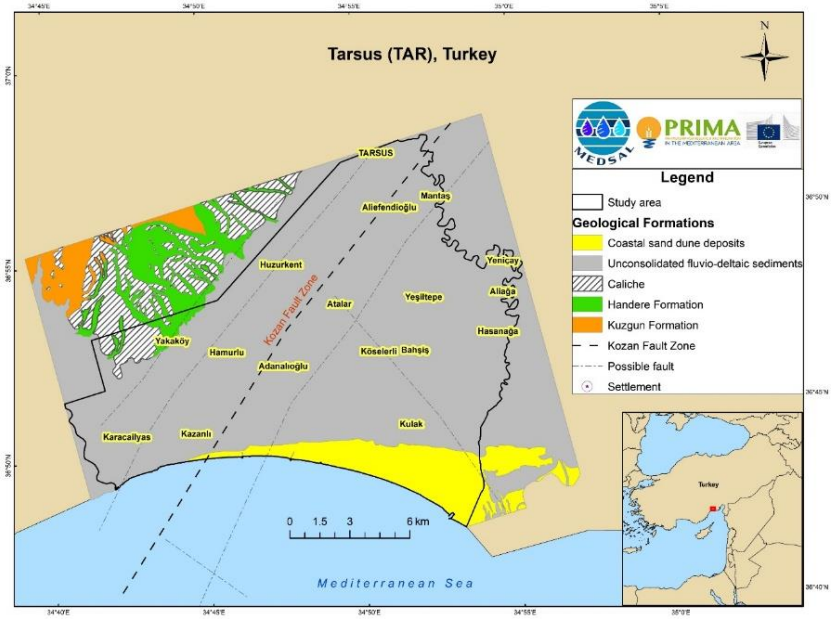

Figure 4: Reference Geological Map (RGM) of the Tarsus Coastal Plain

Mersin ophiolite/ophiolitic mélange is made up of rocks with diverse compositions, which include harzburgite, dunite, gabbro, clinopyroxenite cut by isolated diabase dykes, serpentinite, radiolarite, chert and ophiolitic mélange containing Permian, Jurassic, Cretaceous age exotic rock blocks (decimeter to kilometer in size) found in unevenly altered serpentinitic matrix (Özgül, 1976; Poisson, 1977; Avşar, 1992). Serpentinites possibly formed during suboceanic hydrothermal alteration of their ultramafic protoliths (e.g., harzburgite and dunite) in advance of their emplacement on land during Middle to Upper Cretaceous as a result of Neo-Tethyan Ocean closure. This formation stretches from northeast to southwest, and is about 60 km in length, 25 km in width

(Tekin et al., 2016) and has a thickness of about 6 km (Parlak et al., 1996; Çelik, 2008). Mersin ophiolite/ophiolitic mélange mostly outcrops within deep canyons (carved by Deliçay River) in the northwest part of the study area, which is recognized for its substantial chromite (Cr_2O_3) deposits (Yaman, 1991).

The basement rocks are separated from the overlying Tertiary sedimentary rocks by a distinct unconformity (Figure 5), which marks the Early Miocene transgression in the region (Yalçın and Görür, 1984) and transition from terrestrial to shallow marine environment. Following the emplacement of Late Cretaceous ophiolite/ophiolitic mélange within the Tauride Belt, a number of Neogene sedimentary basins of varying sizes were formed in south-eastern Türkiye. Among these, the Cilicia-Adana Basin Complex (CABC) is the largest (Gül, 2007). The Cenozoic basin fill deposits consist of Tertiary units to the north and Quaternary units to the south, with strata displaying a gentle southward dip (Yalçın and Görür, 1984).

Tertiary sedimentary rocks consist of a thick succession of lacustrine, fluvial, and deep/shallow marine deposits displaying complex lateral and vertical transitions due to fluctuations in the sea level (Ternek, 1953; 1957; Schmidt, 1961; Yetiş et al., 1995; Şenol et al., 1998). Tertiary sedimentary rocks outcrop mostly in the highlands at north of TCP, and from older to younger, include Oligo-Miocene Gildirli formation, Lower-Middle Miocene Karaisalı formation and Güvenç formation, Middle-Upper Miocene Kuzgun formation, and Upper Miocene-Pliocene Handere formation (Schmidt, 1961; Şenol et al., 1998). These units are described in the paragraphs below.

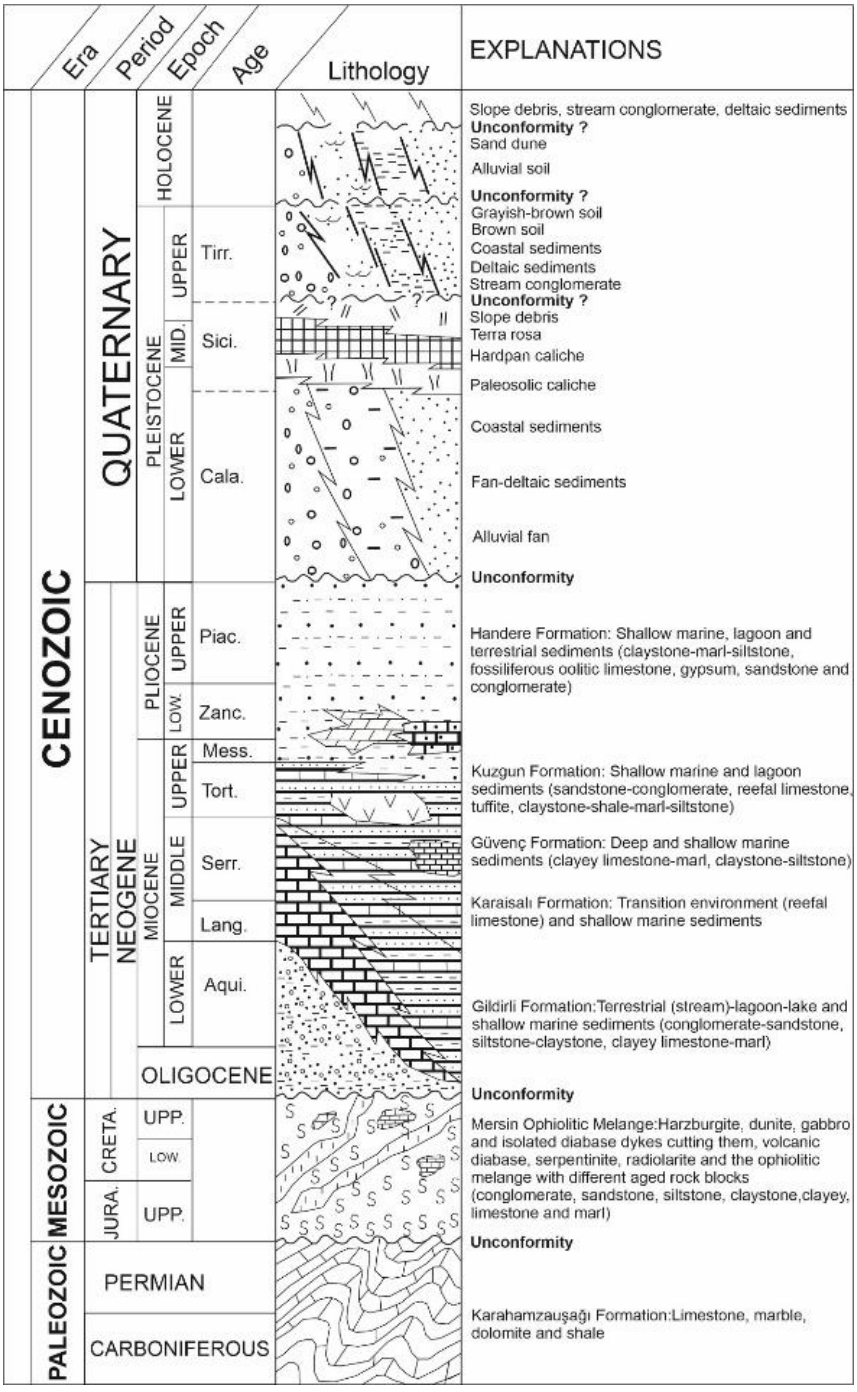

Figure 5: Lithostratigraphic Column of Tarsus Coastal Plain (after Şenol et al., 1998)

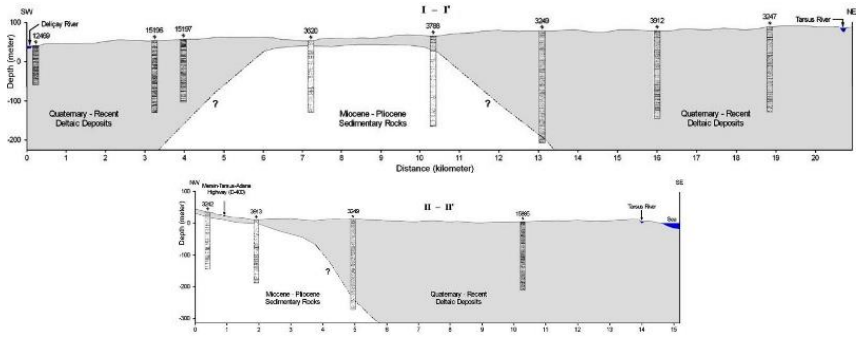

Figure 6: Geological Cross Sections of Tarsus Coastal Plain (after Güler et al., 2012)

Gildirli formation consists of three distinct rock units, mainly conglomerate-sandstone, siltstone-claystone, and clayey limestone-marl (Schmidt, 1961; Şenol et al., 1998). Although they are intertwined and alternate with each other, the conglomerate-sandstone unit dominantly occurs in the lower part, siltstone-claystone unit in the mid part, and clayey limestone-marl unit in the upper part of this formation (Şenol et al., 1998). The conglomerate-sandstone unit is composed of lens and wedge-shaped conglomerate and sandstone layers of 0.5-1.0 m in thickness and 10-300 m in length (Şenol et al., 1998). The clasts of the conglomerate-sandstone unit are firmly attached with clay matrix-carbonate cement and usually derived from the pre-Miocene rocks, including crystallized limestone-marble, ophiolitic rocks, chert, and quartzite. The conglomerate-sandstone unit is mostly poorly graded and cross-bedded with sand and gravel bars (Şenol et al., 1998). Siltstone-claystone unit mostly occurs as wedges and lenses of different sizes and consists of 2-50 cm thick layers, locally containing gravel- and sand-sized clasts (Şenol et al., 1998). The clayey limestone-marl unit consists of 0.5-100 cm thick clayey limestone and marl layers with hundreds of meters of lateral extension. The Gildirli formation is commonly discordant with the underlying units (e.g., ophiolite/ophiolitic mélange) and its thickness range from 1 to 175 m, depending on the paleotopography (Şenol et al., 1998). The facies characteristics of the above-mentioned units suggest a depositional environment for this formation ranging from terrestrial (e.g., flood plain, lake, and lagoon) to shallow marine (Schmidt, 1961; Şenol et al., 1998).

Karaisalı formation is generally composed of well-layered fossiliferous reefal limestones containing corals, algae, foraminifera, echinoderms,

mollusks, bryozoa, and halimeda (Görür, 1979; Şenol et al., 1998; Taraf et al., 2013). Karaisalı formation, although unconformably overlies the pre-Miocene units, it displays vertical transition with the underlying Gildirli formation (if present) and overlying Güvenç formation. The reefal Karaisalı formation was highly controlled by the antecedent topography, clastic input, and sea level fluctuations (Gül, 2007). Thickness of the Karaisalı formation varies depending on the position of the erosion plane and reaches a maximum of 300 m (Şenol et al., 1998). Facies characteristics of the Karaisalı formation suggest a coastal (reefal) depositional setting (Görür, 1979; Şenol et al., 1998).

Güvenç formation consists of sediments dominated by two units, including clayey limestone-marl and claystone-siltstone that were formed in the shallow-deep sea (reef front) environments (Özçelik and Yetiş, 1994; Şenol et al., 1998). In the region, these units are mostly transitional with each other (Şenol et al., 1998). The clayey limestone-marl unit dominates the lower parts of the formation (transitional with Gildirli and Karaisalı formations), whereas the claystone-siltstone unit is mostly found in the mid and upper parts (transitional with Kuzgun formation) (Özçelik and Yetiş, 1994). Deep-sea sediments of the Güvenç formation generally contains significant amount of pyrite, indicating a reducing (i.e., anaerobic) environment (Özçelik and Yetiş, 1994). Near the study area, the visible thickness of the Güvenç formation varies between 50 and 600 m (Şenol et al., 1998).

Kuzgun formation is represented predominantly by sandstones of shallow marine and terrestrial origin (Yetiş et al., 1986; Yetiş, 1988; Büyükutku and Bağcı, 2005). Mainly four units can be distinguished within the Kuzgun formation. These are (from bottom to top) sandstone-conglomerate, reefal limestone, tuffite, and claystone-marl-siltstone, representing shallow marine and transitional environments (e.g., coastal, lagoon, braided river, delta, tidal, and reef) controlled by the fluctuations at the sea levels (e.g., transgressions and regressions) (Şenol et al., 1998). The sandstone-conglomerate unit consists of lens and wedge-shaped sandstone and conglomerate layers, with thicknesses of 0.5-10 m and lengths of 10-500 m (Şenol et al., 1998). The clasts of the sandstone-conglomerate unit are derived from rocks such as ophiolite, quartzite, chert, limestone, and marble, all of which can be related to the pre-Miocene rocks. In some parts of the unit, quartz and feldspar clasts can reach up to 90% (Şenol et al., 1998). The reefal limestone unit is found in several

levels within the sandstone-conglomerate unit, with thicknesses of 5-50 m and hundreds of meters in length. This unit is generally massive and/or layered, laterally and vertically transitive with other units, and contains abundant fossils and gravel/sand clasts composed mainly of quartz and feldspar (Şenol et al., 1998). The tuffite (named as Salbaş tuffite member) geochemically has a tholeitic character and rhyodacitic, trachyandesitic and andesitic composition originated from magmas formed at a volcanic arc environment (Türkmen et al., 2013). Tuffite unit is mainly composed of a mixture of detrital materials (e.g., clay, sand and gravel) and contains fossils (e.g., lamellibranch and gastropod) (Yetiş and Demirkol, 1986) and primary/secondary minerals (e.g., quartz, feldspar, biotite, clays, zeolite, and calcite) (Türkmen et al., 2013). The claystone-marl-siltstone unit generally occurs as lenses 1 to 30 m thick that extend 10 m to several kilometers. This unit does not show lamination or stratification due to intense bioturbation and contains abundant fossils (mainly ostrea and gastropod) (Şenol et al., 1998). Kuzgun formation, varying in thickness between 50 and 1600 m, is conformable with both overlying (Handere) and underlying (Güvenç) formations (İlker, 1975; Şenol et al., 1998).

Handere formation can be divided into four distinct units such as claystone-marl-siltstone, fossiliferous oolitic limestone, gypsum, and sandstone-conglomerate (Şenol et al., 1998). These are generally intertwined with each other, where the first three dominantly occurs in the lower parts and the latter in the upper parts of the formation (Şenol et al., 1998). The deposition of the mixed clastic-carbonate-evaporite succession of Handere formation was caused by the desiccation of the Mediterranean Sea during the Messinian Salinity Crisis (5.60 and 5.33 Ma) (Yetiş et al., 1995; Burton-Ferguson et al., 2005; Faranda et al., 2013). Arid and hot climate conditions prevailing during the Upper Miocene (i.e., Messinian) resulted in deposition of a thick sedimentary succession of marine sediments, in addition to gypsum, anhydrite, and halite (Yetiş and Demirkol, 1986; Darbaş et al., 2008; Darbaş and Nazik, 2010). Later, warm and rainy climate conditions during the Pliocene era and the eustatic sea-level fluctuations (transgressions and regressions) gave rise to development of shallow sea-transitional (e.g., coastal, lagoon, delta, and tidal) and fluvial environments (Şenol et al., 1998; Ilgar et al., 2013). The claystone-marl-siltstone unit consists of layers 5 to 100 m thick that extend 100 to 1000 m (Şenol et al., 1998). Fossiliferous oolitic limestone unit is hard and firmly

cemented. Although oolitic structure is well developed in most parts, it is non-existent or poorly developed in other parts (Şenol et al., 1998). The gypsum unit consists of layers 0.1 to 25 m in thickness and 50 to 250 m in width, where gypsum layers show alternations of clays and silts (Şenol et al., 1998). The sandstone-conglomerate unit typically occurs as layers or lenses and wedges, that range in thickness from a few centimeters to several meters. Although, its dominant lithology is mainly sandstone, conglomerate layers also occur at some places (Şenol et al., 1998). Handere formation conformably overlies the Kuzgun formation with a transitional contact. The exact thickness of the Handere formation is not known because it is largely covered with Quaternary deposits. In the region, the thickness of the Handere formation vary between 50 and 500 m (Şenol et al., 1998).

The surficial geology of TCP is generally characterized by a substantial sequence of Quaternary deposits, which unconformably overlie the Handere formation. Quaternary deposits are heterogeneous mixtures of metamorphic, igneous, and sedimentary rock detritus with laterally discontinuous layers of clay, silt, sand, and gravel deposited by terrestrial processes (e.g., fluvio-deltaic, lacustrine and aeolian) (Şenol et al., 1998; Güler et al., 2012). This Quaternary sedimentary sequence includes alluvial fan deposits, deltaic sediments, coastal sediments, caliche (calcrete), wind-blown sand dune deposits, and stream alluvium/conglomerate (Şenol et al., 1998). The undifferentiated Quaternary deposits overlying the Upper Miocene-Pliocene Handere formation was collectively named as “Kuranşa formation” by some previous researchers (e.g., Yetiş, 1988; Gürbüz and Kelling, 1993). According to the available well log information, the thicknesses of Quaternary sediments varies considerably (from 30 m in the north to over 500 m in the south) and they mostly composed of recent deposits from the Deliçay, Tarsus, and Seyhan rivers (Göney, 1976; DSİ, 1978; Şenol et al., 1998), which are all perennial in character. Tertiary sedimentary rocks are largely covered by the Quaternary fluvio-deltaic sediments in the area (Yetiş and Demirkol, 1986; Ergin, 1996; Şenol et al., 1998). In the majority of localities, these deposits exhibit a high degree of heterogeneity, characterized by laterally discontinuous layers, where clay-rich layers predominate in the southern part of the area (Kurt, 2010). Among the Quaternary deposits, caliche formations and coastal aeolian (windblown) sand dune deposits stand out with their distinctly different

geological and geomorphological characteristics, so they were mapped separately and explained in detail in the present study (Figure 4).

Caliche formations are prevalent in the northern part of the area, where they exhibit terrace-like morphologies at elevations ranging from 25 to 250 m amsl. These formations manifest in diverse forms, including powdery, nodular, tubular, fracture-infill, hardpan, laminar crust, and pisolithic crust (Ternek, 1953; Eren, 2011; Eren et al., 2018). The caliche hardpan has been observed to extend across the lithologically different levels of the Kuzgun formation, in conjunction with alluvial sediments accumulated within erosional troughs (Eren, 2011). Based on previous age dating studies (e.g., Özer et al., 1989), Eren (2011) presumed Middle Pleistocene for the age of caliche formations in Mersin area. Caliche is primarily composed of calcite ($CaCO_3$), with minor components including palygorskite and smectite, as well as accessory mineral phases such as feldspar, quartz, dolomite, and illite (Kadir and Eren, 2008; Eren, 2011).

The coastal part of TCP is predominantly composed of well-sorted, relatively loose Holocene-Recent aeolian sand dune deposits that are generally 1 to 10 m in height and oriented in east-west direction along the Mediterranean coastline, creating an undulating topography (Şenol et al., 1998). Those lacking vegetation covers act under the influence of the wind and change place frequently. In general, the source rocks of the dunes is pre-Miocene metamorphics, magmatics, ophiolites, Miocene and younger units that are found throughout the Deliçay and Tarsus river basins (Şenol et al., 1998). The sand fraction is primarily constituted by opaque minerals (predominantly of ophiolitic origin), accompanied by hornblende, epidote, and chlorite, in addition to calcite, feldspars, biotite and minor quartz (Dinc et al., 1978).

In this region, Tertiary sedimentary rocks are found beneath unconsolidated Quaternary-Recent fluvio-deltaic sediments (Yetiş and Demirkol, 1986). As illustrated in Figure 6, the cross-sections through TCP, were created based on well log data acquired from DSİ (1978). The first transect (I–I') traverses the TCP in a NW-SE direction, and second transect (II–II') traverses the plain in a SW-NE direction. Quaternary-Recent sediments demonstrate substantial variation in thickness (30 m in the NW and ~500 m in the SE corner) and are primarily composed of recent deposits from the Deliçay, Tarsus, and Seyhan rivers (Göney, 1976; DSİ, 1978). These deposits exhibit a

high degree of heterogeneity, characterized by laterally discontinuous layers comprising clay, silt, sand, and gravel, with an increasing percentage of clay towards the north (Kurt, 2010).

2.2. Geomorphology and Surface Hydrology

TCP extends along the 21-km stretch of the Mediterranean Sea coast, where elevations range from 0 to 107 m amsl with a mean elevation of 8.4 m amsl. In the NW corner of TCP, topographic elevations abruptly rise from 20 to 107 m. The mean slope in the low-lying deltaic plain is only 0.4° (degree), where coastal sand dune areas characteristically display a rolling topography. In the eastern part, elevations behind the coastal sand dune field are generally less than 2 m and becomes waterlogged for extended periods after heavy rains and floods. In the area, coastal erosion is a pressing issue, not only threatening the agricultural fields and groundwater resources (due to seawater encroachment), but also the Kazanlı beach, which is a very important nesting site in the Mediterranean for two globally threatened marine turtle species (*Chelonia mydas* and *Caretta caretta*). For instance, a remote sensing study conducted at the southeastern coastal part of TCP revealed a coastline erosion rate of -19.68 m/year over a 30-year period (Kuleli, 2010).

There are two perennial rivers in the area, namely Deliçay and Tarsus, which delineate the western and eastern boundaries of TCP, respectively. The main channels of these rivers were digitized as both polygons and polylines using the GIS software. In addition to that, artificial hydrologic features found within the study area mask, such as irrigation and drainage canals were digitized as polylines. At present, there are no permanent lakes, lagoons, wetlands or springs found within the limits of TCP. However, as previously mentioned, the eastern part was occupied up until 1968 by a marshland called Aynaz (remnant of the ancient lagoon named Rhegma). The government has devoted extensive drainage efforts to reclaim the marshland area (Yilmaz, 1998), which started in 1958 and ended in early 1969, after complete dewatering of the marshland area. The extents of the lagoon and marshland area obtained from a map drawn by Ramsay (1903) were digitized as polygons using the GIS software. In TCP, a total of 339 artificial water bodies (e.g., small ponds) were identified from the satellite imagery. These are mostly formed because of sediment and soil extraction around the agricultural fields. The excavated earth material is used

to level the uneven ground surface near greenhouses or in places, to raise the base level of the property to protect it from flooding (Güler et al., 2012). All the artificial water bodies identified from the high-resolution satellite imagery were digitized using the GIS software. It is important to note that these features are generally transient and subject to frequent modification (Özdemir, 2024). The geomorphologic and hydrologic features previously discussed are illustrated in Figure 7.

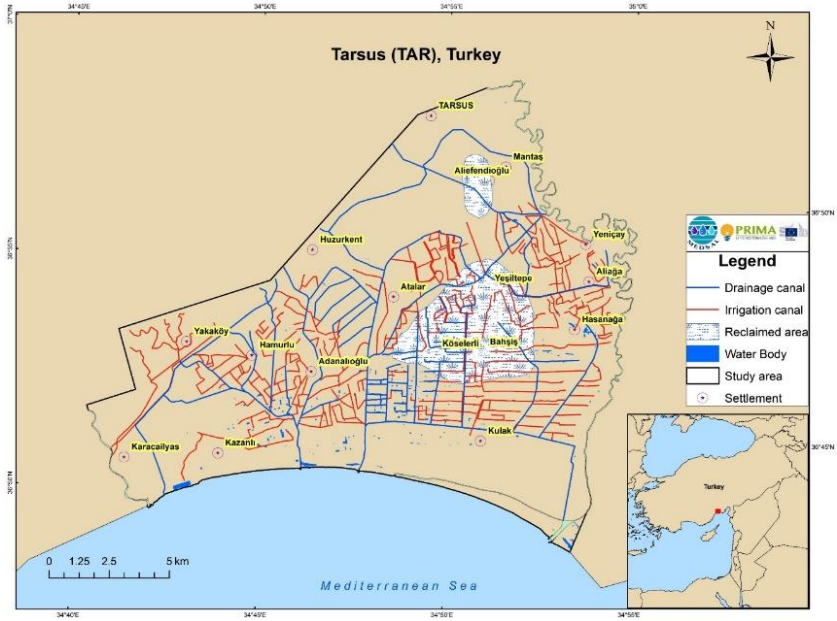

Figure 7: Geomorphologic and Hydrologic Features of Tarsus Coastal Plain

2.3. Soil Resources

Soil and sediment samples collected throughout TCP have been extensively studied to characterize their trace element and mineralogical compositions, textural and hydrological properties, as well as nutrient (e.g., nitrate and nitrite) levels (Kurt et al., 2008a; 2008b; 2009a; 2009b, 2009c; 2010a; 2010b; 2011a; 2014). Kurt et al. (2009a) employed a five-step sequential extraction procedure to determine the trace element pollution in topsoil samples (n = 208) collected from TCP. The high concentrations of Cr, Cu, Mn, Pb and Zn were found around Kazanlı, whereas Pb was particularly high along the Mersin-Tarsus highway (state road D-400) due to heavy vehicle

traffic (Kurt et al., 2009a). The geoaccumulation index calculations also indicated that the concentrations of trace elements (e.g., Cr, Cu, Cd, Co, Ni, Pb, V, and Zn) in soil samples were rather high around both industrial and agricultural areas (Kurt et al., 2010a; 2011a), some of which greatly exceeded soil quality standards of the European Union.

The mineralogical, geochemical, and textural properties of the delta deposits in TCP have also been studied in detail using both depth-specific (in 40 sites from three depth intervals) and spatially distributed soil samples (collected from additional 208 sites) (Kurt et al., 2009c; 2010b; 2014). The area stretching along the Mediterranean Sea coast has significantly high sand fraction due to presence of the coastal sand dunes. However, the proportion of sand show a gradual decrease towards north, where silt and clay generally dominate the soil texture (Kurt et al., 2009c; 2010b; 2014). XRD results indicate the presence of calcite, quartz, feldspar, mica, dolomite, amphibole, and clays in the soils, of which calcite, quartz, feldspar, and clays collectively account for 80% of the total volume (Kurt et al., 2009c; 2010b; 2014). The predominant clay minerals in soil consist of smectite, illite, chlorite, kaolinite, and serpentine, with smectite being most abundant (Kurt et al. 2014). Kurt et al. (2014) also noted that Quaternary-Recent unconsolidated deposits vary in texture in the north-south direction, whereas differences in geochemical and mineralogical properties only occur in east-west direction.

Kurt et al. (2008a) have collected soil/sediment samples (n = 208) from TCP to determine their nitrate and nitrite levels. The results of this study have revealed similar spatial distributions for nitrate and nitrite over the area, and both nutrients display elevated concentrations around greenhouses (e.g., in Kazanlı), whereas lower concentrations are mostly confined to areas around citrus orchards or forests. In a subsequent publication, Kurt et al. (2009b) also compared the spatial distribution of nitrate and nitrite in soil and groundwater samples from the site using GIS techniques, which revealed a weak correlation between the two. According to results obtained from that study, in soil samples, concentrations of nitrate were between 10-1,478 mg/L and nitrite between 0.0-9.6 mg/L. In groundwater samples, however, nitrate concentrations were between 0-1,834 mg/L; whereas nitrite concentrations ranged between 0.0-10.3 mg/L (Kurt et al., 2009b; Kurt et al., 2012).

Soil salinity is also a major problem in the area, especially in places where water levels are close to surface (Scheumann, 1997). The salt accumulation in the shallow soil depths (e.g., plant root zone) is mostly due to high evaporation and sea-spray. Autumn rainfall leaches the accumulated salts, and increases the salt concentration in the groundwater (Scheumann, 1997). In spring, the saline groundwater is drained through the drainage system, resulting in partial improvement in the groundwater quality (Scheumann, 1997).

Four major types of soils occur on the coastal plains of TCP, including vertisols (80.9%), arenosols (14.7%), calcisols (2.6%), and leptosols (1.8%) (GDRS, 2001; Soil Atlas of Europe, 2005) (see Figure 8). Vertisols are the most common soil type in the area and usually consists of abundant silty-clay and calcareous components derived from Tertiary formations. Vertisols typically display shrinking and swelling behavior upon drying and wetting and they form wide cracks in the dry season due to abundance of swelling smectite clays. In the area, arenosols typically occur along the Mediterranean coastline, which increase in width from west to east. The arenosols in the coastal stretch are represented by well-sorted and loose sand dune deposits, which are easily erodible due to poor development of vegetation cover. Calcisols usually develops on marls and older alluvium deposits with significant accumulation of secondary $CaCO_3$, developed under dry climate conditions. The precipitation of $CaCO_3$ occur as nodules or even in continuous layers of soft or hard caliche (Eren, 2011; Eren et al., 2018). Leptosols comprise commonly thin and rocky soils found in the northern part, along the hilly terrain. Because of their shallow depth and limited pedogenic development, they usually do not show structure.

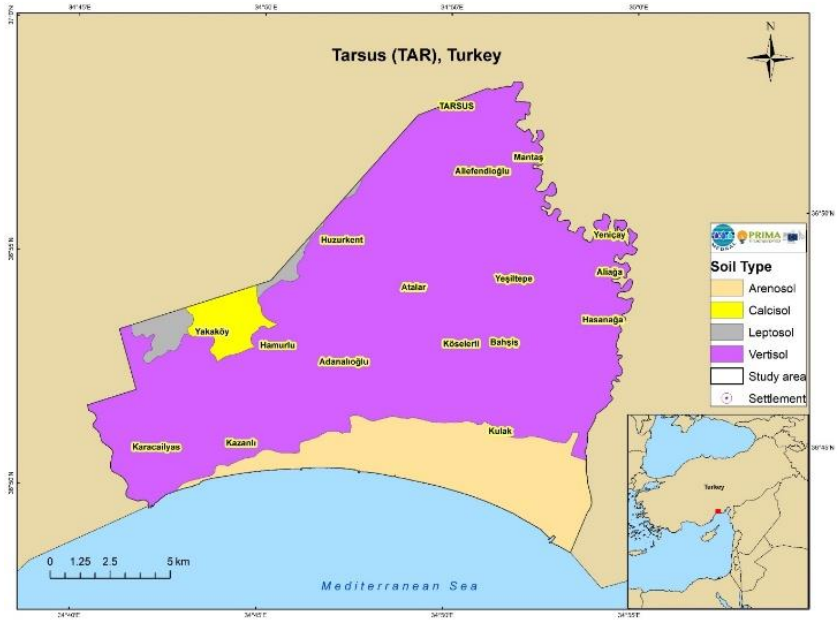

Figure 8: Soil Map of Tarsus Coastal Plain (modified from GDRS, 2001; Soil Atlas of Europe, 2005)

3. HYDROGEOLOGY

3.1. Hydrogeological Overview and Hydro-Lithology

The aquifer system in TCP comprises multiple layers that have developed in Quaternary-Recent unconsolidated basin-fill deposits. The thickness of these layers varies significantly, ranging from approximately 30 m in the NW to around 500 m in the SE corner of the plain. The aquifers in TCP are predominantly confined or semi-confined in nature due to the presence of substantial clay-silt layers or lenses (Güler et al., 2012). The available well log records (unpublished) obtained from DSİ and KHGM, show that laterally discontinuous clay layers/lenses can be found throughout the entire depth of the aquifer. The thickness of individual clay layers/lenses range from 1 to 120 m (average is 13.9 m) and increase towards east. The highlands bounding the coastal plain at its northern side, however, is mostly composed of fractured and/or karstic rock aquifers/aquitards formed in Tertiary sedimentary rocks and Paleozoic-Mesozoic Basement rocks. These older rocks have undergone extensive burial beneath the Quaternary-Recent unconsolidated basin-fill deposits.

In TCP, recharge to the aquifer system occurs through a variety of mechanisms, both natural and artificial in nature. These mechanisms include: (i) infiltration resulting from precipitation, agricultural irrigation, and wastewater discharges; (ii) leakages from streambeds or irrigation and drainage canal systems; (iii) mountain front recharge; and (iv) inflow from the Mediterranean Sea (i.e., seawater intrusion). The discharge from the aquifer system is facilitated by a variety of mechanisms, including (i) evapotranspiration from the shallow groundwater; (ii) subsurface outflow to the Mediterranean Sea; (iii) river runoff; (iv) water abstraction from groundwater wells; and (v) discharge from the drainage canal system to the Mediterranean Sea. The groundwater from the Quaternary-Recent fluvio-deltaic coastal aquifer is utilized extensively for agricultural, industrial, and domestic purposes.

Quaternary-Recent unconsolidated deposits in the northern parts of the TCP demonstrate comparatively low values of hydraulic conductivity, attributable to a gradual increase in the clay proportion towards the north (Kurt, 2010; Güler et al., 2012; 2013). The general direction of groundwater flow is towards the Mediterranean Sea, along which several depression cones are formed due to heavy groundwater pumping (see Güler et al., 2012). The natural flow system was modified by the large-scale irrigation-drainage and dewatering projects that were started in late 1950s. Increase in agricultural activities in 1970s and subsequent development of groundwater resources through shallow and deep wells resulted in decline in groundwater levels and reversal of the flow paths, especially near the coastline. Nevertheless, basin-wide ramifications of these substantial hydrological alterations and present water management methods have been scarcely explored, with the exception of Güler et al. (2012). Furthermore, the discharge of wastewater from a variety of sources, in conjunction with the excessive use of fertilizers, exerts significant pressure on surface water and groundwater resources. Güler et al. (2012) found that the in-situ saturated hydraulic conductivities (K_{fs}) of surficial soils/sediments at a depth of ~35 cm ranged from 2.94×10^{-6} to 9.37×10^{-2} cm/s, with an average of 3.62×10^{-3} cm/s. An evident, albeit gradual, increase in K_{fs} values has been observed from north to south, which corresponds to a decrease in the proportion of clay- and silt-sized fraction in surficial soils/sediments (see Güler et al., 2012).

The geologic and lithostratigraphic units (see Table 2) of the Reference Geological Map (RGM) of TCP were further classified considering their intrinsic hydrogeological properties. The classification process was achieved through the grouping of lithologies exhibiting genetic affinities and demonstrating internal textural and compositional similarities, with the objective of producing a homogenous entity in terms of groundwater flow and storage behavior. To this end, the classification scheme proposed by Struckmeier and Margat (1995) was utilized, which resulted in four "hydrolithological units" for TCP. Using this scheme, the hydrolithological units given in Table 3 were identified and presented in Figure 9.

Table 3: Hydrolithological Units of the Tarsus Coastal Plain

Formation	**HL_class** [1]
Kuzgun Formation	Minor aquifers with local and limited groundwater resources
Handere Formation	Minor aquifers with local and limited groundwater resources
Caliche	Strata with essentially no groundwater resources
Unconsolidated fluvio-deltaic sediments	Extensive but only moderately productive aquifers
Coastal sand dune deposits	Local or discontinuous productive aquifers

[1] HL_class: Hydrolithological Classification, according to Struckmeier and Margat (1995) Classification.

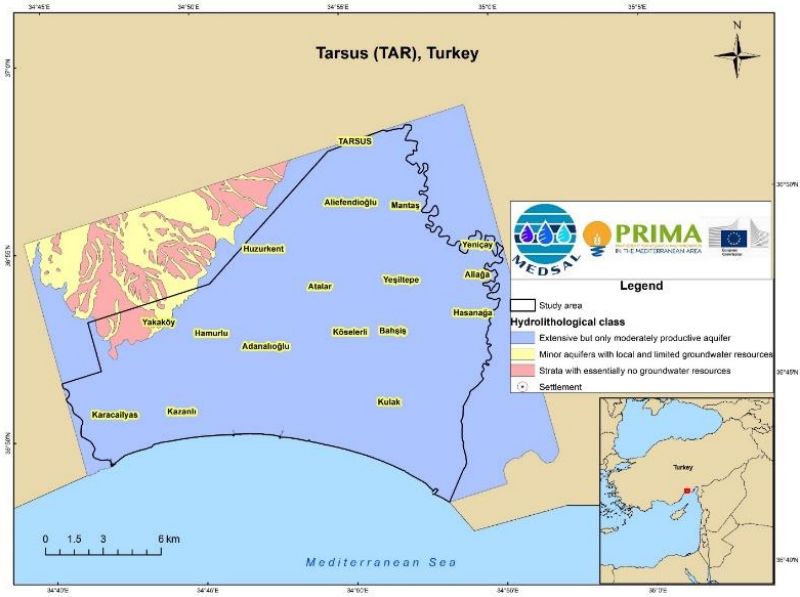

Figure 9: Hydrolithological Map of the Tarsus Coastal Plain According to Struckmeier and Margat (1995) Classification

3.2. Wells

3.2.1. Census of Wells

Based on the previously compiled groundwater well database of TCP, 310 wells have been inventoried and documented in earlier reports and publications (see Figure 10).

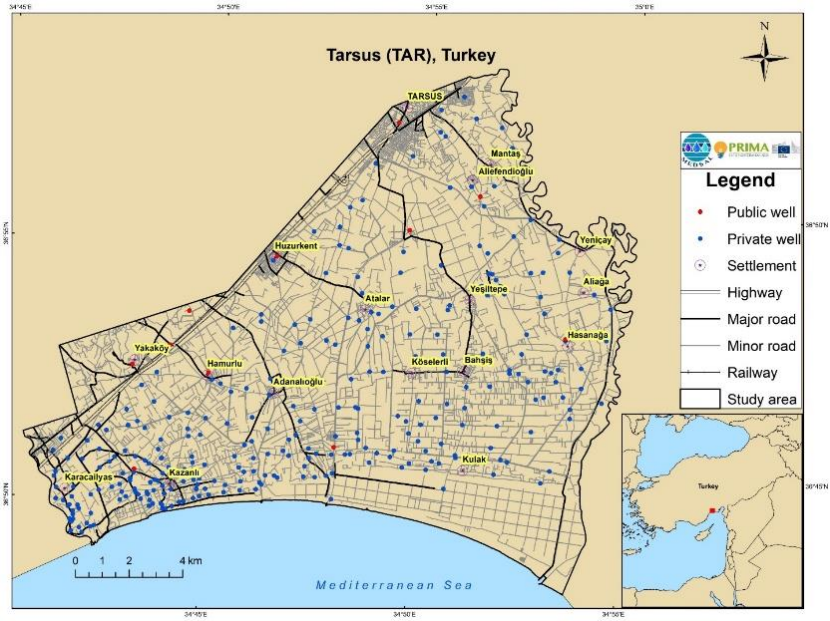

Figure 10: Map Showing the Distribution of Wells (Private and Public) in Tarsus Coastal Plain

According to the most recent PDEU (2018) report, the number of registered wells (actively operating) available in TCP is 1,315, where the actual number is possibly much higher. For instance, in a State Planning Organization (DPT) project conducted by Alpaslan et al. (2009) and a Ph.D. study completed during that project by Kurt (2010) report on groundwater physicochemical data for 193 wells and groundwater level data for 87 wells. In these studies, the wells used for the groundwater sampling and analysis could not be employed for groundwater level measurements due to well owner's objection or lack of consent to disassemble well-equipment on the wellhead, which would have interfered with their daily (irrigation) operations. Therefore, in these studies, the wells (n = 87) used for the water level measurements were selected from

mostly abandoned wells, without installed well equipment. The measured total depths of these (abandoned) wells range from 1.65 to 155 m, where the groundwater levels were between -6.88 and 11.25 m amsl during the August 2008 (dry season) survey (Alpaslan et al., 2009; Kurt, 2010; Güler et al., 2012). There are also a limited number (n = 30) of wells throughout the site with only borehole log information, of which depths range from 54 to 283 m.

In TCP, well head elevations (approximate ground elevation in meters above mean sea level) at well coordinates range from 0.43 to 40 m, with calculated distances from the sea are between 100 to 15,479 m. All the wells recorded in the database are drilled wells, of which 11 can be classified as public and 299 as private. Of the 310 wells in the compiled database, 280 used for agricultural irrigation, 14 for domestic supply, and 16 for industrial purposes. Due to restrictions in access to wells found within the premises of the industrial facilities, their exact numbers are not known, and they are underrepresented in the database. The records of the registered wells obtained from the State Hydraulic Works (DSİ) also include some limited data (unpublished) for 125 wells, most of which are probably included in the database created for this project, however their precise number is not known due to some problem with their coordinate values.

3.2.2. Well Tests (step drawdown)

In TCP, a limited number of step drawdown tests (only in four wells) were performed in the past, nonetheless they only report pumping rates (L/s) and corresponding drawdown (m) values, which is not adequate to evaluate hydraulic properties (e.g., transmissivity (T), hydraulic conductivity (K) and storage coefficient (S)) of the aquifer system. The average specific capacity (i.e., specific discharge) values in these four wells range from 0.61 to 6.82 L/s/m. In additional 25 wells, constant-rate pumping test (pumping durations ranging from 2.5 to 72 hours) results were available, but these also only reported pumping rates (L/s) and corresponding drawdown (m) values for individual wells. Based on this limited information, the specific capacity (i.e., specific discharge) values in the Quaternary-Recent unconsolidated basin-fill deposits range from 0.03 to 51.95 L/s/m (mean value is 5.65 L/s/m), where higher values occur near Kazanlı and Kulak settlements (Güler et al., 2013). The fractured and/or karstic rock aquifers/aquitards formed in older (pre-

Quaternary) formations outcropping in the highlands bounding the coastal plain, however, have generally low yields, where reported specific capacity values reach up to only 0.65 L/s/m (Hatipoglu et al., 2009). As reported by Demirel (2004), transmissivity (T) values of the alluvial deposits varies between 3.5×10^{-2} and 3.5×10^{-4} m^2/s near the Kazanlı region.

3.3. Piezometric Data

Review of the existing literature have revealed that only two (basin-wide) synoptic groundwater levels surveys have been conducted at TCP; the first one is before 1978 (named pre-1978) by DSİ (1978) and the second one in August 2008 by Güler et al. (2012) (see Figure 11).

The historical (pre-1978) water table elevation contours (in meters) shown (red dashed lines) in Figure 11 indicate that most likely the coastal plain aquifer was under quasi-steady-state conditions and the natural groundwater flow occurred from NW to SE direction, towards the Mediterranean Sea. As evident from the water table elevation contours of the pre-1978 and 2008 surveys (Figure 11), hydraulic gradients are higher at the NW part of the plain, which may be explained by the lower hydraulic conductivities of the aquifer material due to increase in clay content towards north (see Kurt, 2010) and the presence of NE-SW trending faults running parallel to the sinistral Kozan Fault Zone (see Figure 4). Nevertheless, as indicated by the directions of groundwater flow in 2008, the aquifer system is fairly disturbed by heavy groundwater pumping, which resulted in reversal of flow directions and formation of several large cones of depression (see Figure 11). A study of hydraulic head measurements conducted in the groundwater wells in 2008 revealed that the confining layers exhibited slight permeability, thereby permitting the gradual upward seepage of groundwater (Güler et al., 2012). Although such occurrences are not commonplace in the present day, earlier studies (e.g., DSİ, 1978) have documented the presence of free-flowing artesian wells in the southeastern portion of the aquifer (in the vicinity of Kulak, Bahşiş, and Köselerli settlements). This portion of the aquifer was once occupied by the Aynaz marshland (relict of the ancient Rhegma lagoon), which completely dewatered in 1968 after great efforts.

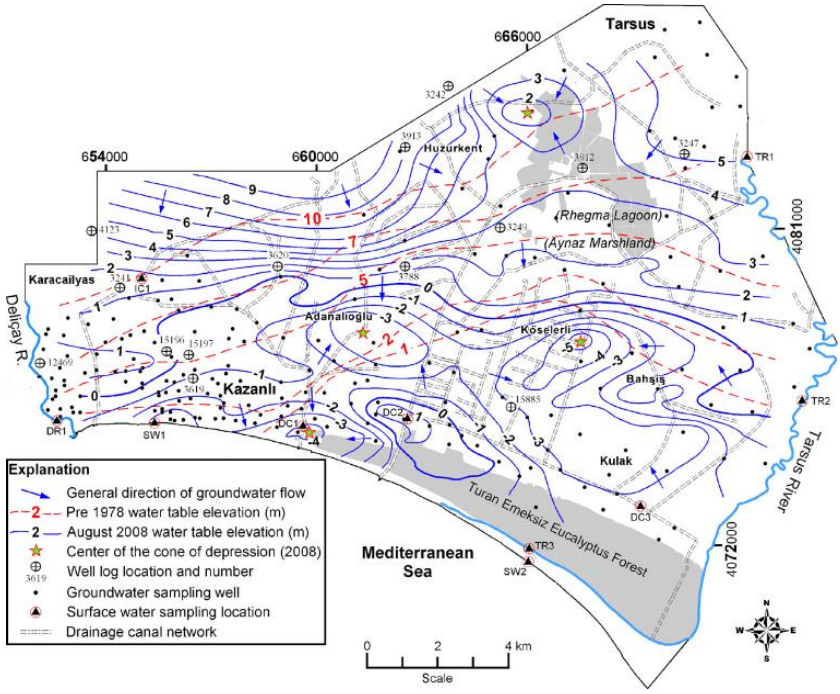

Figure 11: Map Showing the Water Table Elevations (Pre-1978 and 2008) and Groundwater Flow Directions in Tarsus Coastal Plain (after Güler et al., 2012)

A comparison of pre-1978 and 2008 groundwater levels, as illustrated in Figure 11, elucidates the combined impact of substantial groundwater extraction and extensive drainage projects on the hydrology of the region. The anthropogenic impact on the hydrological system of the region is evident in the substantial alterations to groundwater levels and flow directions. These alterations have led to a decline in groundwater levels (-2 to -5 m amsl), and a deterioration in water quality in the coastal areas, reaching levels that are considered unacceptable. According to Güler et al. (2012), increases in both groundwater electrical conductivity (EC) and concentrations of Na^+, Cl^-, B, and Br indicate the occurrence of active seawater intrusion along the coastal zone, mainly in the vicinity of Kazanlı and Kulak (see Figure 11). In the southern part of the transect extending from Kazanlı to Bahşiş, a superficial aquifer has been identified, situated just below the ground surface (<1 m) (Güler et al., 2012). During periods of increased precipitation levels, particularly during winter, a considerable portion of land experiences inundation (Güler et al., 2012).

4. HYDROGEOCHEMICAL DATA

4.1. Previous Surveys on Hydrogeochemistry

Surface and groundwater resources of TCP have been subject to investigations (mostly short-term synoptic sampling) conducted by various researchers. Despite their importance, surface water resources of the area received limited attention in the literature, but they were shown to be polluted by waste discharges from domestic, industrial and agricultural sources (see Kumbur and Vural, 1989; Özer, 2001; Ergene et al., 2007; Kumbur et al., 2008).

Kumbur and Vural (1989) studied the water quality along the Tarsus (Berdan) River by collecting bi-monthly water samples from the selected sampling points during January to May 1989. In this study, surface water samples were analyzed for a variety of parameters, including pH, biochemical oxygen demand (BOD), dissolved oxygen (DO), total solids content, detergents, and various trace elements (e.g., Bi, Ca, Cd, Co, Cr, Cu, Fe, K, Mg, Mn, Ni, Pb, and Zn). Subsequently, a comparison was made between the obtained findings and the established standards for irrigation water quality. The Tarsus River was found to contain elevated levels of certain parameters (e.g., BOD and anionic detergents) and various trace elements (e.g., Cd, Pb, Mn, Ni, Fe, and Zn in excess of the permissible standard levels (Kumbur and Vural, 1989). These elevated levels can be attributed to the discharge of domestic and industrial wastewater. The study by Özer (2001) was a follow up study conducted previously by Kumbur and Vural (1989). Özer (2001) also studied the water quality along the Tarsus River by collecting water samples from eight sampling points during September 1997 and December 2000. In this study, temperature, pH, DO, suspended solids, nitrate, hardness, phosphate, detergents, sulfate, major ions (i.e., Ca, Mg, Na, and K), and trace elements (i.e., Al, B, Cd, Cr, Cu, Fe, Mn, Ni, Pb, and Zn,) were analyzed and comparisons made with the water quality criteria and irrigation water standards. As stated by Özer (2001), the primary sources of contamination in the river are the release of inadequately treated or untreated industrial and residential effluents, as well as the outflow of regions with high pesticide and fertilizer application through the irrigation-drainage canal system constructed by the DSİ. In a later study by Ergene et al. (2007), water samples collected from five locations along the Tarsus River were evaluated for their genotoxicity using an in vivo piscine micronucleus (MN) test. They also analyzed the water samples

for several trace elements and found that the Tarsus River is contaminated with genotoxic pollutants, which are linked to waste discharged into the river. Kumbur et al. (2008) have investigated water quality of irrigation canals, streams and wells used for irrigation supply in four settlements located along the Mediterranean Sea coastline. In the study by Kumbur et al. (2008), the values of the analyzed parameters (i.e., temperature, electrical conductivity, pH, Cr, Cu, Mn, Mo, and Ni) were presented as ranges for each settlement, where water quality were found to be impacted by agricultural activities.

Many hydrogeochemical studies were conducted since 2004 in TCP and in the surrounding region, which greatly differ in scope and sampling density, as well as in areal coverage (e.g., Demirel, 2004; Hatipoğlu, 2004; Demirel and Külege, 2005; Hatipoğlu and Bayarı, 2005; Hatipoglu et al., 2009; Alpaslan et al., 2009; Kurt, 2010; Akbulut et al., 2011; Güler et al., 2012; Hatipoglu-Bagci and Bayari, 2020). Demirel (2004) was first to report groundwater chemistry of the four wells operated by a factory (Soda-chromium industry) located in the Kazanlı area, where seawater intrusion occurred due to heavy pumping of the aquifer. In the premises of the factory, eight wells were located with a total pumping rate of 1,080 L/s. Four out of eight wells were abandoned due to high concentrations of Cl^- (>3000 mg/L) in groundwater. In 2001, new set of wells were drilled >1,000 m away from the coast and old well field was abandoned. The wells not affected by the seawater intrusion had an Mg-Ca-HCO_3 water type. A study conducted by Hatipoğlu (2004) investigated hydrogeochemistry of an area covering 810 km^2, which included 19 groundwater samples from TCP. The hydrogeochemical facies of the samples were changed along the flow path from Ca-HCO_3 to Mg-HCO_3, Na-HCO_3, and Na-Cl near the coastline (Hatipoğlu and Bayarı, 2005; Hatipoglu et al., 2009). Demirel and Külege (2005) investigated hydrogeochemistry of an area covering 400 km^2, which included 13 groundwater samples from TCP. The hydrogeochemical facies of the samples were changed along the flow path from Ca-Mg-HCO_3 to Mg-Ca-HCO_3, Mg-Na-Ca-HCO_3-Cl, Na-Mg-Ca-HCO_3-Cl, and Na-HCO_3-Cl (near the coastline), which were attributed to evaporite dissolution (e.g., gypsum) in Handere formation and seawater intrusion (Demirel and Külege, 2005).

The most comprehensive hydrogeologic/hydrogeochemical study conducted in TCP so far was a project supported by the DPT (State Planning Organization of Türkiye), aiming the assessment of the quality of water and soil

resources in the area (Alpaslan et al., 2009). The results of this project were utilized in a dissertation by Kurt (2010) and in the subsequent publications (Korkut, 2009; Korkut et al., 2011; Akbulut et al., 2011; Kurt et al., 2009b; 2011b; 2012; Güler et al., 2012). As noted by Güler et al. (2012), the source of groundwater salinization is not solely caused by the seawater intrusion, but other processes (i.e., water-rock interaction, ion exchange, agricultural activities (nitrate pollution), and dissolution of evaporitic series (e.g., gypsum, anhydrite, halite, etc.) formed during the Messinian Salinity Crisis) have also major role in groundwater salinization in the area. Previous hydrogeochemical studies (e.g., Alpaslan et al., 2009; Korkut, 2009; Korkut et al., 2011; Kurt, 2010; Kurt et al., 2009b; 2011b; 2012; Güler et al. 2012; Hatipoglu-Bagci and Bayari, 2020) have found that the concentrations of boron, iron, zinc, chromium, sodium, chloride, sulfate, nitrate, and nitrite in groundwater samples taken from the area between Kazanlı and Tarsus exceed drinking water standards. Akbulut et al. (2011) evaluated the hydrochemistry of the aquifer using Stuyfzand hydrogeochemical classification system. Akbulut et al. (2011) found that the $CaHCO_3$+ water type generally dominates the coastal aquifer, while the $MgHCO_3$+ water type typically occurs in the western part of the aquifer. In consideration of the transition from $CaHCO_3$+ to $NaHCO_3$+ water type along the groundwater flow direction, Akbulut et al. (2011) asserted that cation exchange processes influence the groundwater composition in the SW part of the aquifer system. The groundwater samples collected in the NE-SW direction are classified as $CaHCO_3\phi$ water type, suggesting that the cation exchange process is nearly complete and in its last phase (Akbulut et al., 2011).

4.2. Overall Hydrogeochemical Status

Groundwater resources of TCP have been the subject of a number of hydrogeochemical investigations (mostly short-term synoptic sampling) since 2004, which greatly differ in scope and sampling density, as well as in areal coverage (Demirel, 2004; Hatipoğlu, 2004; Demirel and Külege, 2005; Hatipoğlu and Bayarı, 2005; Hatipoglu et al., 2009; Alpaslan et al., 2009; Güler et al., 2012; Hatipoglu-Bagci and Bayari, 2020). Except for Alpaslan et al. (2009) and Güler et al. (2012), the number of groundwater samples collected by other studies (within the limits of TCP) ranged from 4 to 22, which is obviously not adequate for a proper characterization of the groundwater-surface

water system covering an area of ~240 km^2. The most comprehensive hydrogeologic/hydrogeochemical study conducted in TCP so far was a project supported by the DPT, aiming the assessment the quality of the water and soil resources in the area (Alpaslan et al., 2009). The hydrogeochemical data from this project were evaluated in subsequent publications by Kurt (2010), Akbulut et al. (2011) and Güler et al. (2010; 2012). Güler et al. (2012) analyzed 203 water samples collected from TCP, which included groundwater (n = 193), Deliçay River (n = 1), Tarsus River (n = 3), drainage canals (n = 3), an irrigation canal (n = 1), and the Mediterranean Sea (n = 2). The parameters analyzed included physical parameters (EC, pH, DO, temperature), cations (Ca, Mg, Na, K, and Si), anions (Cl^-, SO_4^{2-}, F^-, NO_3^-, NO_2^- HCO_3^-), and trace elements (B, Ba, Br, Cr, Fe, Mn, Ni, Sr, and Zn) (Table 4). Long-term time series data required for demonstrating the temporal evolution of salinization phenomena in TCP is rather scant in the literature because of lack of continuous monitoring efforts. The paper published by Demirel (2004) is the only one reporting on the evolution of chloride (Cl^-) and electrical conductivity (EC) of groundwater in four wells operated by the Soda-chromium industry (in Kazanlı area), where seawater intrusion occurred due to heavy pumping of the aquifer. Four out of eight wells were abandoned in 2001 due to high concentrations of Cl^- (>3000 mg/L) in groundwater. The changes observed in Cl^- concentrations of the abandoned wells are presented in Figure 12.

TCP comprises two distinct hydrogeological domains that are physically connected: (1) fractured and/or karstic rock aquifers/aquitards formed in Tertiary sedimentary rocks and Paleozoic-Mesozoic basement rocks found in highland areas and (2) a multilayer aquifer system developed in the Quaternary-Recent unconsolidated basin-fill deposits found in coastal plain. The multi-layer aquifer formed in the coastal plain is more productive than the fractured/karstic rock aquifers/aquitards with respect to groundwater production (Demirel, 2004; Hatipoglu et al., 2009). However, many previous researchers have noted the presence of elevated salinity, especially in groundwater wells located in the vicinity of coastal settlements such as Kazanlı, Adanalıoğlu, and Kulak (Demirel, 2004; Demirel and Külege, 2005; Kumbur et al., 2008; Güler et al., 2010; 2012; Akbulut et al., 2011).

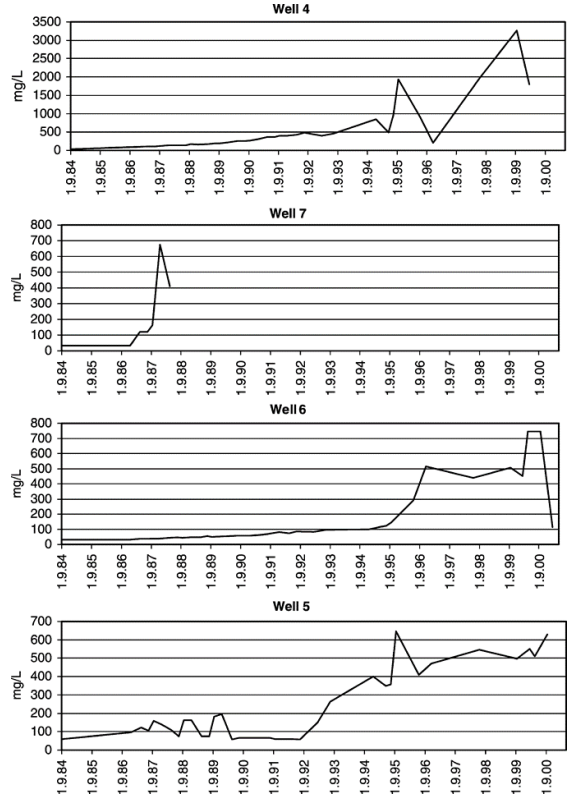

Figure 12: The Change in Chloride (Cl^-) Concentration versus Time in Four Industrial Production Wells Located in Kazanlı (after Demirel, 2004)

Table 4: Statistics of the Parameters of the Surface Water and Groundwater Samples from the Tarsus Coastal Plain (after Güler et al., 2012).

Parameter	Surface water										Groundwater (n = 193)		
	Mediterranean Sea		Deliçay River	Tarsus River			Irrigation Canal	Drainage Canal					
	S1	S2	DR	T1	T2	T3	I	D1	D2	D3	Minimum	Maximum	Median
EC (µS/cm)[1]	57100	58400	657.5	602.0	577.0	705.0	329.0	2270.0	2500.0	1229.0	431.0	2991.0	906
TDS (mg/L)[2]	37246	37794	407.4	442.5	417.4	491.2	266.8	1441.4	1556.4	895.4	336.1	2307.4	704.9
pH	7.8	8.2	8.3	7.9	7.8	7.7	7.8	7.5	7.7	8.3	7.0	8.7	7.5
DO (mg/L)[3]	4.4	4.6	4.0	4.3	3.9	2.2	4.6	2.6	4.0	6.7	0.4	5.2	1.7
Ca^{2+} (mg/L)	785	808	54.2	59.4	56.2	62.3	51.6	89.2	80.9	67.0	8.4	223.3	79.5
Mg^{2+} (mg/L)	1488	1576	27.3	22.7	17.9	23.2	9.4	48.9	58.7	39.4	4.6	176.1	41.8
Na^+ (mg/L)	10200	10190	32.5	44.0	39.1	69.9	11.8	360.9	389.2	157.5	7.8	410.6	53.0
K^+ (mg/L)	449	529	2.1	2.5	3.0	3.6	1.2	18.2	13.9	4.9	0.7	99.1	2.2
Si (mg/L)	3.3	4.1	1.9	4.5	4.6	4.7	7.2	6.7	8.9	6.5	3.9	27.9	15.2
Cl^- (mg/L)	21150	21100	28.3	30.2	51.0	26.8	11.1	560.0	444.8	165.3	6.1	433.0	67.8
SO_4^{2-} (mg/L)	2900	3312	32.5	57.0	53.0	61.0	13.0	130.0	118.0	151.8	1.0	741.0	73.6
HCO_3^- (mg/L)	89.7	86.4	269.6	184.3	161.6	227.0	137.8	213.7	404.1	224.2	140.7	667.8	297.2
F^- (mg/L)	1.9	2.9	0.7	0.2	0.2	0.2	0.2	1.6	0.3	0.4	0.1	1.3	0.34
NO_3^- (mg/L)	5.8	9.3	4.9	5.3	7.5	6.2	2.7	3.5	3.5	0.9	0.4	201.1	11.1
NO_2^- (mg/L)	0.4	0.1	0.6	0.2	0.3	0.3	0.1	0.3	0.1	0.0	0.0	2.4	0.02
B (µg/L)	11780	3387	–	68.8	94.4	106.3	287.8	288.2	987.7	256.4	42.9	1920.0	150.0
Ba (µg/L)	97.5	145.1	30.6	49.0	51.4	43.6	22.2	69.9	39.1	26.8	10.2	249.0	58.2
Br (µg/L)	73960	88330	–	80.1	78.9	140.0	41.2	1945.0	2576.0	481.6	21.9	1532.0	190.3
Cr (µg/L)	102.6	520.9	2.3	1.7	1.3	1.3	0.5	1.2	0.8	1.2	0.1	62.8	3.6
Fe (µg/L)	1058	3710	183.4	476.8	593.1	277.3	78.9	307.2	168.4	252.1	0.1	2052.0	63.9
Mn (µg/L)	915.3	257.5	21.4	43.1	78.9	24.2	7.7	62.6	23.9	24.9	0.1	259.2	2.1
Ni (µg/L)	705.7	449.4	9.4	7.0	7.0	6.6	4.7	5.9	5.2	6.7	1.5	43.7	3.9
Sr (µg/L)	10200	9762	392.4	433.8	404.4	419.2	244.3	952.7	688.5	564.7	116.0	6001.0	839.1
Zn (µg/L)	355.5	4703	11.8	10.6	11.7	10.3	61.4	10.2	3.9	5.8	2.5	4593.0	79.8

[1] Electrical conductivity.
[2] Total dissolved solids.
[3] Dissolved oxygen.

Güler et al. (2012) identified a statistically significant association between the classical hydrogeochemical variables (e.g., Ca^{2+}, Mg^{2+}, SO_4^{2-}, HCO_3^-, Sr, and Ni) resulting from natural water-rock interaction (WRI) processes and nitrate (NO_3^-) and interpreted this as co-occurrence of both natural weathering and anthropogenic pollution (non-point) processes in the recharge areas. According to Güler et al. (2012), this association is attributable to the types of chemical fertilizers that are currently being utilized in the region. These fertilizers, which include ammonium sulfate, calcium nitrate, magnesium nitrate, and, among others, also contain the major ions (Ca^{2+}, Mg^{2+}, SO_4^{2-}, etc.) that typically result from the natural WRI processes. The findings indicate a significant correlation between nitrate and major ions (Ca^{2+} ($r = 0.52$), Mg^{2+} ($r = 0.42$), and SO_4^{2-} ($r = 0.23$)), thereby substantiating the association between geogenic and anthropogenic factors (Güler et al., 2012). This finding also suggests a high degree of vulnerability to agricultural contaminants in the area. The predominance of Ca-Mg-HCO_3 water type in the vicinity of the northern boundary of the site, in conjunction with the supersaturation of calcite and dolomite, suggests that the flow through the fracture network has been sufficiently slow to attain equilibrium conditions prior to the influx of recharge water into the basin (Güler et al., 2012). In addition to seawater intrusion, an increase in SO_4^{2-} concentrations is of local significance in TCP, largely confined to the area between Huzurkent and Adanalıoğlu settlements. This area is distinguished by underlying Miocene-Pliocene formations, which are recognized for their tendency to host substantial gypsum deposits. The study by Güler et al. (2012) revealed that groundwater samples exhibited undersaturation with respect to gypsum (SI<-0.68), thereby indicating that gypsum dissolution is favored within the aquifer system. The aquifer contains a high proportion of smectitic clay (20–67% in the 0–150-cm of topsoil; see Kurt, 2010). This observation suggests the potential for a substantial contribution from ion exchange reactions, wherein Ca^{2+} and Mg^{2+} replace Na^+ within clay minerals (Güler et al., 2012). This also elucidates the observed decrease in Ca^{2+} and Mg^{2+} concentrations and the concurrent increase in Na^+ levels along the ground water flow path (Güler et al., 2012). In TCP, the highest concentrations of Na^+, Cl^-, B, and Br are typically observed in coastal regions that have experienced seawater intrusion. Furthermore, elevated concentrations of Ca^{2+}, Na^+, K^+, F^-, SO_4^{2-}, B, and Sr have been predominantly observed in the

region delineated by the Huzurkent and Adanalıoğlu settlements, where evaporite dissolution (i.e., gypsum) has been identified as the key process influencing the groundwater chemistry (Güler et al., 2012). In the region, the observed increase in the salt content of groundwater samples (i.e., aquifer salinization) can be attributed to various mechanisms, including the intrusion of seawater, the dissolution of evaporitic series (primarily gypsum) from the Handere formation, and ion exchange process. Furthermore, the presence of trapped seawater in the sediments or sea spray has been identified as a probable contributor to the salinization of the groundwater in the region (Güler et al., 2012). In the context of TCP, anthropogenic activities have been identified as a contributing factor to the observed levels of pollution. The presence of various industries, petroleum hydrocarbon storage facilities, and significant vehicular traffic along the D-400 road have been identified as primary sources of pollution. In addition to that, a wide variety of chemicals used in agricultural activities also contributes to the trace element and salinity load of the groundwater in the area.

5. COASTAL AQUIFER CONCEPTUAL MODEL

According to the sketch cross-section by Hatipoğlu (2004) and Hatipoglu et al. (2009), the conceptual model of the groundwater flow system comprises two aquifer systems (i.e., hillside and coastal), having different recharge mechanisms. The hillside aquifer is fed mostly by the recharge from the deeply seated Permo-Carboniferous karstic aquifer and partly by local recharge. Most of the recharge to the coastal aquifer is primarily attributable the Permo-Carboniferous karstic aquifer, which is fed from the headwater regions of the central Taurus Mountains to the north (Hatipoğlu, 2004; Hatipoglu et al., 2009). The presence of waterlogged areas (depth to water <1 m) in the eastern half of the coastal plain near Yeşiltepe-Hasanağa-Kulak triangle (Figure 7) and the fault in Figure 4 indicate that this particular coastal area is probably the discharge location of the regional flow system, directed upward by faults concealed within the thick unconsolidated Quaternary deposits. The existence of these concealed faults were previously not known, and they only occur in recent publications (see Aksu et al., 2014 and references therein). These waterlogged areas were the places where the ancient Rhegma lagoon (later Aynaz marshland) once existed, which has reportedly fed by the springs of its

own and by occasional overflow from the Tarsus River (see Ramsay, 1903). As demonstrated by Güler et al. (2012), Deliçay and Tarsus rivers are in hydraulic connection with the coastal aquifer in their lower reaches. Furthermore, a considerable volume of groundwater is observed to be flowing along the 6th-century pre-diversion Tarsus River channel and within the area that formerly constituted the site of the ancient Rhegma lagoon (later Aynaz marshland). Despite their subterranean position, the presence of hydrogeochemical evidence indicates the potential for groundwater flow to occur along pathways established by pre-existing subsurface paleo-river channels and deposits that fill the ancient lagoon area (Güler et al., 2012). In TCP deep and shallow aquifers are also closely connected, especially in places where the confining layers are slightly permeable or discontinuous (Güler et al., 2012).

5.1. Groundwater Exploitation

The estimated recharge rates reported in the literature for the alluvial aquifer are highly variable and range from 74×10^6 m^3/year (Demirel, 2004) to 148×10^7 m^3/year (Hatipoglu et al., 2009), although the latter study also covers the neighboring small basins to the west. In a hydrogeologic survey conducted by DSİ (1978) in the Tarsus plain and its neighboring Efrenk plain (in the west) reports the total groundwater volume as 54.7×10^6 m^3. According to the most recent provincial environmental status report (PDEU, 2018), there are 1,315 registered wells in the Tarsus Plain, with a groundwater withdrawal rate of $\sim72\times10^6$ m^3/year. However, considering the number of unregistered wells, it can be postulated that probably 1,500 to 2,000 wells are actively being used for agricultural irrigation and industrial water supply in the area.

5.2. Groundwater Salinization

In order to assess the salinization resulting from the intrusion of seawater, Güler et al. (2012) employed a methodology based on the estimation of the seawater fraction (f_{sea}) of groundwater samples (see Appelo and Postma, 1994). This estimation was derived from the analysis of chloride (Cl^-) contents, as reported in samples collected in August 2008. The calculations were executed under the assumption that Cl^- originates exclusively from two sources: seawater intrusion and sea spray. Figure 13 illustrates the distribution of f_{sea} (%) in groundwater samples and the areas impacted by the seawater intrusion.

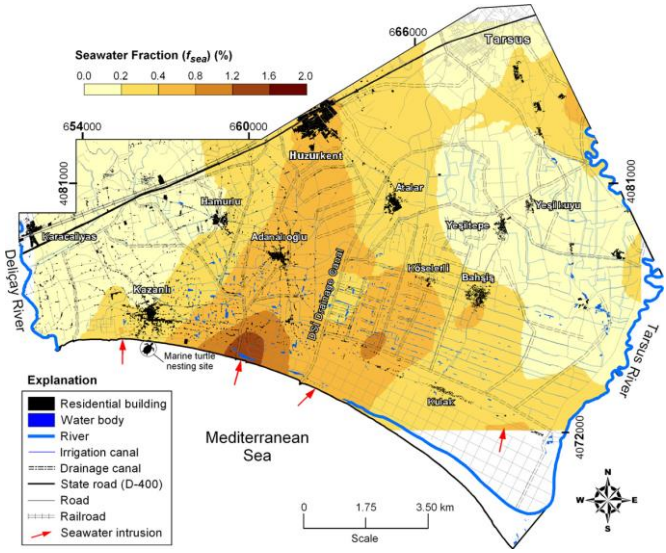

Figure 13: Spatial Distribution of Seawater Fraction (f_{sea}) in Groundwater Samples from the Tarsus Coastal Plain (after Güler et al., 2012)

In the area, seawater intrusion is evident in the southern part between Kazanlı and Kulak settlements, where the seawater fractions (f_{sea}) of the groundwater samples range from 0.09% to 1.99%, as depicted in Figure 13. In the sampling campaign conducted by Güler et al. (2012) in 2008, 7.8% of the groundwater samples were found to contain concentrations of Cl^- above 200 mg/L. In TCP, the increase in the salt content of groundwater (i.e., aquifer salinization) can be primarily attributed two mechanisms: (i) seawater intrusion and (ii) dissolution of evaporites (e.g., gypsum and halite) hosted by the Handere formation (Güler et al., 2012). Furthermore, the salinization of the groundwater in the area is likely attributable to the presence of trapped seawater in the sediments, sea-spray, and ion exchange reactions (Güler et al., 2012).

5.3. Current Management Practices

Türkiye has initiated a transformation of its legal and institutional frameworks to align with the principles of Integrated River Basin Management (IRBM). This development follows the enactment of the European Commission (EC) Water Framework Directive (WFD) (2000/60/EC), accepted in December 2000 (Delipınar and Karpuzcu, 2017). The WFD stipulates that European

Union (EU) member states and/or accession countries are obligated to formulate and execute river basin management plans. These plans are to be meticulously designed and updated to incorporate integrated and coordinated participatory processes within a collaborative framework (Delipınar and Karpuzcu, 2017). As an accession country, Türkiye, has been conducting studies on the establishment of new legal and institutional structures based on basin units. These studies constitute an integral component of the transposition process of the WFD into Turkish national legislation (Delipınar and Karpuzcu, 2017). In this context, numerous legal regulations and associated basin institutions have been implemented. The General Directorate of State Hydraulic Works (DSİ) has delineated 25 river basins in Türkiye and is executing basin studies based on this delineation. Since the second half of the 20th century, policies concerning water and natural resources in Türkiye have undergone continuous reform. In Türkiye, the administration of water and environmental affairs is divided among various ministries, a system that has been shown to result in challenges in the execution of water and environmental projects due to the overlap in the legal duties and responsibilities of these ministries.

In Türkiye, groundwater is under the jurisdiction and disposition of the State and is a public domain. Therefore, in order to benefit from this resource, there is an obligation to act according to the laws and regulations determined by the State. Prospection, use and protection of groundwater was determined by the "Law on Groundwater, No. 167" (Resmi Gazete, 1960) and the authority was given to the DSİ. The implementation of the law is carried out in accordance with the principles of the "Groundwater Regulation and the Groundwater Technical Regulations". According to the Law No. 167 (Resmi Gazete, 1960), waters below a certain depth (10 m from the surface) are considered as groundwater and for all groundwater facilities (wells, galleries, tunnels, etc.) constructed, it is obligatory to obtain the necessary permissions from the DSİ. Currently, there are no restrictions on the use of groundwater resources, as long as the required permits are obtained from the DSİ. Despite this, many unregistered groundwater wells are found throughout TCP that are not accounted for in the basin-wide water usage. Many improperly abandoned old wells are found in the study area, which threaten the quality of the groundwater resources. Such wells can provide short-circuit pathways between the surface water-shallow aquifer and the lower confined aquifers allowing

movement and mixing of fresh waters and waters containing contaminants and/or high salinity.

6. CONCLUSIONS

Coastal delta environments are multifaceted regarding geology, hydrogeology, biology, and land use activities; therefore, their sustainable use and management can be an extremely challenging task due to their multilayer structure and utterly complex, sometime mysterious nature. TCP consists of multiple aquifer systems formed within the Quaternary-Recent unconsolidated basin-fill deposits of the Tarsus coastal plain (Mersin, SE Türkiye) and covers an area of ~240 km^2. Bordered by the Deliçay River on the west, Tarsus River on the east, and Bolkar Mountain range on the north, this coastal aquifer is an important regional water resource, which is currently intensely utilized to meet ever-increasing agricultural and industrial water demands by means of a large number of shallow (<40 m) and deep (<300 m) wells drilled through the underlying basin-fill deposits, which varies in thickness from 30 m in the NW to locally ~500 m in the SE corner of the site. TCP is situated in an economically and ecologically important area providing not only space for agriculture, heavy industry, settlement, and transportation, but also offers a natural habitat for globally threatened two sea turtle species (i.e., *Caretta caretta* and *Chelonia mydas*). During the past six decades, this area has witnessed an unprecedented increase in population, industrial development, and agricultural activities, which have jointly resulted in deterioration of soil and groundwater resources. In this semi-arid coastal region, water quality issues have become a primary concern due to substantial pollution loads stemming from various point and diffuse sources, compounded by the ongoing increase in water demands. Furthermore, the environmental pollution in the area has caused worrying consequences for the local environment, which threatens the viability of the globally endangered sea turtle species nesting in the area. Therefore, sustainable use and management of groundwater resources in the region necessitates a comprehensive understanding of groundwater circulation patterns and the prevailing hydrologic and hydrogeochemical processes impacting water quality and quantity.

Despite the recent insights gained from onshore/offshore seismic reflection profiles, which have elucidated the previously uncharted structural

framework of the basin, there is a considerable amount of research yet to be conducted to comprehensively characterize this intricate aquifer system. The effects of the newly discovered geological structures (i.e., fault zones) on the groundwater movement (e.g., water logging) and ground water quality (e.g., salinization) have not been investigated by the previous studies so far. Trend of salinization is not known in the area, except for some short-term monitoring studies and synoptic groundwater sampling campaigns. The sensors that will be installed in the study area will definitely shed some light onto the long-term trends in salinization and groundwater level changes.

Apart from industrial use, availability of safe and adequate water for agricultural irrigation is crucial for this area, the residents of which are predominantly small-scale farmers historically engaged in a wide variety of fruit (mainly citrus) and vegetable cultivation. In this area, agricultural activities continues all year long due to fertile alluvial soil and mild climate that favors cropping two to three times per year. Therefore, the water and soil resources of the site are under the influence of environmental pollution and degradation resulting from intense agricultural activities, together with industrial and urban wastewater discharges. The environmental problems caused by the anthropogenic pollution from various point and diffuse sources are greatly exacerbated by the lack of basin-wide management strategies and monitoring efforts. The coastal area of TCP is also highly vulnerable to seawater intrusion due to overpumping of the aquifers and its low-lying topography. In addition, dissolution of the evaporitic series formed (in Handere formation) during the Messinian Salinity Crisis is also important in terms of salinization, in certain parts of the aquifer system. In TCP, high water levels, water logging, flooding, sand extraction, coastal erosion, and sea-level rise are also important environmental problems affecting large areas and results in degradation of water quality and economic losses in agricultural areas. Despite their importance, surface water resources of the area have received inadequate attention in the literature, however they were shown to be polluted by wastewater discharges from domestic, industrial, and agricultural sources.

In the area, protecting vulnerable ecosystems and preventing groundwater resources from further deterioration is only possible by adapting new strategies. Such strategies should include; regulation of the amount and type of agrochemicals applied to agricultural soils, monitoring both

groundwater pumping rates and wastewater disposals from industrial and domestic sources, and establishing a groundwater monitoring network for the assessment of temporal changes occurring in its quality and quantity.

REFERENCES

Akbulut, C., Güler, C., Kurt, M. A., & Alpaslan, M. (2011). *Stuyfzand hydrogeochemical classification system: Application to Kazanlı-Tarsus (Mersin) coastal aquifer*. In Türkiye Jeoloji Kurultayı (pp. 117-118). MTA, Ankara. (In Turkish).

Akgül, M. A. (2018). Sentetik açıklıklı radar verilerinin taşkın çalışmalarında kullanılması: Berdan Ovası taşkını. *Geomatik Dergisi*, *3*(2), 154–162.

Aksu, A. E., Walsh-Kennedy, S., Hall, J., Hiscott, R. N., Yaltırak, C., Akhun, S. D., & Çifçi, G. (2014). The Pliocene–Quaternary tectonic evolution of the Cilicia and Adana basins in the eastern Mediterranean: Special reference to the development of the Kozan Fault zone. *Tectonophysics*, *622*, 22-43. https://doi.org/10.1016/j.tecto.2014.03.025

Alan, İ., Şahin, S., Keskin, İ., Bakırhan, B., Balvı, V., Böke, N., Saçlı, L., Pehlivan, Ş., Kop, A., Hanilçi, N., & Çelik, Ö. F. (2007*). Orta Torosların jeodinamik evrimi Ereğli (Konya)-Ulukışla (Niğde)-Karsantı (Adana)-Namrun (İçel) yöresi [The geodynamic evolution of the Central Taurus in the Ereğli (Konya)-Ulukışla (Niğde)-Karsantı (Adana)-Namrun (İçel) region]*. MTA, Ankara (in Turkish).

Alpaslan, M., Güler, C., Gizir, A. M., Temel, A., Sangün, M. K. (2009). *Mersin Doğusunda Bulunan Tarımsal ve Endüstriyel Kökenli Toprak ve Su Kirletici Kaynakların Araştırılması*. Devlet Planlama Teşkilatı (DPT) Proje No: 2006 K 120770 (in Turkish).

Appelo, C. A. J., & Postma, D. (1994). *Geochemistry, groundwater and pollution*. A. A. Balkema.

Avşar, N. (1992). Namrun (İçel) yöresi paleojen bentik foraminifer faunası. *MTA Dergisi*, *114*, 127-144 (in Turkish).

Baran, I., & Kasparek, M. (1989). *Marine turtles Türkiye: Status survey 1988 and recommendations for conservation and management*. World Wide Fund for Nature (WWF).

Burak, S., Doğan, E., & Gazioğlu, C. (2004). Impact of urbanization and tourism on coastal environment. *Ocean & Coastal Management*, *47*(9-10), 515-527. https://doi.org/10.1016/j.ocecoaman.2004.07.007

Burton-Ferguson, R., Aksu, A. E., Calon, T. J., & Hall, J. (2005). Seismic stratigraphy and structural evolution of the Adana basin, eastern

Mediterranean. *Marine Geology*, *221*(1-4), 189-222. https://doi.org/10.1016/j.margeo.2005.03.009

Büyükutku, A. G., & Bağcı, A. S. (2005). Clay controls on reservoir properties in sandstone of Kuzgun formation and its relevance to hydrocarbon exploration, Adana basin, Southern Türkiye. *Journal of Petroleum Science and Engineering*, *47*, 123-135. https://doi.org/10.1016/j.petrol.2005.03.003

Canbolat, A. F. (2004). A review of sea turtle nesting activity along the Mediterranean coast of Türkiye. *Biological Conservation*, *116*(1), 81-91. https://doi.org/10.1016/S0006-3207(03)00179-4

Çelik, A., Kaska, Y., Bağ, H., Aureggi, M., Semiz, G., Kartal, A. A., & Elçi, L. (2006). Heavy metal monitoring around the nesting environment of green sea turtles in Türkiye. Water Air and Soil Pollution, 169, 67-79. https://doi.org/10.1007/s11270-006-1562-0

Çelik, Ö. F. (2008). Detailed geochemistry and K-Ar geochronology of the metamorphic sole rocks and their mafic dykes from the Mersin Ophiolite, southern Türkiye. *Turkish Journal of Earth Sciences*, *17*, 685-708.

Darbaş, G., & Nazik, A. (2010). Micropaleontology and paleoecology of the Neogene sediments in the Adana Basin (South of Türkiye). *Journal of Asian Earth Sciences*, *39*(3), 136-147. https://doi.org/10.1016/j.jseaes.2010.03.002

Darbaş, G., Nazik, A., Temel, A., & Gürbüz, K. (2008). A paleoenvironmental test of the Messinian Salinity Crisis using Miocene–Pliocene clays in the Adana Basin, Southern Türkiye. *Applied Clay Science*, *40*(1-4), 108-118. https://doi.org/10.1016/j.clay.2007.09.007

Delipınar, Ş., & Karpuzcu, M. (2017). Policy, legislative and institutional assessments for integrated river basin management in Türkiye. Environmental *Science & Policy*, *72*, 20-29. https://doi.org/10.1016/j.envsci.2017.02.011

Demirel, Z. (2004). The history and evaluation of saltwater intrusion into a coastal aquifer in Mersin, Türkiye. *Journal of Environmental Management*, *70*(3), 275-282. https://doi.org/10.1016/j.jenvman.2003.12.007

Demirel, Z., & Külege, K. (2005). Monitoring of spatial and temporal hydrochemical changes in groundwater under the contaminating effects

of anthropogenic activities in Mersin region, Türkiye. *Environmental Monitoring and Assessment*, *101*(1–3), 129-145. https://doi.org/10.1007/s10661-005-9145-x

Demirkol, C. (1989). Pozantı-Karsantı-Karaisalı (Doğu Toros) arasında yer alan karbonat platformunun stratigrafisi ve jeolojik gelişimi. *MTA Dergisi*, *109*, 33-44 (in Turkish).

Dinc, U., Yesilsoy, S. M., Kapur, S., Berkman, A., & Ozbek, H. (1978). Formation of sand dunes in the East Mediterranean coast and their physical, chemical and mineralogical properties. *Annals of the University of Çukurova, Faculty of Agriculture*, *2*, 81-105.

DSİ (General Directorate of State Hydraulic Works). (1978). *Mersin, Berdan ve Efrenk Ovaları Hidrojeokimyasal Etüd Raporu*. Ankara (in Turkish).

DSİ (General Directorate of State Hydraulic Works). (2019*). DSİ Akım Gözlem Yıllıkları (1959-2015) ve EİE Akım Gözlem Yıllıkları (1935-2011)*. Retrieved from http://www.dsi.gov.tr/faaliyetler/akim-gozlem-yilliklari

Duran, C., Gunek, H., & Sandal, E. K. (2012). Effects of urbanization on agricultural lands and river basins: case study of Mersin (South of Türkiye). *Journal of Environmental Biology*, *33*(2), 363-371.

Enerji Atlası. (2020). *Hidroelektrik Santralleri*. https://www.enerjiatlasi.com/hidroelektrik/ (Accessed May 14, 2020)

Eren, M. (2011). Stable isotope geochemistry of Quaternary calcretes in the Mersin area, southern Türkiye – A comparison and implications for their origin. *Chemie der Erde*, *71*, 31-37. https://doi.org/10.1016/j.chemer.2010.12.002

Eren, M., Kaplan, M. Y., Kadir, S., & Kapur, S. (2018). Biogenic (β-fabric) features in the hard-laminated crusts of the Mersin and Adana regions, southern Türkiye and the role of soil organisms in the formation of the calcrete profiles. *Catena*, *168*, 34-46. https://doi.org/10.1016/j.catena.2017.12.021

Ergene, S., Çavaş, T., Çelik, A., Köleli, N., & Aymak, C. (2007). Evaluation of river water genotoxicity using the piscine micronucleus test. *Environmental and Molecular Mutagenesis*, *48*(6), 421-429. https://doi.org/10.1002/em.20291

Ergin, M. (1996). Subaerially exposed Late-Quaternary basinal shelf of the inner Mersin Bay, Eastern Mediterranean: Paleoenvironmental evidence. *Geo-Marine Letters*, *16*, 95-100. https://doi.org/10.1007/BF02202603

Erol, O. (2003). Ceyhan deltasının jeomorfolojik evrimi. *Ege Coğrafya Dergisi*, *12*, 59-81 (in Turkish).

Faranda, C., Gliozzi, E., Cipollari, P., Grossi, F., Darbaş, G., Gürbüz, K., Nazik, A., Gennari, R., & Cosentino, D. (2013). Messinian paleoenvironmental changes in the easternmost Mediterranean Basin: Adana Basin, southern Türkiye. *Turkish Journal of Earth Sciences*, *22*, 839-863. https://doi.org/10.3906/yer-1205-11

GDRS (General Directorate of Rural Services). (2001). *Soil characteristics maps of scale 1/25,000*. Ankara.

Göney, S. (1976). *Adana Ovaları* I. İstanbul Üniversitesi Yayın No: 2162, Coğrafya Enstitüsü Yayın No: 88, İstanbul (in Turkish).

Görür, N. (1979). Karaisalı kireçtaşının (Miyosen) sedimantolojisi. *Türkiye Jeoloji Kurumu Bülteni*, *22*, 227-233 (in Turkish).

Gül, M. (2007). Effects of antecedent topography on reefal carbonate deposition: Early-Middle Miocene of the Adana Basin, S Türkiye. *Journal of Asian Earth Sciences*, *31*, 18-34. https://doi.org/10.1016/j.jseaes.2007.03.002

Güler, C. (2009). Site characterization and monitoring of natural attenuation indicator parameters in a fuel contaminated coastal aquifer: Karaduvar (Mersin, SE Türkiye). *Environmental Earth Sciences*, *59*(3), 631-643. https://doi.org/10.1007/s12665-009-0060-2

Güler, C., Alpaslan, M., Kurt, M. A., & Temel, A. (2010). Deciphering factors controlling trace element distribution in the soils of Karaduvar industrial-agricultural area (Mersin, SE Türkiye). *Environmental Earth Sciences*, *60*(1), 203-218. https://doi.org/10.1007/s12665-009-0180-8

Güler, C., Kurt, M. A., Alpaslan, M., & Akbulut, C. (2012). Assessment of the impact of anthropogenic activities on the groundwater hydrology and chemistry in Tarsus coastal plain (Mersin, SE Türkiye) using fuzzy clustering, multivariate statistics and GIS techniques. *Journal of Hydrology*, *414–415*, 435-451. https://doi.org/10.1016/j.jhydrol.2011.11.021

Güler, C., Kurt, M. A., Korkut, R. N., & Korkut, R. N. (2013). Assessment of groundwater vulnerability to nonpoint source pollution in a Mediterranean coastal zone (Mersin, Türkiye) under conflicting land use practices. *Ocean & Coastal Management*, *71*, 141-152. https://doi.org/10.1016/j.ocecoaman.2012.10.010

Gürbüz, K. (1999). An example of river course changes on a delta plain: Seyhan Delta (Çukurova plain, southern Türkiye). *Geological Journal*, *34*(1–2), 211-222. https://doi.org/10.1002/(SICI)1099-1034(199901/06)34:1/2<211::AID-GJ822>3.0.CO;2-0

Gürbüz, K. (2003). *Berdan Nehri'nin Kuvaterner'deki evrimi ve Tarsus'un tarihçesine jeolojik bir yaklaşım*. Kuvaterner Çalıştayı IV. İTÜ Avrasya Yer Bilimleri Enstitüsü, 79-83 (in Turkish).

Gürbüz, K., & Kelling, G. (1993). Provenance of Miocene submarine fans in the northern Adana Basin, southern Türkiye: A test of discriminant function analysis. *Geological Journal*, *28*(3–4), 277-293. https://doi.org/10.1002/gj.3350280307

Güven, O., Yıldırım, Ü., Güler, C., & Kurt, M. A. (2024). Land use and land cover classes affected by the possible sea level rise in Mersin city center (Türkiye). *Advanced GIS*, *4*(1), 15-23.

Hatipoğlu, Z. (2004). *Mersin-Tarsus kıyı akiferinin hidrojeokimyası (Unpublished doctoral dissertation)*. Hacettepe Üniversitesi, Fen Bilimleri Enstitüsü, Ankara.

Hatipoğlu, Z., & Bayarı, C. S. (2005). Mersin-Tarsus kıyı ve yamaç akiferinin hidrojeokimyası. *Türkiye Jeoloji Bülteni*, *48*(2), 59–72.

Hatipoglu, Z., Motz, L. H., & Bayari, C. S. (2009). Characterization of the groundwater flow system in the hillside and coastal aquifers of the Mersin-Tarsus region (Türkiye). *Hydrogeology Journal*, *17*, 1761. https://doi.org/10.1007/s10040-009-0504-5

Hatipoglu-Bagci, Z., & Bayari, C. S. (2020). CrVI and trace element contaminated groundwater systems connected with ophiolitic rocks. *Bulletin of Environmental Contamination and Toxicology*, *106*, 415–420. https://doi.org/10.1007/s00128-020-02887-w

Ilgar, A., Nemec, W., Hakyemez, A., & Karakuş, E. (2013). Messinian forced regressions in the Adana basin: A near-coincidence of tectonic and

eustatic forcing. *Turkish Journal of Earth Sciences*, *22*(5), 864-889. https://doi.org/10.3906/yer-1208-3

İlker, S. (1975). *Adana baseni kuzeybatısının jeoloji ve petrol olanakları, T.P.A.O*. Arama Arşiv No: 973 (unpublished). Ankara.

IUCN. (2020). *The IUCN Red List of Threatened Species*. https://www.iucnredlist.org/ (Accessed May 10, 2020).

Kadir, S., & Eren, M. (2008). The occurrence and genesis of clay minerals associated with Quaternary caliches in the Mersin area, southern Türkiye. *Clays and Clay Minerals*, *56*, 244-258. https://doi.org/10.1346/CCMN.2008.0560208

Kafalı Yılmaz, F. (2008). *Adana Ovaları'nda İklim-Tarım İlişkisi ve Tarım Politikalarının Yansıması*. Afyon Kocatepe Üniversitesi Yayın No: 70, AKÜ, Afyonkarahisar (in Turkish).

Karaca, M., & Nicholls, R. J. (2008). Potential implications of accelerated sea-level rise for Türkiye. *Journal of Coastal Research*, *24*(2), 288-298. https://doi.org/10.2112/07A-0003.1

Karayakar, F., Erdem, C., & Cıcık, B. (2007). Seasonal variation in copper, zinc, chromium, lead, and cadmium levels in hepatopancreas, gill, and muscle tissues of the mussel Brachidontes pharaonis Fischer, collected along the Mersin coast, *Türkiye. Bulletin of Environmental Contamination and Toxicology*, *79*, 350-355. https://doi.org/10.1007/s00128-007-9246-z

Kaska, Y., Çelik, A., Bağ, H., Aureggi, M., Özel, K., Elçi, A., Kaska, A., & Elçi, L. (2004). Heavy metal monitoring in stranded sea turtles along the Mediterranean coast of Türkiye. *Fresenius Environmental Bulletin*, *13*(8), 769-776.

Kasparek, M., Godley, B. J., & Broderick, A. C. (2001). Nesting of the green turtle, Chelonia mydas, in the Mediterranean: A review of status and conservation needs. *Zoology in the Middle East*, *24*(1), 45-74. https://doi.org/10.1080/09397140.2001.10637885

Koleli, N., & Halisdemir, B. (2005). Distribution of chromium, cadmium, nickel, and lead in agricultural soils collected from Kazanlı-Mersin, Türkiye. *International Journal of Environment and Pollution*, *23*(4), 409-416. https://doi.org/10.1504/IJEP.2005.007603

Korkut, R. N. (2009). *Researching nitrate and nitrite pollution in ground waters in the area between Deliçay-Tarsus River (Mersin) (Unpublished master's thesis)*. Mersin Üniversitesi, Fen Bilimleri Enstitüsü, Mersin.

Korkut, R. N., Güler, C., Akbulut, C., & Kurt, M. A. (2011). Spatial distribution of nitrate-nitrite pollution in Tarsus Plain (Mersin) groundwaters and their relationship with various physical parameters. *Türkiye Jeoloji Kurultayı*, 49–50.

Kuleli, T. (2010). Quantitative analysis of shoreline changes at the Mediterranean Coast in Türkiye. *Environmental Monitoring and Assessment*, *167*, 387-397. https://doi.org/10.1007/s10661-009-1057-8

Kumbur, H., Özsoy, H. D., & Özer, Z. (2008). Effects of agricultural chemicals on water quality in Mersin Province. *Ekoloji*, *68*, 54–58. https://doi.org/10.5053/ekoloji.2008.687

Kumbur, H., Vural, N. (1989). Investigation of metal and detergent pollution in Berdan Creek. *Gazi University Journal of Engineering and Architecture*, *4*(1-2), 25-41.

Kurt, M. A. (2010). *Mineralogy of soil profiles, soil and water pollution in the area between Deliçay and Tarsus Creek (Mersin)*. (Unpublished doctoral dissertation). Mersin Üniversitesi, Fen Bilimleri Enstitüsü, Mersin.

Kurt, M. A., Alpaslan, M., & Güler, C. (2008a). *Determination of nitrate and nitrite pollution and their origin in agricultural soils of the area between Mersin-Tarsus using GIS*. In Mersin Sempozyumu (pp. 137–145). Mersin Valiliği Sempozyum Dizisi.

Kurt, M. A., Alpaslan, M., Güler, C., & Temel, A. (2011a). *Evaluation of environmental geology and geochemistry of the Berdan Plain (Mersin) using GIS*. In 64th Türkiye Jeoloji Kurultayı (pp. 56–57). MTA, Ankara.

Kurt, M. A., Alpaslan, M., Güler, C., & Temel, A. (2009a). *Spatial distribution of heavy metals in agricultural soils between Deliçay-Tarsus rivers (Mersin) using GIS*. Türkiye Jeoloji Kurultayı, 62, Abstract Book I, 544-545. (in Turkish)

Kurt, M. A., Alpaslan, M., Güler, C., & Temel, A. (2010a). *Classification of soil areas between Deliçay and Tarsus stream (Mersin) according to geoaccumulation indices*. Türkiye Jeoloji Kurultayı, 63, Abstract Book, 279-280. (in Turkish)

Kurt, M. A., Alpaslan, M., Temel, A., & Güler, C. (2009c). *Mineralogical properties and soil texture of the cultivated topsoils between Mersin and Tarsus*. Türkiye Jeoloji Kurultayı, 62, Abstract Book I, 124-125. (in Turkish)

Kurt, M. A., Alpaslan, M., Temel, A., & Güler, C. (2010b*). Differences in the origins of the delta deposits in the area between Deliçay and Tarsus rivers: Geochemical and mineralogical evidence*. IV. Ulusal Jeokimya Sempozyumu, Elazığ, 41-42. (in Turkish)

Kurt, M. A., Alpaslan, M., Güler, C., & Temel, A. (2014). Mineralogical and geochemical characteristics of Quaternary sediments from the area between Deliçay and Tarsus (Berdan) Rivers. *Türkiye Jeoloji Bülteni*, *57*(1), 1-17.

Kurt, M. A., Güler, C., Alpaslan, M., & Akbulut, C. (2009b). *Comparison of the nitrate and nitrite levels in soils and ground waters of the area between Mersin-Tarsus*. Türkiye Jeoloji Kurultayı, 62, Abstract Book I, 524-525. (in Turkish)

Kurt, M. A., Güler, C., Alpaslan, M., & Akbulut, C. (2011b). *Assessment of the quality and suitability of ground waters from the area between Mersin and Tarsus for human consumption*. Türkiye Jeoloji Kurultayı, 64, Abstract Book, 50-51. (in Turkish)

Kurt, M. A., Güler, C., Alpaslan, M., & Akbulut, C. (2012). Determination of nitrate and nitrite origins in the soils and ground waters of the area between Mersin-Tarsus (Turkey) using geographic information systems. *Carpathian Journal of Earth and Environmental Sciences*, *7*(4), 181-188.

Kurt, M. A., Güler, C., Alpaslan, M., & Temel, A. (2008b). *Karaduvar (Mersin) tarım topraklarındaki bazı ağır metallerin kökeni ve dağılımının faktör analizi ve CBS yardımıyla belirlenmesi*. 61. Türkiye Jeoloji Kurultayı, Bildiri Özleri Kitabı, 17. (in Turkish)

Leloğlu, U. M., Tunalı, E., & Ozaner, F. S. (2003). *Creation of a low-cost digital photogrammetry for monitoring coastal zones of Türkiye*. In Studying Land Use Effects in Coastal Zones with Remote Sensing and GIS (pp. 71-79). Kemer, Antalya.

MDPAF (Mersin Directorate of Provincial Agriculture and Forestry). (2018). *2017 yılı Faaliyet Raporu*. https://mersin.tarimorman.gov.tr/Belgeler/Duyuru/Brifing%202017.pdf

MEDASSET. (2019). *Update Report: Follow-up of Recommendation No. 95 (2002) on the conservation of marine turtles in Kazanli beach (Türkiye)*. https://www.medasset.org/?s=KAZANLI

Ozaner, F. S. (1994). *Anamur, Kazanlı (Mersin) ve Samandağ (Antakya) Kıyılarında Kıyı (Plaj) Erozyonunun Araştırılması*. TÜBİTAK Proje No: DEBAG-62, Ankara.

Özçelik, N., & Yetiş, C. (1994). Adana baseni Güvenç formasyonunun (Tersiyer) fasiyes ve ortamsal nitelikleri. *Türkiye Jeoloji Bülteni*, *37*(2), 73-85.

Özdemir, C. S. (2024). *Investigation of morphometric and physicochemical properties of artificial water bodies in Tarsus (Berdan) plain (Mersin)*. M.Sc. thesis, Mersin Üniversitesi, Fen Bilimleri Enstitüsü.

Özer, A. M., Wieser, A., Göksu, H. Y., Müller, P., Regulla, D. F., & Erol, O. (1989). ESR and TL age determination of caliche nodules. International Journal of Radiation Applications and Instrumentation. Part A. *Applied Radiation and Isotopes*, *40*(10-12), 1159-1162. https://doi.org/10.1016/0883-2889(89)90057-9

Özer, Z. (2001). *Berdan Çayının Kirlilik Durumunun Araştırılması ve Coğrafik Bilgi Sistemi (CBS)'nin Oluşturulmasına Yönelik Kriterlerin Belirlenmesi*. M.Sc. thesis, Department Environmental Engineering, Institute of Pure and Applied Sciences, Mersin University, Mersin.

Özgül, N. (1976). Toroslar'ın bazı temel jeoloji özellikleri. *Türkiye Jeoloji Kurumu Bülteni*, *19*(1), 65-78.

Özgüler, H. (2007). *Dams in flood mitigation in Türkiye. International Congress on River Basin Management, Turkey Ministry of Energy and Natural Resources*, 22-24 March 2007, Antalya.

Öztürk, H. K. (2004). Present status and future prospects of hydroelectric energy in Türkiye. *Energy Sources*, *26*(9), 829-840. https://doi.org/10.1080/00908310490451385

Parlak, O., Delaloye, M., & Bíngöl, E. (1996). Mineral chemistry of ultramafic and mafic cumulates as an indicator of the arc-related origin of the

Mersin ophiolite (southern Türkiye). *Geologische Rundschau*, *85*, 647. https://doi.org/10.1007/BF02440102

PDEU (Provincial Directorate of Environment and Urbanization). (2019). *Mersin İli 2018 Yılı Çevre Durum Raporu*. https://webdosya.csb.gov.tr/db/ced/icerikler/mers-n_-cdr2018-20200110072526.pdf

Poisson, A. (1977). *Recherches Géologiques Dans Les Taurides Occidentales (Turquie)*. Ph.D. dissertation, Universite Paris Sud.

Ramsay, W. M. (1903). Cilicia, Tarsus, and the Great Taurus Pass. *The Geographical Journal*, *22*(4), 357-410. http://www.jstor.org/stable/1775456

Resmi Gazete. (1960). *Yeraltı suları hakkında Kanun (No. 167)*. Resmi Gazete No. 10688, 23.12.1960. http://www.resmigazete.gov.tr/arsiv/10688.pdf

Resmi Gazete. (1969). 25 Nisan 1969, Sayı: 13183, p. 6. https://www.resmigazete.gov.tr/goruntule.html?t=1969-04-25

Russell, R. J. (1954). Alluvial morphology of Anatolian rivers. *Annals of the American Geographers*, *44*(4), 363-391. http://www.jstor.org/stable/2561397

Sandal, E. K., & Gürbüz, M. (2003). The examination of spatial expansion of the city of Mersin and misuse of agricultural lands. *Coğrafi Bilimler Dergisi*, *1*(1), 117-130.

Scheumann, W. (1997). *Managing Salinization: institutional analysis of public irrigation systems*. Springer-Verlag.

Schmidt, G. C. (1961). *Stratigraphic nomenclature for the Adana region Petroleum District VII*. Turkish Petroleum Administration Bulletin, 6, 47-63.

Şenol, M., Şahin, Ş., & Duman, T. Y. (1998). *Adana-Mersin Dolayının Jeoloji Etüd Raporu (1/100.000 Ölçekli Mersin O33 Paftası)*. MTA Doğu Akdeniz Bölge Müdürlüğü.

Simav, Ö., Şeker, D. Z., & Gazioğlu, C. (2013). Coastal inundation due to sea level rise and extreme sea state and its potential impacts: Çukurova Delta case. *Turkish Journal of Earth Sciences*, *22*, 671-680. https://doi.org/10.3906/yer-1205-3

Soil Atlas of Europe. (2005). *European Soil Bureau Network, European Commission*.

Tekin, U. K., Bedi, Y., Okuyucu, C., Göncüoglu, M. C., & Sayit, K. (2016). Radiolarian biochronology of upper Anisian to upper Ladinian (Middle Triassic) blocks and tectonic slices of volcano-sedimentary successions in the Mersin Mélange, southern Türkiye: New insights for the evolution of Neotethys. *Journal of African Earth Sciences*, *124*, 409-426. https://doi.org/10.1016/j.jafrearsci.2016.09.039

Ternek, Z. (1953). Mersin-Tarsus kuzey bölgesinin jeolojisi. *MTA Dergisi*, *44*(44), 18–62.

Ternek, Z. (1957). Adana havzasının Alt Miosen (Burdigalien) formasyonları, bunların diğer formasyonlarla olan münasebetleri ve petrol imkânları. *MTA Dergisi*, *49*, 48–66.

Turkish State Meteorological Service (TSMS). (2019). *TÜMAS*. http://www.mgm.gov.tr/veridegerlendirme/il-ve-ilceler-istatistik.aspx?m=MERSIN#sfB (Accessed November 10, 2019).

Türkmen, S., Öner, F., & Taga, H. (2013). Kuzgun formasyonu tüfitinin jeokimyası ve endüstriyel hammadde potansiyeli. *Çukurova Üniversitesi Mühendislik Mimarlık Fakültesi Dergisi*, *28*(2), 61-76. (in Turkish)

Ünlü, T. S., & Ünlü, T. (2009). *Mersin from Railway Station to the Lighthouse*. Mersin Book Series - 1. Mersin Chamber of Commerce and Industry.

Ünlügenç, U. C. (1986). *Kızıldağ-Yayla (Adana) Dolayının Jeolojik İncelemesi* (Master's thesis, Çukurova Üniversitesi). (in Turkish)

Uslu, T. (1989). *Geographical Information on Turkish Coastal Dunes*. European Union for Dune Conservation and Coastal Management Publication.

Wolf, U. (2001). *Kazanlı environmental pollution in March 2001: Report on the chemical analysis of samples—Preliminary results of a rapid assessment* (Unpublished report).

Yalçın, M. N., & Görür, N. (1984). *Sedimentological evolution of the Adana basin*. In O. Tekeli & M. C. Göncüoğlu (Eds.), International Symposium on the Geology of the Taurus Belt (pp. 165-172). MTA.

Yaman, S. (1991). *Mersin ofiyolitinin jeolojisi ve metallojenisi*. In Acar, A. (Ed.), Çukurova Üniversitesi Mühendislik-Mimarlık Fakültesi (pp. 255-268).

Yetiş, C. (1988). Reorganization of the tertiary stratigraphy in the Adana Basin, Southern Türkiye. *Newsletters on Stratigraphy*, *20*(1), 43-58. https://doi.org/10.1127/nos/20/1988/43

Yetiş, C., & Demirkol, C. (1986). *Adana Baseni Batı Kesiminin Detay Jeoloji Etüdü* I. MTA Raporu No: 8037. (in Turkish)

Yetiş, C., Demirkol, C., & Kerey, E. (1986). Adana havzası Kuzgun formasyonunun (Üst Miyosen) fasiyes ve ortamsal nitelikleri. *Türkiye Jeoloji Kurumu Bülteni*, *29*, 81-96. (in Turkish)

Yetiş, C., Kelling, G., Gökçen, S. L., & Baroz, F. (1995). A revised stratigraphic framework for later Cenozoic sequences in the northeastern Mediterranean region. *Geologische Rundschau*, *84*(4), 794-812. https://doi.org/10.1007/BF00240569

Yilmaz, K. T. (1998). Ecological diversity of the Eastern Mediterranean region of Türkiye and its conservation. *Biodiversity and Conservation*, *7*(1), 87-96. https://doi.org/10.1023/A:1008811829956

CHAPTER 4

POLLINATION WITH ROBOTIC SYSTEMS IN FRUIT AND VEGETABLE FARMING

Prof. Dr. Ümmügülsüm ERDOĞAN[1]

DOI: https://dx.doi.org/10.5281/zenodo.17847592

[1] Bayburt University, Engineering Faculty, Department of Food Engineering, Bayburt, Turkey. gulsum25@gmail.com, ORCID ID: 0000-0002-0490-2285

INTRODUCTION

Pollination, the transfer of pollen from the anther of the male organ to the stigma of the female organ, is a crucial stage in the life cycle of all flowering plants (Westwood, 1993). Pollination is the foundation of plant production, and fruit and seed production are impossible in many plant species without pollination. In nature, wind, water, humans, birds, some mammalian species, and insects serve as pollinators (Sıralı & Cınbırtoğlu, 2011). Insects are the most effective pollinators because they directly target flowers. Bees hold the most important place among insect pollinators (Yılmaz, 2016). In terms of pollination, plants are classified into three groups: polyphyletic, oligophyletic, and monophyletic plants; and pollinators are classified as polytrophic, oligotrophic, and monotrophic species. All pollinators except the honeybee fall into one of these groups. However, although the honeybee is polytropic, it exhibits a very unique characteristic, ranging from polytropic to monotropic (Doğaroğlu, 1985).

Honeybees produce products with high nutritional and pharmacological values, such as honey, beeswax, royal jelly, bee venom, and propolis. Furthermore, they pollinate plants, which are even more important, ensuring a superior product quality and quantity (Özkök & Sorkun, 2001). Bees also enable the survival of thousands of species from various groups that use plants for food, shelter, or nesting, thus maintaining biodiversity.

The decline in bee populations observed in recent years has become a global problem known as the "pollinator crisis." Factors such as climate change, pesticide use, habitat loss, and pathogen and parasite pressure are seriously reducing the number and effectiveness of natural pollinators (Bağrıaçık, 2017). This situation leads to yield declines and economic losses, particularly in fruit and vegetable cultivation. Rapid advances in agricultural technologies in recent years have led to the development of robotic and AI-supported pollinator systems. Robotic pollinators are autonomous systems equipped with sensors and image processing technologies that mimic the behavior of natural pollinators. These devices can identify morphological characteristics of flowers and precisely transfer pollen at the appropriate time (Garip, 2022).

Robotic pollinator technologies are attracting attention with their potential to increase agricultural productivity, reduce seasonal dependence, and support sustainable production. However, further research is needed on issues

such as cost, energy efficiency, sensor accuracy, and adaptation to production conditions before these technologies can be widely implemented.

1. POLLINATION IN FRUITS AND VEGETABLES

Many fruit and vegetable species require an effective pollination process for yield and quality. Pollination occurs when pollen from the male organs is transferred to the pistil stigma, and this process forms the basis for fertilization and fruit formation. Pollination effectiveness is influenced by many factors, including the plant's flower morphology, environmental conditions, pollinator availability, and the species' genetic makeup (Şahinler & özge Toy, 2022).

A significant number of economically important fruit and vegetable species are zoophilically pollinated. Yield and fruit quality are directly related to the level of pollination, particularly in species such as apple, pear, cherry, strawberry, tomato, squash, melon, and pepper (Genç & Dodoloğlu, 1993). For example, in strawberry (*Fragaria × ananassa*), adequate pollination reduces fruit deformities, ensures uniform color distribution, and increases fruit weight (Chang, Lee, & Mah, 2000; Erdoğan & Erdoğan, 2009). Similarly, in tomato (*Solanum lycopersicum*), bees (*Bombus spp*.) are the most effective natural pollinators because flowers require vibration to release pollen (Ozols, Gailis, Jakobija, Jaško, & Zagorska, 2022).

However, in recent years, the effectiveness of natural pollinators has been limited, especially in greenhouse and closed-circuit production systems. Controlled environmental conditions, high temperature and humidity fluctuations, reduce natural bee activity, leading producers to resort to manual or mechanical pollination methods. While these methods offer short-term solutions, they are unsustainable due to their high labor requirements, time-consuming, and uneven pollen distribution (Partap & Ya, 2012).

To meet the pollination needs of fruit and vegetable species, a combination of biological and technological methods should be considered. Robotic pollinator systems hold significant potential as a complement to natural pollination. By optimizing these systems based on plant flowering phenology, they can address pollination deficiencies related to time and environmental conditions.

2. ROBOTIC POLLINATOR TECHNOLOGIES

Robotic pollinators are advanced engineering solutions that integrate image processing, artificial intelligence, sensor technologies, robotic mechanical systems, and precise pollen application mechanisms. The development of robotic pollinators first began with biomimetic pollination experiments conducted in Japan. These systems are based on "flower sensing technologies." Researchers have developed a microdrone prototype that transfers pollen from flower to flower using gelatin-based ionic liquid gels bonded to horsehair fibers (Chechetka, Yu, Tange, & Miyako, 2017). Morphological features (flower shape, position, and opening stage) were detected using high-resolution RGB cameras and depth sensors integrated into mini unmanned aerial vehicles (UAVs). Targeted artificial pollination approaches are being developed using deep learning-based flower recognition algorithms on this image data (Gallmann et al., 2022; Schnalke, Funk, & Wagner, 2025; Shi, Li, & Song, 2019). In the 2020s, the integration of artificial intelligence and machine learning algorithms into agricultural technologies has significantly increased the autonomous mobility of robotic pollinators. These systems detect the three-dimensional position of flowers, minimizing the risk of collision and increasing energy efficiency. Furthermore, the use of biodegradable and electrostatic pollinator materials has supported environmental sustainability goals. Studies conducted by Chinese AI groups and in the United States show that YOLOv8 and CNN-based models can achieve over 90% accuracy in flower detection (R. Singh, Kumar, N., Patel, H., Singh, A., 2024).

Autonomous navigation systems, on the other hand, enable robots to navigate within greenhouses, orchards, or vertical farming structures without collisions. For this purpose, wheeled autonomous robots, rail systems, or drone-based aerial vehicles are used (Wu et al., 2024). The pollinator tip mechanism is the most critical part of robotic systems. Nozzles that produce airflow or vibration are used in species requiring vibratory pollination, such as tomatoes. Liquid or dry pollen spray mechanisms are used in species requiring cross-pollination, such as apples (Bhattarai et al., 2025). Artificial hair or silicone-surfaced tips that provide a soft mechanical touch are preferred for delicate flowering species, such as strawberries (Nishimoto et al., 2023). Furthermore, pollen measurement sensors on the robots monitor pollen density in real time,

providing a standard dosage. This not only increases pollination performance but also reduces pollen waste (Sapkota et al., 2023).

Today, robotic pollinators can be classified into three main categories:

1. Autonomous aerial vehicles (microdrons): These are small-sized systems capable of precise pollination, especially used in greenhouses.
2. Land-based robotic systems: They move between rows and transfer pollen to flowers through mechanical contact.
3. Mechanical manipulator arms: These are systems adapted from industrial robots, providing highly accurate flower recognition and contact with multi-joint structures.

However, the development of robotic pollinators is still in its early stages. Technical hurdles such as high production costs, energy requirements, navigational difficulties in open spaces, and sensitivity to environmental variables must be overcome. However, the increasing affordability of sensor technologies, the development of artificial intelligence algorithms, and the integration of renewable energy solutions strengthen the potential for the future widespread use of these systems. The development of robotic pollinator technologies has been shaped by the combination of nature-inspired engineering and digital agriculture. These technologies are poised to become a key component of sustainable fruit and vegetable production, complementing natural pollinators in the near future.

3. THE USE OF ROBOTIC POLLINATORS IN FRUIT AND VEGETABLE PRODUCTION

Adequate pollination in strawberry plants is critical for fruit shape, weight, and sugar content. Nishimoto et al. (2023) conducted a study to compare pollination methods for strawberries in a plant factory. The study evaluated the performance of robotic pollinators and traditional hand pollination. The results showed that robotic systems can effectively recognize flower clusters and transfer pollen; no significant difference was found between robotic and hand pollination in terms of fruit weight, volume, sugar content, or marketable fruit ratio. The study also demonstrates that robotic systems are a viable alternative in greenhouse environments, particularly when bee populations are limited or absent.

A robotic pollination study conducted in apple orchards by Washington State University used a 6-axis manipulator mounted on a mobile platform and an image processing based machine vision system. The robot detected flower clusters and targetedly applied pollen using electrostatic sprayers. In field trials conducted in 2022, the system successfully targeted 56% of flower clusters, achieving successful pollen transfer. In subsequent improvements, the accuracy rate for detecting the first flowers to open in the beam using the YOLOv8 algorithm increased to 91%, and the successful pollination rate reached 84%. Furthermore, the manipulator application time to a flower cluster was reduced from 6.5 seconds to 4.8 seconds, increasing operation speed. Trials have shown that the robotic system provides fruit set and quality comparable to natural bee pollination (Sapkota et al., 2023).

Tomato flowers require vibrational pollen release. Image processing and artificial intelligence (AI)-based algorithms have demonstrated significant success in tomato pollination with robotic systems. In their study, Hiraguri et al. (2023) classified the morphological shapes of tomato flowers in a greenhouse environment using a convolutional neural network (CNN); This system performed with over 70% accuracy when integrated with a robot or drone, and the effect of ideal flower shape on fruit yield was verified. Additionally, a deep learning and visual feedback-controlled system was developed: Using depth data obtained from a 3D camera, an AI-based model predicts flower orientation, and the robotic articulated arm is guided to this position to perform pollination. This approach has been demonstrated to be highly accurate (average accuracy of ~91.2%) and have a low positioning error (~1.1 cm) in laboratory experiments (R. Singh, Seneviratne, & Hussain, 2025).

Because the effectiveness of natural pollinators is limited in greenhouse conditions, robotic pollination systems offer significant potential to address this gap. A review by Kushwah et al. (2025) noted that robotic systems used in greenhouse agriculture are equipped with various mechanisms for pollen transfer, such as robotic arms, vibrating tips, and electrostatic sprayers. These systems can target flowers with high precision and increase productivity. However, there are technical, economic and environmental challenges to the widespread use of robotic pollination; in particular, maintaining pollen quality, scalability of the systems and cost-effectiveness stand out as important obstacles.

4. ADVANTAGES AND DISADVANTAGES OF ROBOTIC POLLINATION

Robotic pollination systems hold the potential to provide sustainable yields in agriculture today, as agricultural risks such as the decline of natural pollinators and climate fluctuations increase. These systems can operate in controlled environments or greenhouses, unaffected by weather, humidity, and light conditions, and can target flowers using high-precision sensors and image processing algorithms. Positive effects on fruit set and quality have been observed (Bagagiolo, Matranga, Cavallo, & Pampuro, 2022; Bhattarai et al., 2025). Robotic systems also have data collection capabilities; the pollination status of each flower can be monitored and processes can be optimized, resulting in more predictable results in agricultural management. The use of robotic pollinators offers continuity and flexibility in production by reducing labor dependency, providing significant advantages, particularly in situations where bee colony collapses or biological risks exist (Bagagiolo et al., 2022).

However, robotic pollination also has limitations. In greenhouse or open field conditions, robots can be affected by environmental factors such as humidity, chemical agents, dust, or leaf obstacles, and their performance may degrade (Bagagiolo et al., 2022). High initial installation costs, maintenance, and energy requirements are economic factors that limit commercial applicability. Furthermore, most systems are currently designed for a single function, with limited adaptability to different plant species and flower morphologies. Ecological and ethical dimensions should also be considered; some studies highlight those robotic pollinators cannot fully compensate for biodiversity and may create energy consumption and electronic waste (e-waste) risks in production processes. Despite these limitations, the development of robotic systems integrated with artificial intelligence, sensor technologies, and the Internet of Things (IoT) could make robotic pollination more intelligent, autonomous, and suitable for large-scale applications, thus offering sustainable solutions in terms of both yield and quality in agricultural production (Bagagiolo et al., 2022; Bhattarai et al., 2025).

5. CONCLUSION

Honeybees, who perform a crucial role through pollination, in a sense, ensure the continuity of nature. Honeybees not only increase the quantity and

quality of crops by pollinating cultivated plants, but also assist in the pollination of plants in the wild when other pollinators are absent or scarce. They also protect endangered plant species, enabling their proliferation and spread, the development of wildlife, and the increase in plant and animal diversity.

Pollination in fruits and vegetables plays a critical role in determining crop yield and quality. It transports the pollen necessary for flower fertilization, fruit formation, and growth; inadequate pollination can lead to a decrease in fruit number, deformities, and weight loss. Yield, particularly in species such as tomatoes, strawberries, apples, and peppers, is directly dependent on the effectiveness of pollinators. Furthermore, pollination supports the preservation of genetic diversity in plants and the maintenance of a healthy ecosystem. Therefore, a decrease in natural pollinators or adverse environmental conditions can cause significant losses in agricultural production.

Robotic pollinators offer technological solutions that can fill this gap. Robotic systems, supported by image processing and artificial intelligence, can detect the position of flowers and perform targeted pollen transfer, thus reducing yield losses caused by the lack of manual or natural pollinators. Furthermore, thanks to their repeatability and continuity, robotic systems enable standardized pollination throughout the year.

The use of robotic pollinators is an important technological approach for increasing productivity, improving quality, and reducing dependence on natural pollinators in fruit and vegetable production. The development and dissemination of these systems is critical for sustainable agriculture and food security.

REFERENCES

Bagagiolo, G., Matranga, G., Cavallo, E., & Pampuro, N. (2022). Greenhouse robots: Ultimate solutions to improve automation in protected cropping systems—a review. *Sustainability, 14*(11), 6436.

Bağrıaçık, N. (2017). Polinatör böcekler ve küresel tozlaşma krizi. *Journal of the Institute of Science Technology, 7*(4), 37-41.

Bhattarai, U., Sapkota, R., Kshetri, S., Mo, C., Whiting, M. D., Zhang, Q., & Karkee, M. (2025). A vision-based robotic system for precision pollination of apples. *Computers Electronics in Agriculture, 234*, 110158.

Chang, Y.-D., Lee, M.-Y., & Mah, Y. (2000). *Pollination on Strawberry in the Vinyl House by Apis mellifera L. and A. cerana Fab.* Paper presented at the VIII International Symposium on Pollination-Pollination: Integrator of Crops and Native Plant Systems 561.

Chechetka, S. A., Yu, Y., Tange, M., & Miyako, E. (2017). Materially engineered artificial pollinators. *Chem, 2*(2), 224-239.

Doğaroğlu, M. (1985). Bitkisel üretimde verimliliği artırmada bal arısının yeri ve önemi. *Yem Sanayi Dergisi, 48*, 11-15.

Erdoğan, U., & Erdoğan, Y. (2009). Üzümsü meyvelerin tozlaşmasında bal arılarının yeri ve önemi. In.

Gallmann, J., Schüpbach, B., Jacot, K., Albrecht, M., Winizki, J., Kirchgessner, N., & Aasen, H. (2022). Flower mapping in grasslands with drones and deep learning. *Frontiers in plant science, 12*, 774965.

Garip, Z. (2022). Seri Robot Manipülatöründe Ters Kinematik Problemi Çözmek İçin Kaotik Tabanlı Çiçek Tozlaşma Algoritmasının Uygulanması. *Journal of the Institute of Science Technology, 12*(1), 80-90.

Genç, F., & Dodoloğlu, A. (1993). Arıcılığın temel esasları (Ders notu). *Atatürk Üniv. Zir. Fak. Yay*(149), 286.

Hiraguri, T., Kimura, T., Endo, K., Ohya, T., Takanashi, T., & Shimizu, H. (2023). Shape classification technology of pollinated tomato flowers for robotic implementation. *scientific reports, 13*(1), 2159.

Kushwah, A., Bhandari, A., Chandra, V., Sindhu, M., Navyashree, R., Devi, S., . . . Kumar, V. (2025). Robotic Pollination in Greenhouse Farming:

Current Innovations, Challenges, and Future Prospects. *Oriental Journal of Chemistry, 41*(4).

Nishimoto, Y., Lu, N., Ichikawa, Y., Watanabe, A., Kikuchi, M., & Takagaki, M. (2023). An evaluation of pollination methods for strawberries cultivated in plant factories: robot vs hand. *Technology in Horticulture, 3*(1).

Ozols, N., Gailis, J., Jakobija, I., Jaško, J., & Zagorska, V. (2022). Bumblebee pollination activity in a commercial tomato greenhouse during the winter season. *Rural. Sustain. Res, 48*, 45-53.

Özkök, A., & Sorkun, K. (2001). Apiterapide kullanılan önemli arı ürünlerinden: bal, polen ve propolis. *Teknik Arıcılık, 72*, 4-10.

Partap, U., & Ya, T. (2012). The human pollinators of fruit crops in Maoxian County, Sichuan, China. *Mountain Research Development, 32*(2), 176-186.

Sapkota, R., Ahmed, D., Khanal, S. R., Bhattarai, U., Mo, C., Whiting, M. D., & Karkee, M. (2023). Robotic pollination of apples in commercial orchards. *arXiv preprint arXiv:.10755*.

Schnalke, M., Funk, J., & Wagner, A. (2025). Bridging technology and ecology: enhancing applicability of deep learning and UAV-based flower recognition. *Frontiers in plant science, 16*, 1498913.

Shi, L., Li, Z., & Song, D. (2019). *A flower auto-recognition system based on deep learning.* Paper presented at the IOP Conference Series: Earth and Environmental Science.

Singh, R., Kumar, N., Patel, H., Singh, A. (2024). Deep learning-based flower detection enabling robotic tomato pollination. Scientific Reports. *14*, 8821. doi:https://doi.org/10.1038/s41598-024-57409-3

Singh, R., Seneviratne, L., & Hussain, I. (2025). Robust pollination for tomato farming using deep learning and visual servoing. *Robotica, 43*(1), 86-109.

Sıralı, R., & Cınbırtoğlu, Ş. (2011). Bal arılarının tozlaşmadaki ve bitkisel üretimdeki önemi. *Arıcılık Araştırma Dergisi, 10*(1), 28-33.

Şahinler, N., & özge Toy, N. (2022). Polinasyonda Arılar ve Küresel Isınmanın Arılara Etkisi. *Turkish Journal of Agriculture-Food Science Technology, 10*, 2882-2887.

Westwood, M. N. (1993). Temperate-zone pomology: physiology and culture. In: Timber Press (OR).

Wu, P., Lei, X., Zeng, J., Qi, Y., Yuan, Q., Huang, W., . . . Lyu, X. (2024). Research progress in mechanized and intelligentized pollination technologies for fruit and vegetable crops. *International Journal of Agricultural Biological Engineering, 17*(6), 11-21.

Yılmaz, K. (2016). Bal arılarının bitkisel üretimdeki önemi. *Ordu'da Tarım, 20*(118), 1-2.

CHAPTER 5

MODELING THE POLLUTION SUSCEPTIBILITY OF THE ERDEMLİ COASTAL AQUIFER USING DRASTIC METHOD

MSc. Nazire ORTAK[1]

Prof. Dr. Mehmet Ali KURT[2]

Assoc. Prof. Dr. Ümit YILDIRIM[3]

Prof. Dr. Cüneyt GÜLER[4]

Lecturer Onur GÜVEN[5]

DOI: https://dx.doi.org/10.5281/zenodo.17847599

[1] Mersin University, Institute of Science, Mersin, Türkiye. kekliknazire@gmail.com, ORCID ID: 0000-0002-6190-0809.

[2] Mersin University, Engineering Faculty, Department of Environmental Engineering, Mersin, Türkiye. malikurt@mersin.edu.tr, ORCID ID: 0000-0001-7255-2056

[3] Bayburt University, Faculty of Applied Sciences, Emergency Aid and Disaster Management Department, Bayburt, Türkiye. umityildirim@bayburt.edu.tr, ORCID ID: 0000-0002-7631-7245

[4] Mersin University, Engineering Faculty, Department of Geological Engineering, Mersin, Türkiye. cguler@mersin.edu.tr, ORCID ID: 0000-0001-8821-6532

[5] Bayburt University, Central Research Laboratory and Research Centre, Bayburt, Türkiye. onurguven@bayburt.edu.tr, ORCID ID: 0000-0001-5608-7633

INTRODUCTION

With the Industrial Revolution, synthetic materials entered our lives alongside natural products. The diversification of the required production technologies has increased human living standards. However, pollutants released into the environment as a result of human-induced activities have posed risks and led to the degradation of agricultural lands. Consequently, both water and soil resources have been contaminated, reducing agricultural productivity and deteriorating the quality of water and crops.

Coastal aquifers are polluted by anthropogenic activities, including industrial and agricultural operations such as improper waste disposal and excessive pumping. In addition, they may also be contaminated by geogenic sources associated with the geochemical characteristics of the natural rock formations within the aquifer system.

The study area is the Erdemli Coastal Aquifer (ECA), located in Erdemli district of Mersin Province. Erdemli is a region where agricultural activities are carried out year-round, and its economy is largely based on agricultural production. Irrigation water for agricultural practices is mostly supplied from groundwater wells through pumping. Excessive fertilization and the widespread use of septic tanks in rural areas are the primary anthropogenic factors causing groundwater pollution in the study area.

In recent years, migration, unplanned urbanization, and industrial activities in Mersin have created numerous problems in coastal aquifers, one of which is the Erdemli Coastal Aquifer. The area is dominated by agricultural lands such as greenhouses and citrus orchards, where groundwater is widely utilized. Meeting the increasing water demand in the future and reducing pollution requires the implementation of proper water management strategies.

The aim of this study is to determine some physical and chemical properties of soil samples taken from the ECA region in Mersin and to assess the aquifer's susceptibility to pollution through DRASTIC modeling.

According to 2018 TÜİK data (TSI, 2018), the population of Erdemli district and its villages is 140,331. The district consists of 11 municipalities (Arpaçbahşiş, Ayaş, Çeşmeli, Erdemli, Esenpınar, Kargıpınarı, Kızkalesi, Kocahasanlı, Kumkuyu, Limonlu, and Tömük), 71 neighborhoods, and 50 villages. The most populated neighborhoods are Merkez, Kargıpınarı, Akdeniz,

Alata, and Tömük, while the least populated are Tozlu, Kuşluca, Evdilek, Hacıalanı, Sinap, and Akpınar.

1. GEOGRAPHICAL SETTING

The study area covers a surface area of 45 km². It is naturally bounded by the Arpaçbahşiş Stream in the east, the Kocahasanlı Stream in the west, and the Mediterranean Sea in the south (Figure 1). The elevation of the area ranges between 0 and 255 m and is located between the latitudes 36°34′–36°39′N and longitudes 34°14′–34°21′E. The southeastern part of the ECA, close to the Mediterranean coast, is mainly characterized by deltaic deposits transported by the Alata Stream, the largest river in the study area, as well as partially by the Kocahasanlı, Kargıcak, Kargıpınarı, and Arpaçbahşiş streams. These deposits form extensive alluvial plains. In contrast, the northeastern parts are composed predominantly of carbonate rocks. Groundwater in the region is primarily supplied from Quaternary and modern fluvial–deltaic coastal aquifers located along the Mediterranean coast and, to a lesser extent, from karstic aquifers in areas with steeper slopes. These groundwater resources are extensively used for both agricultural irrigation and domestic water supply.

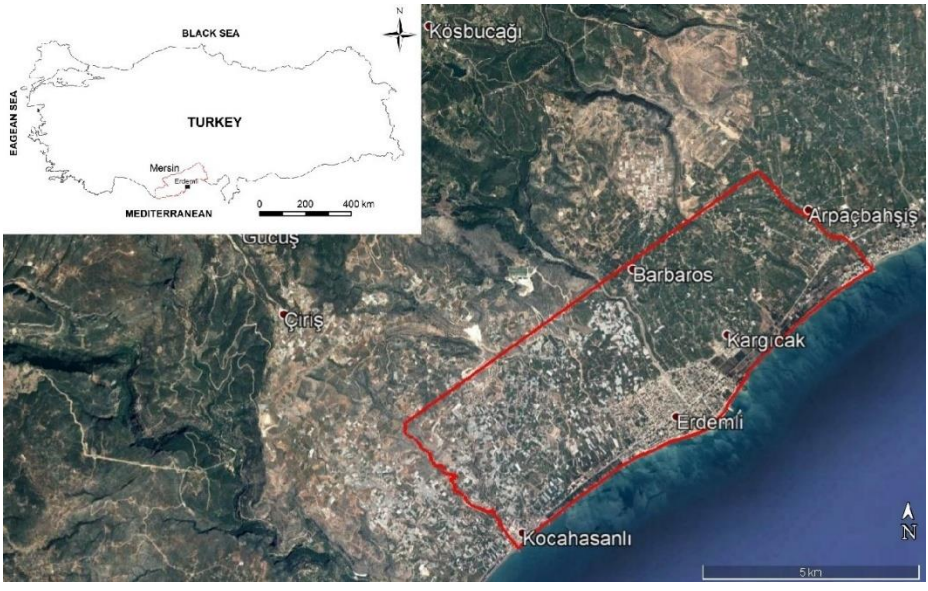

Figure 1: The Location Map of the Study Area

2. MORPHOLOGY

The district of Erdemli in Mersin Province lies within the Mediterranean Region, situated on the Erdemli Plain south of the foothills of the Central Taurus Mountains. The study area is bounded by Mersin in the east, the Taurus Mountains in the north, the Mediterranean Sea in the south, and Silifke district in the west. The elevation of the district center ranges between 0 and 255 meters above sea level, while the slope of the terrain varies between 0° and 63°. Slope values increase from the coastal areas toward the north. In terms of areal distribution, 64.4% of Erdemli consists of mountainous areas, 23.5% of plateaus, and 9.1% of plains.

3. CLIMATE AND VEGETATION

Erdemli is an agricultural district where greenhouse cultivation is particularly intensive. The climate is typically Mediterranean, characterized by hot and dry summers and mild, rainy winters. In the higher elevations of the district, a continental climate is observed, with precipitation generally beginning in the autumn.

The land stretching from the coastal strip to the upland plateaus is highly suitable for a wide variety of agricultural crops. The most cultivated products are lemon, orange, banana, and tomato. Notably, Erdemli produces about 65% of Türkiye's lemon supply. The region is also rich in carob, wild pistachio, laurel, oleander, willow, and plane trees. At higher elevations, thyme, mint, pennyroyal, and Gundelia species are common, along with pine forests.

The upland areas of Erdemli contain some of the world's richest cedar (Cedrus libani) forests (Dürgen, 2012). These forests are commonly found around the villages of Aydınlar, Hacıalanı, Sorgun, and Çerçili. In addition, extensive pine forests occur in the upper reaches of the Alata Stream, whereas pine trees become less abundant around the Lamas Stream and are gradually replaced by olive trees.

4. LAND USE

Land use classes in the study area were derived by digitizing up-to-date Google Earth images. Land use classes were categorized into open fields, industrial area, houses, orchards, forest, green houses, agricultural area, and summer houses. Among these classes, citrus orchards and greenhouses account

for the largest share, while industrial areas represent the smallest proportion. The distribution of land use types is shown in Figure 2. These results clearly indicate that the economy of the Erdemli region is predominantly agriculture-based.

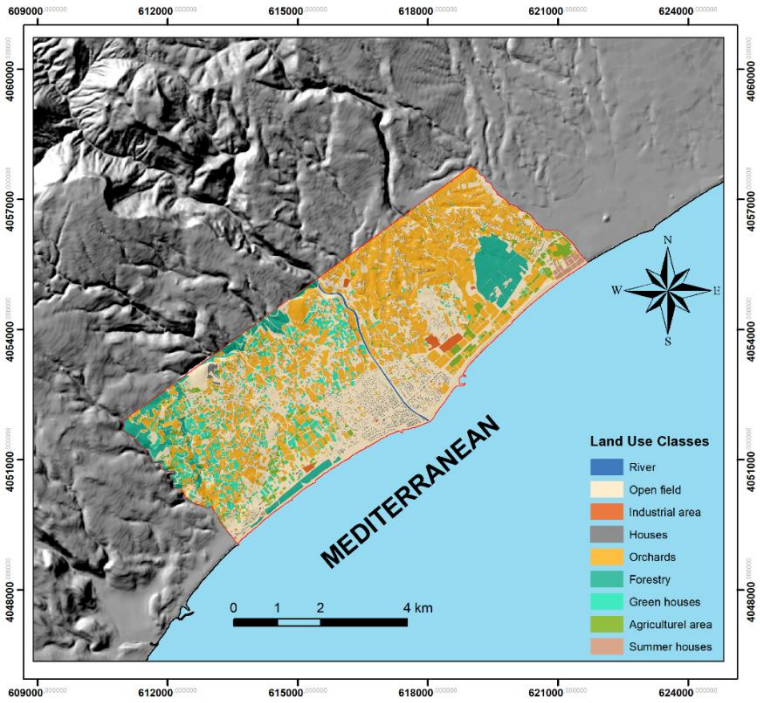

Figure 2: The land Use Classes of the Study Area.

5. SOURCES AND IMPACTS OF POTENTIALLY TOXIC ELEMENTS IN SOIL

Soil, which provides the essential nutrients required for sustaining life, is also contaminated by toxic pollutants of anthropogenic origin. Among these, trace elements are considered the most hazardous group. Metals with atomic numbers greater than 20 and specific gravity above 5 g/cm³ are defined as heavy metals (Kurt, 2010). Heavy metals located between groups 2A and 6A of the periodic table are chemically stable and cannot be degraded in nature (Okcu et al., 2009; Wickfors and Ukeles, 1982).

Approximately 70 elements are included in the trace element group, of which 20 are ecologically significant. These include Fe, Mn, Zn, Cu, Mo, V,

Co, Ni, Cr, Pb, Be, Tl, Sb, Se, Sn, Al, As, Cd, Hg, and Ag. Some of these (Fe, Cu, Zn, Mn, Mo, and Ni) are micronutrients for plants and animals (Okcu et al., 2009).

Soil contamination may occur not only due to anthropogenic activities but also from geogenic sources such as mining, earthquakes, floods, and volcanic eruptions. Acid rain decreases soil pH, leading to heavy metal accumulation and mobilization. Natural concentrations of potentially toxic elements in soils vary depending on mineralogical, physical, and chemical properties and the soil formation process. Soils with high clay content tend to adsorb trace elements, forming soluble compounds (Yalçın, 2019).

Trace elements are integral components of ecosystems and occur naturally. For example, copper (Cu) and zinc (Zn) are essential for life, with zinc playing a crucial role in metabolic regulation. In contrast, lead (Pb) and mercury (Hg) serve no biochemical function and are toxic to living organisms (Raven et al., 1999). While Cu and Zn are micronutrients required for many enzymatic processes, Pb and Hg are toxic even at very low concentrations.

Under natural conditions, soils can neutralize high concentrations of elements and prevent toxic effects on living organisms. However, trace element pollution is exacerbated in agricultural lands due to uncontrolled pesticide and fertilizer application (Mikanov, 2006). Traffic on highways also contributes to the contamination of agricultural soils with elements such as Pb, Cd, and Ni (Hakerlerler et al., 1995).

Soil is one of the most important components of the biosphere. Therefore, trace element pollution not only reduces soil productivity and crop quality but also poses serious risks to environmental quality and human health (Kocaer and Başkaya, 2003). Elements such as Pb, Cd, Co, Zn, and Ni can cause severe health problems in humans. In soils, trace element-induced biochemical changes affect respiration activity and organic matter mineralization. The concentration of trace elements varies depending on parent material composition, soil properties, and the toxicity of these elements to biological processes (Dökmeci, 2005).

The toxic effects of metals on humans depend on several factors, including immune resistance, exposure dose, age, nutritional status, and overall health. Their impacts vary depending on the duration they remain in the body:

Pb and Hg primarily affect the central nervous system, Ni affects the lungs, and Cd affects the kidneys (Muslu, 1985).

In soils with low organic matter, potentially toxic elements accumulated in coarse-textured soils can leach into groundwater depending on pH. Conversely, soils with high cation exchange capacity (CEC) and clay content tend to retain heavy metals and form insoluble compounds.

According to the World Health Organization (WHO), approximately 65% of chronic diseases are associated with toxic metal pollution (Güleç, 2013). Inorganic contaminants such as As, Mn, Cu, Zn, Cl, Ni, and Fe have severe toxic effects, causing poisoning and even death in living organisms (Dündar et al., 2012).

6. SOURCES AND IMPACTS OF POTENTIALLY TOXIC ELEMENTS IN SOIL

The susceptibility of aquifers to pollution refers to their natural ability to resist contamination (Gogu et al., 2003). Groundwater vulnerability is assessed by considering the source of pollutants, their distance to groundwater, and the physical and chemical properties of the aquifer system. Susceptibility assessments are divided into two categories: specific vulnerability and intrinsic vulnerability (Vrba and Zaporozec, 1994). The former considers the characteristics of the contaminant and its pathway, while the latter reflects the natural properties of groundwater and its environment.

Vulnerability maps are created to determine aquifer susceptibility to pollution. These maps classify areas into different susceptibility levels using numerical values. If vulnerability varies spatially, susceptibility classes range from low to high (Remesan and Panda, 2008; Yıldırım, 2023).

Methods used in vulnerability mapping include:

- Observation-based methods: Maps are generated using data from monitoring wells without considering the contaminant source or its distance to groundwater.
- Statistical methods: These methods rely on available data and correlations to evaluate regions with limited or incomplete information, without explicitly considering groundwater flow.

- Process-based methods: These involve approximate predictions and simulation models that incorporate contaminant sources, transport pathways, and aquifer properties.
- Index-based methods: These evaluate pollution pathways by assigning ratings to parameters that influence contaminant movement to groundwater.

One of the most commonly used index-based methods is the DRASTIC model. The DRASTIC method was developed by Aller et al. (1987) to assess the vulnerability of aquifers to contamination. Based on point count models, this method has been increasingly applied with the advancement of Geographic Information System (GIS) technology. Since GIS technology supports the DRASTIC model, these two methods are now commonly used together, enabling the determination of groundwater pollution potential.

DRASTIC modeling is divided into two parts: the classification of hydrogeologically significant parameters and the weighting of these classified parameters. The first part encompasses all hydrogeological and geological factors that govern the movement of water, while in the second part, the parameters are evaluated and the index is calculated. The mappable hydrogeological parameters are derived from the combination of factors that influence water movement in the first stage, whereas the second stage involves calculating the index through the relative rating of the parameters.

The DRASTIC model is based on four fundamental principles: (i) the presence of a contaminant at the ground surface, (ii) the transport of the contaminant to groundwater by precipitation, (iii) the movement of the contaminant with groundwater flow, and (iv) the applicability of the method to areas larger than 0.4 km² (Yavuz, 2017).

This model, which considers the hydrological, geological, and topographic structure of aquifers, is environmentally compatible and widely used. The method evaluates seven different parameters: depth to groundwater (D), net recharge (R), aquifer media (A), soil media (S), topography (T), impact of the vadose zone (I), and hydraulic conductivity (C). Each parameter has a specific weight depending on its relative influence on contamination. In addition to the weight value, each parameter is also assigned a rating value, which varies depending on the study area. The DRASTIC Index value is calculated by multiplying the weight and rating values of each of the seven

parameters and summing the results. A higher value of this index indicates a greater vulnerability of groundwater to contamination (Türkay, 2015, Yıldırım; 2023).

7. MATERIALS AND METHODS

In this study, soil samples collected from the coastal region of Erdemli district, Mersin Province, were used as the primary material. A total of 32 soil samples were taken from surface soils (0–20 cm). As base layers for the GIS analysis, up-to-date Google Earth imagery of the study area and 1:25,000 scale Silifke O-32-c1 and O-32-c4 topographic maps were used. Groundwater depth data for the Erdemli coastal aquifer were compiled from boreholes drilled in the region for various purposes in previous studies.

The pH, electrical conductivity (EC), and salinity of the soil samples were measured using a multiparameter device in a 1:5 soil-to-pure water suspension after 24 hours of equilibration, following the procedure described by Rayment and Higginson (1992).

The soil samples were oven-dried at 105°C for 1.5 hours, ground for 5 minutes at 900 rpm using a ring mill, and subjected to total dissolution for elemental analysis. For this procedure, a hot plate was preheated to 270°C, and 0.1 g of ground soil sample was placed in Teflon crucibles. One milliliter of hydrofluoric acid (HF) was added to dissolve the silicate phases of the soil. After complete evaporation of HF, 8 mL of aqua regia (1:3 HNO_3:HCl) was added to the crucibles to dissolve the remaining soil components. The solution was transferred into 50 mL Falcon tubes and diluted to 50 mL with ultrapure water. Trace element concentrations were determined using an ICP-MS instrument.

The grain size distribution of the soil samples was determined by sieve analysis using sieves of 4, 2, 0.5, 0.25, 0.2, 0.125, and 0.045 mm mesh sizes. From the resulting particle size distribution curves, parameters D10, D50, and Io were calculated. These parameters were then used to estimate the permeability values of the surface soils in the study area according to the Alyamani-Sen method (Alyamani and Sen, 1993).

7.1. Creation and Weighting of DRASTIC Layers

7.1.1. D: Depth to Groundwater

The depth-to-groundwater (D) parameter indicates the vertical distance from the land surface to the groundwater table. It is considered one of the most critical parameters in the DRASTIC method, as it represents the path a pollutant must travel to reach groundwater (Aller et al., 1987).

In this study, groundwater depths were obtained from previously drilled wells in the study area. The point data were interpolated to generate a depth-to-groundwater map, which was then reclassified according to the classes given in Table 1. Each class was assigned rating values as indicated.

Table 1: Area, Elevation, and Flow Path Length Values of Catchments.

Depth to Groundwater (m)	Rating (Dr)
0.00–1.52	10
1.52–4.57	9
4.57–9.14	7
9.14–15.24	5
15.24–22.86	3
22.86–30.48	2
>30.48	1

7.1.2. R: Recharge

The recharge (R) parameter represents aquifer replenishment through infiltration from the surface. The classification values of the recharge parameter (Piscopo, 2001) were calculated using data layers of annual precipitation, topography, and permeability for the study area. For the RA parameter, annual precipitation data from the meteorological stations were utilized. A precipitation map and a weighted precipitation map were generated by converting point precipitation data into raster format.

For the topography (T) parameter, a slope map (expressed in percentages) and a weighted slope map were produced in a GIS environment using the Digital Elevation Model (DEM) of the study area.

For the permeability (SP) parameter, soil samples were collected from 32 different locations within the study area, and grain size distribution analyses were conducted in the laboratory to produce grain size distribution curves. As described by Alyamani and Sen (1993), the permeability value of each location was calculated based on the grain size distribution. The calculated permeability

values were transferred into the GIS environment to generate both a permeability map and a weighted permeability map for the study area.

The resulting slope map was reclassified according to Table 2, and the T values specified in the table were assigned to each cell of the respective classes. For the permeability parameter, the saturated hydraulic conductivity layer was divided into very high, high, moderate, low, and very low hydraulic conductivity classes, and the SP values given in Table 2 were assigned to these classes.

Table 2: Ranges and Classification Values of The Parameters Used in the Determination of the Recharge (R) Parameter (Piscopo, 2001).

Precipitation (mm/year)		**Rating (RA)**		**Permeability**		**Recharge Value (R)**	
Rating	RA	Rating	T	Rating	SP	Rating	R
>850	4	<2	4	Very High	5	11–13	10
700–850	3	2–10	3	High	4	9–11	8
500–700	2	10–33	2	Medium	3	7–9	5
<500	1	>33	1	Low	2	5–7	3
				Very Low	1	3–5	1

7.1.3. A: Aquifer Media

Aquifers are geological formations capable of storing and transmitting groundwater. The aquifer media (A) parameter significantly influences the rate of contaminant transport (Aller et al., 1987).

The aquifer media map was created using the geological map of the study area and available well logs. Raster classification was based on aquifer material types and the corresponding ratings provided in Table 3.

Table 3: Aquifer Media Ratings (Aller et al., 1987).

Aquifer Material	**Rating Range**	**Mean Rating (Ar)**
Massive shale	1–3	2
Metamorphic/Volcanic rock	2–5	3
Weathered metamorphic/volcanic	3–5	4
Glacial deposits	4–6	5
Bedded sandstone, limestone	5–9	6
Massive sandstone	4–9	6
Massive limestone	4–9	8
Sand and gravel	4–9	8
Basalt	2–10	9
Karstic limestone	9–10	10

7.1.4. S: Soil Media

The soil media (S) parameter represents the uppermost soil layer. The type of soil material influences the infiltration capacity of water percolating downward. In addition, this parameter affects the quantity of water retained in the unsaturated zone and the amount of contaminants reaching the groundwater through percolation (Aller et al., 1987).

The soil map of the study area was prepared by converting the vector format digital soil map into raster format. Class values were assigned according to soil types, considering their permeability characteristics, and a weighted soil media map was produced using the classification values given in Table 4.

Table 4: Soil Media Classification Values (Aller et al., 1987).

Soil Material	**Rating (Sr)**
Thin or absent (soil)	10
Gravel	10
Sand	9
Peat	8
Shrinking and aggregated clay	7
Sandy loam	6
Loam	5
Silty loam	4
Clay loam	3
Muck	2
Nonshrinking and unaggregated clay	1

7.1.5. T: Topography

The topography (T) parameter expresses the slope of the land surface. To calculate this parameter, all contour lines and peak points within the study area were digitized to generate a DEM. Using ArcGIS, a slope map of the study area was prepared, and each slope class was assigned ratings according to Table 5, resulting in a weighted topography map.

Table 5: Topography Classification Values (Aller et al., 1987).

Slope (%)	**Rating (Tr)**
0–2	10
2–6	9
6–12	5
12–18	3
> 18	1

7.1.6. I: Impact of the Vadose Zone

The vadose zone (unsaturated zone) refers to the region between the land surface and the groundwater table. Since it determines the travel path and residence time of contaminants, this parameter is critical. Processes such as filtration and evaporation often occur in this zone, increasing or decreasing contaminant impacts.

The vadose zone media were classified according to lithological data from the study area, and ratings were assigned as shown in Table 6 to produce the weighted vadose zone map.

Table 6: Vadose Zone Classification Values (Aller et al., 1987).

Vadose Zone Material	Rating (Ir)
Impermeable layer	1
Silt–clay	2–6
Limestone	2–5
Sandstone	2–7
Interbedded limestone and sandstone	4–8
Sand and gravel with clay/silt	4–8
Sand and gravel	4–8
Basalt	2–10
Karstic limestone	8–10

7.1.7. C: Hydraulic Conductivity

Hydraulic conductivity (C) represents the ability of the aquifer to transmit water. It is influenced by porosity and hydraulic gradient. Areas with high porosity result in higher groundwater flow velocities, which facilitate contaminant transport (Aller et al., 1987). Hydraulic conductivity values were assigned based on previous hydrogeological studies in the region and the lithology of the study area. A hydraulic conductivity distribution map was produced and reclassified according to Table 7.

Table 7: Hydraulic Conductivity Classification Values (Aller et al., 1987).

Hydraulic Conductivity (m/day)	Rating (Cr)
0.04075–4.075	1
4.075–12.225	2
12.225–28.525	4
28.525–40.75	6
40.75–81.5	8
>81.5	10

7.2. Calculation of the DRASTIC Index

The calculation of the DRASTIC index involves two stages: classification and weighting. In the classification stage, each parameter of the DRASTIC model is considered a factor influencing contamination, and numerical values ranging from 1 to 10 are assigned to these factors according to their relative significance. These assigned values are referred to as class values and are denoted by the subscript "r." In the weighting stage, each parameter of the DRASTIC model is assigned a value between 1 and 5, based on its potential impact on pollution, and this is referred to as the weight value, denoted by the subscript "w" (Aller et al., 1987). Table 8 presents the weight values of the parameters that constitute the DRASTIC model, while Table 9 shows the degrees of aquifer vulnerability to contamination according to the calculated DRASTIC Index (DI) values.

Table 8: Weights of DRASTIC Parameters (Aller et al., 1987).

Symbol	Parameter	Weight (Dw)
D	Depth to groundwater	5
R	Recharge	4
A	Aquifer media	3
S	Soil media	2
T	Topography	1
I	Vadose zone impact	5
C	Hydraulic conductivity	3

Table 9: Classification of Aquifer Vulnerability Based on DRASTIC Index (Aller et al., 1987).

DRASTIC Index Value	Vulnerability Classes	Explanation
$DI \leq 80$	Very low	Low risk of pollution
$80 < DI \leq 120$	Low	Slight vulnerability to contamination
$120 < DI \leq 160$	Moderate	Moderate risk of pollution
$160 < DI \leq 200$	High	Highly vulnerable, management plan required
$DI > 200$	Very high	Extremely vulnerable, urgent management needed

8. RESULTS AND DISCUSSION

8.1. Physical Properties of the Study Area Soils

To evaluate the impact of surface soils on aquifer vulnerability, 32 soil samples were collected, and their physical and chemical properties were

determined. The maximum, minimum, and average values of pH, electrical conductivity (EC), salinity, nitrate, total dissolved solids (TDS), and $CaCO_3$ contents are presented in Table 10. The maximum, minimum, and average pH values of the soils were 8.77, 7.44, and 7.83, respectively, indicating that the soils of the study area are generally alkaline. The maximum, minimum, and average EC values were 658, 112, and 226 µS/cm, respectively. The maximum, minimum, and average salinity values were 0.23, 0.05, and 0.10 ppt, respectively. Since dissolved salts increase electrical conductivity in both soil and water, these low salinity values indicate that there is not yet a salinization problem in the study area. The maximum, minimum, and average nitrate values were 136, 1.94, and 19.03 mg/L, respectively. These values demonstrate that nitrate load is high in the soils of Erdemli. The elevated nitrate concentrations are mainly attributed to the use of chemical and organic fertilizers and domestic waste. Nitrate accumulation in soils increases particularly during fertilization periods, leading to nitrate pollution in shallow aquifers. The maximum, minimum, and average TDS values of the soils were 313, 73, and 139 mg/L, respectively. The maximum, minimum, and average calcium carbonate ($CaCO_3$) contents were 48.84%, 4.14%, and 20.57%, respectively. The generally high $CaCO_3$ content is attributed to the widespread presence of limestone formations in the region, especially in elevated areas, which physically weather and accumulate in more level areas.

Table 10: Maximum, Minimum, and Average Physical Properties of soil Samples (n=32).

Statistics	EC (µS/cm)	TDS (mg/L)	Salinity (ppt)	pH	Nitrate (mg/L)	$CaCO_3$ (%)
Max.	658	313	0.23	8.77	136	48.84
Min.	112	73	0.05	7.44	1.94	4.14
Mean	226	139	0.10	7.83	19.03	20.57

8.2. Trace Element Concentrations of Soil in the Study Area

A total of 32 soil samples collected from the study area were subjected to complete dissolution using a hot plate digestion method. The resulting soil solutions were analyzed for the elements B, P, Ti, V, Mn, Ba, Fe, Cr, Ni, Cu, Zn, As, and Pb. The maximum, minimum, and mean concentrations of trace elements in the soil samples from the study area are presented in Table 11. The

table also includes the maximum, minimum, and mean reference values of these elements in soils reported by Bowen (1979). The concentrations obtained in this study were compared with Bowen's (1979) values to evaluate the presence or absence of potential contamination.

Table 11: Descriptive Statistics of Trace Elements in the Soils of the Study Area and Reference Values Reported by Bowen (1979).

		Concentration (mg/kg)											
		B	P	V	Cr	Mn	Fe	Ni	Cu	Zn	As	Ba	Pb
This Study (n=32)	Max.	33.7	3514	182	256	987	40588	652	29.6	403	12.4	186	26.4
	Min.	6.2	109	35.8	74.1	259	12399	53.6	6.3	1.2	0.01	31.0	9.2
	Mean	18.8	1113	77.5	138	569	25759	203	19.7	97.8	3.4	104	16.8
Bowen (1979)	Max.	270	5300	500	1500	10000	550000	750	250	900	40	3000	300
	Min.	2	35	3	5	20	2000	2	2	1	0.1	100	2
	Mean	20	800	90	70	1000	40000	50	30	90	6	500	35

According to Bowen (1979), the concentration of boron (B) in soils ranges between 2 and 270 mg/kg, with a mean value of 20 mg/kg. In the soils of the ECA, boron concentrations range between 6.17 and 33.73 mg/kg, with an average value of 18.75 mg/kg (Table 11). The boron concentrations in the study area fall within the limits reported by Bowen (1979), while the mean value is lower than Bowen's (1979) global average. It can therefore be inferred that boron pollution, particularly originating from domestic wastes (such as detergent residues) through percolation from the soil surface, is currently absent or remains at a limited level in the study area.

Phosphorus (P) tends to accumulate in agricultural soils primarily as a result of the use of phosphorus-based fertilizers. According to Bowen (1979), the concentration of phosphorus in soils ranges from 35 to 5300 mg/kg, with an average value of 800 mg/kg (Table 11). In the soils of the ECA, phosphorus concentrations vary between 109 and 3514 mg/kg, with a mean concentration of 1113 mg/kg. Although these concentrations fall within the limits reported by Bowen (1979), the mean value (1113 mg/kg) is higher than the global average of 800 mg/kg. This finding suggests that phosphorus fertilizers are used locally

in agricultural activities in the region. The critical question here is whether the phosphorus present in surface soils can reach the aquifer. A study conducted by Ece (2021) on the groundwater quality of the ECA reported orthophosphate concentrations as high as 0.353 mg/L. This indicates that the aquifer may be sensitive to phosphorus contamination. Anthropogenic sources of phosphorus include phosphate fertilizers, detergents, septic tanks, and animal wastes. To prevent potential phosphorus pollution in the ECA, it is essential to ensure the optimal use of phosphorus-based fertilizers in agricultural practices and to replace septic systems, particularly in rural settlements, with proper sewerage infrastructure.

The minimum and maximum concentrations of vanadium (V) in soils are reported as 3 mg/kg and 500 mg/kg, respectively, with a global average of 90 mg/kg (Bowen, 1979). In the surface soils of the ECA, the minimum, maximum, and mean concentrations of vanadium are 35.75 mg/kg, 182 mg/kg, and 77.54 mg/kg, respectively (Table 11). These values indicate that the vanadium concentrations in the study area soils do not exceed the reported global values.

According to Bowen (1979), the minimum and maximum concentrations of manganese (Mn) in soils are 20 mg/kg and 10,000 mg/kg, respectively, with a global average of 1000 mg/kg. In the surface soils of the study area, the minimum, maximum, and mean concentrations are 259 mg/kg, 987 mg/kg, and 569 mg/kg, respectively. The mean manganese concentration in the study area soils is therefore considerably lower than the global average concentration.

Iron (Fe), an essential nutrient element for all living organisms, has minimum and maximum concentrations in soils of 2000 mg/kg and 550,000 mg/kg, respectively, with a global average of 40,000 mg/kg (Bowen, 1992). In the soils of the study area, the minimum and maximum concentrations of iron are 12,399 mg/kg and 40,588 mg/kg, with a mean value of 25,759 mg/kg. The mean iron concentration in the study area soils is therefore considerably lower than the global average concentration reported by Bowen (1979).

The minimum and maximum concentrations of barium (Ba) in soils are reported as 100–3000 mg/kg, with an average value of 500 mg/kg (Bowen, 1979). In the surface soils of the study area, the minimum and maximum concentrations of barium are 31 mg/kg and 186 mg/kg, respectively, with a mean value of 104 mg/kg.

The chromium (Cr) concentrations in soil range from 5 to 1500 mg/kg, with an average concentration of 70 mg/kg (Bowen, 1979). In the surface soils of the ECA, the minimum, maximum, and mean concentrations of Cr are 74 mg/kg, 256 mg/kg, and 138 mg/kg, respectively (Table 11). Although the Cr concentrations in the study area fall within the global limits reported by Bowen (1979), the mean value is approximately twice the global average. There are no industrial activities in Erdemli and its surroundings that could account for elevated chromium levels in soils. The relatively high chromium concentrations in the surface soils of the ECA are instead attributed to the ophiolitic rocks outcropping in the region. The soils of the ECA are predominantly alluvial in nature, formed by clastic materials transported from higher elevations by numerous streams in the area, particularly the Alata Stream. Similarly, the mean nickel (Ni) concentration in the soils of the study area (203 mg/kg) is considerably higher than the global average of 50 mg/kg reported by Bowen (1979). The elevated Ni levels, like those of Cr, are also associated with ophiolitic rocks in the source areas. These ophiolitic units are exposed in the northern sections of the study area, where the Alata Stream traverses deep valleys. Within the boundaries of Gücüş village, numerous chromite deposits have been mined and subsequently abandoned, further supporting the geogenic contribution of Cr and Ni. Kurt (2018), in a study of surface soils (0–15 cm) in the eastern parts of Mersin Province, reported mean Cr and Ni concentrations of 117 mg/kg and 228 mg/kg, respectively, and attributed these elevated levels to the presence of ophiolitic rocks in the source region. This indicates that the soils of the lowland areas of Mersin generally contain elevated Cr and Ni concentrations. The critical issue is whether the relatively high Cr and Ni concentrations in the surface soils of the region dissolve and migrate into the groundwater system. A study by Ece (2021) on the water quality of the ECA reported that only one groundwater sample exceeded the WHO (2011) drinking water limit for Ni (50 μg/L), while no exceedances were observed for Cr. Nevertheless, it must be noted that the downward migration of elements from the unsaturated zone to the aquifer accelerates during rainy periods. Therefore, the groundwater of the ECA possesses a significant potential for contamination by geogenic chromium and nickel.

According to Bowen (1979), the maximum, minimum, and average concentrations of copper (Cu) in soils are 250 mg/kg, 2 mg/kg, and 30 mg/kg,

respectively. In the soils of the study area, the maximum and minimum Cu concentrations are 29.56 mg/kg and 6.26 mg/kg, with a mean value of 19.71 mg/kg. Similarly, Bowen (1979) reported the maximum, minimum, and average concentrations of zinc in soils as 900 mg/kg, 1 mg/kg, and 90 mg/kg, respectively. In the soils of the study area, the maximum, minimum, and mean Zn concentrations are 403 mg/kg, 1.39 mg/kg, and 97.82 mg/kg, respectively. These findings indicate that the mean concentrations of both copper and zinc in the surface soils of the ECA are fairly close to the global average values reported by Bowen (1979).

The concentration of arsenic (As) in soils ranges between 0.1 and 40 mg/kg, with an average value of 6 mg/kg (Bowen,1979). In the surface soils of the ECA, the maximum, minimum, and mean concentrations of arsenic are 12.45 mg/kg, 0.01 mg/kg, and 3.37 mg/kg, respectively (Table 11). These results indicate that arsenic concentrations in the study area soils fall within the global limits reported by Bowen (1979), while the mean value is lower than that of the global average (Table 11).

Regarding lead (Pb), the maximum, minimum, and mean concentrations in the surface soils of the ECA were all found to be lower than the corresponding values reported by Bowen (1979) (Table 11).

8.3. Soil Permeability of the Study Area

Grain size analyses were performed on the soil samples collected from the study area to determine their particle size distributions, and the corresponding graphs were plotted. Based on these grain size distribution curves, the D_{10}, D_{50}, and Io values were determined, and permeability values were subsequently calculated using the method proposed by Alyamani and Sen (1993). The spatial distribution map of the permeability values of the study area soils is presented in Figure 3. It is evident that permeability values are higher in zones dominated by coarse particles (sand). Overall, the central and coastal sections of the study area are characterized by relatively high permeability values (Figure 3).

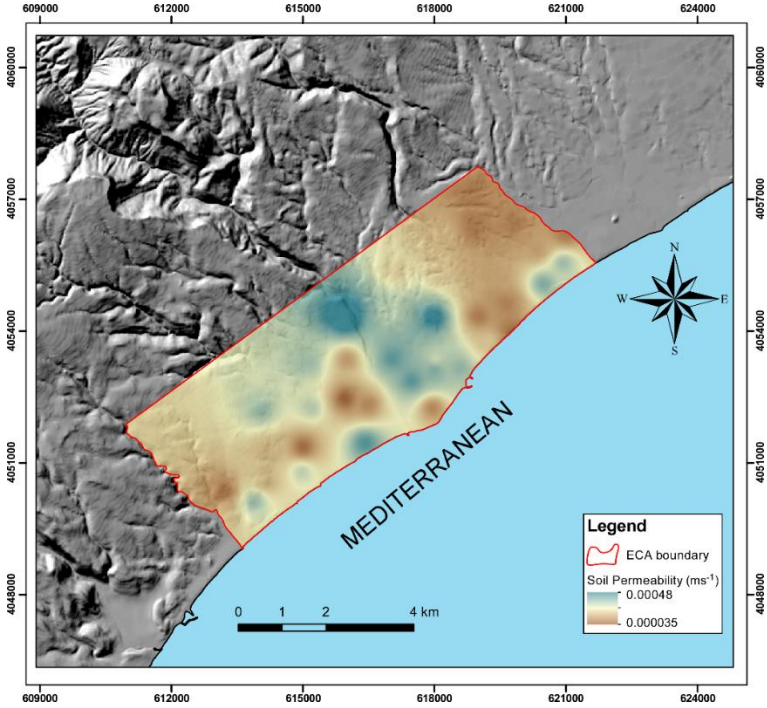

Figure 3: Spatial Distribution of Soil Permeability in the Study Area

8.4. DRASTIC Index Map of the Study Area

The DRASTIC index map of the ECA was calculated in accordance with the methodology described by Aller et al. (1987). The map was produced by multiplying the weight values assigned to each parameter by their respective class values and then summing the results. For this study, the DRASTIC index map of the study area was generated in ArcGIS using seven different parameter maps. Within ArcGIS, the "Raster Math" tool in the "Arc Toolbox" menu was employed to multiply the class values of each parameter with their respective weight values. All the resulting weighted parameter maps had a pixel resolution of 25 m and were aligned with identical row and column dimensions. Subsequently, the weighted parameter maps were combined using the "Raster Math" tool in ArcGIS to generate the unclassified DRASTIC index map (Figure 4). According to the DRASTIC index map, the minimum and maximum DRASTIC index values of the ECA were calculated as 95 and 195, respectively. Since pollution susceptibility is directly proportional to the DRASTIC index, areas with higher index values correspond to greater vulnerability.

As a result of the analyses, the ECA was classified into three vulnerability categories: low, moderate, and high. Each vulnerability class was represented by different colors, as shown in Figure 5: purple for low vulnerability (DI = 80–120), green for moderate vulnerability (DI = 120–160), and red for high vulnerability (DI = 160–200). Low-vulnerability zones are primarily observed along a northeast–southwest trending belt in the central part of the study area (Figure 5). Toward the west, this belt narrows and transitions into moderate and high vulnerability zones (Figure 5). These low-vulnerability areas are predominantly agricultural, especially citrus farming, with lemons being the main crop. It should be emphasized that agricultural activities are among the most significant contributors to groundwater pollution, and the vulnerability class is strongly influenced by both the type of land use and the pollutants associated with these activities.

Moderate-vulnerability areas are located between the high-vulnerability coastal zones (marked in red) and the low-vulnerability zones (marked in purple), generally forming an east–west oriented band (Figure 5). Land use in these moderate-vulnerability zones includes both agricultural lands and residential areas. Most of the settlement area of Erdemli town lies within this zone. Within the moderate-vulnerability areas, agricultural activities dominate the land use, with citrus orchards (mainly lemon) to the east of the Sorgun Stream, and citrus orchards, banana plantations, and tomato greenhouses to the west. In these zones, both agricultural and urban pollutants have the potential to affect the aquifer.

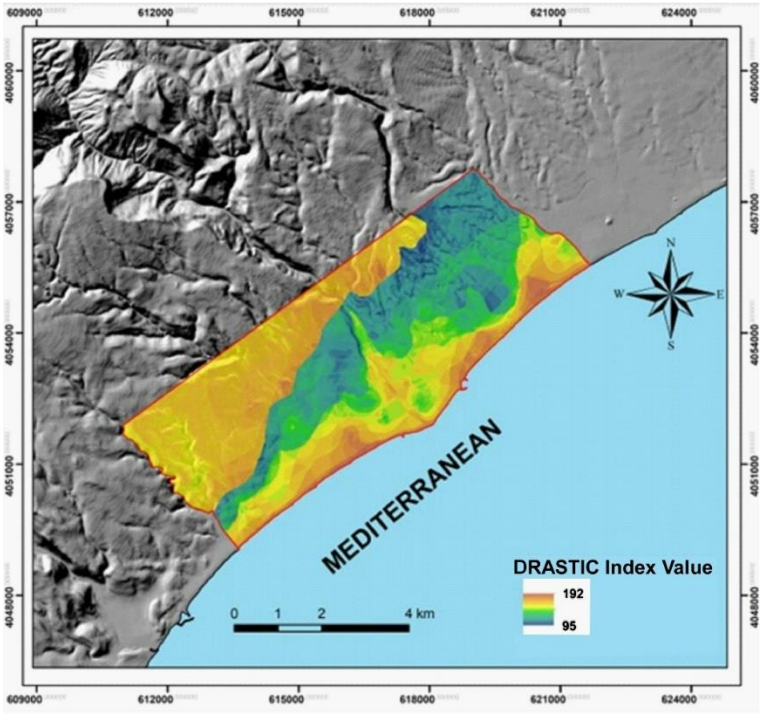

Figure 4: DRASTIC Index Map of the Study Area

The third vulnerability class in the study area corresponds to zones with high pollution susceptibility, which are observed in two distinct areas (Figure 5). The first zone extends along the Mediterranean coast, locally penetrating inland by 1–1.5 km. This coastal zone encompasses both residential areas and agricultural lands (Figure 5). It includes the most densely populated settlements of the study area. Furthermore, this coastal strip represents the section with the heaviest urban and intercity traffic and contains the highest concentration of summer houses and holiday resorts. In this zone, the groundwater table lies closer to the surface compared to other parts of the study area. The coastal zone also exhibits a high potential for seawater intrusion. Ece (2021) reported that seawater intrusion has already been observed in certain parts of the ECA. The number of summer houses and tourism facilities in this coastal zone continues to increase, along with groundwater abstraction, which is expected to exacerbate the inland advance of saline water front in the future. For all these reasons, this coastal section is considered the most vulnerable area to pollution, with the potential to transition to a very high vulnerability class in the near

future. The second high-vulnerability zone (marked in red) is located farther inland, in the central and western parts of the study area, and expands westward. This zone corresponds to a karstic aquifer system. Land use in this area is dominated by agricultural activities and small settlements (neighborhoods or vineyard/orchard houses). Agricultural practices primarily include greenhouse farming (banana and tomato) and citrus cultivation. In recent years, citrus farming has increasingly been replaced by greenhouse farming. In these transformed areas, banana cultivation—requiring higher irrigation demand—has become predominant. This trend is likely to increase water stress in the region in the future, particularly within these high-vulnerability zones.

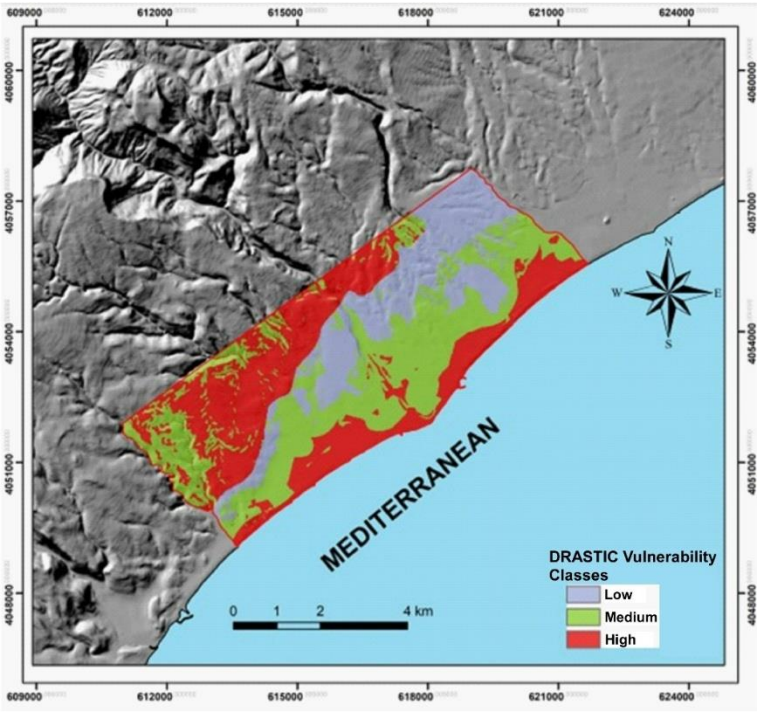

Figure 5: DRASTIC Index Vulnerability Classification Map of the Study Area

9. CONCLUSION AND RECOMMENDATIONS

The most dominant land use in the study area is agriculture, consisting mainly of citrus orchards (particularly lemon), greenhouses (for banana and tomato production), and open-field production. This study revealed that citrus

orchards are gradually being replaced by greenhouse cultivation, while both urban and rural residential areas are expanding rapidly.

To assess the impact of surface soils on aquifer vulnerability, soil samples were collected, and their physical and chemical properties were analyzed. The results indicate that the soils of the Erdemli Coastal Aquifer (ECA) are generally alkaline in nature, with relatively high nitrate and calcium carbonate contents. The elevated nitrate levels can be attributed to the excessive use of chemical and organic fertilizers. It was also determined that nitrate accumulation during fertilization periods can lead to pollution in shallow aquifers.

The study further revealed elevated concentrations of phosphorus (P), chromium (Cr), and nickel (Ni) in some parts of the study area. The high P values are linked to the use of phosphorus fertilizers in agricultural activities, while Cr and Ni are associated with ophiolitic rocks and chromite mines located in the northern parts of the basin.

The DRASTIC model results indicated that the DRASTIC Index values in the ECA range between 95 and 192. Based on these values, the aquifer was classified into three vulnerability zones: low, moderate, and high.

- Low vulnerability areas occur mainly along a northeast–southwest axis in the central part of the basin, gradually narrowing toward the west.
- Moderate vulnerability areas form a transitional east–west zone, consisting of both agricultural and residential land use.
- High vulnerability areas are located along the Mediterranean coast and in inland karstic zones in the western part of the aquifer. The coastal zone is particularly at risk due to shallow groundwater levels, urbanization, tourism facilities, and potential seawater intrusion.

The results emphasize that agricultural and urban activities are the primary contributors to groundwater contamination risk in the ECA. Without adequate management, the coastal zone may shift from high to very high vulnerability in the future due to increased groundwater use, expansion of summer houses, and intensified greenhouse farming.

In the context of global warming and increasing droughts, groundwater use has become more critical, while contamination risks are simultaneously rising due to anthropogenic activities. Coastal aquifers are among the most vulnerable systems in this regard. The ECA, which plays a vital role in

sustaining agricultural production in the region, is under growing pressure from rising population and agricultural water demand.

Therefore, the implementation of sustainable water management practices is crucial. Specifically, the 4R principles (Reduce, Recycle, Reuse, and Recover) should be urgently applied in order to minimize contamination risk and ensure the long-term sustainability of the aquifer

REFERENCES

Aller, L., Bennett, T., Lehr, J. H., Petty, R. J., & Hackett, G. (1987). *DRASTIC: A standardized system for evaluating ground water pollution potential using hydrogeologic settings*. USEPA, Ada, Oklahoma, USA.

Alyamani, M. S., & Sen, Z. (1993). Determination of hydraulic conductivity from grain-size distribution curves. *Groundwater*, *31*, 551-555.

Bowen, H. J. M. (1979). *Environmental chemistry of the elements*. Academic Press.

Dökmeci, A. H. (2005). *Gala Gölü ve gölü besleyen su kaynaklarındaki ağır metal kirliliğinin araştırılması*. [Master's thesis, Trakya Üniversitesi Fen Bilimleri Enstitüsü].

Dündar, M., Altundağ, H., Kaygaldurak, S., Şar, V., & Acar, A. (2012). Çeşitli endüstriyel atık sularda ağır metal düzeylerinin belirlenmesi. *SAÜ Fen Bilimleri Dergisi*, *16*(1), 6-12.

Dürgen, G. A. (2012). *Mersin ili Erdemli ilçesi'nin sosyo-ekonomik ve kültürel yapısı*. [Master's thesis, Niğde Üniversitesi].

Ece, F. (2021). *Erdemli (Mersin) kıyı akiferinin su kalitesinin araştırılması*. [Master's thesis, Mersin Üniversitesi].

Gogu, R. C., Hallet, V., & Dassargues, A. (2003). Comparison of aquifer assessment techniques application to the Neblon River Basin (Belgium). *Environmental Geology*, *44*, 886.

Güleç, A. (2013). *Türkiye'de organik ve klasik yöntemlerle üretilen zeytinyağlarının ağır metal içeriğine yönelik bir araştırma* [Doctoral dissertation, Hacettepe Üniversitesi Sağlık Bilimleri Enstitüsü].

Hakerlerler, H., Okur, B., & Yağmur, B. (1995). *Gediz havzasında yollara yakın arazilerde motorlu araç trafiğinden kaynaklanan ağır metal kirlenmesi üzerine bir araştırma*. Gediz Havzası Erozyon ve Çevre Sempozyumu Bildiriler Kitabı, 10-11 Ekim 1995, 138-148.

Kocaer, O., & Başkaya, H. (2003). Metallerle kirlenmiş toprakların temizlenmesinde uygulanan teknolojiler. *Uludağ Üniversitesi Mühendislik-Mimarlık Fakültesi Dergisi*, *8*(1), 121-131.

Kurt, M. A. (2010). *Deliçay ve Tarsus Çayı (Mersin) arasında kalan alandaki toprak profillerinin mineralojisi, toprak ve su kirliliğinin araştırılması.* [Doctoral dissertation, Mersin Üniversitesi].

Kurt, M. A. (2018). Comparison of trace element and heavy metal concentrations of top and bottom soil in a complex land use area. *Carpathian Journal of Earth and Environmental Sciences*, *13*(1), 47-56.

Lynch, S. D., Reynders, A. G., & Schulze, R. E. (1994). Preparing input data for a national-scale groundwater vulnerability map of southern Africa. *Water South Africa*, *20*, 239-246.

Mikanov, O. (2006). Effects of heavy metals on some biological parameters. *Journal of Geochemical Exploration*, *88*, 220-223.

Muslu, Y. (1985). *Su temini ve çevre sağlığı* [Master's thesis, İstanbul Teknik Üniversitesi].

Okcu, M., Tozlu, E., Kumlay, M. A., & Pehluvan, M. (2009). Ağır metallerin bitkiler üzerine etkileri. *Alınteri Zirai Bilimler Dergisi*, *17*(B), 14-26.

Piscopo, G. (2001). *Groundwater vulnerability map, explanatory notes, Castlereaght catchment, NSW*. Department of Land and Water Conservation.

Raven, J. A., Evans, M. C. W., & Korb, R. E. (1999). The role of trace metals in photosynthetic electron transport in O2-evolving organisms. *Photosynthesis Research*, *60*(2), 111-149.

Rayment, G. E., & Higginson, F. R. (1992). *Australian laboratory handbook of soil and water chemical methods*. Reed International Books Australia.

Remesan, R., & Panda, R. K. (2008). Groundwater vulnerability assessment, risk mapping, and nitrate evaluation in a small agricultural watershed: Using the DRASTIC model and GIS. *Environmental Quality Management*, *18*(1), 53-74.

Turkish Statistical Institute. (2025). *The results of address based population registration system (ABPRS)*. https://biruni.tuik.gov.tr/medas/?kn=95&locale=tr (accessed September 10, 2025).

Turyay, Z. (2015). *Köyceğiz-Dalyan havzasının yeraltı suyu kirlenme potansiyelinin DRASTIC yöntemi kullanılarak belirlenmesi* [Master's thesis, İstanbul Teknik Üniversitesi].

Vrba, J., & Zaporozec, A. (1994). *Guidebook on mapping groundwater vulnerability*. Hannover: Heinz Heise.

Wickfors, G. H., & Ukeles, R. (1982). Growth and adaptation of estuarine unicellular algae in media with excess copper, cadmium, or zinc. *Marine Ecology Progress Series*, *7*, 191–206.

World Health Organization. (2011). *Guidelines for drinking water quality (4th ed.)*. WHO Publications.

Yalçın, S. (2019). *İncesu ile Kayseri bölge toprakları arasındaki ağır metallerin kökeninin ve alansal dağılımının belirlenmesi* (Unpublished master's thesis). Mersin Üniversitesi, Mersin.

Yavuz, V. S. (2017). *Batman Ovası'nın yeraltı suyu potansiyeli ve kalitesinin coğrafi bilgi sistemi ile modellenmesi* (Unpublished doctoral dissertation). Dicle Üniversitesi, Diyarbakır.

Yıldırım, Ü. (2023). Evaluation of groundwater vulnerability in the Upper Kelkit Valley (Northeastern Turkey) using DRASTIC and AHP-DRASTIC-LU models. *ISPRS International Journal of Geo-Information*, *12*(6), 251. https://doi.org/10.3390/ijgi1206025151

CHAPTER 6

THE IMPACT OF GREENHOUSE GASES ON CLIMATE CHANGE

Assist. Prof. Dr. Cihan PALOLUOĞLU[1]

DOI: https://dx.doi.org/10.5281/zenodo.17847624

[1] Bayburt University, Faculty of Art and Design, Department of Interior Architecture and Environmental Design, Bayburt, Türkiye. cpaloluoglu@bayburt.edu.tr, ORCID ID: 0000-0002-8635-8315

INTRODUCTION

Climate change has been a natural process since the Earth's creation, continuing to the present day. These processes are a system that moves through various formations. This system encompasses the multilayered atmosphere that surrounds the Earth and extends to the outermost layer of the Earth's atmosphere. Another important component of the system is the hydrological cycle. The components of this other system can be listed as the biosphere, terrestrial lands, and oceans. Thus, the climate system supports the formation of these important and active systems. This climate system, which is formed by natural processes, can also undergo fragmentation due to unnatural processes. Greenhouse gases are among the most significant anthropogenic effects. Greenhouse gases have very detrimental effects on the climate and living organisms. The most important known greenhouse gases are CO_2 (Carbon dioxide), CH_4 (Methane), Nitrous Oxide (N_2O), water vapor, and fluorinated gases (CFCs) (Table 1). These gases are released into the atmosphere from various anthropogenic sources and surround the Earth as a gas cloud. These gases can also trap radiation waves that should travel from the Earth to space. The greater the presence of these heat-trapping greenhouse gases, the greater the temperature difference between the Earth's crust and the atmosphere. In fact, the presence of these heat-trapping gases in the atmosphere at normal levels is a natural process. Their absence also poses significant risks. At the same time, if these heat-trapping gases are present at lower-than-normal levels, the Earth's surface cools excessively. If these gases are present at higher-than-normal levels, the Earth's temperature increases, triggering global warming (Manabe, 2019). However, in the last century, especially with the Industrial Revolution, these greenhouse gases have been produced in excessive quantities and released into the atmosphere. This situation is currently demonstrating its destructive, destructive, and disruptive effects, starting with global warming and ultimately leading to climate change (Filonchyk et al., 2024).

Greenhouse gases, which have highly detrimental effects today, can be emitted from various anthropogenic sources. The primary reason for the increase in greenhouse gases resulting from industrial and technological demands stems from the excessive use of fossil fuels for energy and heating. Another contributing factor is the uncontrolled expansion of urban settlements into agricultural land. Literature indicates that greenhouse gases released from

artificial/anthropogenic sources are the gases that most significantly impact climate change and are a determining factor (Cassia, 2018; Bilgili, 2024). This unintentional increase in greenhouse gases leads to increased heat retention in the atmosphere, thereby significantly altering the Earth's energy balance. It also leads to an increase in the Earth's current average surface temperature. This, in turn, leads to changes in seasonal changes and weather events occurring in different regions of the world. This also increases the intensity and frequency of these weather events.

The effects of greenhouse gases on climate change can be summarized as follows: 1. Increased temperatures and heat stress resulting from a rise in the average global temperature. 2. Increased melting of glaciers and winter snow cover, resulting in rising sea levels. Heat storage in the oceans also contributes to temperature increases. 3- Adaptation to these processes or deterioration in the biosphere and ecosystem structures, which are climate systems. 4- Acceleration of climate feedback due to climate change. This can be explained as follows: Temperature increases are likely to be even greater year after year (Bilgili, 2024). Furthermore, as agricultural lands are converted into urban areas, the degradation of these natural sources of CO2 also increases. Thus, some models clearly demonstrate the decrease in the amount of natural carbon-holding sinks (forests, vegetation, trees, etc.) (Denisov et al., 2021). As mentioned above, greenhouse gases not only increase Earth's temperature. They can also increase ocean acidification rates. They also contribute to the extinction of biodiversity and the loss of species. They also alter the hydrological cycle. Most importantly, they have serious and destructive effects on human health. CH_4 and N_2O, the most concentrated greenhouse gases, have shorter half-lives than CO_2 but also have greater heat-trapping properties than CO_2 (Filonchyk et al., 2024). When these conditions are examined, greenhouse gases not only affect the physical structure of the Earth. Along with physical processes, they also significantly impact human health, social structures, and the economy, making them one of the most pressing environmental issues of our time.

Greenhouse gases disrupt the Earth's energy balance by trapping radiation reflected from the Earth's surface and atmosphere, as well as trapping infrared radiation from the Sun within the atmosphere. Thus, a significant process is underway that causes temperature increases. CO_2 is the most

dominant greenhouse gas. The primary source of this is the burning of fossil fuels and the transition to different methods in agricultural lands. Furthermore, because CO_2 has a longer half-life (the time it remains in the atmosphere) than other greenhouse gases, it is a significant contributor to heat accumulation (Fawzy et al., 2020). Another greenhouse gas is methane. Unlike CO_2, methane has a short half-life. However, it has a significant heat storage capacity in the atmosphere. Recently, its amounts have been increasing in direct proportion to the growth of the agricultural and energy sectors (Saunios et al., 2020). N_2O is among the primary causes of climate change, as it settles in the ozone layer and poses a threat from both sides. Fertilization processes in agricultural activities are among their primary sources (Tian et al., 2020).

Furthermore, fluorinated greenhouse gases, which cause significant global warming due to their high heat-trapping properties, have become a significant threat on a global scale. The primary sources of fluorinated gases are cooling systems (air conditioners, etc.) and the electronics industry (Velders et al., 2022). Tropospheric ozone and water vapor, as well as other greenhouse gases with short atmospheric lifetimes, contribute to global warming through feedback mechanisms and pose a significant risk (Zhang et al., 2023). To mitigate the apparent impacts of these greenhouse gases and maintain effective climate change policies, greenhouse gases must be monitored rigorously. At the same time, urgent efforts to reduce and control policies must be implemented (Table 1).

This book chapter provides a detailed presentation under the title "The Impact of Greenhouse Gases on Climate Change." First, the nature, sources, and growth trends of greenhouse gases will be examined from different perspectives. Then, their direct and indirect effects on climate change will be investigated. Temporal and spatial changes will be discussed, and the policies and response methods of various countries will be examined. This chapter also explains greenhouse gases and their effects in Türkiye, and clarifies Turkey's current position on this issue. Their interactions in the field of air pollution will be presented, particularly from the perspective of an environmental engineer. Thus, greenhouse gases will be discussed alongside air pollutants, and their potential impact on climate change will be reported. Thus, this book will provide a detailed overview of the topics from an environmental engineering perspective, and by combining them with scientific

assessments, the current status will be presented in a clear and organized manner.

Table 1: Greenhouse Gases, Their Sources and Effects.

Greenhouse Gas	Main Formation Sources	Primary Climate Impacts	Scientific Explanation and Recent Literature
Carbon Dioxide (CO_2)	Fossil fuel combustion, cement production, deforestation, land-use change	Primary driver of global warming; long atmospheric lifetime; ocean acidification	CO_2 is the dominant component of total anthropogenic greenhouse gas emissions and can persist in the atmosphere for centuries. The energy sector and industrial processes are the main contributors to increasing CO_2 levels (Fawzy et al., 2020).
Methane (CH_4)	Agriculture (ruminant livestock), rice paddies, landfills, natural gas and oil extraction	Much higher warming potential than CO_2 (GWP ~28–34); strong short-term warming effect	CH_4 is a short-lived climate pollutant but exhibits a warming effect up to 80 times stronger than CO_2 over short timeframes. Global methane concentrations have been rising rapidly in recent years (Saunois et al., 2020).
Nitrous Oxide (N_2O)	Nitrogen-based fertilizers, agricultural soils, biomass and fossil fuel combustion, industrial processes	Very high global warming potential; contributes to stratospheric ozone depletion	N_2O is a long-lived greenhouse gas and currently the only major anthropogenic gas responsible for ongoing ozone layer depletion. Agriculture accounts for nearly two-thirds of global N_2O emissions (Tian et al., 2020).
Fluorinated Gases (HFCs, PFCs, SF_6, NF_3)	Refrigeration/air-conditioning systems, semiconductor manufacturing, aluminum and magnesium industries	Extremely high GWP (thousands of times greater than CO_2); very long atmospheric persistence	Even small quantities of fluorinated gases exert strong climate forcing. Particularly, SF_6 and PFCs can remain in the atmosphere for thousands of years (Velders et al., 2022).
Tropospheric Ozone (O_3)	Photochemical reactions of NO_x and VOC emissions	Short-lived climate pollutant; warming effect; adverse health impacts	Tropospheric O_3 is a short-lived climate pollutant formed through human-driven emissions and significantly contributes to near-term warming trends (Zhang et al., 2023).
Water Vapor (H_2O)	Natural evaporation processes; increased atmospheric moisture due to warming	Strong natural greenhouse effect; positive feedback mechanism	Although not directly anthropogenic, warming increases atmospheric H_2O concentrations, amplifying greenhouse warming through

1. STUDY AREA

1.1. Effects of Greenhouse Gases on Climate Change

Greenhouse gases are hazardous gases that absorb radiation reflected from the Earth's surface and then reflect infrared (IR) radiation to the Earth's surface. They are recognized as the primary cause of global warming. The effects of greenhouse gases can be categorized into two groups: natural and anthropogenic. The natural greenhouse effect, specifically the greenhouse

effect that existed before the industrial revolution in Earth's history, is a series of natural processes that maintain the Earth at livable temperatures. The anthropogenic greenhouse effect is a hazardous process that emerged after the Industrial Revolution and contributes to global warming (Figure 1). Greenhouse gases, which have contributed to increasing global warming over the last 50 years, have become a central focus of climate change studies. These studies provide detailed information on the structure of greenhouse gases, their sources of formation, and their movement in the atmosphere (Fawzy et al., 2020).

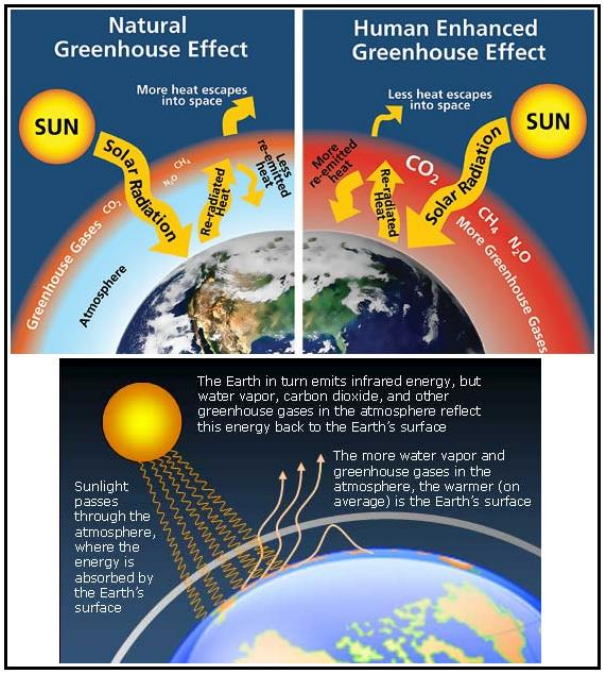

Figure 1: Greenhouse Gases and the Greenhouse Effect (URL-1)

2.2. Greenhouse Gases and their Properties

2.2.1 Carbon Dioxide (CO_2)

With the Industrial Revolution, the burning of fossil fuels, including oil, coal, and natural gas, released substantial amounts of anthropogenic CO_2 into the atmosphere. At the same time, the destruction of forests, which are the primary source of sinks, and industrial activities increase the amount of anthropogenic CO_2. CO_2 is one of the gases that contributes most significantly

to global warming. This is due to its long atmospheric half-life and its strong heat-trapping properties. CO_2 also plays a significant role in ocean acidification. This occurs when excessive anthropogenic CO_2 released from the ocean surface is absorbed, disrupting the carbonate balance. For these reasons, CO_2 can have dual effects, having both thermal and chemical effects (Table 1) (Fawzy et al., 2020).

2.2.2. Methane (CH_4)

Methane gas, despite its short half-life in the atmosphere, is a very potent greenhouse gas. Methane is approximately 28-34 times more potent than CO_2 in terms of its global warming impact. Methane gases released from livestock farming, rice production, waste storage facilities, household composting, and leaks from fossil fuel-burning plants have a significant impact on global warming (Table 1) (Saunios et al., 2020).

2.2.3. Nitrous Oxide (N_2O)

Nitrogen monoxide gases are among the primary greenhouse gases that contribute to the depletion of the stratospheric ozone layer. Their most significant sources are nitrogen fertilizers used in agriculture. Increasing agricultural activities in our age are also causing significant increases in N_2O emissions (Tian et al., 2020). Furthermore, the long-term lifespan of N_2O greenhouse gases in the atmosphere, which spans up to 120 years, indicates that their impact on climate change will continue to increase in the long term (Table 1).

2.2.4. Fluorinated Gases (CFCs)

Fluorinated gases such as HFCs, PFCs, SF_6, and NF_3 originate from industrial sources and are considered hazardous greenhouse gases. Therefore, they can increase the global warming potential thousands of times that of CO_2. These fluorinated gases, commonly used in air conditioning systems, are primarily sourced from cooling systems. They are also known to originate from the foam production, electronics sector, and perfume industry. Even very small amounts can easily increase the global warming potential. Therefore, fluorinated gases are among the most critical components of climate change policies (Table 1) (Velders et al., 2022).

2.2.5. Ozone and Water Vapor

Tropospheric ozone is formed as a result of photochemical reactions between NO_x and VOCs in the atmosphere. Due to this formation pattern, they are classified as short-lived air pollutants. Ozone gases are known to trigger global warming. They also pose a serious threat to human health through respiration (Zhang et al., 2023). Water vapor, another greenhouse gas, is not an anthropogenic greenhouse gas; however, it increases atmospheric water vapor concentration with increasing temperatures. Furthermore, it can cause temperature increases by strengthening positive feedback systems (Table 1).

The effects of natural and anthropogenic greenhouse gases on climate change should not be limited to temperature alone. In addition to their capacity to increase temperature, these gases also have profound impacts on various climatic processes currently occurring worldwide. These include melting glaciers, rising sea levels, increased frequency and severity of extreme weather events, disruptions to the hydrological system, ecosystem degradation, and severe impacts on human health. Furthermore, considering the physical and chemical reactions that anthropogenic greenhouse gases released into the atmosphere interact with one another, they appear to trigger feedback mechanisms within the atmosphere. Thus, their unpredictable and irreversible risks to climate systems are increasingly evident (Zhang et al., 2023) (Figure 2).

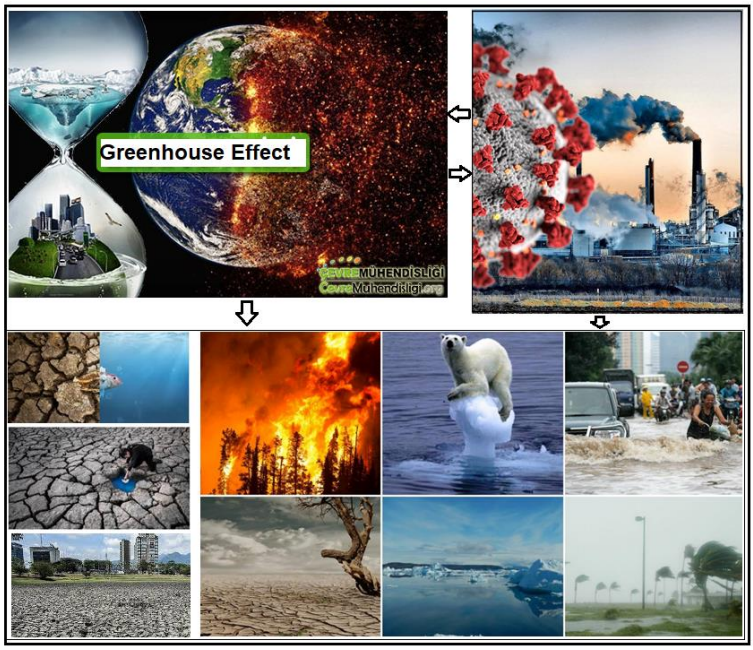

Figure 2: Adverse Effects of the Greenhouse Effect on Climate Change (URL-2; URL-3)

When all greenhouse gases are examined, and their mechanisms of action are understood, the picture that emerges is that they are the most critical components determining the balance of the climate system. In particular, anthropogenic CO_2, CH_4, N2O, and fluorinated gases are the primary drivers of global warming. In our age, countries must develop action policies to combat these gases as quickly as possible to address the ever-increasing risks. These policies should be actively pursued by implementing a range of applications and methodologies, including emission reduction strategies, energy conversion practices, agricultural management practices, and innovative climate modeling methods in industrial studies.

2.3. Effects of Greenhouse Gases on Human Health

The rise in temperatures and the greenhouse effect, resulting from increased greenhouse gases in the atmosphere, are being felt worldwide. These undesirable increases have a direct or indirect impact on human health. Long-lived greenhouse gases, primarily CO_2, released into the atmosphere significantly alter the frequency and intensity of heat waves. Changing heat

waves trigger numerous adverse human health issues, including respiratory failure and cardiovascular disease (Table 2). Numerous studies have found that changing heat waves increase mortality rates, particularly among the elderly and children, as well as those with other chronic diseases (Vicedo-Cabrera et al., 2021).

Methane, another greenhouse gas, is recognized as both a heat-trapping gas that exacerbates the warming effect of climate change and a primary component in tropospheric ozone formation. Tropospheric ozone can cause respiratory diseases, asthmatic conditions such as bronchitis, and permanent lung damage. Increased levels of methane, a greenhouse gas in the atmosphere, and consequently increased tropospheric ozone, cause severe damage, particularly in patients with asthma and COPD (Table 2). Numerous studies in the literature emphasize that ozone-related respiratory diseases are increasing in parallel with the accelerated greenhouse effect (Zhang et al., 2023).

N_2O, another greenhouse gas with a significant risk, depletes the stratospheric ozone layer. UV-B radiation can easily reach the Earth's surface from this thinning layer. People exposed to UV-B radiation are also at increased risk of developing skin cancer. It also causes cataracts in the eyes and weakens the immune system (Tian et al., 2020). Furthermore, increasing global warming has been linked to a rise in the rate of spread of infectious diseases. These diseases, in particular, are contributing to the increasing incidence of malaria, dengue fever, West Nile virus, and Lyme disease. These diseases have been found to spread both at their source and by expanding northward (Ryan et al., 2020).

One of the greenhouse effect's most significant impacts is on climate change systems. Both physical changes (floods, storms, extreme weather events, forest fires, etc.) and risky events such as the increase in direct food-borne and water-borne diseases are developing simultaneously within climate systems. In particular, rising temperatures lead to the proliferation of Vibrio and Salmonella bacteria, which cause acute gastroenteritis, a contagious disease characterized by abdominal pain, nausea, vomiting, and diarrhea (Table 2). At the same time, the risk of highly contagious diseases, such as cholera, increases due to the increased prevalence of these viruses and bacteria (Phillips et al., 2021). Studies on the diagnosis, frequency, and recurrence of certain diseases have found an increase in deaths from cardiovascular diseases. One of the

primary reasons for this is the recent release of high concentrations of PM2.5 into the atmosphere, attributed to the increase in forest fires resulting from rising temperatures associated with global warming (Chen et al., 2021).

Considering all these results, greenhouse gases cannot be considered solely as a result of global warming and rising temperatures. They should also be considered and evaluated as a complex process that has a direct impact on human health. To reduce the risk of widespread and infectious diseases that humanity may face in the future, it is crucial to rapidly control greenhouse gases, which have long half-lives, and air pollutants, which have shorter half-lives than greenhouse gases, and accelerate their removal at the source.

Table 2: Greenhouse Gases and the Effects of the Greenhouse Effect on Human Health and the Diseases They May Cause.

Greenhouse Gas / Climate Stressor	Formation Sources	Human Health Effects	Diseases Associated with Greenhouse Effect
Carbon Dioxide (CO_2)	Fossil fuel combustion, industrial processes, deforestation	Increases heatwave frequency, causing heat stress	Heatstroke, cardiovascular stress, respiratory distress, dehydration
Methane (CH_4)	Agriculture, landfills, oil/gas infrastructure	Enhances tropospheric ozone formation, impairing lung function	Asthma, COPD exacerbations, upper respiratory infections
Nitrous Oxide (N_2O)	Agricultural soils, fertilizer use, biomass burning	Indirectly contributes to warming; promotes ozone depletion	UV-related skin cancer, cataracts, immune suppression
Fluorinated Gases (HFCs, PFCs, SF_6)	Refrigeration systems, electronics industry	High GWP leads to long-term global warming	Heat-related cardiovascular events, spread of vector-borne diseases
Tropospheric Ozone (O_3)	NO_x + VOC photochemistry	Strong respiratory toxin; causes lung inflammation	Asthma attacks, bronchitis, reduced lung function
Rising Temperatures (Due to Greenhouse Effect)	Anthropogenic increase in greenhouse gases	Thermal stress, electrolyte imbalance	Heatstroke, cardiac arrhythmias, kidney failure
Extreme Weather Events	Climate change	Traumatic injuries, waterborne illnesses	Leptospirosis, cholera, salmonella, increased infectious diseases
Spread of Biological Agents	Increased temperature and humidity	Expansion of mosquito, tick, and animal pathogen ranges	Malaria, dengue fever, Lyme disease, West Nile virus
Deterioration of Air Quality (PM, O_3, smoke)	Fossil fuel use, wildfires, industrial emissions	Respiratory and cardiovascular toxicity	COPD, asthma, lung cancer, myocardial infarction, stroke

3. MATERIALS AND METHODS

3.1. How to Reduce Greenhouse Gases and the Greenhouse Effect? Key Precautions and Measures to be Taken

As a result of the increasing amount of anthropogenic greenhouse gases released into the atmosphere during the Industrial Revolution, the greenhouse effect is becoming increasingly stronger. This strengthening greenhouse effect is the primary cause of climate change, particularly global warming. Therefore, all countries around the world must immediately take measures to reduce greenhouse gas emissions. Adequately combating the greenhouse effect will both reduce pressures on the climate system and pave the way for sustainability in the fight against the long-term effects of the greenhouse effect. Two primary methods should be selected to reduce greenhouse gas emissions. The first is to strengthen control and removal mechanisms at the source. The second is to strengthen natural sinks (protecting existing forests and trees, reducing forest fires, and increasing the number of trees and forests by urgently replanting trees in burned forest areas) (Fawzy et al., 2020).

Another method for reducing greenhouse gases is to deviate from existing norms and implement new transformations in the energy sector. Fossil fuels are the most commonly burned fuels for energy production in industry. As a result, CO_2 emissions are higher than usual. To reverse these increases, fossil fuels must be replaced with clean, environmentally friendly renewable energy models such as solar energy, wind energy, hydroelectric energy, biomass, and geothermal energy. Furthermore, recent price reductions in renewable energy costs across countries have significantly contributed to both the realization of these energy transformations and their increasing numbers (IEA, 2022). Thus, the increasing number of applications for renewable energy projects, both individually and institutionally, will reduce the reliance on fossil fuels and ultimately lead to reductions in CO_2 levels.

The second important step in reducing CO_2 emissions is to reduce the carbon footprint of land, air, rail, and maritime transportation systems. Key steps in this area include increasing the prevalence of electric vehicles and increasing public transportation capacity. Designing more and more practical bicycle and walking paths will also contribute to a gradual reduction in CO_2 and NO_x emissions from the overly demanding transportation sector.

Furthermore, a medium-term solution would be the implementation of fuel cell conversions and hydrogen technologies (Creutzig et al., 2022).

Among the primary measures to reduce CH_4 and N_2O emissions are agricultural activities and land management. Livestock production is the sector that emits the most methane. The establishment of biogas plants in this sector is essential. Furthermore, improving feed conversion and waste management is crucial for reducing methane gas. Water management processes used in rice planting and harvesting, particularly in rice fields, should be modified to improve efficiency. Instead, increasing dryland farming techniques will significantly reduce methane emissions (Saunois et al., 2020). Meanwhile, reducing nitrogen fertilizer use will also have a significant impact on N_2O emissions. Furthermore, controlling fertilizer distribution and regularly monitoring cooling system maintenance are measures that will significantly reduce N_2O emissions.

Measures taken against fluorinated gases used in industrial areas, cooling systems, and air conditioners are among the methods that will significantly reduce the greenhouse effect. In combating fluorinated gases such as HFC and SF_6, the initial step should be to replace gases with high global warming capacity with those with low global warming capacity. This will both reduce leaks and ensure regular maintenance of cooling systems (Velders et al., 2022).

Another measure to reduce the greenhouse effect in daily life is to strengthen carbon sinks. Forests, in particular, as well as land and oceans, can absorb a significant portion of the CO_2 released into the atmosphere. Therefore, all countries around the world must rapidly reverse the deforestation they are either consciously or unconsciously causing on their lands. Together, everyone should prioritize reforestation. New trees destroyed by forest fires should be planted to replace them. Expanding the surface area of forests is also a crucial step in maintaining the carbon balance through ecosystem reconstruction (Houghton & Nassikas, 2020). In addition to sinks, expanding marine and ocean carbon ecosystems, expanding seagrass meadows, protecting and increasing the number of forests with high carbon sequestration capacity, such as mangrove forests, and protecting and restoring coastal marshes will all help resolve stalled climate policies as they develop high carbon sequestration capacities.

In addition to these natural control methods, anthropogenic sinks, which are also highly effective, serve as additional control methods. Anthropogenic sinks enable carbon capture and storage (CCS). These are highly innovative methods that can reduce and eliminate carbon dioxide at its source. These innovative methods can significantly reduce the amount of CO_2 released from cement factories, iron and steel plants, and power generation facilities, which all emit high amounts of greenhouse gas emissions (Fawzy et al., 2020). Furthermore, controlling other short-lived air pollutants released into the atmosphere from urban and rural areas will significantly reduce the impact of greenhouse gases and thus reduce the strength of the greenhouse effect. Furthermore, controlling and combating gases such as methane, tropospheric ozone, water vapor, and black carbon will also reduce temperature increases, albeit in the short term, thereby mitigating the impact of global warming (Zhang et al., 2023).

On the other hand, if the international agreements reached by countries (such as the Paris Agreement, emissions trading systems, carbon taxes, etc.) are fully implemented, global emissions will be significantly reduced. Furthermore, specific policies will support the acceleration of climate change implementation in developing countries. Chief among these are climate finance, green investment mechanisms, and technological transfer tools.

From a general perspective, multifaceted approaches must be addressed to reduce the greenhouse effect globally. This will be achieved through rigorous implementation that encompasses agriculture, energy, industry, transportation, ecosystem management, and similar processes. Furthermore, technological and political solutions must work together collectively. This will achieve global climate goals and truly combat the greenhouse effect. Otherwise, the global failure to adequately combat greenhouse gases will only lead to the summary results we have seen and will experience (Figure 3).

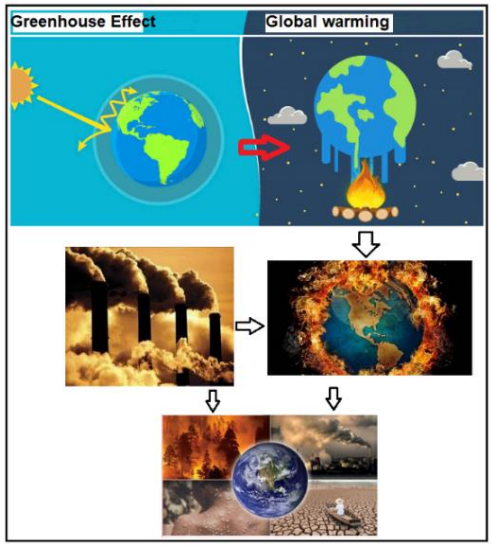

Figure 3: Negative Situations the World Faces if the Greenhouse Effect is Not Combated (URL-4; URL-5)

As can be seen from Table 3, the precautionary policies to be taken regarding the above-mentioned greenhouse gases are presented below in summary form;

Table 3. Main measures that can be taken against the greenhouse effect

Mitigation Area	Recommended Application	Expected Impact	Scientific Basis / Explanation
1. Energy Transition	Transition from fossil fuels to renewable energy (solar, wind, biomass, geothermal)	Significant reduction in CO_2 emissions	Renewable energy technologies reduce fossil fuel dependence in global energy systems, lowering greenhouse gas emissions (IEA, 2022).
2. Energy Efficiency	Insulation, low-energy appliances, efficient industrial systems	Decrease in energy demand; reduction in emissions	Efficiency measures are among the fastest strategies for immediate CO_2 reduction (Fawzy et al., 2020).
3. Decarbonization of Transportation	Electric vehicles, public transportation, cycling infrastructure	Reduction in transport-related CO_2, NO_x, and PM	Electric mobility significantly reduces carbon emissions and air pollutants in urban areas (Creutzig et al., 2022).
4. Agricultural and Livestock Management	Biogas plants for methane reduction, feed modification; precision fertilizer management	Reduction in CH_4 and N_2O emissions	Agricultural improvements reduce short-lived climate pollutants and nitrous oxide emissions (Saunois et al., 2020; Tian et al., 2020).
5. Industrial Emission Control	Replacing fluorinated gases with low-GWP alternatives	Strong reduction of high-impact HFC, PFC, and SF_6 emissions	Fluorinated gases have extremely high carbon-equivalent impacts; mitigation offers major climate benefits (Velders et al., 2022).
6. Strengthening Carbon Sinks	Forest conservation, afforestation, ecosystem restoration	Natural reduction of atmospheric CO_2	Forests and soil carbon sinks play a critical role in the global carbon cycle (Houghton & Nassikas, 2020).
7. Carbon Capture and Storage (CCS/CCU)	Capturing and storing CO_2 from industrial facilities	Rapid mitigation in high-emission sectors	CCS is effective in cement, energy, and metallurgical industries (Fawzy et al., 2020).
8. Reduction of Short-Lived Climate Pollutants (SLCPs)	Methane, black carbon, and tropospheric ozone control	Rapid temperature decline; short-term climate benefits	Mitigating SLCPs provides climate benefits within 10–20 years (Zhang et al., 2023).

4. RESULTS AND DISCUSSIONS

4.1. Current Status of the Greenhouse Effect in Türkiye

Türkiye is geographically located in the global transition zone between the Middle East and the Eastern Mediterranean. Due to its location, it is considered one of the country's most affected by the greenhouse effect. While excessive warming due to the greenhouse effect is observed regionally in Türkiye, it also experiences extreme weather events. The greenhouse effect, as detailed above, is the result of CO_2, water vapor, methane, N_2O, and similar gases accumulated in the atmosphere, which reflect sunlight off the Earth's surface and trap long-wave radiation from the Sun. This directly disrupts the global energy balance. From Turkey's perspective, the ever-increasing emissions released into the atmosphere from various regions and industries in Türkiye contribute to the global accumulation. Furthermore, due to both this contribution to the global accumulation and increasing greenhouse gas emissions, statistics measuring drought, heat, precipitation, storms, and many other extreme weather events in Türkiye are changing.

In Türkiye, thanks to the Turkish Statistical Institute (TÜİK, 2025), numerical and statistical data are available on our global greenhouse gas contribution. According to the "Greenhouse Gas Emission Statistics for 1990-2023" report published by TÜİK, greenhouse gas emissions for 2023 increased by 6.9% compared to the previous year. This increase resulted in CO_2 reaching 598.9 Mt. Per capita emissions were also calculated to be equivalent to 7 tons of CO_2. Furthermore, the study revealed that the energy sector accounts for the highest total emissions in Türkiye, accounting for 73.8%. The remaining percentages are listed as follows: agriculture accounts for 12%, product use and industrial processes account for 11.8%, and the waste sector accounts for 2.3%. Furthermore, an examination of the Istanbul Commodity Exchange tables reveals that greenhouse gas emissions in Türkiye are primarily caused by energy and fuel consumption.

A review of international energy statistics, in conjunction with national statistics, yields similar results. According to the International Energy Agency (IEA), Turkey's energy-related CO_2 emissions are estimated to have reached 392 Mt as of 2023. This CO_2 emission in Türkiye has been reported to account for approximately 1.1% of global CO_2 emissions. Furthermore, the use of fossil fuels, such as coal and natural gas, in Türkiye's energy production significantly

increases greenhouse gas emissions. This increase primarily stems from increased CO_2 levels resulting from the generation of electricity and heating. Although renewable energy plants have been supporting electricity generation in recent years, unless the number of facilities that use coal to generate energy decreases, CO_2 emissions will continue to rise. This is one of the fundamental factors that significantly strengthen the greenhouse effect. This can be best illustrated in Figure 4, which shows Türkiye's resources used in electricity generation.

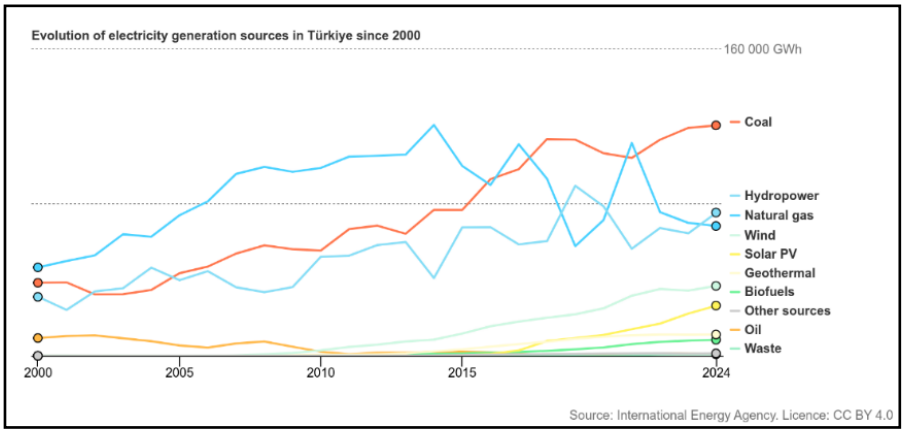

Figure 4. Distribution of Resources Used in Electricity Generation in Türkiye Since 2000 (URL-6).

In Türkiye, assessing the greenhouse effect solely by emissions may not reflect accurate results. It should also be evaluated in relation to the state's climate policy targets. Turkey has declared its net-zero greenhouse gas emissions target by 2053, having accepted the Paris Agreement. At the same time, the NDC (National Determined Contribution) declaration has been updated to the United Nations Framework Convention on Climate Change. With this declaration, Turkey also projects an emission reduction of up to 41%. It was announced that emissions would peak in 2038. Subsequently, the authorities announced that greenhouse gas emissions would be zero by 2053. For these targets to be credible, Türkiye's coal consumption must first be eliminated. Then, decarbonization policies must be implemented in the electricity sector. However, when examining the 2023 data, it becomes clear that CO2 emissions are continuing in Türkiye, and that the current rate of

increase can be reduced to zero emissions. Therefore, if Türkiye wants to mitigate the greenhouse effect, it is clear that this cannot be achieved solely through technical transformations. These transformations must be accompanied by comprehensive climate management policies that encompass transportation, energy, agriculture, industry, and land use. Thus, only through collective and feasible efforts can Türkiye's greenhouse gas emissions, and therefore the greenhouse effect, be reduced.

5. CONCLUSION

This section examines greenhouse gas emissions, the greenhouse effect, global warming, and the current status of the greenhouse effect in Türkiye. The increasing strength of the greenhouse effect worldwide poses a serious threat to important environmental, social, and economic processes, both globally and regionally. Carbon dioxide, water vapor, methane, nitrous oxide, and fluorinated gases, the most commonly released gases used for energy or heating and from various sources, are accumulating in the atmosphere at ever-increasing levels. This increase disrupts the world's energy balance. At the same time, temperature increases continue, significantly impacting hydrological cycle systems and triggering water shortages and ecosystem extinctions. Considering Türkiye's rapidly increasing energy demand and its geographical location, Türkiye is one of the most vulnerable countries to the effects of climate change.

Studies have shown that Türkiye predominantly uses fossil fuels for energy production. The combustion of coal and natural gas, among these fuels, contributes significantly to the greenhouse effect. Furthermore, considering the short- to medium-term impact on the greenhouse effect, other sources in Türkiye primarily include methane and nitrous oxide emissions from agriculture, industry, and transportation. In response to these contributions, Türkiye's greenhouse gas emission neutralization policies, including its national declaration contribution, are promising in reducing greenhouse gases. Furthermore, the recent increase in renewable energy resources in Türkiye supports this goal. However, achieving these goals requires intense, feasible, and collective action, as well as the implementation of decisive climate policies.

In line with these goals, several recommendations are presented below to enable Türkiye to reduce its greenhouse gas emissions truly.

a- Increasing Energy Conversions: A clear deadline for the end of coal and coal derivatives should be set, and coal use should be eliminated in Türkiye before this date. Renewable energy production should be rapidly increased instead. Energy efficiency programs should also be expanded nationally.

b- Decarbonization in the transportation sector: The number of electric vehicles, which has increased in recent years, should be further increased. Public transportation should be further strengthened. The number and ease of use of bicycle and pedestrian paths should be increased. This will reduce CO_2 and NO_x emissions from transportation.

c- Emission Control Management in Agriculture and Livestock: Precision agriculture practices, especially those needed to reduce methane and N_2O emissions, should be rapidly implemented. The storage and consumption of fertilizers produced should be managed in a systematic manner. Water use, especially in rice paddies with high water requirements, should be controlled. Support efforts should also be undertaken to expand biogas plants, which have increased in number in recent years.

d- Extremely Low-Carbon Technologies in Industry: Fluorinated gases should be replaced with alternatives with lower global warming capacity. In particular, efforts must be intensified to relocate cement factories and the metallurgical sector using carbon capture and storage (CCS) technologies.

e- Increasing and Strengthening the Number of Natural Sinks: Forested areas that have been deliberately or inadvertently burned must be protected with serious deterrent measures to prevent further damage. New forests should be established to replace those that have been burned or cleared. Degraded ecosystems should be restored, and the number of trees should be increased by planting resilient and long-lived trees.

f- Reducing Other Air Pollutants That Damage the Climate: Efforts should be undertaken to reduce air pollutants such as black carbon, methane, and tropospheric ozone. This will reduce temperature increases in the short term, though not necessarily in the long term. Ultimately, climate governance will be achieved.

g- Strengthening National Climate Management and Implementation: Türkiye should intensify its efforts to reduce greenhouse gas emissions by upholding its international commitments (such as the Paris Agreement). It should also support emissions trading and carbon taxes, which are economic instruments that can help mitigate climate change.

h- Increasing Awareness and Scientific Studies in Education: Official efforts should be undertaken to enhance the effective use of central research laboratories affiliated with universities. This will ensure the full implementation of climate science to reduce the greenhouse effect. Furthermore, increasing scientific studies will ensure both the healthy operation and the increased number of carbon management and sustainable technological fields.

In conclusion, reducing or eliminating the greenhouse effect, which results from greenhouse gas emissions, should not be viewed as a one-sided environmental problem. On the contrary, it has a direct impact on many areas, including health, the economy, agriculture, energy efficiency, and social well-being. In this context, reducing the greenhouse effect and increasing climate resilience in Türkiye should not be addressed unilaterally, but holistically. Climate strategies should be implemented with determination by establishing a comprehensive and collective framework, particularly in relation to transportation, agriculture, energy, and land use. To achieve these goals, a sustainable vision should be established, and long-term policy decisions, informed by science, should be made and implemented. This will reduce both greenhouse gas emissions and, consequently, the greenhouse effect. It will also play a critical role in leaving future generations a more livable, healthy, and breathable environment.

REFERENCES

Anadolu Ajansı. (2025, 26 Mart). Türkiye'nin sera gazı emisyonu 2023'te yüzde 6,9 arttı. https://www.aa.com.tr

Bilgili, M. (2024). Comprehensive overview on the present state and future prospects of climate change. Arabian Journal for Science and Engineering, 49, 12345–12367.

Cassia, R. (2018). Climate change and the impact of greenhouse gasses. Frontiers in Plant Science, 9, 1234.

Chen, R., Yin, P., Meng, X., Wang, L., Liu, C., Niu, Y., Liu, Y., Liu, J., Qi, J., & Zhou, M. (2021). Associations between wildfire smoke exposure and cardiovascular mortality in multiple countries. The Lancet Planetary Health, 5(9), e612–e620.

Climate Action Tracker. (2024). Turkey country assessment – Current policies and net zero target. Climate Analytics & NewClimate Institute. https://climateactiontracker.org

Creutzig, F., Nemet, G. F., Fischer, S., Torabi, S., Jochem, P., Edelenbosch, O. Y., ... & Minx, J. C. (2022). The underestimated potential of solar energy to mitigate climate change. Nature Energy, 7, 102–110.

Denisov, S. N., Eliseev, A. V., & Mokhov, I. I. (2021). Model estimates for contribution of natural and anthropogenic CO? and CH? emissions into the atmosphere from the territory of Russia, China, USA and Canada to global climate changes in the 21st century. arXiv. https://arxiv.org

Fawzy, S., Osman, A. I., Doran, J., & Rooney, D. W. (2020). Strategies for mitigation of climate change: A review. Environmental Chemistry Letters, 18(6), 2069–2094.

Filonchyk, M., et al. (2024). Greenhouse gases emissions and global climate change. Science of the Total Environment, XXXX, YYYY–YYYY.

Houghton, R. A., & Nassikas, A. A. (2020). Global and regional fluxes of carbon from land use and land-cover change 1850–2015. Global Biogeochemical Cycles, 34(3), e2019GB006321.

International Energy Agency (IEA). (2022). World Energy Outlook 2022. IEA Publications.

International Energy Agency. (2024). Türkiye – Countries & regions: Emissions and energy mix. IEA. https://www.iea.org/countries/turkiye

Intergovernmental Panel on Climate Change (IPCC). (2022). Climate Change 2022: Impacts, Adaptation, and Vulnerability. Cambridge University Press.

IPCC. (2022). Climate Change 2022: Mitigation of Climate Change. Working Group III Contribution to the Sixth Assessment Report.

Phillips, C. A., Caldas, A., Cleetus, R., Dahl, K. A., Declet-Barreto, J., Licker, R., ... & Carlson, C. J. (2021). Compound climate risks in the COVID-19 pandemic. Nature Climate Change, 11, 598–608.

Republic of Türkiye. (2023). Türkiye – Updated first nationally determined contribution (NDC). UNFCCC.

Ryan, S. J., Carlson, C. J., Mordecai, E. A., & Johnson, L. R. (2020). Global expansion and redistribution of Aedes-borne virus transmission risk with climate change. PLOS Neglected Tropical Diseases, 13(6), e0007213.

Saunois, M., Stavert, A. R., Poulter, B., Bousquet, P., Canadell, J. G., Jackson, R. B., Raymond, P. A., Dlugokencky, E. J., Houweling, S., Patra, P. K., ... Zheng, B. (2020). The Global Methane Budget 2000–2017. Earth System Science Data, 12(3), 1561–1623.

Tian, H., Xu, R., Canadell, J. G., Thompson, R. L., Winiwarter, W., Suntharalingam, P., Davidson, E. A., Ciais, P., Jackson, R. B., Janssens-Maenhout, G., ... Saikawa, E. (2020). A comprehensive quantification of global nitrous oxide sources and sinks. Nature, 586, 248–256.

TÜİK. (2025). Sera Gazı Emisyon İstatistikleri, 1990–2023 (Bülten No. 53974). Türkiye İstatistik Kurumu.

UNDP. (2023). Türkiye – Climate Promise country profile. United Nations Development Programme.

URL-1: https://mrgeogwagg.wordpress.com/2015/06/24/greenhouse-effect-and-anthropogenic-warming

URL-2: https://www.cevremuhendisligi.org/index.php/sozluk/94-haberler/yazar-ciy/1959-kuresel-isinma-ve-iklim-degisikliginin-etkileri#google_vignette

URL-3: https://yeserenerji.com/iklim-degisikligi-ve-salgin-hastaliklar/

URL-4: https://www.cevreizni.com/sera-gazi-emisyonu

URL-5: https://turkinform.com.tr/kuresel-isinma-nedir-sebepleri-nelerdir-nasil-onlenir-etkili-cozumler-ve-alinabilecek-onlemler

URL-6: https://www.iea.org/countries/turkiye/electricity?utm_source=chatgpt.com

Velders, G. J. M., Ravishankara, A. R., Daniel, J. S., Andersen, S. O., & Molina, M. J. (2022). Preserving the ozone layer and protecting the climate. Science, 378(6626), 952–960.

Vicedo-Cabrera, A. M., Scovronick, N., Sera, F., Royé, D., Schneider, R., Tobias, A., ... & Gasparrini, A. (2021). The burden of heat-related mortality attributable to recent human-induced climate change. Nature Climate Change, 11, 492–500.

Zhang, H., Chen, G., Li, M., Wang, Y., Wu, X., & Zhao, B. (2023). Short-lived climate forcers and their role in near-term climate mitigation. Atmospheric Environment, 299, 119600.

CHAPTER 7

MEDICINAL AROMATIC PLANTS AND CLIMATE CHANGE

Assoc. Prof. Dr. Betül GIDIK[1]

DOI: https://dx.doi.org/10.5281/zenodo.17847636

[1] Bayburt University, Faculty of Applied Sciences, Department of Organic Agriculture Management, Bayburt, Türkiye. betulgidik@bayburt.edu.tr, ORCID ID: 0000-0002-3617-899X

INTRODUCTION

Nowadays, a variety of industries, including food, cosmetics, paint, textiles, medicine, and agriculture, use medicinal and fragrant plants. Depending on a nation's degree of development, different plants are used for different reasons. Eighty percent of people in poor nations receive treatment with herbal products. This rate is significantly lower in wealthy nations, yet it can reach up to 95% in some Middle Eastern, Asian, and African nations. For instance, this percentage is between 40 and 50 percent in Germany, 42 percent in the USA, 48 percent in Australia, and 49 percent in France. Turkey has a wide variety of plant species due to its diverse flora (Türkan et al., 2006; Bayraktar et al., 2017; Acubuca and Budak, 2018; Göktaş and Gıdık, 2019)

Medicinal plants are those that contain specific bioactive substances, such as alkaloids, terpenoids, or phenolic compounds, in any or all of their organs, including leaves, flowers, roots, bulbs, tubers, bark, seeds, and fruits. One or more plants that contain chemicals with therapeutic qualities and health benefits are considered medicinal and aromatic plants (Bayram et al., 2010; Marshall, 2011; Gerçek et al., 2022).

The climate has changed continuously from the ice ages to the creation of the planet, but it has accelerated due to humanity's quick progress toward civilization and its careless devastation of the natural world. The industrial revolution of the 1860s broke the natural climate change equilibrium by bringing about rapid industrialization, urbanization based on skewed settlement patterns, incorrect land use, deforestation, and rapid degradation of the natural environment. Natural climate changes stopped occurring during the Industrial Revolution and the rise in human activity in the 20th century, and global warming-related climate change took their place (Hekimoğlu and Değer, 2008; Demirbaş and Aydın, 2020). The effects of climate change on medicinal aromatic plants are shown in Figure 1.

The aim of this study is to determine the relationship between medicinal aromatic plants, whose economic value and areas of use have rapidly increased in recent years, and climate change, which has had the greatest impact on agricultural activities in recent years. In order to answer the question of what the effects of climate change are on medicinal aromatic plants, a general assessment was made by reviewing studies conducted in recent years.

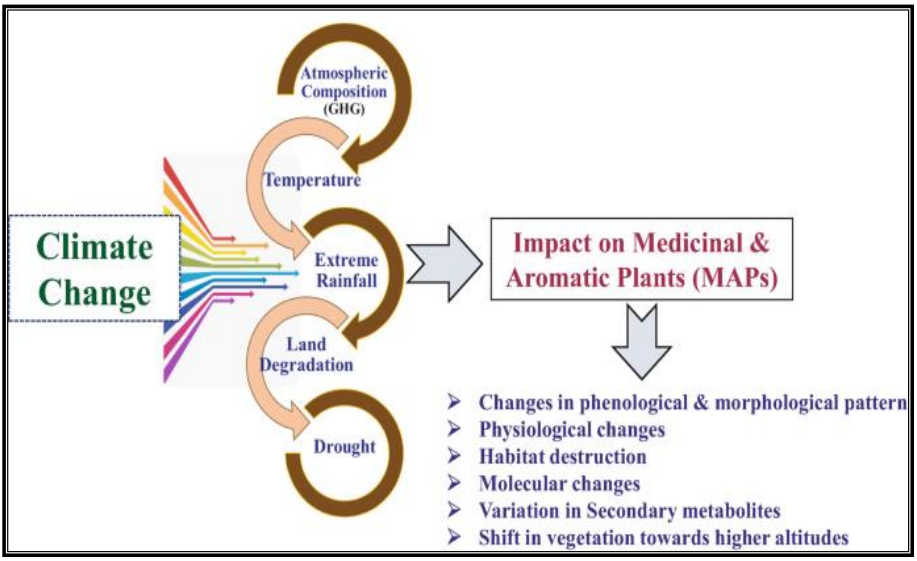

Figure 1: The Effects of Climate Change on Medicinal Aromatic Plants (Pandey, 2024)

1. MEDICINAL AND AROMATIC PLANTS

Aromatic medicinal plants are also added to cuisine. They are used for their coloring, sweetening, antioxidant, and preservation qualities. The active components of plant-based essential oils have been shown in numerous studies to possess a variety of qualities, including antibacterial, antioxidant, antifungal, and inhibitory actions. Additionally, some plants are used as colorants: paprika for red, saffron for yellow, tomato for red, marigold for yellow-orange, pomegranate for red-purple, annatto (bixa orellana tree) for red, safflower for red and yellow, and turmeric for yellow (Toker et al., 2015). Herbal products have become more popular in recent years, and a lot of study has been done on their bioactive properties, which include anti-inflammatory, antioxidant, antibacterial, and anticancer benefits (Göktaş and Gıdık, 2019; Sefalı, 2023).

Healers of the Aztec and Maya Native American cultures of Mexico and Central America are known to have experimented with some natural remedies and used at least medicinal plants to cure particular illnesses around 1,000 years ago (Evans, 2004; Berdan, 2005; Kumar and Jnanesha, 2016).

BOTANICAL NAME	FAMILY	USES
Abelmoschus moschatus	Malvaceae	Eye disorders, Vomiting, Carminative, Gastric
Adhatoda vesica	Acanthaceae	Cough, cold, bleeding, menstrual problems
Andrographis paniculata	Scanthaceae	Fevers, jaundice, diabetes
Asparagus racemosus	Liliaceae	Strength, acidity and liver complaints, Diabetes
Bacopa monnieri	Plantaginaceae	Mental clarity and longevity, Ulcers, tumors, asthma
Cassia angustifolia	Fabaceae	Laxative, Indigestion, jaundice, Anaemia
Centella asiatica	Apiaceae	Memory enhancer, Neurosis, Physical strength
Costus speciosus	Costaceae	Fever, cough, Diabetes, Digestive, Stimulant
Clitoria ternatea	Fabaceae	Diuretic, Ulcer, Visceralgia
Commiphora mukul	Burseraceae	Arthritis, Gout, Fever, Facial paralysis
Cymbopogon flexuosus	Poaceae	Skin Disorders & Perfumes
Cymbopogon martini	Poaceae	Cardio tonic, leprosy & perfumes
Cymbopogon winterianus	Poaceae	Antiseptic, Bactericidal, Mosquito repellent
Eclipta alba	Asteraceae	Hair, skin, Intestinal worms
Ocimum bacilicum	Lamiaceae	Perfumery, Cosmetic industries
Ocimum sanctum	Lamiaceae	Fever, Cold, cough and skin diseases
Ocimum gratissimum	Lamiaceae	Skin diseases, bakery, Icecream
Plectranthus amboinicus	Lamiaceae	Coughs, sore throats and nasal congestion
Plumbago zeylanica	Plumbaginaceae	Anaemia, Fever, Skin diseases
Tinospora cardifolia	Menispermaceae	Jaundice, Fever, Diabetes, Respiratory disorders
Vetiveria zizanioides	Poaceae	Vetiver root is cooling, Stimulant and tonic
Vitex negundo	Lamiaceae	Ulcer, Eye & ear diseases, Pain
Withania somnifera	Solanaceae	Immunity, Skin diseases, Depression, Strength

Figure 2: Some Medicinal Aromatic Plants and their Uses (Kumar and Jnanesha, 2016)

Certain fragrant and therapeutic plants are cultivated. Others are gathered from the natural world. Cumin, anise, thyme, fenugreek, poppy, fennel, mint, and coriander are all grown in Turkey. Natural sources include bay leaf, mahlep, linden blossom, sage, rosemary, licorice root, and juniper bark. Due to its geographical location, Anatolia has played an important role in the trade of herbal medicines and spices from ancient times to the present day. It is stated that 70 plants were traded during the Republican era in relation to the drug trade. Today, 347 plant species are collected from nature and traded domestically and internationally. It is also said that there are around 200 plants with export potential (Faydaoğlu et al., 2011).

Aromatic and medicinal plants are employed in landscape design for aesthetic, practical, ecological, and financial reasons. They are also utilized in

the pharmaceutical sector to prevent sickness, preserve health, or treat illness (Faydaoğlu and Sürücüoğlu 2011; Kara 2020).

Teas made from medicinal and fragrant herbs are used in both ancient and contemporary medicine to treat illnesses, maintain health, and prevent disease. Additionally, they are used in nutrition as spices, herbal tastes, and dietary supplements. They are utilized in many different industries, including pesticides, in addition to being used in cosmetics and perfumery as body care products and scents. Additionally, some plants are utilized as prepared, dried sections known as medicines. Since ancient times, people have believed that plants have therapeutic qualities. The Chinese emperor Shin-Nong is credited with writing the earliest treatise on aromatic and medicinal herbs in 3700 BC. Over 200 plants are mentioned by the emperor in his book. The Egyptians used and sold herbal remedies at the same time as the Chinese, according to writings and paintings discovered in ancient tombs (Ceylan, 1995; Arslan et. al., 2015).

Turkey is far behind major actors in the trade of aromatic and medicinal plants, like China, India, South Korea, Pakistan, and Bulgaria.

According to Güner (2012), there are presently over 12,000 taxa in Turkey's flora, of which about 3% are plant taxa. As is evident, this problem has not yet been thoroughly assessed for Turkey, a market that appears to have a very promising future. Because of this, the relationships between Turkish herbalists and consumers should be thoroughly examined, herbal products and medications should be purchased appropriately, and the unintentional gathering and ingestion of plants in the wild should be avoided (Özgüven et al., 2005; Schippmann et al.,. 2006; Göktaş and Gıdık, 2019).

2. CLIMATE CHANGE

The climate has changed continuously from the ice ages until the world's formation, but humanity's quick progress toward civilization and careless devastation of the natural world have sped up this process (Kadıoğlu, 2012). The equilibrium of natural climate change was broken by the industrial revolution of the 1860s, which brought about rapid industrialization, urbanization based on distorted settlement patterns, incorrect land use, deforestation, and rapid degradation of the natural environment (Demir, 2009; Demirbaş and Aydın, 2020).

High temperatures, droughts, forest fires, the depletion of water supplies, unusual and severe weather events, and warming and rising oceans are all consequences of global climate change, according to the European Commission's most recent report. Additionally, it results in losses in a number of important social and economic sectors, including energy, transportation, tourism, and agricultural production. Health issues, food insecurity, poverty, and mass migration are all caused by these factors. Global climate change is an environmental issue that affects all societies worldwide, endangering food security as well as the living conditions and basic means of subsistence of a significant portion of the world's population. (Çelen, 2018; European Comission, 2024; Ayaz and Çiğdem, 2025).

Greenhouse gases absorb some of the long-wave terrestrial radiation that the Earth's warm surface emits before it naturally escapes into space and is then re-emitted. This characteristic allows natural greenhouse gasses to control the rise in global temperatures. Thus, life on Earth is made feasible by the natural greenhouse effect. However, the natural greenhouse effect has been disrupted and a period marked by unnatural temperature increases and climate change has begun due to excessive increases in these gases' emissions, especially from the late 19th century (Türkeş et al., 2000; Türkeş, 2008).

3. CLIMATE CHANGE AND MEDICINAL AROMATIC PLANTS

Natural green areas are progressively disappearing due to global urbanization, necessitating the building of parks, gardens, and playgrounds with botanical landscaping (Çay, 2010). Turkey has a very high species diversity and endemism rate, with 11,466 plant taxa, 3,649 of which are endemic. Natural plants possess traits that enable them to adjust to their surroundings. These features include location-specific soil, climate, precipitation, drought, and frost (Güner et al., 2012).

Different parts of Turkey will be impacted by climate change in different ways and to differing degrees because of its orographic features, steep topography, and natural sea encirclement on three sides. Significant issues with water supplies may emerge as a result of climate change, which will alter the natural habitats of plants and animals in agricultural activities. The problems with water resources in Turkey's arid and semi-arid regions, particularly in

cities, will be exacerbated by climate change that may occur in the upcoming decades, depending on the increase in greenhouse gas accumulation in the atmosphere; the need for water for drinking and agriculture may also rise (Türkeş, 2020; Yaldız and Şekeroğlu, 2013).

Given that our nation will experience warmer and drier weather in the future, it is essential to find agricultural plant types that can withstand these conditions, as well as to create and fund research initiatives pertaining to this topic. In fact, the detrimental effects of drought on agriculture and, in turn, on farmers will compel some farmers to modify their goods in accordance with changing seasonal features. In this regard, it is crucial to develop medicinal and aromatic plants which are still mostly gathered from our nation's natural flora under cultivation conditions in appropriate ecologies, even though their significance and regions of application have increased recently (Yaldız and Şekeroğlu, 2013).

Reduced yields are one way that global warming affects agriculture, especially in dry areas where intense heat is a problem. Even with sufficient irrigation, plants in areas where irrigated agriculture is practiced suffer from heat stress, which lowers yields. Extreme heat causes irrigation to occur more frequently in irrigated areas, which results in an overuse of surface and groundwater resources (Türkeş, 2008; Yaldız and Şekeroğlu, 2013).

Some medicinal aromatic plants may be more tolerant to climate change than others. Identifying these plants and expanding their production areas can be considered an important measure to be taken against climate change, particularly in plant production.

Acantholimon spp. (Figure 3) is indigenous to Turkey and goes by several names, including goat's beard, sheep's beard, shepherd's pillow, and pig's thistle. Although it may grow in any kind of soil, it likes poor, dry, sandy, permeable, and well-drained soils. The plant is especially useful in erosion control initiatives because of its extreme heat tolerance (Kıvçak, 1956; Yaldız and Şekeroğlu, 2013).

Figure 3: General Appearance of the *Acantholimon* Plant (Govaerts, 1995)

Safflower (*Carthamus tinctorius* L.) (Figure 4), also known by names such as false saffron, American saffron, and dyer's saffron, is a drought-resistant oil plant. Medicinally, safflower is used to increase blood flow in the arteries in cardiovascular disorders, allowing tissues to receive more oxygen, thereby lowering high blood pressure, and as a pain reliever and fever reducer in the treatment of swelling and pain resulting from trauma. This plant, which has a high adaptability to different climatic conditions, is a valuable oilseed and medicinal aromatic plant that could be cultivated more widely in the context of global warming and climate change (Zhang, and Cheng, 2005; Konar et al. 2010).

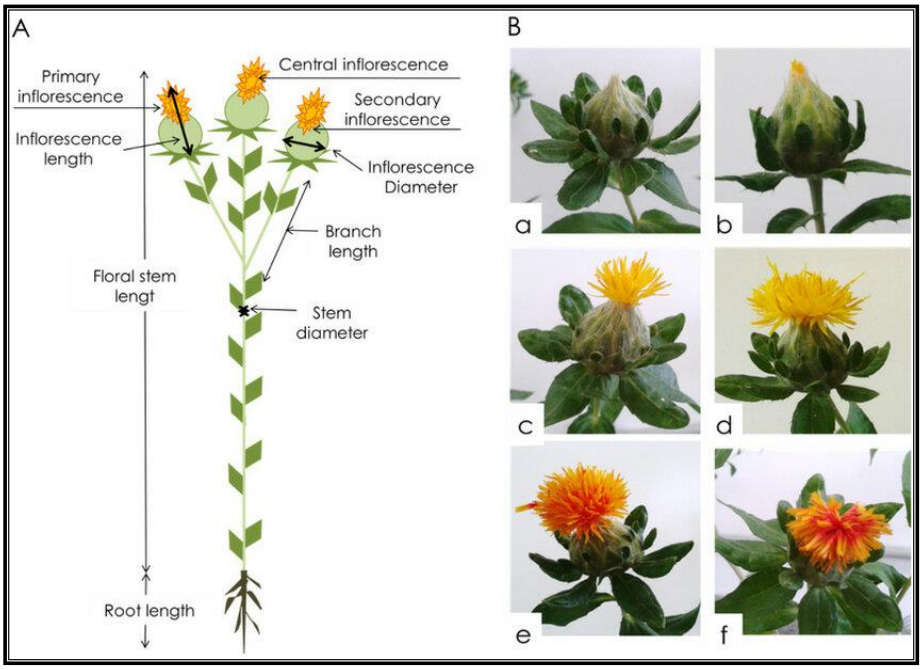

Figure 4: Parts of the Safflower Plant

4. CONCLUSION

Studies conducted in recent years show that the effects of climate change are becoming more noticeable. The negative effects of climate change are increasing due to many factors such as the growing world population, developing industrialization and production techniques, and environmental factors.

It is important that agricultural activities are carried out under sustainable conditions. In particular, the continuity of the production of medicinal aromatic plants, which have different uses, is important. For all these reasons, it is necessary to recognize and understand the inevitable climate change and take measures in the necessary areas. Measures that can be taken include cultivating medicinal aromatic plants in wider areas and producing varieties that are resistant to different climatic conditions and stress factors.

Research on medicinal aromatic plants should be increased. Varieties that are resistant to heat and drought stress should be identified and cultivated over larger areas.

REFERENCES

Acıbuca V. and D.B. Budak, "Dünya'da ve Türkiye'de Tıbbi ve Aromatik Bitkilerin Yeri ve Önemi," Çukurova Tarım ve Gıda Bilimleri Dergisi., vol. 33, no. 1, p. 37-44, 2018.

Arslan N, Baydar H, Kızıl S, Karik Ü, Şekeroğlu N, Gümüşçü A. Tıbbi ve Aromatik Bitkiler Üretiminde Değişimler ve Yeni Arayışlar. TMMOB Ziraat Mühendisliği VIII. Teknik Kongresi,12–16 Ocak, Bildiriler Kitabı–I, Sayfa 483–505, Ankara. 2015

Ayaz, M., and Çiğdem, Z. A General Overvıew of Agrıcultural Measures That Can Be Taken to Reduces the Negatıve Effects That May Occur In Agrıculture Durıng the Adaptatıon Process to Global Clımate Change. ICONTECH INTERNATIONAL JOURNAL, 8(3), 208–220. 2025. https://doi.org/10.5281/zenodo.15745627

Bayraktar Ö.V., G. Öztürk and D. Arslan, "Türkiye'de Bazı Tıbbi ve Aromatik Bitkilerin Üretimi ve Pazarlamasındaki Gelişmelerin Değerlendirilmesi," Tarla Bitkileri Merkez Araştırma Enstitüsü Dergisi., vol. 26, no. 2, p. 216-229, 2017.

Bayram, E., Kırıcı, S., Tansı, S., Yılmaz, G., Arabacı, O., Kızıl, S., Telci, İ. Tıbbi ve aromatik bitkiler üretiminin arttırılması olanakları. Türkiye Ziraat Mühendisliği VII. Teknik Kongresi Bildiriler Kitabı, 11-15. 2010.

Ceylan A Tıbbi Bitkiler I. Ege Üniversitesi Ziraat Fakültesi Yayınları No:312, III. Baskı, İzmir. 1995.

Çay, E. 'Ankara üniversitesi rektörlük kampüsü bitkisel tasarımında dekoratif amaçlı kullanılan ağaç ve çalıların saptanması üzerine bir araştırma'. Yüksek Lisans Tezi. Gazi Üniversitesi Eğitim Bilimleri Enstitüsü, Ankara. 2010.

Demir, A. Küresel İklim Değişikliğinin Biyolojik Çeşitlilik ve Ekosistem Kaynakları Üzerine Etkisi. Ankara Üniversitesi Çevrebilimleri Dergisi, 1(2), 37-54. 2009. https://doi.org/10.1501/Csaum_0000000013

Demirbaş, M. ve Aydın, D., Ecological Life Sciences (NWSAELS), 5A0143, 2020; 15(4):163-179. 2020.

European Commission. 2024. Consequences of Climate Change, Erişim adresi: https://ec.europa.eu/clima/climate-change/consequences-climate-change_enErişim tarihi:17.05.2024

Faydaoğlu, E. ve ark., Geçmişten Günümüze Tıbbi ve Aromatik Bitkilerin Kullanılması ve Ekonomik Önemi, Kastamonu Üniversitesi Orman Fakültesi Dergisi, 11(1):52–67. 2011.

Faydaoğlu, E., Sürücüoğlu, M.S.. Geçmişten günümüze tıbbi ve aromatik bitkilerin kullanılması ve ekonomik önemi. Kastamonu Üniversitesi Orman Fakültesi Dergisi 11(1):5267. 2011

Gerçek YC, Acar Şhain A, Nesrin Ecem Bayram NE, Çelik S, Sefalı A, Gıdık B, Cevahir Öz G, Pinar NM. Anatomy, trichome micromorphology and phytochemical profile of Stachys rizeensis R. Bhattacharjee from Turkey. S Afric J Bot. 149:19–28. 2022.

Govaerts, R. World Checklist of Seed Plants 1(1, 2): 1-483, 529. MIM, Deurne.,1995.

Göktaş, Ö., and Gıdık, B. Tıbbi ve Aromatik Bitkilerin Kullanım Alanları. Bayburt Üniversitesi Fen Bilimleri Dergisi, 2019,; 2(1), 145-151.

Güner A., Türkiye Bitkileri Listesi (Damarlı Bitkiler). Nezahat Gökyiğit Botanik Bahçesi Yayınları, Flora Dizisi 1, İstanbul. 2012.

Güner, A., Aslan, S., Ekim, T., Vural, M., Babaç, M. T. Türkiye bitkileri listesi:(damarlı bitkiler), Nezahat Gökyiğit Botanik Bahçesi Yayınları, İstanbul, p: 377-455. 2012.

Kadıoğlu, M., Türkiye'de İklim Değişikliği Risk Yönetimi. Türkiye'nin İklim Değişikliği II. Ulusal Bildiriminin Hazırlanması Projesi Yayını, Ankara. 2012

Kara, B.. Isparta iklim koşullarında yetişen bazı tıbbi ve aromatik bitkilerin şifa bahçeleri örneğinde kullanımı. Yüksek Lisans Tezi, Süleyman Demirel Üniversitesi Fen Bilimleri Enstitüsü, Isparta. 2020

Kıvçak, M. S., Astragalus-Geven. İstanbul Üniv. Orman Fak. Derg., 6 (1), 76-79. 1956.

Konar, V., Aşkın, Y., Türkoğlu, İ.., 2010.Yabani Aspir (Carthamus persicus Wild) Bitkisinin Yağ Asidi Bileşiminin İncelenmesi. Fırat Üniv. Fen Bil. Dergisi Fırat Univ. Journal of Science 22(1),29-36,2010 22(1),29-36, 2010.

Kumar A., and Jnanesha A.C., Medicinal and Aromatic Plants Biodiversity inIndia and Their Future Prospects: A Review. nd. J. Unani Med., Vol. IX, Iss. 1, pp. 10-17, 2016

Marshall, E. Health and wealth from medicinal aromatic plants. Rural Infrastructure and Agro-Industries Division, Food & Agriculture Organization of the United Nations, 68 p. 2011.

Özgüven M, Sekin S, Gürbüz B, Şekeroğlu N, Ayanoğlu F, Erken S Tütün, Tıbbi ve Aromatik Bitkiler Üretimi ve Ticareti. In: VI. Türkiye Ziraat Mühendisliği Teknik Kongresi Bildiriler Kitabı. Ankara, ss: 481-501. 2005.

Pandey, H. 2024. Consequences of Climate Change on Medicinal and Aromatic Plants in the Indian Himalayan Region: An Overview. In: Tripathi, S., Bhadouria, R., Garkoti, S.C. (eds) Warming Mountains. Springer, Cham. https://doi.org/10.1007/978-3-031-62197-0_20

Sefalı, A. Bayburt İlinde Yetişen Yabani Meyvelerin Tespiti ve Bazı İncelemeler. Osmaniye Korkut Ata Üniversitesi Fen Bilimleri Enstitüsü Dergisi, 6(1), 52-67. 2023. https://doi.org/10.47495/okufbed.1100152

Schippmann U, Leaman D, Cunningham AB A Comparison of Cultivation and Wild Collection of Medicinal and Aromatic Plants Under Sustainability Aspects. In: Bogers RJ (Ed.) Medicinal and Aromatic Plants. Springer, Dordrecht, pp. 75-95.2006.

Toker, R., Gölükcü M. and Tokgöz H., "Tıbbi Ve Aromatik Bitkilerin Gıda Sanayisinde Kullanım Alanları," Türkiye Tohumcular Birliği Dergisi., vol. 4, no. 15, p. 54-59, 2015.

Türkan Ş., H. Malyer, S.Ö. Aydın and G. Tümen, "Ordu İli ve Çevresinde Yetişen Bazı Bitkilerin Etnobotanik Özellikleri," Süleyman Demirel Üniversitesi, Fen Bilimleri Enstitüsü Dergisi., vol. 10, no. 2, p. 162-166, 2006.

Türkeş, M.,. İklim Değişikliği ve Küresel Isınma Olgusu:Bilimsel Değerlendirme,s:21-57. Yay. 2008

Türkeş M., 2002. İklim Değişikliği: Türkiye - İklim Değişikliği Çerçeve Sözleşmesiilişkileri Ve İklim Değişikliği Politikaları Devlet Meteoroloji İşleri Genel Müdürlüğü, PK 401, Ankara Vizyon 2023: Bilim ve Teknoloji Stratejileri Teknoloji Öngörü Projesi, Çevre ve Sürdürülebilir Kalkınma Paneli Vizyon ve Öngörü Raporu için hazırlanmıştır (Ekim, 2002)

Türkeş, M., Sümer, U.M., Çetiner, G., 2000. "Kyoto Protokolü Esneklik Mekanizmaları", hazırlayan: T.C. Çevre Bakanlığı ÇEKÖK Hava

Yönetimi Dairesi Başkanlığı, Ankara, 13 Nisan 2000 tarihinde İstanbul Sanayi Odası'nda düzenlenen T.C. Çevre Bakanlığı Birleşmiş Milletler İklim Değişikliği Çerçeve Sözleşmesi Semineri Notları,2000,s.33-54

Yaldız, G., and Şekeroğlu, N. Küresel İklim Değişikliğinde Tıbbi ve Aromatik Bitkilerin Önemi. Turkish Journal of Scientific Reviews(1), 85-88. 2013.

Zhang, HJ., Cheng, YY. 2005. An HPLC/MS Method for İdentifying Major Constıtuents in the Hypocholesterolemic Extracts of Chinese Medicine Formula 'Xue-Fu-Zhu-Yu Decoction'. Biomed. Chromatogr.

CHAPTER 8

EFFECTS OF INCREASING WINTER TEMPERATURES ON HONEY BEE (*Apis mellifera* L.) COLONY METABOLISM

Assoc. Prof. Dr. Yaşar ERDOĞAN[1]

DOI: https://dx.doi.org/10.5281/zenodo.17847648

[1] Bayburt University, Department of Veterinary Medicine, Demirözü Vocational High School, Bayburt, Türkiye. yasarerdogan@hotmail.com, ORCID ID: 0000-0002-3897-2003

INTRODUCTION

Global climate change is not merely a one-dimensional process of increasing global average temperatures; it is a multi layered transformation affecting all components of the climate system. This transformation is causing irregularities in seasonal temperature regimes, an increase in the frequency of extreme weather events, changes in frost-thaw cycles, shifts in precipitation patterns, and, in particular, an increase in winter minimum temperatures. The IPCC's Sixth Assessment Report (IPCC., 2023) reveals that winter temperatures have increased by +1.4°C globally over the past 50 years, and between +2.5 and +3.2°C in mid-latitude regions. This temperature increase, in particular, affects nighttime minimum temperatures, which has critical consequences for organisms that rely on metabolic slowdowns to adapt to low winter temperatures.

For honeybees (*Apis mellifera*), winter is a key period in colony biology. During this period, the colony conserves energy by reducing its metabolism to sustain survival; brood rearing capacity is reduced or completely halted, and thermoregulation is achieved through a tight cluster structure called the "winter cluster" (Seeley & Visscher, 1985). Winter bees can successfully adapt to these low temperatures thanks to their high vitellogenin levels, developed fat body reserves, and long-lived physiological structures (Amdam et al., 2004).

However, the warming of winters associated with climate change directly disrupts these natural physiological and behavioral strategies. Numerous ecological studies show that warm winters increase energy consumption in bee colonies, advance the brood rearing period, and create metabolic stress within the colony (Stabentheiner, Kovac, & Brodschneider, 2010). Carbohydrate consumption, which is normally minimal during the winter, increases by 30–60% with increasing temperature. Because bees are more active, honey supplies are rapidly depleted. Early brood rearing requires high energy levels and necessitates maintaining a constant temperature of 34–35°C within the colony, significantly increasing the metabolic burden on worker bees (Jones & Oldroyd, 2006).

Winter warming affects not only energy metabolism but also the immune and pathogen dynamics that determine colony health. For example, while *Varroa destructor* reproduction is normally limited due to low brood numbers in winter, high winter temperatures cause an expansion of brood size, thus

allowing varroa to reproduce continuously (Stabentheiner et al., 2010). Similarly, *Nosema ceranae* increases its infectivity under warm and humid winter conditions, reducing energy efficiency by causing damage to the intestinal epithelium (Higes, 2010; Ptaszyńska et al., 2018). This has been directly linked to the observed increase in colony losses.

Consequently, warming winters have become not merely a "temperature bias" for honey bees, but a holistic stress factor affecting all components of colony metabolism. In this section, the effects of rising winter temperatures on energy metabolism, thermoregulatory strategies, immune balance, behavioral dynamics, and pathogen pressure in bee colonies will be addressed from a multifaceted perspective, drawing on the literature, and the ecological implications will be discussed in detail.

1. WINTER WARMING TRENDS: SCIENTIFIC BACKGROUND

One of the fastest-moving components of climate change is the increase in winter temperatures. While global average temperature increases are often associated with summer, current scientific data indicate that winter minimum temperatures are rising faster than summer (IPCC., 2023). This is primarily due to the direct impact of radiative cooling processes, which determine nighttime temperatures, on atmospheric greenhouse gas concentrations. The atmosphere's increased heat-trapping capacity results in warmer nights, particularly the coldest nights, placing significant pressure on winter dynamics. Large scale climate datasets such as NOAA, ECMWF, and ERA5 also confirm this trend, revealing that over the past four decades, winter minimum temperatures have been 2–6°C higher than the 20th-century average, winter minimums have increased on average 35% faster than summer increases, and freeze thaw cycles have decreased significantly in many regions. This trend places significant stress on organisms whose winter metabolisms are geared to low temperature conditions. In social insects, such as honeybees, which are highly sensitive to environmental temperature, even a few degrees of increase in winter temperature can significantly affect colony physiology and homeostasis mechanisms.

1.1. Global Winter Minimum Temperature Increase

Climate models and long-term observations reveal that winter minimum temperatures have increased significantly in many regions of the world. According to reports by the (IPCC., 2023) and (NOAA., 2023), winter minimum temperatures have increased to over +3°C in cold climate zones such as Northern Europe, Siberia, and Canada, while in mid-latitude regions such as Turkey, the Balkans, and the Caucasus, this increase has been in the range of +2.5–4.5°C. Rising nighttime minimum temperatures lead to fewer frost days and shorter snow cover, radically altering the nature of winter conditions. These changes have critical consequences not only from a meteorological perspective but also for ecosystem functioning: plants' cold storage requirements are disrupted, soil microorganism activity increases, pest insects' survival rate increases, and species composition shifts over time. From the perspective of honeybees, this increase in winter minimum temperatures has direct impacts on all fundamental biological processes, including colony thermoregulation, energy metabolism, immune system dynamics, and, in particular, the reproductive cycle of *Varroa destructor*.

Table 1: Winter Minimum Temperature Increase Between 1980 and 2020.

Region	Average Increase (°C)	Increase in Coldest Nights (°C)	Decrease in Frost Days (%)
Europe	+2.1	+3.4	–27
Türkiye–Caucasus	+2.8	+4.1	–33
Northern United States	+1.6	+2.5	–21
Central Asia	+3.2	+5.0	–38

*(Copernicus Climate Change Service, (2023); IPCC., 2023; NOAA., 2023)

These data indicate that winters are no longer "cold," but rather "mild," and sometimes "temperate," with varying temperatures. This leads to metabolic and behavioral incompatibilities in honeybees, whose winter biology evolved to accommodate cold, stable conditions.

2. WINTER BIOLOGY IN HONEYBEES: BASIC MECHANISMS

Honeybee colonies have developed highly effective adaptations to extreme winter conditions thanks to the complexity of their social structures. Winter biology consists of a combination of physiological resistance and collective behavior.

2.1. Physiology of Winter Bees

The physiological makeup observed in honeybees during winter is completely different from that of summer workers. Summer workers are short-lived (4–6 weeks), while winter bees can live for 4–6 months. The most important reasons for this are:

a) High Vitellogenin Levels

Vitellogenin is not only an egg yolk protein but also a multipurpose protein associated with antioxidant defense, immune modulation, and longevity (Amdam et al., 2004). Vitellogenin levels in winter bees are 3–5 times higher than in summer workers.

b) Increased Fat Body Cells

In honeybees, the fat body is a key metabolic organ that assumes the functions of both the liver and adipose tissue. In winter bees, this structure has significantly higher lipid reserves, increased energy storage capacity, and stronger detoxification enzyme activity. These characteristics serve as a critical protective buffer for maintaining colony metabolism during the long winter and for worker bees to withstand environmental stress. These rich fat body reserves are one of the key physiological factors contributing to the longevity of winter bees.

c) Strong Immunity

Winter bees have an inherently more stable immune system due to cold weather, low pathogen activity, and reduced metabolic stress.

d) Longevity Mechanism

This combination allows winter bees to assume the role of the "bridge of life" that sustains the colony throughout the season.

Because this physiological structure evolved for cold and stable winter conditions, warm winters can easily disrupt the metabolic balance of winter bees. 3.2. Colony Thermoregulation

The fundamental requirement for honeybees to successfully survive the winter is thermoregulation at the colony level. During the winter, worker bees cluster together to form a structure called the "winter cluster." Within this collective structure, the temperature in the center is maintained between 20–35°C and 7–12°C in the outer shell (Seeley & Visscher, 1985). Heat production is achieved by the bees vibrating their flight muscles, a process that is metabolically costly. When the ambient temperature rises, the cluster relaxes, the bees' mobility increases, and their muscle vibrations become more irregular, resulting in a significant increase in colony energy consumption. Especially on days above 10–15°C, bees are more likely to venture out; however, because there is no nectar or pollen outside, these flights only result in unnecessary energy loss. This disruption of the winter cluster directly reduces colony metabolic efficiency and, as will be discussed in the following sections, constitutes one of the primary biological mechanisms responsible for increased winter losses.

3. EFFECTS OF INCREASING WINTER TEMPERATURES ON COLONY METABOLISM

Increasing winter temperatures are one of the most critical climatic processes affecting the physiological and behavioral integrity of honeybee colonies. This section details the multifaceted effects of increasing winter temperatures on colony metabolism and evaluates existing literature findings. Colony strategies, naturally based on low energy consumption, limited mobility, and minimal brood rearing during winter, are significantly disrupted by rising temperatures. Increased energy consumption, suppression of the immune system, increased pathogen pressure, and changes in colony behaviors are among the primary stress factors that warm winters impose on honeybee biology (Stabentheiner, Kovac, Mandl, & Käfer, 2021).

3.1. Impact on Energy Metabolism

Energy metabolism is one of the physiological processes most affected by increasing winter temperatures. Low energy expenditure during winter is a fundamental prerequisite for colony survival. However, this balance is disrupted during warm winters.

3.1.1. Increased Carbohydrate Consumption

Honey bees' primary energy source during winter is honey. During cold winters, the colony remains in a compact cluster, and energy consumption is minimal. However, increasing temperatures cause the cluster to loosen and the bees to move more. This directly increases carbohydrate consumption.

In cold winter conditions, the average honey consumption per colony is 8–12 kg, while in warm winter conditions, the average honey consumption per colony is 12–18 kg. This represents a 30–60% increase (Stabentheiner et al., 2021).

This increase is associated not only with metabolic activity but also with unnecessary external flight attempts, increased ventilation behavior, and premature brood rearing activities. The collapse of colonies from starvation and depletion of their honey reserves at the end of winter is often linked to mild winters.

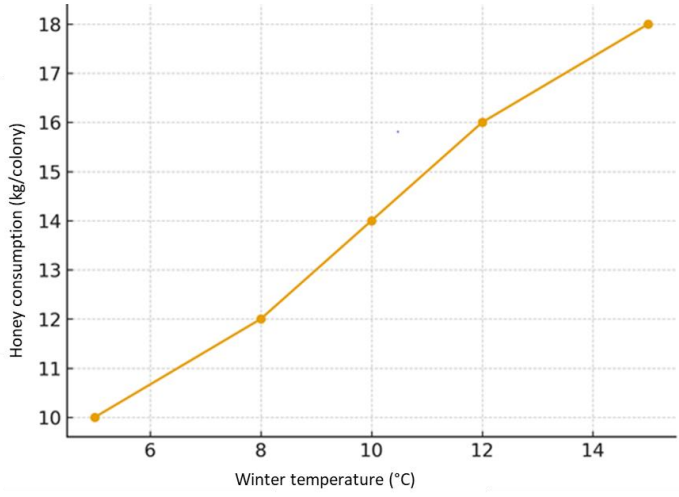

Figure 1: Honey Consumption Curve Versus Temperature Increase

3.1.2. Increased Muscle Activity and Metabolic Rate

During warm winters, thermoregulation in honeybees is maintained through a mechanism based on flight muscle tremors. Increased environmental temperature causes increased mobility of worker bees within the colony and a looser winter cluster structure. Under these conditions, more frequent and irregular muscle tremors are required to maintain thermal stability within the colony, resulting in significantly increased ATP consumption and oxygen consumption. As reported by de Villepin (2024), metabolic rate increases approximately 2–3 times in warm winter conditions compared to cold winters. This increase in muscle activity leads to a faster depletion of bees' adipose tissue reserves, thus negatively impacting their wintering performance.

3.1.3. Early Depletion of Fat Reserves

The key physiological factor determining the longevity of winter bees is their high levels of stored fat body reserves. These reserves are critical for energy production, maintaining immune system functions, and maintaining tolerance to various environmental stresses. However, increased metabolic activity during warm winters leads to the depletion of these fat reserves much earlier than expected. This accelerated loss of fat tissue shortens the lifespan of winter bees by approximately 15–30%, slows down intra-colony population renewal in the spring, and consequently hinders colony development. This results in reduced spring honey yield and supports the view that warm winters are one of the primary biological reasons for colonies' poor start to the season.

3.2. Early Onset of Brood Production

One of the most significant effects of rising winter temperatures is the earlier than normal onset of brood rearing within the colony. While brood production is generally minimal in cold climates until the end of January and February, during warm winters, this process can be observed as early as December. Because honey bees must maintain a constant brood temperature of approximately 35°C during brood rearing, the colony faces a significant thermoregulatory burden. Maintaining this temperature increases energy expenditure by approximately 5–7 times, honey consumption by 2–3 times, and muscle activity by approximately 3 times (Jones & Oldroyd, 2007). Therefore,

warm winter conditions cause the colony's metabolism to accelerate much earlier than expected, leading to a rapid depletion of energy reserves.

Table 2: Brood Area Changes in Warming Winters.

Temperature	Brood Area	Energy Consumption	Colony Risk
Cold (≤5°C)	Minimum	Low	Low
Warm (6–12°C)	Increased	Middle	Middle
Abnormally Hot (>12°C)	Continually	High	Very high

Early brood rearing also prevents varroa mite reproduction from stopping; this is discussed in detail in the following subsections.

3.3. Effects on Immunity

The immune system is normally stable during winter; however, warm winters disrupt this balance, increasing pathogen pressure.

3.3.1. Nosema ceranae Dynamics

Nosema ceranae is a microsporidian with a high proliferative capacity in warm and humid conditions, and increases in winter temperatures significantly accelerate the development of this pathogen. Under milder winter conditions, the rate of spore production increases, resulting in damage to the intestinal epithelial tissue of worker bees and energy losses due to impaired sugar digestion. These physiological disruptions increase the stress burden at the colony level and lead to increased late-winter mortality. Indeed, temperatures between 8–12 °C have been reported to cause a significant increase in N. ceranae burden (Ptaszyńska et al., 2018).

3.3.2. *Varroa destructor* Reproductive Cycle

Under normal winter conditions, *Varroa destructor* reproduction is significantly limited because brood cell closure is short-lived, narrowing the biological window for the parasite to multiply. However, the uninterrupted brood production during warm winters allows varroa reproduction to continue and the parasite load to rapidly increase. Under these conditions, varroa

reproduction rates are reported to increase by 50–80%, and the Deformed Wing Virus (DWV) infection load also increases significantly. The extreme parasite pressure experienced by colonies at the end of winter is considered one of the most powerful biological mechanisms contributing to colony losses during warm winters.

4. BEHAVIORAL AND ECOLOGICAL IMPACTS

Rising winter temperatures profoundly affect not only the physiological processes of honeybee colonies but also their behavioral dynamics and ecosystem interactions. Winter is a period when bees generally avoid flight, enter a metabolic conservation mode, and the colony's interaction with the external environment is minimal. However, temperature fluctuations disrupt these natural behavioral patterns. This section details the multifaceted effects of increasing winter temperatures on honeybee behavior and the ecosystem.

4.1. Increased Winter Flights

Winter temperatures exceeding 10–12°C can trigger extroversion activity in honeybees, which is normally minimal. While flights during the winter are generally limited to short, defecation-only "cleaning flights," under cold climate conditions, the tendency for worker bees to extrovert significantly increases during mild winters. The intense work of flight muscles during these extroversions leads to high energy consumption; however, because nectar and pollen are not readily available during the winter months, this behavior results in a net loss rather than an energy gain. This unnecessary energy expenditure, especially in older winter workers, leads to a rapid depletion of fat reserves. Indeed, the literature has reported that the number of extroversions increases 3–5 times during mild winters compared to normal winters, and the success rate of returning to the colony after flight decreases significantly (Abou-Shaara, 2014).

4.2. Energy Loss and Increased Mortality

Flight behavior in honeybees is a highly energy-intensive process, and the aerobic metabolism of flight muscles consumes approximately 5–7 times more energy than at rest. Because winter bees are physiologically adapted to low temperatures, they struggle to meet this intense energy requirement during

warm winter conditions and may experience energy depletion, particularly during return flights. This significantly increases the incidence of adverse outcomes such as death by freezing outside the hive, declines due to energy depletion, and disorientation during flight.

Increased winter temperatures affect not only flight behavior but also the navigational capacity of honeybees. Bee navigation depends on multiple environmental and physiological parameters, such as the position of the sun, polarized light patterns, the Earth's magnetic field, and circadian rhythms (Dyer, 1987). The occurrence of warmer days than expected during winter months can lead to misinterpretation of some of these parameters, distorting timing signals and, consequently, decreasing navigation accuracy. The Effect of Temperature Fluctuations on Circadian Rhythm

The prevailing low and stable temperatures during winter allow honeybees to maintain a stable circadian rhythm. However, interday temperature differences of 12–15°C, the occurrence of short "spring-like" temperatures, and rapid warming-cooling cycles cause bees to fail to correctly adjust their timing mechanisms. This circadian disruption manifests itself in flight timing errors, inability to find the hive, decreased return success, and, especially, an increase in the loss of older workers (Scheiner et al., 2020). Another reason why temperature fluctuations weaken the navigation system is the emergence of temperature-sensitive neurophysiological changes in the mushroom body regions of the bee brain. These changes are thought to be closely related to the sudden colony losses frequently reported in late winter.

4.3. Plant Bee Phenology Mismatch

One of the most important ecological consequences of increasing winter temperatures is the disruption of the natural synchrony between plant phenology and early spring activity of honeybees. Honeybees are highly dependent on pollen and nectar sources in early spring, and the timing of plant flowering is largely dependent on winter cold requirements. Mild winters lead to earlier plant emergence, increased frequency of early flowering, and, despite this, persistent frost risk due to unstable spring temperatures. The short-term abundance of pollen and nectar experienced under these conditions is often followed by a sudden cold snap or frost, which destroys early-flowering flowers and eliminates food resources. The resulting food gap leads to protein

deficiency in the colony, slowing or completely halting brood development. Indeed, phenological incompatibilities have been reported to be a major determinant of late-winter weakness in colonies (Kudo & Cooper, 2019).

4.4. Ecosystem-Level Impacts

The effects of warming winter conditions are not limited to early spring performance of honeybees; they also disrupt pollinator-plant interactions at broader ecological scales. Increased winter temperatures can shift the timing between pollinator and flowering periods, alter the structure and dynamics of pollinator communities, reshape interspecies competitive relationships, and cause significant yield losses in some plants. This process creates a comprehensive chain of disruptions that affects not only honeybees but also all pollinator communities and their dependent plant species within the ecosystem.

5. HUMIDITY, CONDENSATION, AND MICROBIAL RISK WITHIN THE HIVE

The microclimate within the hive plays a decisive role in the survival of honeybee colonies throughout the winter. An optimal winter environment is characterized by low metabolic activity, moderate humidity, stable temperature, and minimal pathogen activity. However, rising winter temperatures disrupt this delicate microclimate balance, negatively impacting humidity, condensation, and microbial load within the hive.

The temperature-humidity relationship exhibits a nonlinearity in closed systems. As temperature increases, the moisture-holding capacity of the air increases; However, because temperatures fluctuate frequently between days in winter, water vapor produced by bees can condense into drops within the hive. This process not only puts the colony under "wet-cold stress" but also creates a favorable environment for pathogens.

5.1. Increased Winter Temperatures and Humidity Dynamics

During hot winter days, the increased metabolic activity of honeybees causes the amount of water vapor released within the hive to increase. This moisture production increases even further when brood rearing begins early, and under conditions of inadequate hive ventilation, humidity builds up inside

the hive. Relative humidity levels reaching 70–90% within the hive are particularly risky, as high humidity causes bees to lose body heat rapidly, increase their need to generate heat through shivering, and consequently, increase energy consumption, thus increasing the overall physiological burden on the colony. Therefore, it is emphasized that "dry cold" conditions are relatively safe for bees during the winter months, while the real danger lies in the "wet-cold" microclimate conditions triggered by temperature fluctuations.

5.2. Condensation Formation and Its Effects

Water vapor produced by honeybees' respiratory and metabolic activities can condense and fall to the bottom as drops if the hive ceiling remains cooler than the surrounding environment. The fall of these drops on the winter cluster causes the bees' body temperature to rapidly decrease, while the increased humidity in the honeycombs increases the risk of fermentation and spoilage. This condensation becomes even more pronounced in poorly insulated hives. Rising winter temperatures and increasing day-night temperature differences make condensation processes more unstable, disrupting the stability of the intra-colony microclimate. Condensation is known to be particularly harmful to young larvae and pupae, as wet and cold conditions negatively affect larval metabolism and increase susceptibility to pathogens.

5.3. Increased Microbial Risks

Warmer winters create an ideal breeding ground for pathogens and microbial agents within the hive. The most notable of these are Nosema ceranae, molds, *Paenibacillus larvae (*AFB), and *Melissococcus plutonius* (EFB).

5.3.1. Nosema ceranae

Nosema ceranae is a microsporidian with a high proliferation capacity in warm and humid conditions, and studies have shown that spore density can increase by up to 200% as relative humidity within the hive exceeds 70% (Higes, 2010). High humidity supports this increase in pathogen load through multiple biological mechanisms. Increased humidity causes the intestinal epithelial tissue of worker bees to become more sensitive, leading to increased honey consumption due to increased energy requirements and, consequently,

increased spore intake. Furthermore, the balance of the gut microbiota is disrupted, and winter bees' immune systems are suppressed, increasing their susceptibility to infection. The combined effect of these mechanisms leads to a significant increase in the risk of *N. ceranae* infection in warm and humid winter conditions.

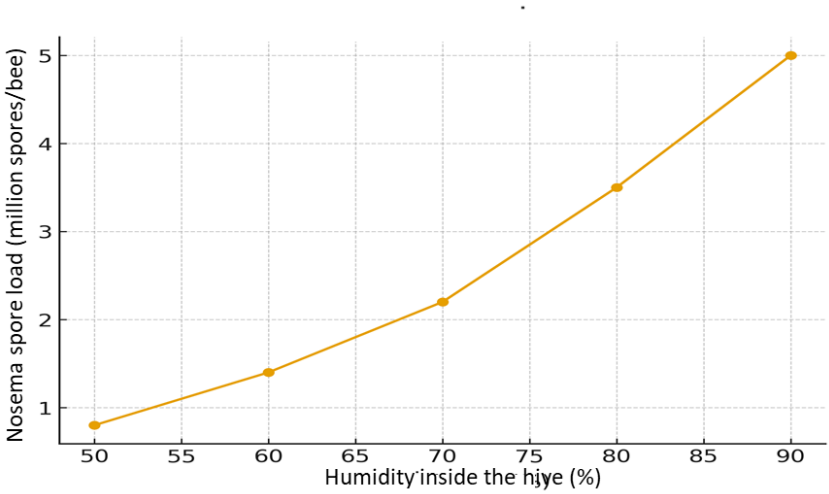

Figure 2: Humidity Nosema Relationship Graph

This graph shows that spore load increases exponentially as humidity increases.

5.3.2. Mold Fungi (Ascosphaera, Aspergillus, Penicillium)

High humidity levels within the hive create a favorable microenvironment for the development of mold and other fungal pathogens. During mild winters, the likelihood of fungal species such as Ascosphaera apis (the causative agent of chalk disease), Aspergillus flavus, and Penicillium commune proliferating in the colony increases. These microorganisms cause larval mortality, characteristic mummification of larvae, and the accumulation of various toxins within the colony, negatively impacting both brood health and overall colony strength. The increased reporting of chalk disease during warming winter conditions is considered a typical reflection of this mechanism, which promotes fungal growth due to increased humidity.

5.3.3. AFB (American foulbrood) and EFB (European foulbrood) Risk

AFB *(American foulbrood) – Paenibacillus larvae*

EFB *(European foulbrood) – Melissococcus plutonius*

Bacterial brood diseases normally have limited spread due to low winter temperatures. However, during mild winters, uninterrupted brood rearing allows the disease cycle to continue. Increased humidity within the hive supports bacterial growth, and physiologically weakened winter bees become more susceptible to pathogens. Under these conditions, European foulbrood (EFB) can emerge as an "early spring epidemic," particularly in stressed colonies associated with warm winters (Forsgren, 2010).

5.4. Knock On Effects of Hive Microclimate Disruption

Increased winter temperatures initiate a series of knock-on processes that directly affect the intra-colony microclimate. As temperatures rise, humidity within the hive increases, resulting in condensation and a significant increase in the reproduction rate of various pathogens. This microclimatic disruption leads to a suppression of the winter bees' immune system and increased metabolic energy loss; as a result, the winter bees' lifespan is shortened, and the colony enters spring with a weakened worker population. The combined effect of these processes is considered one of the primary determinants of colony collapses observed in the late winter and early spring period.

6. MODELING AND FUTURE PROJECTIONS

The acceleration of global climate change not only affects current ecosystem processes but also poses serious future risk projections. Given the sensitivity of honeybee colonies to winter temperatures, the combined evaluation of climate models and colony dynamics models offers important insights into bee health and colony losses in the coming years. International research conducted by the COLOSS (Prevention of Honeybee Colony Losses) network includes large-scale modeling studies on how colony losses will change under various temperature scenarios.

According to (Gray et al., 2023) data, climate scenarios will place significant pressures on honeybee colonies through 2050. These projections

were derived using both climate models (CMIP6, IPCC SSP2–4.5, and SSP5–8.5 scenarios) and biological simulations that model intra-colony population dynamics.

6.1. Winter Loss Projections

Modeling in recent years indicates that if winter temperatures continue to rise, there will be a significant increase in colony mortality. Based on COLOSS data, it is noteworthy that global colony losses reported for 2020 averaged 12–22%, while projections for 2050 project an additional 15–25% increase. These projections indicate that winter losses could reach levels of 30–40% in many regions. The primary biological mechanisms behind this increase in the literature are: These effects are summarized as increased varroa and related virus load, increased energy consumption, earlier start of the brood rearing period, faster physiological exhaustion of winter bees and disruption of the microclimate balance within the hive (Brodschneider, Gray, & Project, 2022).

6.2. Increasing Number of Warm Winters

The IPCC's SSP2–4.5 intermediate climate scenario projects a significant increase in the number of warm winter days (≥12°C) in the coming years. The average number of warm winter days, recorded as 3–5 days per year during the 1980–2000 period, is expected to increase to 7–14 days by 2050 and 15–25 days by 2100. In the SSP5–8.5 scenario, which projects even faster warming, the increase is even more dramatic; the number of warm winter days is projected to approximately double by 2050 and triple by 2100. This change is not merely a climatic indicator; it translates directly to metabolic disruptions, increased energy consumption, and an early break in winter physiology for honeybees biologically adapted to long winters.

6.3. Weakening of Spring Populations

The strength of the colony population in the spring depends largely on how the winter is handled. Models reveal that particularly warm winter conditions have a significant debilitating effect on colony populations. First, high winter temperatures increase worker bees' energy expenditure, causing their fat reserves to deplete much earlier than expected. This shortens winter

bees' lifespan, and the colony enters the season with a lower-than-required number of workers.

A second consequence of warm winters is the inability to generate a sufficient young worker population in the spring. Early brood rearing leads to high energy and resource consumption, making it difficult for the colony to quickly replenish its population both in late winter and early spring. This results in a weak start to the season for the colony, which should normally exhibit strong growth.

A third critical factor is the persistence of varroa mite pressure throughout the winter. Because brood production is not interrupted in mild winters, *Varroa destructor* reproduction continues, and the parasite load reaches high levels as spring approaches. This cycle is considered one of the most important factors suppressing the spring population.

Population modeling studies also confirm this pattern. Colony dynamics models such as BEEHAVE and ApisRAM show that spring worker populations remain 18–35% lower under warm winter scenarios, second-generation brood emergence is significantly delayed, and seasonal honey yield decreases by an average of 20–30% (Romero-Leiton, Gutierrez, Benavides, Molina, & Pulgarín, 2022).

6.4. Ecosystem-Level Projections for 2050

The impacts of increasing winter temperatures are not limited to honey bee colonies; the entire pollination ecosystem is directly affected by this change. 2050 projections indicate that flowering times for many plant species will shift earlier by 3–5 weeks, further exacerbating bee-plant phenological mismatches. A decrease in the protein content of pollen produced by heat-stressed plants translates to a decrease in nutritional quality for both honey bees and other pollinators (Descamps, Quinet, & Jacquemart, 2021). Damage to early-flowering species from frost events in March can increase flower loss and disrupt the continuity of pollen and nectar sources in spring. Furthermore, warming winters negatively impact not only honeybees, which form social colonies, but also solitary bees, whose population dynamics are more sensitive. All these changes combined indicate that the ecological network formed by honeybees and natural pollinators is gradually weakening, jeopardizing the sustainability of ecosystem services.

6.5. General Assessment of Model Results

Overall, current modeling studies suggest a significant increase in colony winter losses by 2050. The primary drivers of this increase are understood to be metabolic stress, varroa and related virus pressure, and a mismatch between bee and plant phenology. The emergence of mild winter conditions as the "new norm" in many regions indicates that traditional colony management practices will not be sufficient and that beekeeping strategies must be restructured with climate-adapted approaches. In this context, strengthening regional monitoring systems, establishing early warning mechanisms sensitive to temperature anomalies and developing sustainable beekeeping policies appropriate to local ecological conditions are of great importance.

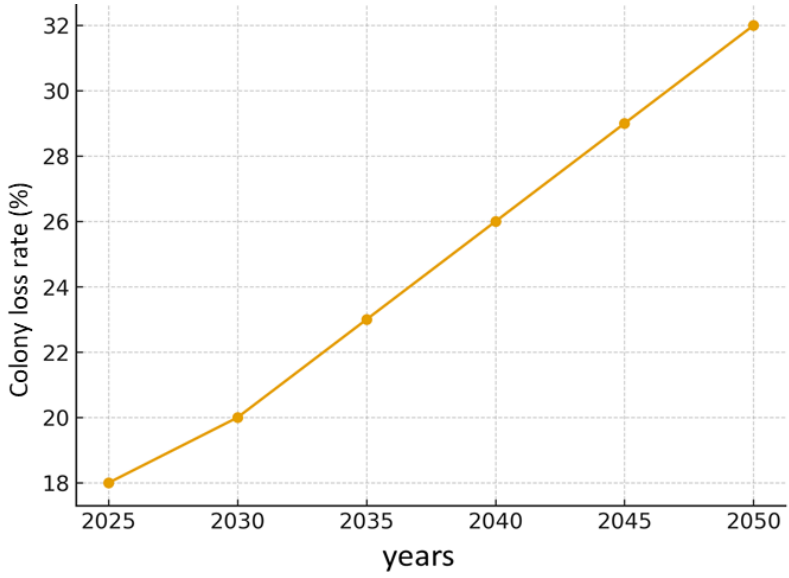

Figure 3: Colony Loss Projection

7. MANAGEMENT RECOMMENDATIONS AND ADAPTATION STRATEGIES

With increasing winter temperatures, the metabolic, behavioral, and pathogen-related stress factors faced by honeybee colonies have changed significantly. Therefore, it has become imperative to review traditional beekeeping practices and develop strategies adapted to new climate conditions. This section discusses comprehensive management strategies for warming

winters, based on recommendations from scientific studies and international beekeeping monitoring programs (COLOSS, Apimondia, USDA-ARS).

7.1. Feeding Strategies

Increasing winter temperatures require restructuring feeding strategies because they affect the colony's energy consumption and brood rearing period.

7.1.1. Increasing Winter Stocks

While an average of 8–12 kg of honey is sufficient for a colony under traditional winter conditions, this amount should be increased to 12–18 kg in mild winter scenarios. This increase is necessary both to offset the energy consumption resulting from cluster relaxation and to meet the needs of the early brood stage.

Research shows a 30–60% increase in honey consumption during mild winters (Tosi et al., 2021).

7.1.2. Protein Supplementation

The early onset of brood rearing at the end of winter naturally increases protein requirements within the colony. However, failure to meet this requirement during periods when pollen sources are not yet available leads to both increased brood losses and a shorter lifespan for winter bees. Protein insufficiency leads to a weak spring population, preventing colony development from achieving the necessary momentum. Therefore, the use of high-quality protein cakes for supplementation is recommended during January and February, provided that temperature trends and colony condition are carefully assessed.

7.1.3. Periodic Monitoring and Supplemental Feeding During Warm Winters

Regular monitoring is crucial during warm winters, as colonies consume energy more rapidly and brood activity begins earlier than expected. During such periods, weekly colony checks are recommended, particularly to monitor for excessive honey consumption and to supplement with controlled amounts of cake when necessary. However, careful planning of the feeding program is

necessary, as overfeeding can increase humidity levels within the hive, increasing secondary risks such as condensation and pathogen development. In this context, ensuring that the breeding cycle of *Varroa destructor* is not interrupted, one of the most critical problems posed by warm winters, necessitates restructuring varroa management to suit warming climate conditions.

7.2. Mid Winter Oxalic Acid Application

Brief periods during the winter months when the colony is completely free of brood constitute the most effective timeframes for oxalic acid (OA) drip or steam application. However, because brood rearing is often uninterrupted during warm winters, the traditional application schedule becomes ineffective, and varroa control must be rescheduled. COLOSS protocols recommend regular varroa load measurements in December and January and OA application only during short meteorological windows when there are no brood. This approach is considered one of the most viable strategies for interrupting the varroa cycle, even under warm winter conditions.

7.2.1. Brood Break Strategies

Because warm winter conditions encourage continuous brood production in the colony, the complete absence of brood production during certain periods makes it difficult to break the varroa cycle. In such cases, creating an artificial "brood break" using biotechnical methods becomes an effective option. Practices such as short-term queen caging, creating a new broodless period by splitting the colony, or queen replacement allow for the interruption of the *Varroa destructor* reproductive cycle by temporarily removing the brood curtain. These methods, used in conjunction with chemical treatments in warming climates, are considered among the most important integrated varroa management tools.

7.2.2. Regular Monitoring

The increasing frequency of warm winters necessitates that varroa management shift from a solely seasonal practice to a year-round monitoring-based system. The recommended monitoring interval for mild winters includes natural shedding checks every three to four weeks and accurate varroa load

measurements using alcohol wash at the end of winter. Warm winters pose a serious risk, especially in colonies with high varroa levels; parasite populations increase rapidly during periods of continuous brood production, and the colony enters the end of winter under extreme biological stress, tending to collapse.

7.3. Hive Air Conditioning

Because the winter warming disrupts the humidity and temperature balance within the hive, hive air conditioning has become an even more critical management area.

7.3.1. Humidity Control

Increased humidity levels within the hive are one of the primary factors triggering numerous negative processes, from the proliferation of Nosema ceranae to mold growth, from condensation on ceiling surfaces to the emergence of various brood diseases. Therefore, to maintain colony health, it is recommended that the relative humidity within the hive be maintained as evenly as possible, ideally between 55–75%. This range provides the most suitable microclimate conditions that both limit microorganism growth and support the bees' thermoregulatory capacity.

7.3.2. Avoiding Over Insulation

During winter months, when temperatures fluctuate frequently, heavy insulation can exacerbate the temperature-humidity imbalance within the hive, increasing the risk of condensation. Therefore, it is recommended to use top ventilation holes to maintain a more stable microclimate, to choose breathable, air-permeable cover fabrics, and to use appropriate interior materials that support hygrothermal balance. These practices help both reduce condensation and more effectively control humidity, which is critical for colony health.

7.3.3. Sensor Technologies (Hygrothermal Sensors)

Sensor systems such as HOBO, BroodMinder, and Arnia Hive Monitor, used in modern beekeeping, allow for real-time monitoring of critical parameters such as hive temperature, humidity, consumption dynamics, and even acoustic activity. These technologies are particularly valuable during

warming winter conditions; Because sensors enable early detection of condensation risk, more accurate estimation of honey consumption, monitoring of changes in colony activity levels, and indirect detection of shifts in the varroa-brood cycle. Therefore, as warm winters become increasingly common, beekeepers are strongly encouraged to adopt a technology-supported colony management approach.

7.4. Genetic Adaptation

The genetic basis of tolerance to warm winters is becoming increasingly important. Different honeybee subspecies respond differently to changes in winter temperatures.

7.4.1. Caucasian Honeybee (*Apis mellifera caucasica*)

Some honeybee lines stand out for their high adaptability to cold and humid climates. These genetic traits allow the colony to exhibit more stable cluster behavior throughout the winter, to avoid premature brood rearing, and, consequently, to maintain low winter honey consumption. One of the most notable advantages of these lines is that consumption behavior does not fluctuate excessively even during warm winter conditions and that intra-colony energy management proceeds more harmoniously. These features constitute an important resistance mechanism against metabolic stress caused by mild winters that are becoming more frequent with climate change.

7.4.2. Carniolan Bee (*Apis mellifera carnica*)

The Carniolan bee is one of the lines known for its strong winter conservation ability and controlled population growth. Because it can efficiently manage energy within the colony, it avoids unnecessary consumption throughout the winter and enters the spring with a balanced worker population. Furthermore, relatively high varroa tolerance has been reported in some Carniolan populations, providing a significant advantage, particularly in mild winters when parasite pressure increases. One of the Carniolan line's most notable characteristics is its behavioral flexibility to heat-cold fluctuations; this flexibility helps maintain colony stability in the increasingly irregular winter conditions that are becoming more frequent with climate change.

7.4.3. Anatolian Local Genotypes

The high climatic resilience, adaptability to different winter temperatures, hardiness, and low consumption characteristics of local bee ecotypes found in Central Anatolia, Eastern Anatolia, and the Caucasian transition zone in Turkey have been emphasized in many studies (Kandemir, Kence, Sheppard, & Kence, 2006). These ecotypes are an important biological resource that supports colony sustainability in warming climates because they exhibit a genetically more resilient structure to fluctuations in winter conditions. Therefore, preserving local genetic lines and actively using them in breeding programs is considered a critical strategy against the risks posed by warm winters.

8. CONCLUSION

Increased winter temperatures are not only a change in the physical environment for honeybee (*Apis mellifera*) colonies, but also a multifaceted stress factor affecting all biological, ecological, and pathological processes that determine colony survival. The effects of warming winters on colonies are manifested in a wide range of aspects, from energy metabolism and immune functions to behavioral adaptations, plant-bee interactions, pathogen dynamics, and long-term population patterns.

First, increased energy consumption during winter causes colonies to rapidly deplete their honey reserves and prematurely deplete the physiological reserves of winter bees. This not only reduces the chances of survival during the winter but also restricts colony development in the spring, negatively impacting honey yield, pollination efficiency, and colony regeneration. Rising temperatures cause brood rearing to begin earlier than usual, increasing metabolic load while also paving the way for parasites such as *Varroa destructor* to reproduce continuously throughout the year.

From an immune system perspective, warm and humid winter conditions facilitate the proliferation of microsporidia, particularly Nosema ceranae, causing damage to the intestinal epithelium and a significant increase in winter mortality. Humidity and condensation mechanisms within the hive contribute to the proliferation of molds and the triggering of brood diseases, placing colonies under microbial pressure. This microbial stress, combined with behavioral disruptions, further weakens colony resilience.

At the ecosystem level, rising winter temperatures cause incompatibilities in plant-bee phenology, creating critical nutritional gaps for bees as a result of the coincidence of early flowering and frost events. This incompatibility can impact both the balance of pollinator communities and crop production systems in the long term. Modeling indicates that if current temperature trends continue, there could be an additional 15–25 percent increase in winter losses by 2050. This highlights the need to update beekeeping practices, colony management protocols, and breeding strategies with a climate-adaptive approach.

Consequently, the impacts of warming winter conditions on honeybees are interconnected, multi component, and increasingly severe. Therefore, comprehensive management strategies that both address basic bee biology and adapt to the impacts of climate change are needed. Practices such as in-hive air conditioning, sensor technologies, genetic adaptation, feeding strategies, and integrated varroa mite management will play a key role in increasing colony resilience to warmer winter conditions in the future. Furthermore, preserving local ecotypes and developing sustainable beekeeping models are critical for establishing more resilient pollinator communities to climate change.

REFERENCES

Abou-Shaara, H. F. (2014). The foraging behaviour of honey bees, *Apis mellifera*: a review. *Veterinarni medicina, 59*(1).

Amdam, G. V., Simões, Z. L., Hagen, A., Norberg, K., Schrøder, K., Mikkelsen, Ø., . . . Omholt, S. W. (2004). Hormonal control of the yolk precursor vitellogenin regulates immune function and longevity in honeybees. *Experimental gerontology, 39*(5), 767-773.

Brodschneider, R., Gray, A., & Project, C. M. C. (2022). How COLOSS monitoring and research on lost honey bee colonies can support colony survival. *Bee World, 99*(1), 8-10.

Copernicus Climate Change Service, C. D. S. ((2023)). ERA5 hourly data on single levels from 1940 to present. Copernicus Climate Change Service (C3S) Climate Data Store (CDS). (Accessed on DD-MMM-YYYY). doi:DOI: 10.24381/cds.adbb2d47

de Villepin, F. E. (2024). Thermoregulation in Honey Bees. *American Bee Journal*.

Descamps, C., Quinet, M., & Jacquemart, A.-L. (2021). Climate change induced stress reduce quantity and alter composition of nectar and pollen from a bee-pollinated species *(Borago officinalis, Boraginaceae)*. *Frontiers in plant science, 12*, 755843.

Dyer, F. C. (1987). Memory and sun compensation by honey bees. *Journal of Comparative Physiology A, 160*(5), 621-633. doi:10.1007/BF00611935

Forsgren, E. (2010). European foulbrood in honey bees. *Journal of invertebrate pathology, 103*, S5-S9.

Gray, A., Adjlane, N., Arab, A., Ballis, A., Brusbardis, V., Bugeja Douglas, A., . . . Brodschneider, R. (2023). Honey bee colony loss rates in 37 countries using the COLOSS survey for winter 2019–2020: the combined effects of operation size, migration and queen replacement. *Journal of Apicultural Research, 62*(2), 204-210. doi:10.1080/00218839.2022.2113329

Higes, M., Martín-Hernández, R. Meana, A. . (2010). *Nosema ceranae* in Europe: An Emergent Type C Nosemosis. . *Apidologie,*(41), 375-392. doi:http://dx.doi.org/10.1051/apido/2010019

IPCC. (2023). Climate Change 2023: Synthesis Report. Contribution of Working Groups I, II and III to the Sixth Assessment Report of the Intergovernmental Panel on Climate Change. Geneva, Switzerland: IPCC.

Jones, J. C., & Oldroyd, B. P. (2006). Nest thermoregulation in social insects. *Advances in insect physiology, 33*, 153-191.

Kandemir, I., Kence, M., Sheppard, W. S., & Kence, A. (2006). Mitochondrial DNA variation in honey bee (Apis mellifera L.) populations from Turkey. *Journal of Apicultural Research, 45*(1), 33-38.

Kudo, G., & Cooper, E. J. (2019). When spring ephemerals fail to meet pollinators: mechanism of phenological mismatch and its impact on plant reproduction. *Proc Biol Sci, 286*(1904), 20190573. doi:10.1098/rspb.2019.0573

NOAA. (2023). Global Climate Report – 2022. National Centers for Environmental Information.

Ptaszyńska, A. A., Gancarz, M., Hurd, P. J., Borsuk, G., Wiącek, D., Nawrocka, A., . . . Paleolog, J. (2018). Changes in the bioelement content of summer and winter western honeybees (Apis mellifera) induced by Nosema ceranae infection. *PLoS one, 13*(7), e0200410.

Romero-Leiton, J. P., Gutierrez, A., Benavides, I. F., Molina, O. E., & Pulgarín, A. (2022). An approach to the modeling of honey bee colonies. *Web Ecology, 22*(1), 7-19.

Scheiner, R., Frantzmann, F., Jäger, M., Mitesser, O., Helfrich-Förster, C., & Pauls, D. (2020). A novel thermal-visual place learning paradigm for honeybees (Apis mellifera). *Frontiers in Behavioral Neuroscience, 14*, 56.

Seeley, T. D., & Visscher, P. K. (1985). Survival of honeybees in cold climates: the critical timing of colony growth and reproduction. *Ecological Entomology, 10*(1), 81-88.

Stabentheiner, A., Kovac, H., & Brodschneider, R. (2010). Honeybee colony thermoregulation–regulatory mechanisms and contribution of individuals in dependence on age, location and thermal stress. *PLoS one, 5*(1), e8967.

Stabentheiner, A., Kovac, H., Mandl, M., & Käfer, H. (2021). Coping with the cold and fighting the heat: thermal homeostasis of a superorganism, the

honeybee colony. *Journal of Comparative Physiology A, 207*(3), 337-351.

Tosi, S., Nieh, J. C., Brandt, A., Colli, M., Fourrier, J., Giffard, H., . . . Simon-Delso, N. (2021). Long-term field-realistic exposure to a next-generation pesticide, flupyradifurone, impairs honey bee behaviour and survival. *Communications Biology, 4*(1), 805. doi:10.1038/s42003-021-02336-2

CHAPTER 9

X-RAY ANALYSIS TECHNIQUES USED IN THE DETERMINATION OF HEAVY METAL POLLUTION IN AGRICULTURAL AND ENVIRONMENTAL MATRICES: A COMPARATIVE EVALUATION

Assoc. Prof. Dr. Bünyamin ALIM[1]

Assoc. Prof. Dr. Erdem ŞAKAR[2]

DOI: https://dx.doi.org/10.5281/zenodo.17847661

[1] Bayburt University, Technical Sciences Vocational School, Department of Electricity and Energy, Bayburt, Türkiye. balim@bayburt.edu.tr, ORCID ID: 0000-0002-4143-9787

[2] Atatürk University, Faculty of Science, Department of Physics, Erzurum, Türkiye. erdem@atauni.edu.tr, ORCID ID: 0000-0002-1359-4464

INTRODUCTION

Multi-factorial anthropogenic factors such as the deterioration of the geochemical balance of natural environments with the increasing energy demand due to population growth, increased sewage discharges with growing urbanization, increased industrial activities, fossil fuel emissions, mining processes, agricultural inputs and atmospheric deposition have caused an increase in heavy metal concentration levels in agriculture and the environment (Tóth et al., 2016; Alloway, 2013; Adriano, 2001). This situation directly affects not only environmental quality parameters but also the yield of agricultural products, their nutrient composition and the biological functions of ecosystems.

The fundamental characteristic that distinguishes heavy metals from other pollutants is their persistence in all ecosystems due to their inability to biodegrade. This inability and persistence allow heavy metals to spread among different ecosystems over time through mobilization and redistribution processes without losing any of their characteristics (Wuana & Okieimen, 2011). This spread accelerates the transport of toxic heavy metals, especially ^{24}Cr, ^{25}Mn, ^{26}Fe, ^{28}Ni, ^{33}As, ^{48}Cd, ^{80}Hg and ^{82}Pb, into the food chain, causing vital effects on human health and the agricultural economy (Muhammad et al., 2021; Nagajyoti et al., 2010). Additionally, World Health Organization reports indicate that heavy metal contamination in agricultural foods is one of the most widespread food safety problems on a global scale (WHO, 2017). Therefore, determining the proportion of heavy metals and/or the level of contamination of these metals in agricultural and environmental matrices is of great global importance for ecosystem health, food security, human health, and sustainable development goals, and constitutes a critical area of scientific research.

The toxicity level of heavy metals is related to processes such as chemical speciation, bioavailability, mobility, bioaccumulation, biotransformation, and biomagnification along the food chain. Accurately determining the quantitative and qualitative characteristics of heavy metal concentrations in environmental and agricultural matrices is possible not only by measuring the total metal amount but also by assessing the metal's chemical form, oxidation state, complexation behavior, and biological interaction potential (Manceau et al., 2002). Therefore, heavy metal analysis represents a multifaceted, multidisciplinary field of study, situated at the intersection of ecotoxicology, soil science, plant nutrition, and environmental engineering with

current analytical methodologies. In multidisciplinary studies, the use of advanced techniques is essential because the matrices to be examined exhibit high analytical heterogeneity and significant matrix effects can emerge in heavy metal measurements. Moreover, the need for these techniques is not only a scientific necessity but also a necessity for the applicability of international environmental management policies. For example, the European Union's Water Framework Directive and soil strategy require heavy metal monitoring studies to be conducted using high-resolution analytical techniques (European Commission, 2019). In addition, the World Health Organization (WHO, 2017) and the United Nations Environment Programme (UNEP, 2020) recommend the use of certain technical standards in heavy metal monitoring studies and encourage the use of high-resolution analytical techniques for data accuracy.

The accuracy of analytical measurements depends not only on the instrument's sensitivity but also on the sample preparation method, preservation of metal speciation, reduction of matrix effects, quality control procedures, and interlaboratory agreement. Therefore, to determine the analytical technique to be used for determining heavy metal pollution in agricultural and environmental ecosystems, it is essential to know all analytical techniques that perform this type of measurement. Choosing the right analytical technique for determining heavy metal pollution is critical for both the reliability of the measurement results and the effectiveness of environmental and agricultural management strategies. Each analytical method has its own limitations and advantages, such as detection limit, selectivity, sensitivity to matrix effects, sample preparation requirements, and cost. Choosing the appropriate method ensures both the prevention of false-positive/negative results and the scientific basis of environmental risk assessments. Furthermore, choosing the right analytical technique plays a strategic role in monitoring agricultural production safety, rehabilitating contaminated sites, monitoring contamination throughout the food chain, and generating reliable data for regulatory authorities.

Modern analytical techniques used for the analytical determination of heavy metal contamination in agricultural and environmental matrices can be categorized as spectroscopic techniques, mass spectroscopic techniques, electroanalytical techniques, chromatographic techniques, thermal analysis techniques, microscopic and surface analysis techniques, nuclear techniques, and next-generation sensor technologies. Among these techniques,

spectroscopic techniques determine the concentrations of atoms in the matrix based on absorption and emission, and therefore provide the most sensitive measurements.

In this book chapter, the fundamentals, strengths and weaknesses of X-ray analysis techniques, which are spectroscopic techniques used in the analytical determination of heavy metal pollution in agricultural and environmental matrices, are explained in detail and a comparative analysis is made with other techniques.

1. CLASSIFICATION OF ANALYTICAL MEASUREMENT TECHNIQUES USED IN HEAVY METAL DETERMINATION

Analytical techniques used in heavy metal determination can be classified according to their measurement principles, sensitivity levels, and application areas. In general, these techniques can be classified as follows:

- **Spectroscopic Techniques:** These techniques are based on determining the presence of metals at the atomic and molecular levels. This group includes AAS (Atomic Absorption Spectroscopy), AES (Atomic Emission Spectroscopy), AFS (Atomic Fluorescence Spectroscopy), XAS (X-Ray Absorption Spectroscopy), XRF (X-Ray Fluorescence) and XRD (X-Ray Diffraction), which perform analysis at the atomic level. At the molecular level, they include FTIR (Fourier Transform Infra-Red) Spectroscopy, UV-Vis spectrophotometry, and Raman spectroscopy.
- **Mass Spectroscopic Techniques:** Provide the separation of elements based on their mass/electric charge ratio; in this field, Inductively Time of Flight-Mass Spectrometry (TOF-MS) and Coupled Plasma-Mass Spectrometry (ICP-MS) are used in the determination of trace elements with high sensitivity.
- **Electroanalytical Techniques:** These techniques are based on the deposition of metal ions on the electrode surface and the measurement of voltage-current relationships. They are grouped as DPV (Differential Pulse Voltammetry), CSV (Cathodic Stripping Voltammetry) and ASV (Anodic Stripping Voltammetry).

- **Chromatographic Techniques:** They are grouped as HPLC (High-Performance Liquid Chromatography), IC (Ion Chromatography) and GC (Gas Chromatography). They are critical techniques used in analyzing metal speciation and complex formations.
- **Thermal Analysis Techniques:** These are grouped as TGA (Thermo-Gravimetric Analysis), DTA (Differential Thermal Analysis) and DSC (Differential Scanning Calorimetry). These techniques reveal the dissolution and stability profiles of metal components by examining the thermal behavior of metal-containing minerals and waste materials.
- **Microscopic and Surface Analysis Techniques:** These techniques enable the morphological and chemical characterization of metal particles and are used to determine details such as microdistribution and particle size. These techniques are grouped as TEM-EDS (Transmission Electron Microscopy-Energy Dispersive Spectroscopy), SEM-EDS (Scanning Electron Microscopy-Energy Dispersive Spectroscopy), SPR (Surface Plasmon Resonance) and AFM-IR (Atomic Force Microscopy-based InfraRed spectroscopy).
- **Nuclear Techniques:** These are preferred for radionuclide determination and the determination of certain heavy metal isotopes. These techniques are grouped as PIXE (Proton-Induced X-Ray Emission and NAA (Neutron Activation Analysis) and gamma spectrometry for the determination of radioactive metal isotopes.
- **Next-Generation Sensor Technologies:** Optical biosensors and electrochemical nanosensors fall into this group. They are used in heavy metal determinations, such as the detection of Pb metal in vegetable extracts and real-time monitoring in wastewater treatment plants.

This classification of techniques is critical in selecting analytical methods, considering both the properties of the target element and the nature of the matrix. For example, ICP-MS or AAS are preferred for trace element determination and the determination of low concentrations, while X-ray techniques are preferred when mineralogical and speciation information is required. Electroanalytical and chromatographic techniques offer distinct advantages in field or laboratory settings, while portable devices and sensors play a strategic role in rapid decision-making processes and continuous monitoring systems. This multi-layered classification allows comparison of

parameters such as analytical accuracy, precision, sample preparation time, cost and field suitability, providing a holistic approach to environmental risk assessment and agricultural management practices (Margui et al., 2022; Ravansari et al., 2020; Silva et al., 2019; Alloway, 2013; Kabata-Pendias, 2010; Sparks, 2003; Van Grieken & Markowicz, 2001).

2. X-RAY ANALYSIS TECHNIQUES USED IN HEAVY METAL DETERMINATION

Spectroscopic techniques for heavy metal determination are among the most fundamental and widespread techniques used to identify heavy metal contamination in agriculture and the environment and are based on the interactions between metal atoms and electromagnetic radiation. X-ray-based analytical methods are powerful spectroscopic techniques that allow the quantitative and qualitative determination of metals based on the interactions between the inner shell energy levels of atomic electrons and X-ray photons. It is particularly advantageous for the determination of heavy metals, as elements with medium and high atomic numbers ($Z \geq 13$) interact strongly with X-rays. These analytical techniques can be divided into three main categories: XRF, XRD and XAS. These methods are widely used in the analysis of environmental and agricultural matrices. Their common feature is that they provide non-destructive, multi-element, and rapid analysis, in most cases without requiring sample preparation.

2.1. X-Ray Fluorescence (XRF) Technique

In XRF analysis, the sample is excited by an X-ray source. This excitation excites electrons from the inner shell of atom (e.g., K or L shells), creating a vacancy in the shell. Electrons transition from the outer shells, resulting in the emission of characteristic X-ray fluorescence. Because the energy of this characteristic X-ray emitted is specific to the element, the element is identified using a detector and quantitative determination is achieved by analyzing its fluorescence intensity.

XRF is divided into two types: WDXRF (Wavelengt Dispersive X-Ray Fluorescence) and EDXRF (Energy Dispersive X-Ray Fluorescence), which are laboratory-grade methods offering high accuracy and good analytical

performance. A schematic representation of the operating principle of XRF analysis is shown in Figure 1. Additionally, micro-XRF (μ-XRF), which allows for chemical mapping of surfaces or micro-areas using a focused X-ray beam, and portable XRF (p-XRF) devices are available, suitable for rapid field analysis without requiring laboratory preparation and offering a practical solution for soil, sediment, and waste analysis (Jenkins et al., 2025; Morgui et al., 2022; Yang et al., 2022; Ravansari et al., 2020; Castillo-Michel et al., 2017; Weindorf et al., 2012; Jang, 2010; Strawn & Baker, 2008).

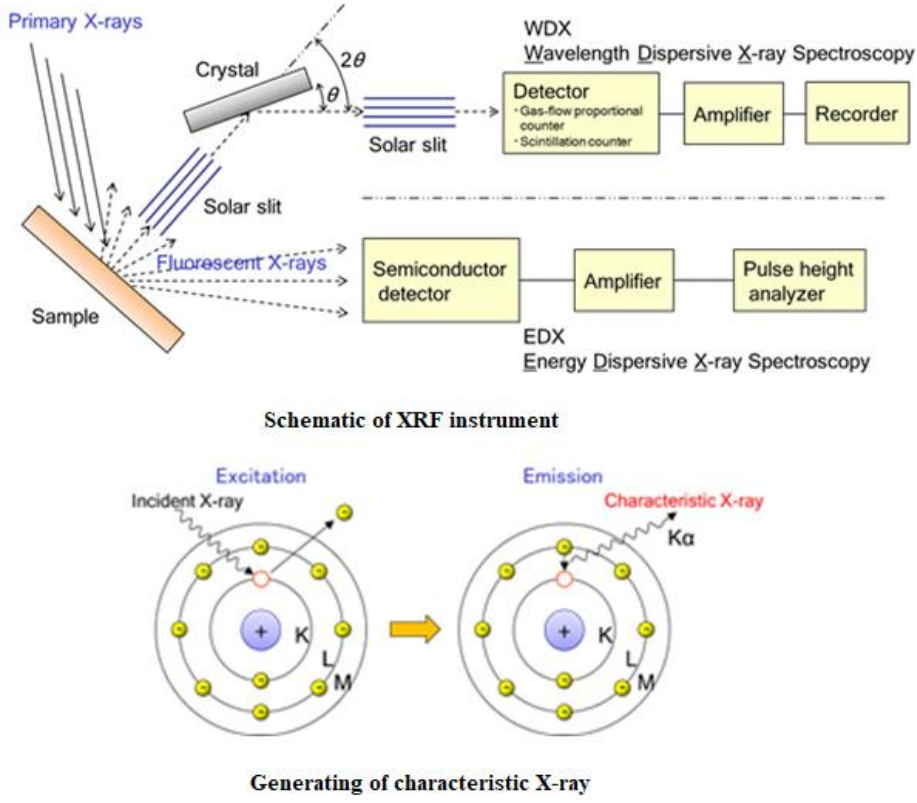

Figure 1: Schematic Representation of the Working Principle of XRF Analysis (Toray Research Center, Inc. 2025)

The advantages of this technique can be listed as follows;

- Minimal sample preparation required (non-destructive analysis),
- Multi-element analysis can be performed and many metals can be determined simultaneously,

- Fast analysis time (seconds to minutes) makes it particularly practical for field analyses,
- High accuracy and sensitivity with proper calibration.

The disadvantages of this technique can be listed as follows;

- The limit of detection (LoD) is generally higher than with laboratory methods; accuracy may decrease, especially at very low concentrations,
- Detection of light elements (low-Z) is difficult—XRF is more effective for heavier elements,
- Matrix effects: Moisture, organic matter, particle size, and surface irregularities can affect measurement accuracy,
- The use of appropriate calibration materials (Certified Reference Materials, CRM) is necessary for quantitative analysis.

This technique is widely used in soil and sediment contamination analyses. Additionally, it is widely used in complex analyses such as metal distribution in environmental samples, particle-scale analysis, biocarbon/plant metal interactions, soil organic matter-metal binding, and multi-element soil analyses.

2.2. X-Ray Diffraction (XRD) Technique

XRD is based on the principle that X-rays are diffracted by atomic planes in crystalline materials. This diffraction phenomenon is described by **Bragg's Law:**

$$n\lambda = 2dsin\theta$$

where, n is the diffraction coefficient, λ is the X-ray wavelength used, d is the distance between crystal planes, and θ is the diffraction angle. A schematic representation of Bragg's law and X-ray diffraction is given in Figure 2.

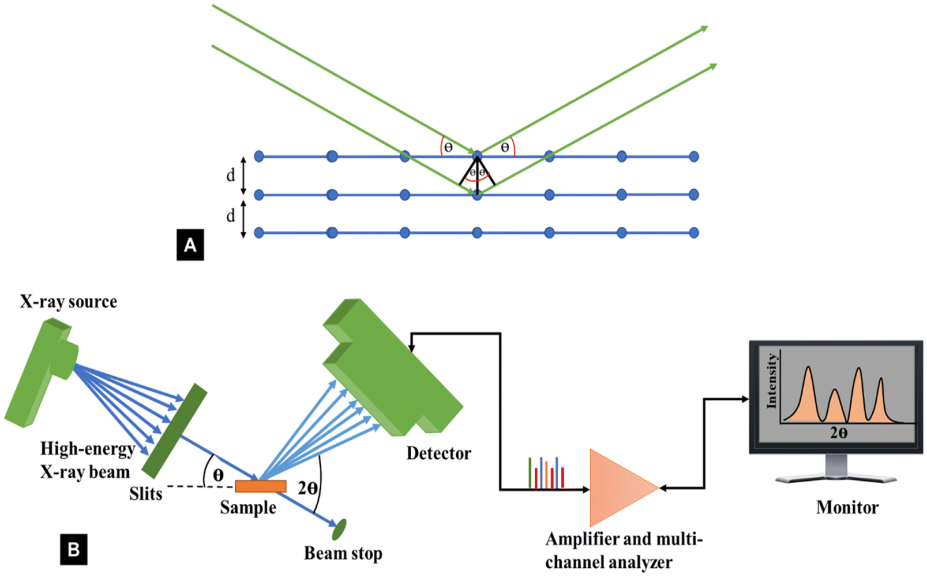

Figure 2: Schematic Representation of Bragg's law (A) and X-ray Diffraction (XRD) (B) (Salem et al., 2023).

In XRD analysis, samples are prepared and analyzed in powder, glass, or pellet form. Soil, sediment, or mineral samples are ground to a homogeneous powder. Mo-Kα (λ = 0.7093 Å) or Cu-Kα (λ = 1.5406 Å) sources are typically used to excite the samples with X-rays. Classic Geiger-Müller scintillation or modern CCD (Charged Coupled Device) detectors are used. The resulting diffraction patterns are compared with reference databases (ICDD – International Centre for Diffraction Data). This allows for phase identification and quantification. The XRD technique does not directly provide the concentration of heavy metals in the matrix, but it is critical for determining the bonding patterns and chemical forms of heavy metals within mineral phases.

The advantages of this technique can be listed as follows;

- Non-destructive analysis does not alter the sample structure,
- Determines phase and mineral composition, revealing the chemical form of the metal,
- Provides critical information for environmental risk and mobility estimation,
- Widely used in soil, sediment, and waste samples.

The disadvantages of this technique can be listed as follows;

- Does not provide direct element concentration; must be combined with other techniques (XRF, ICP-OES/MS) for quantitative determination,
- Sample preparation and particle size affect the accuracy of the analysis,
- Low detection limit; not suitable for ultra-trace element determination,
- Reference databases are not economical.

With this technique, the binding status of metals such as Cr, Pb, Zn, Cu as oxide, sulfate or carbonate phases can be determined in soil and sediment samples, the phase distribution of metal-containing wastes in waste and industrial material analyses and the identification of metallic minerals can be performed (Bakker et al., 2018; Garzon et al., 2017; Andrist-Rangel et al., 2013; Mathanker et al., 2013).

2.3. X-Ray Absorption Spectroscopy (XAS)

XAS is an advanced structural analysis technique that measures the X-ray absorption behavior of an element within a specific energy range, thereby providing information about its electronic structure, local coordination, oxidation state, and atomic environment. The interaction of X-rays with atomic orbitals results in the ionization of nuclear electrons, resulting in distinct absorption features in the energy range near this ionization threshold. X-ray absorption is generally expressed by the **Beer–Lambert law:**

$$I = I_0 e^{-\mu(E)t}$$

where, I_0; the incident X-ray intensity, I ; the X-ray intensity passing through the sample, t ; the sample thickness and $\mu(E)$; the energy dependent absorption coefficient.

XAS is divided into two main components: XANES (X-ray Absorption Near Edge Structure) and EXAFS (Extended X-ray Absorption Fine Structure). A schematic representation of the operating principle of this technique is presented in Figure 3.

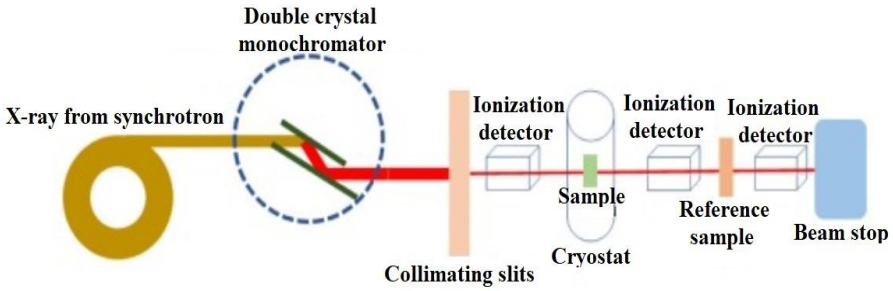

Figure 3: Schematic Representation of the Working Principle of XAS Analysis (Sarker and Nahar, 2022)

XAS is one of the most powerful techniques for heavy metal species determination, particularly in environmental and agricultural matrices. While techniques such as AAS, ICP-MS, and XRF provide only elemental quantities, XAS provides the metal species, which determine the metal's oxidation state, complex structure, binding to soil minerals, chemical form of the metal in plant tissue, bioavailability, and toxicity. Additionally, in XAS analyses, samples can be solid, liquid, biological tissue, or thin film. Transmission measurement should be used to determine high metal content in the sample, fluorescence measurement to determine trace elements, and electron current measurement for surface analysis.

The advantages of this technique can be listed as follows;

- It is one of the few techniques capable of chemical species determination,
- It is non-destructive,
- It does not depend on any crystalline structure (unlike XRD, it can also analyze amorphous materials),
- It provides information (fluorescence mode) even at very low concentrations (ppb),
- It is suitable for use in plants, soil, water, and biological materials.

The disadvantages of this technique can be listed as follows;

- A synchrotron facility is required,
- The experimental process is complex,
- Data analysis requires advanced expertise,
- It is costly and has limited access for routine laboratories.

With this technique, the determination of the binding status of heavy metals in soil and sediments, plant tissues, water and waste matrices, the

prediction of biological mobility and toxicity, and information on oxidation-reduction processes can be provided (Schmidh et al., 2022; Lucas et al., 2022; Qin et al., 2017; Castillo-Michel et al., 2017; Rivard et al., 2016; Lopez-Moreno et al., 2010; Strawn & Baker, 2009; Beauchemin et al., 2003; Parsons et al., 2002; Salt et al., 2002; Xia et al., 1999; Fendorf et al., 1994).

3. COMPARISON OF X-RAY ANALYSIS TECHNIQUES USED IN HEAVY METAL DETERMINATION WITH OTHER ANALYTICAL TECHNIQUES

When determining heavy metals in environmental and agricultural matrices, simply knowing the total metal concentration may not always be sufficient. In complex matrices such as soil, water, sediment, and plants, the metal's form, distribution, mineral phase, or chemical bonding state are critical for bioavailability and ecotoxicity. Therefore, the selection of analytical techniques should be based on multidimensional criteria such as sensitivity, specificity, sample preparation requirements, analysis speed, cost, and practicality. In this context, X-ray analysis techniques (especially X-ray fluorescence-XRF) stand out with their advantages of non-destructive analysis, multi-element determination and rapid sampling in the field, while classical methods (ICP-MS, AAS, etc.) continue to be the gold standard in high sensitivity and trace element determination.

Recent comparative studies demonstrate the relationship between XRF and mass spectrometry methods in environmental soil analyses. One study compared portable-XRF (p-XRF) and conventional acid digestion+ICP-MS data for the determination of lead (Pb) in soil samples. The findings demonstrated a strong linear relationship ($R^2 \approx 0.89$) and statistically significant agreement between the two methods (Maliki et al., 2017). This demonstrates that XRF is a reliable and rapid screening tool for field studies and large sampling campaigns.

Advantages of XRF include minimal sample preparation, non-destructive nature, simultaneous detection of multiple elements, and rapid analysis time. These features are particularly advantageous for contamination mapping across large geographic areas, hotspot identification, or combined field-laboratory analysis strategies (McComb et al., 2014). Despite these advantages, XRF does not always provide the same sensitivity as ICP-MS. XRF

detection limits are generally higher than those of ICP-MS/ICP-OES, particularly for trace element concentrations and in heterogeneous matrices; for some elements (e.g., V, Cd, As), XRF can yield either misleadingly low values or exhibit variation (Guargliardi et al., 2025). Therefore, XRF is generally recommended as a "screening" method to identify potential contamination areas; for precise controls and quantitative analysis, ICP-MS, AAS, or similar high-sensitivity techniques are recommended.

XRF provides only the total elemental concentration but does not provide information about the metal's chemical form, oxidation state, or the mineral phase to which it is bound. Particularly in environmental risk assessments, the form of the metal (e.g., free ion, carbonate/oxide, adsorbed, organic complex, etc.) can be critical. Techniques such as chromatography + mass spectrometry (e.g. HPLC-ICP-MS), voltammetric speciation, and XAS are usually required for this type of information. In addition, XRF results can be affected by matrix effects (grain size, sample homogeneity, moisture, density, surface roughness, etc.), which can reduce accuracy, especially in heterogeneous, natural soil and sediment samples (Guargliardi et al., 2025; Fedeli et al., 2024). Therefore, especially when low concentrations, speciation or bioavailability analyses are involved, classical solubilization + mass spectrometry and/or chromatography-based analyses should be preferred.

The comparison of X-ray analysis techniques with other analytical techniques used in the determination of heavy metals in agriculture and the environment in terms of technical properties is given in Table 1.

Literature data (Guargliardi et al., 2025; Jenkins et al., 2025; Lu et al., 2022; Sikora et al., 2021; Ravansari et al., 2020; Mijovilovich et al., 2020;) show that the most reliable and comprehensive analysis results are usually obtained with a multi-stage and multi-technique approach. For example, after contamination screening and hot-spot mapping with pXRF for the field and large sample volume in the first stage, confirmation and quantitative analysis are performed with ICP-MS/ICP-OES/AAS for critical/highly contaminated matrices or low concentration samples. If metal form, speciation, bioavailability or bond phase information are required, techniques such as chromatography + mass spectrometry, XAS, or mineralogical analysis (e.g., XRD + SEM-EDS) can be used. This hybrid strategy provides a reliable approach in terms of analytical depth while being balanced in terms of time and cost.

Table 1: Comparison of the Most Commonly Used Analytical Techniques for Heavy Metal Determination in Agriculture and the Environment.

Technical Specification	XRF	XRD	XAS	ICP-MS	ICP-OES	AAS	ASV
Non-Destructive	√	√	√	√	√	√	√
Sensitivity (LoD)	**M**	**N.E**	**M**	**V.H**	**H**	**M**	**H**
Multi-element analysis	√	–	√	√	√	X	X
Field use	√ (p-XRF)	X	X	X	X	X	**P**
Mineral phase analysis	X	√	X	X	X	X	X
Valence/bonding analysis	X	X	√	X	X	X	X
Sample preparation time	**V.L**	**L**	**M**	**H**	**H**	**M**	**M**
Measurement time	**S**	**Mt**	**Mt-H**	**Mt**	**Mt**	**Mt**	**Mt**

Abbreviations in table

M: Medium; **N.E:** Non Elemental; **V.H:** Very High; **H:** High; **P:** Partially; **V.L:** Very Low; **L:** Low; **S:** Seconds; **Mt:** Minute; **Mt-H:** Minute-Hour

4. CONCLUSION AND EVALUATION

Determining heavy metal pollution in agricultural and environmental matrices requires not only concentration measurement but also the evaluation of multidimensional parameters such as the metal's chemical form, mineral phase distribution, oxidation state, and environmental mobility. In this context, X-ray-based analytical techniques (XRF, XRD, XAS) provide significant advantages over classical spectroscopic and mass spectrometric techniques due to the distinctive information they provide at the structural and atomic levels. Indeed, the non-destructive and rapid analysis capabilities of XRF have been demonstrated in many studies to enable in-situ heavy metal determination in soil and plants (Ravansari et al., 2020; Weindorf et al., 2012). Additionally, many studies have shown that pXRF measurements are affected by matrix

factors such as moisture, organic matter, and particle size, requiring appropriate sample preparation, CRM-based calibration, and statistical corrections for reliability (Lu et al., 2022; Ravansari et al., 2020). XRD allows for the estimation of heavy metals' environmental mobility by determining which minerals hold them. XAS, on the other hand, provides atomic-level information on the pollutant's environmental behavior by analyzing the oxidation state, coordination chemistry, and binding environment of heavy metals. In these respects, X-ray techniques provide a unique structural analysis approach that complements concentration-focused methods in understanding heavy metal pollution.

In contrast, classical atomic spectroscopic and mass spectrometric techniques such as ICP-MS, AAS, AFS, and AES offer high sensitivity at ultra-trace levels, making them among the most powerful tools for reliable elemental determination. The accuracy of ICP-MS in heavy metal determination down to the ppt level is particularly indispensable for trace analysis of toxic elements such as As, Cd and Pb. Furthermore, these techniques generally require a sample solubilization step, which both degrades the metal's chemical form and provides no information about the metal's environmental binding pattern or mineral phase composition. For example, while the total amount of Pb in a soil sample can be determined with high accuracy with ICP-MS, whether Pb is present in the carbonate, sulfate, or silicate phase cannot be determined without structural techniques such as XRD or XAS. This creates a critical knowledge gap, particularly regarding the metal's mobility, phytotoxicity, and risk analysis.

In this context, the structural, mineralogical, and chemical speciation information provided by X-ray-based methods such as XRF, XRD, and XAS enable multidimensional assessments in agricultural and environmental research. These findings demonstrate that X-ray techniques are not only measurement tools but also key methods for scientifically understanding the environmental fate of heavy metal contamination.

Consequently, several recommendations for future studies emerge. First, hybrid analytical approaches using combined techniques such as XRF–ICP-MS, XRD–XAS, or XRF–XRD–XAS should be expanded; no single method can simultaneously provide complete information on the concentration, mineral phase, and chemical speciation of heavy metals. Second, it is important to develop portable XRF and micro-XAS studies for field applications of X-ray

techniques in agricultural soils, waters, and plant tissues. Third, integrating structural data obtained from X-ray methods with geochemical modeling software will enable more accurate predictions of the long-term environmental fate of pollution. Finally, multidisciplinary studies linking X-ray techniques to heavy metal bioavailability, phytoremediation efficiency, and soil health indices will contribute scientifically to sustainable agriculture and environmental management.

REFERENCES

Adriano, D. C. (2001). Trace elements in terrestrial environments: biogeochemistry, bioavailability, and risks of metals (Vol. 860). New York: Springer. https://doi.org/10.1007/978-0-387-21510-5

Al Maliki, A., Al-lami, A. K., Hussain, H. M., & Al-Ansari, N. (2017). Comparison between inductively coupled plasma and X-ray fluorescence performance for Pb analysis in environmental soil samples. Environmental Earth Sciences, 76(12), 433. https://doi.org/10.1007/s12665-017-6753-z

Alloway, B. J. (2013). Heavy metals in soils: Trace metals and metalloids in soils and their bioavailability (3rd ed.). Springer. https://doi.org/10.1007/978-94-007-4470-7

Andrist-Rangel, Y., Simonsson, M., Öborn, I., & Hillier, S. (2013). Acid-extractable potassium in agricultural soils: Source minerals assessed by differential and quantitative X-ray diffraction. Journal of Plant Nutrition and Soil Science, 176(3), 407-419. https://doi.org/10.1002/jpln.201200465

Bakker, E., Hubert, F., Wander, M. M., & Lanson, B. (2018). Soil development under continuous agriculture at the Morrow plots experimental fields from X-ray diffraction profile modelling. Soil Systems, 2(3), 46. https://doi.org/10.3390/soilsystems2030046

Beauchemin, S., Hesterberg, D., Chou, J., Beauchemin, M., Simard, R. R., & Sayers, D. E. (2003). Speciation of phosphorus in phosphorus-enriched agricultural soils using X-ray absorption near-edge structure spectroscopy and chemical fractionation. Journal of environmental quality, 32(5), 1809-1819. https://doi.org/10.2134/jeq2003.1809

Castillo-Michel, H. A., Larue, C., Del Real, A. E. P., Cotte, M., & Sarret, G. (2017). Practical review on the use of synchrotron based micro-and nano-X-ray fluorescence mapping and X-ray absorption spectroscopy to investigate the interactions between plants and engineered nanomaterials. Plant Physiology and Biochemistry, 110, 13-32. https://doi.org/10.1016/j.plaphy.2016.07.018

European Commission (2019). Water Framework Directive. https://environment.ec.europa.eu/topics/water/water-framework-directive_en

Fedeli, R., Di Lella, L. A., & Loppi, S. (2024). Suitability of XRF for routine analysis of multi-elemental composition: a multi-standard verification. Methods and Protocols, 7(4), 53. https://doi.org/10.3390/mps7040053

Fendorf, S. E., Sparks, D. L., Lamble, G. M., & Kelley, M. J. (1994). Applications of X-ray absorption fine structure spectroscopy to soils. Soil Science Society of America Journal, 58(6), 1583-1595. https://doi.org/10.2136/sssaj1994.03615995005800060001x

Garzón, E., Morales, L., Martínez-Blanes, J. M., & Sánchez-Soto, P. J. (2017). Characterization of ashes from greenhouse crops plant biomass residues using X-ray fluorescence analysis and X-ray diffraction. https://doi.org/10.1002/xrs.2801

Guagliardi, I., Ricca, N., & Cicchella, D. (2025). Comparative Evaluation of Inductively Coupled Plasma Mass Spectrometry (ICP-MS) and X-Ray Fluorescence (XRF) Analysis Techniques for Screening Potentially Toxic Elements in Soil. Toxics, 13(4), 314. https://doi.org/10.3390/toxics13040314

Jang, M. (2010). Application of portable X-ray fluorescence (pXRF) for heavy metal analysis of soils in crop fields near abandoned mine sites. Environmental Geochemistry and Health, 32(3), 207-216. https://doi.org/10.1007/s10653-009-9276-z

Jenkins, E. M., Galbraith, J., & Paltseva, A. A. (2025). Portable X-ray fluorescence as a tool for urban soil contamination analysis: accuracy, precision, and practicality. Soil, 11(2), 565-582. https://doi.org/10.5194/soil-11-565-2025

Kabata-Pendias, A. (2010). Trace elements in soils and plants (4th ed.). CRC Press. https://doi.org/10.1201/b10158

López-Moreno, M. L., de la Rosa, G., Hernández-Viezcas, J. A., Peralta-Videa, J. R., & Gardea-Torresdey, J. L. (2010). X-ray absorption spectroscopy (XAS) corroboration of the uptake and storage of CeO2 nanoparticles and assessment of their differential toxicity in four edible plant species. Journal of agricultural and food chemistry, 58(6), 3689-3693. https://doi.org/10.1021/jf904472e

Lu, J., Guo, J., Wei, Q., Tang, X., Lan, T., Hou, Y., & Zhao, X. (2022). A matrix effect correction method for portable X-ray fluorescence data. Applied Sciences, 12(2), 568. https://doi.org/10.3390/app12020568

Lucas, E., Mosesso, L., Roswall, T., Yang, Y. Y., Scheckel, K., Shober, A., & Toor, G. S. (2022). X-ray absorption near edge structure spectroscopy reveals phosphate minerals at surface and agronomic sampling depths in agricultural Ultisols saturated with legacy phosphorus. Chemosphere, 308, 136288. https://doi.org/10.1016/j.chemosphere.2022.136288

Manceau, A., Marcus, M. A., & Tamura, N. (2002). Quantitative speciation of heavy metals in soils and sediments by synchrotron X-ray techniques. Reviews in mineralogy and geochemistry, 49(1), 341-428. https://doi.org/10.2138/gsrmg.49.1.341

Marguí, E., Queralt, I., & De Almeida, E. (2022). X-ray fluorescence spectrometry for environmental analysis: Basic principles, instrumentation, applications and recent trends. Chemosphere, 303, 135006. https://doi.org/10.1016/j.chemosphere.2022.135006

Mathanker, S. K., Weckler, P. R., & Bowser, T. J. (2013). X-ray applications in food and agriculture: a review. Transactions of the ASABE, 56(3), 1227-1239. https://doi.org/10.13031/trans.56.9785

McComb, J. Q., Rogers, C., Han, F. X., & Tchounwou, P. B. (2014). Rapid screening of heavy metals and trace elements in environmental samples using portable X-ray fluorescence spectrometer, a comparative study. Water, Air, & Soil Pollution, 225(12), 2169. https://doi.org/10.1007/s11270-014-2169-5

Mijovilovich, A., Morina, F., Bokhari, S. N., Wolff, T., & Küpper, H. (2020). Analysis of trace metal distribution in plants with lab-based microscopic X-ray fluorescence imaging. Plant Methods, 16(1), 82. https://doi.org/10.1186/s13007-020-00621-5

Muhammad, M., Habib, I.Y., Hamza, I., Mikail, T. A., Yunusa, A., Muhammad, I. A., Hamza, I., & Bello, A. A., (2021). Heavy metals contamination of agricultural land and their impact on food safety. European Journal of Nutrition & Food Safety, 13(1), 104-111. https://doi.org/10.9734/EJNFS/2021/v13i130354

Nagajyoti, P. C., Lee, K. D., & Sreekanth, T. V. M. (2010). Heavy metals, occurrence and toxicity for plants: a review. Environmental chemistry letters, 8(3), 199-216. https://doi.org/10.1007/s10311-010-0297-8

Parsons, J. G., Aldrich, M. V., & Gardea-Torresdey, J. L. (2002). Environmental and biological applications of extended X-ray absorption fine structure (EXAFS) and X-ray absorption near edge structure (XANES) spectroscopies. Applied Spectroscopy Reviews, 37(2), 187-222. https://doi.org/10.1081/ASR-120006044

Qin, H. B., Zhu, J. M., Lin, Z. Q., Xu, W. P., Tan, D. C., Zheng, L. R., & Takahashi, Y. (2017). Selenium speciation in seleniferous agricultural soils under different cropping systems using sequential extraction and X-ray absorption spectroscopy. Environmental Pollution, 225, 361-369. https://doi.org/10.1016/j.envpol.2017.02.062

Ravansari, R., Wilson, S. C., & Tighe, M. (2020). Portable X-ray fluorescence for environmental assessment of soils: Not just a point and shoot method. Environment International, 134, 105250. https://doi.org/10.1016/j.envint.2019.105250

Rivard, C., Lanson, B., & Cotte, M. (2016). Phosphorus speciation and micro-scale spatial distribution in North-American temperate agricultural soils from micro X-ray fluorescence and X-ray absorption near-edge spectroscopy. Plant and soil, 401(1), 7-22. https://doi.org/10.1007/s11104-015-2494-5

Salem, K. S., Kasera, N. K., Rahman, M. A., Jameel, H., Habibi, Y., Eichhorn, S. J., ... & Lucia, L. A. (2023). Comparison and assessment of methods for cellulose crystallinity determination. Chemical Society Reviews, 52(18), 6417-6446. https://doi.org/10.1039/D2CS00569G

Salt, D. E., Prince, R. C., & Pickering, I. J. (2002). Chemical speciation of accumulated metals in plants: evidence from X-ray absorption spectroscopy. Microchemical journal, 71(2-3), 255-259. https://doi.org/10.1016/S0026-265X(02)00017-6

Sarker, S. D., & Nahar, L. (2022). Characterization of nanoparticles. In Advances in nanotechnology-based drug delivery systems (pp. 45-82). Elsevier. https://doi.org/10.1016/B978-0-323-88450-1.00011-9

Schmidt, E. J., Zanoni, G., Bumguardner, A., Šegvić, B., Lewis, K., Abdala, D., & Siebecker, M. G. (2022). Soil chemical extractions can alter potassium

coordination in agricultural soils: A combined wet chemical and X-ray absorption spectroscopic approach. Geoderma, 422, 115914. https://doi.org/10.1016/j.geoderma.2022.115914

Sikora, A. L., Maguire, L. W., Nairn, R. W., & Knox, R. C. (2021). A comparison of XRFS and ICP-OES methods for soil trace metal analyses in a mining impacted agricultural watershed. Environmental Monitoring and Assessment, 193(8), 490. https://doi.org/10.1007/s10661-021-09275-9

Silva, E. A., Weindorf, D. C., Silva, S. H., Ribeiro, B. T., Poggere, G. C., Carvalho, T. S., ... & Curi, N. (2019). Advances in tropical soil characterization via portable X-ray fluorescence spectrometry. Pedosphere, 29(4), 468-482. https://doi.org/10.1016/S1002-0160(19)60815-5

Sparks, D. L. (2003). *Environmental soil chemistry* (2nd ed.). Academic Press. https://doi.org/10.1016/B978-0-12-656446-4.X5000-2

Strawn, D. G., & Baker, L. L. (2008). Speciation of Cu in a contaminated agricultural soil measured by XAFS, μ-XAFS, and μ-XRF. Environmental science & technology, 42(1), 37-42. https://doi.org/10.1021/es071605z

Strawn, D. G., & Baker, L. L. (2009). Molecular characterization of copper in soils using X-ray absorption spectroscopy. Environmental Pollution, 157(10), 2813-2821. https://doi.org/10.1016/j.envpol.2009.04.018

Toray Research Center, Inc. (2025). X-ray Fluorescence Spectrometry (XRF). https://www.toray-research.co.jp/en/technical-info/analysis/XRF.html

Tóth, G., Hermann, T., Da Silva, M. R., & Montanarella, L. J. E. I. (2016). Heavy metals in agricultural soils of the European Union with implications for food safety. Environment international, 88, 299-309. https://doi.org/10.1016/j.envint.2015.12.017

UNEP (2020). Global Chemicals Outlook II. https://www.unep.org/resources/report/global-chemicals-outlook-ii-legacies-innovative-solutions

Van Grieken, R., & Markowicz, A. (2001). Handbook of X-ray spectrometry (2nd ed.). CRC Press. https://doi.org/10.1201/9780203908709

Weindorf, D. C., Zhu, Y., Chakraborty, S., Bakr, N., & Huang, B. (2012). Use of portable X-ray fluorescence spectrometry for environmental quality

assessment of peri-urban agriculture. Environmental Monitoring and Assessment, 184(1), 217-227. https://doi.org/10.1007/s10661-011-1961-6

WHO. (2017). Guidelines for Drinking Water Quality. https://www.who.int/publications/i/item/9789241549950

Wuana, R. A., & Okieimen, F. E. (2011). Heavy metals in contaminated soils: a review of sources, chemistry, risks and best available strategies for remediation. International Scholarly Research Notices, 2011(1), 402647. https://doi.org/10.5402/2011/402647

Xia, K., Skyllberg, U. L., Bleam, W. F., Bloom, P. R., Nater, E. A., & Helmke, P. A. (1999). X-ray absorption spectroscopic evidence for the complexation of Hg (II) by reduced sulfur in soil humic substances. Environmental science & technology, 33(2), 257-261. https://doi.org/10.1021/es980433q

Yang, W., Li, F., Zhao, Y., Lu, X., Yang, S., & Zhu, P. (2022). Quantitative analysis of heavy metals in soil by X-ray fluorescence with PCA–ANOVA and support vector regression. Analytical Methods, 14(40), 3944-3952. https://doi.org/10.1039/d2ay00593j

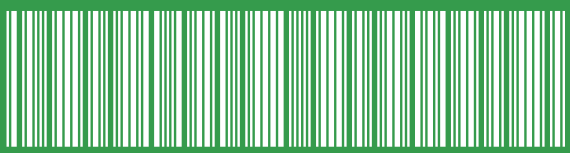

ISBN: 978-625-378-421-8